



THE UNIVERSITY *of* EDINBURGH

This thesis has been submitted in fulfilment of the requirements for a postgraduate degree (e.g. PhD, MPhil, DClinPsychol) at the University of Edinburgh. Please note the following terms and conditions of use:

This work is protected by copyright and other intellectual property rights, which are retained by the thesis author, unless otherwise stated.

A copy can be downloaded for personal non-commercial research or study, without prior permission or charge.

This thesis cannot be reproduced or quoted extensively from without first obtaining permission in writing from the author.

The content must not be changed in any way or sold commercially in any format or medium without the formal permission of the author.

When referring to this work, full bibliographic details including the author, title, awarding institution and date of the thesis must be given.

**UNRAVELLING THE ROLES OF SHIGA TOXIN AND SHIGA
TOXIN-ENCODING BACTERIOPHAGES IN
ENTEROHAEMORRHAGIC *ESCHERICHIA COLI*
(EHEC) O157:H7 COLONISATION OF
THE BOVINE INTESTINE**

Nur Indah Ahmad

Thesis submitted for the Degree of

Doctor of Philosophy

University of Edinburgh

2015

Author's Declaration

I declare that the work contained in this thesis is my own and has not been submitted for any other degree or award.

Nur Indah Ahmad

Abbreviations

A/E	Attaching and effacement
A4GALT	A4-galactosyltransferase
ANOVA	Analysis of variance
APC	Antigen presenting cells
BCA	Bicinchoninic acid assay
Bcl	B-cell lymphoma 2
BiP	Binding protein
BTRM	Bovine terminal rectal mucus
CDK	Cell-dependent kinase
CFU	Colony forming unit
CI	Confidence interval
CL	Containment level
ConA	Concavalin A
CTL	Cytotoxic T lymphocyte
CT-SMAC	Cefixime tellurite-Sorbitol MacConkey
DH₂O	Distilled water
DMEM	Dulbecco's modified Eagle medium
DMSO	Dimethyl sulfoxide
DNA	Deoxyribonucleic acid
DPBS	Dulbecco's phosphate-buffered saline
EGF	Epidermal growth factor
ELISA	Enzyme-linked immuno-assay
FACS	Fluorescence activated cell sorting
FAE	Follicle-associated epithelium
FCS	Fetal calf serum
FL	Fluorescence channel
g	Gram
GADD	Growth arrest and DNA-damage-inducible protein
GALT	Gut-associated lymphoid tissue
Gb3	Globotriaosylceramide
Gb4	Globotetraosylceramide
GUD	Glucuronidase
h	Hour

HBSS	Hank's balanced salt solution
HC	Haemorrhagic colitis
HEPES	(4-(2-hydroxyethyl)-1-piperazineethanesulfonic acid)
HUS	Haemorrhagic uraemic syndrome
HUVEC	Human umbilical vein endothelial cell
IEL	Intra-epithelial leukocyte
IFN-γ	Interferon-gamma
IFNAR	Type 1 Interferon receptor
IMS	Immuno-magnetic sorting
IPRAVE	International Partnership Research Award in Epidemiology
IVOC	<i>In vitro</i> organ culture
JAK	Janus kinase
JNK	c-Jun NH2-terminal Kinase
Lac-MAC	Lactose MacConkey
LB	Lysogeny broth
LEE	Locus of enterocyte effacement
LPS	Lipopolysaccharide
MAPK	Mitogen-activated protein kinase
MEM	Modified Eagle's medium
MFI	Mean/medium of fluorescence intensity
MHC	Major histocompatibility complex
min	Minute
MMC	Mitomycin C
NALT	Nasal-associated lymphoid tissue
NFκB	Nuclear factor kappa B
NK	Natural killer
OCT	Optimum cutting temperature
OD	Optical density
PBMC	Peripheral bovine mononuclear cell
PBS	Phosphate-buffered saline
PBST	Phosphate-buffered saline with Tween 20
PCK	Pancytokeratin
PCNA	Proliferation cellular nuclear antigen
PE	Phycoerythrin
PFA	Paraformaldehyde

PFGE	Pulse field gel electrophoresis
PHA	Phyto-haemagglutinin
PI	Propidium iodide
PStx	Purified Shiga toxin
PT	Phage type
pY-STAT	Phosphorylated signal transducer and activator of transcription protein
RAMALT	Recto-anal mucosal-associated lymphoid tissue
RCF	Relative centrifugal force
RPM	Revolutions per minute
RPMI	Roswell Park Memorial Institute
rRNA	Ribosomal ribonucleic acid
RT-qPCR	Quantitative reverse transcription polymerase chain reaction
SAPK	Stress-activated protein kinase
SDS-PAGE	Sodium dodecyl sulfate polyacrylamide gel electrophoresis
SD	Standard deviation
SEERAD	Scottish Executive Environment and Rural Affairs Department
SEM	Standard error mean
sRNA	Small nuclear ribonucleic acid
SSC	Side-scatter light
STAT	Signal transducer and activator of transcription
STEC	Shiga toxin-producing <i>Escherichia coli</i>
Stx	Shiga toxin
T3SS	Type 3 secretion system
TBST	Tris-buffered saline with Tween 20
TLR	Toll-like receptor
ΦStx2a	Shiga toxin 2a-encoding phage
ΦStx2c	Shiga toxin 2c-encoding phage

Acknowledgements

I would like to express my gratitude to Prof. Dr. David Gally and Dr. Andreas Lengeling for never giving up on me throughout the past four years of great supervision with persistency and patience. Special thanks as well to my previous supervisor, Dr. Arvind Mahajan for his help and guidance during my first year in Edinburgh.

To the Malaysian Ministry of Higher Education and Universiti Putra Malaysia, thank you for funding my studies and accomodating the needs while my family and I were in Edinburgh. Not to forget my superiors and colleagues back home in Malaysia at the Faculty of Veterinary Medicine, UPM, thank you for the continuous trust, support and assistance provided.

A very special thank you to Edith Paxton, who not only taught and shared her marvellous laboratory skills, but also for her help and support throughout the past four years especially with the endless biscuit supplies in her magical drawer. Also to Sean McAteer, thank you for sharing your vast knowledge and assistance throughout the "bacteriology phase" of my work and CL3. A big thank you as well to Dr. Jo Stevens for her kindness in helping me through CL3 and the larvae infection model.

I would also like to express my appreciation to all the past and present CMG and ZAP members, thank you so much for always being there for me. To Eliza and Jo (for the sisterly advice and sharing daily Ph.D survival tips), Alex (for all the bovine terminal rectal samples and for always initiating wonderful critical discussion on anything), Sam (for sharing with me the protocols, syringes and everything larvae and beyond), Amin (for all the serious discussions on life and help with cryosection immunostainings and fluorescence microscopy) and Geoffrey (for being a great friend and sharing my ups and downs in the lab). Most of my final year work followed up from the findings of Kirsty Hughes' Ph.D findings, thank you for supplying me with bovine terminal rectal mucus and your protocols. To the tea timers especially Marie O' Shea, LBEP group, Hazel and Louise, a big warm thank you to all of you for making it bearable for me to overcome the hurdles for the past 4 years!

To Xiao Ying, Zeenath, Janice, Bushra and all my fellow Malaysian friends over here in the Roslin Institute; Nadot, Hamimah, Fahmi, Boon Chin, CK and Zen, thank you for the support and shoulders to cry on. To my mum and dad, brothers, sisters and all the in-laws, thank you for always keeping me in your prayers and providing me with endless help and support, emotionally and financially!

Lastly, this work is dedicated to the most patient, kind, understanding, supportive and tolerant husband in the world, Fazlan, and to my son Faris, for cheering mummy up with your cheekiness and keeping up with mummy's non-sensical rantings throughout the first three years of your life. I love both of you so much!

Table of Contents

Author's Declaration	2
Abbreviations	3
Acknowledgements	6
List of Figures	14
List of Tables	19
Abstract	21
Lay Summary	21
Chapter 1: Introduction	23
1.1 <i>Escherichia coli</i> (<i>E. coli</i>)	24
1.2 Pathogenic <i>E. coli</i>	25
1.3 EHEC as an emerging public health concern	25
1.4 Reservoir and transmission of EHEC to humans	26
1.5 Examples of EHEC O157:H7 outbreaks	28
1.6 EHEC O157:H7 Prevalence in Scotland	29
1.7 Virulence factors of EHEC O157:H7	30
1.7.1 Shiga toxin	33
1.7.1.1 The discovery of Shiga toxin (Stx).....	33
1.7.1.2 Shiga toxin-encoding bacteriophages.....	33
1.7.1.3 Shiga toxin expression	37
1.7.1.4 The structure of Shiga toxin.....	40
1.7.1.5 Globotriaosylceramide (Gb3) as the receptor for Shiga toxins.....	42
1.7.1.6 Shiga toxin internalisation by eukaryotic cells via retrograde transport.....	45
1.7.1.7 Shiga toxin early interaction with and translocation across epithelial monolayers.....	46
1.7.1.8 Shiga toxin in EHEC O157:H7 pathogenesis	48
1.7.2 Type three secretion system (T3SS)	52
1.7.3 Other bacterial factors involved in adherence	57
1.7.4 Plasmid encoding virulence factors	58
1.8 Diagnosis of EHEC infection	59
1.9 Aims of the thesis	60
1.9.1 Shiga toxin in EHEC O157:H7 colonisation of the intestine	60

1.9.2 Shiga toxin-encoding bacteriophages and EHEC O157:H7	
colonisation of the intestine	61
Chapter 2:	64
<i>Assessing the significance of Shiga toxin interaction(s) with Gb3 at the bovine</i>	
<i>intestinal epithelium during EHEC O157:H7 colonisation</i>	64
Chapter 2	65
Introduction.....	65
2.1 Gb3 distribution in humans and cattle	66
2.2 Gb3 as a determinant for Stx cytotoxicity	67
2.3 The mechanism of actions of Stx-induced cytotoxicity	68
2.4 Stx and intestinal epithelial cell proliferation	72
Chapter 2	76
Materials and methods.....	76
2.1 Routine cell culture techniques.....	77
2.2 Vero cells	78
2.3 Caco-2 cells	78
2.4 T84 cells.....	78
2.5 HeLa cells	78
2.6 EBL cells.....	79
2.7 Chinese Hamster Ovary (CHO)-K1 cells.....	79
2.8 Bovine primary terminal rectal cell culture	79
2.9 Shiga toxin	81
2.10 Shiga toxin cytotoxicity assay	81
2.11 Flow cytometry	83
2.11.1 Flow cytometry buffer	83
2.11.2 Immuno-staining.....	83
2.11.3 Data acquisition and analyses	84
2.12 Tissue section harvest and cryosection production	87
2.13 Immuno-fluorescent staining of bovine cryo-sections	88
2.14 Haematoxylin and Eosin staining of cryo-sections.....	91
2.15 Stx and cell cycle/proliferation.....	91
2.15.1 DNA staining solution	91

2.15.2 Cell counting and fixation.....	91
2.15.3 Shiga toxin cell stimulation	92
2.15.4 DNA staining and flow cytometry	92
2.15.5 Data acquisition and DNA content analysis by flow cytometry	93
2.15.6 Detection of proliferating cells.....	95
Chapter 2	96
Results	96
2.1 Gb3 expression on different immortalised cell lines	97
2.2 Sensitivity of different immortalised cell lines towards Shiga toxins	99
2.3 Gb3 expression by cells of the bovine primary terminal rectal culture	
.....	103
2.4 Gb3 detection on bovine cryosections	105
2.4.1 Gb3 and Pancytokeratin co-staining.....	105
2.4.3 Gb3 and Major Histocompatibility Class II (MHC II) co-staining ...	113
2.5 The effect of Stx on intestinal epithelial cell cycle and proliferation	
.....	116
Chapter 2	119
Discussion	119
2.1 Gb3 expression in continuous cell lines	121
2.2 Gb3 expression at the bovine terminal rectum	123
2.3 Shiga toxin and epithelial cell cycle/proliferation	125
Chapter 3	128
<i>Assessing immuno-modulation by Shiga toxin at the follicle-associated</i>	
<i>epithelial mucosa during EHEC O157:H7 colonisation of the bovine intestine</i>	128
Chapter 3	129
Introduction.....	129
(i) Analysis of the effects of Shiga toxin 2 on the immune cell composition of	
the bovine terminal rectum mucosa during EHEC O157:H7 colonisation.....	Error!
Bookmark not defined.	
3.1 Overview of the rectum.....	130
3.2 Gut-associated lymphoid tissue (GALT)	131

3.3 Recto-anal mucosal associated lymphoid tissue (RAMALT)	131
3.4 Leukocyte composition of the GALT	134
3.5 T helper lymphocyte (CD3+/CD4+)	137
3.5.1 Th1 response.....	137
3.5.2 Th2 response.....	138
3.6 T cytotoxic lymphocyte (CD3+/CD8+).....	138
3.7 Natural Killer cell (CD16+/NKp46+)	139
3.8 T Gamma Delta cell (CD3+/ $\gamma\delta$ +)	140
3.9 B lymphocytes (CD21+).....	142
3.10 Monocytes and macrophages (Signal Regulatory Protein-alpha, SiRP- α or SiRP-1 α +)	142
3.11 Interaction of bacterial pathogens with the follicle-associated- epithelium (FAE).....	143
3.12 Shiga toxin and host immunomodulation	146
3.13 Interferon-gamma (IFN- γ) and EHEC O157:H7 colonisation	148
3.14 IFN- γ and epithelial cell proliferation/cell cycle	150
Chapter 3	152
Materials and methods	152
3.1 Harvest of terminal rectal mucosal cells.....	153
3.2 Immunostaining bovine terminal rectal mucosal cells for flow cytometry	155
3.3 Flow cytometry data acquisition and analyses	156
3.4 Measurement of IFN- γ levels released by bovine terminal rectal mucosal cells.....	159
3.5 Interferon- γ stimulation of intestinal epithelial cell lines.....	159
3.6 Cell fixation for propidium iodide staining of DNA	160
3.7 DNA staining by propidium iodide for flow cytometry analysis	160
3.8 Data acquisition and DNA content analysis by flow cytometry	161
3.9 Detection of proliferating cells.....	161
3.10 Caco-2 cell stimulation with purified Shiga toxin 2 or culture supernatants from Stx-producing strains and IFN- γ	161
3.11 Cell lysate collection and storage	162
3.12 Estimation of total protein content in cell lysate	163

3.13 Separation of protein bands by Sodium Dodecyl Sulfate- Polyacrylamide Electrophoresis (SDS-PAGE)	164
3.14 Semi-dry membrane transfer of proteins from SDS-PAGE gel to nitrocellulose membrane	164
3.15 Immuno-staining of proteins on nitrocellulose membrane	165
3.16 Protein band detection	165
3.17 Nitrocellulose membrane reprobing	166
Chapter 3	167
Results	167
3.1 Immuno-phenotyping select mucosal terminal rectal cells	168
3.2 ELISA measurement of IFN- γ release by cultured terminal rectum mucosal cells	178
3.3 The effect of Interferon- γ on the cell cycle of epithelial cell lines	180
3.4 The effect of Shiga toxin on IFN- γ -activated JAK/STAT1 pathway ...	186
Chapter 3	192
Discussion	192
3.1 Cell surface marker expression and Interferon-gamma (IFN- γ) quantified from cells harvested from the bovine terminal rectal mucosa	193
3.2 The effect of IFN- γ on epithelial cell proliferation	197
3.3 Shiga toxin and IFN- γ influence on epithelial signalling of the JAK/STAT1 pathway	197
Conclusion	198
Chapter 4: <i>Shiga toxin-encoding bacteriophages and EHEC O157:H7</i> <i>colonisation of the bovine intestine</i>	200
Chapter 4	201
Introduction.....	201
4.1 Shiga toxin production and cytotoxicity of bovine and human associated EHEC O157:H7 strains	206
4.2 The growth and fitness of EHEC O157:H7 in bovine terminal rectal mucus	207
4.3 The binding capacity of EHEC O157:H7 strains possessing different Stx-prophages	208

4.4 Assessing the effect of Stx-prophages on the virulence of EHEC O157:H7 in a <i>Galleria mellonella</i> infection model.....	209
Chapter 4	211
Materials and Methods.....	211
4.1 Production of culture supernatants.....	214
4.2 Shiga toxin ELISA	215
4.3 Verocytotoxicity assay.....	216
4.4 Growth competition assay.....	217
4.5 Bacterial adherence assay.....	218
4.6 Immunofluorescence staining for H7 and EspA (T3SS effectors)	220
4.7 Western blotting for H7 and EspD (T3SS effectors)	220
4.8 <i>Galleria mellonella</i> larvae killing assay	222
Chapter 4	224
Results	224
4.1 Shiga toxin levels detected by ELISA from different growth conditions	225
4.1.1 Bovine-isolated strains.....	225
4.1.2 Comparison of Stx production between bovine and human-isolated strains.....	227
4.2 Verocytotoxicity assay.....	229
4.2.1 EHEC O157:H7 strains grown in 10% bovine terminal rectal mucus	229
4.2.2 Toxicity assays for EHEC O157:H7 strains cultured in lysogeny broth (LB).....	232
4.2.3 Toxicity of EHEC O157:H7 strains cultured in lysogeny broth (LB) supplemented with Mitomycin C (MMC)	234
4.2.4 Verocytotoxicity levels of bovine and human strains of EHEC O157:H7 in lysogeny broth (LB) under non-induced and induced culture conditions	236
4.3 Growth Competition Assay.....	239
4.3.1 Pairwise comparison of <i>E. coli</i> strains in 10% bovine terminal rectal mucus (BTRM).....	239
4.3.1.1 <i>E. coli</i> MG1655NK and <i>E. coli</i> K-12-Sp5 stx2A::kan (K-12-Sp5).....	239

4.3.1.2 <i>E. coli</i> MG1655NK and <i>E. coli</i> K-12-Sp5 <i>stx2A::kan ΔlacZ</i> (K-12-Sp5)	239
4.3.1.3 EHEC O157:H7 Sakai <i>stx2A::kan</i> and EHEC O157:H7 SakaiΔSp5	243
4.3.1.4 EHEC O157:H7 Strain 9000 and EHEC O157:H7 Strain 10671	243
4.3.1.5 EHEC O157:H7 Strain 9000 and EHEC O157:H7 Strain 9000ΔΦStx2a/ΦStx2c	244
4.4 Bacterial adherence to epithelial cells	248
4.4.1 Bovine EHEC O157:H7 strains binding to HeLa cells	248
4.4.2 Bovine EHEC O157:H7 strains binding to EBL cells	248
4.5 Expression of H7 and EspA (Type Three Secretion) in 10% bovine terminal rectal mucus (BTRM)	251
4.6 <i>Galleria mellonella</i> larvae survival upon EHEC O157:H7 challenge	256
4.6.1 EHEC O157:H7 Strain 9000 and isogenic Stx2-phage mutants	256
4.6.2 EHEC O157:H7 Strain 10671 and Strain 10671ΔΦStx2c	256
4.6.3 EHEC O157:H7 Sakai and Sakai ΔSp5	257
Chapter 4	260
Discussion	260
4.1 Shiga toxin production and potency on Vero cells	262
4.2 Growth of EHEC O157:H7 in competitive environments	264
4.3 EHEC O157:H7 adherence to epithelial cell lines	267
4.4 Assessing virulence between different EHEC O157:H7 strains in <i>Galleria mellonella</i> larvae infection model	269
4.5 Conclusion	271
Chapter 5	273
General Discussion and Conclusion	273
General Discussion	274
Conclusion	281
References	284
Appendix	326

List of Figures

CHAPTER 1

INTRODUCTION

Figure 1.1 The evolution of EHEC O157 in the UK.....	32
Fig. 1.2 Different phases in the life of a phage.....	36
Fig. 1.3 The transcription of <i>stx1</i> and <i>stx2</i> genes.....	39
Fig. 1.4 Phage-mediated expression of the <i>stx2</i> genes.....	39
Fig. 1.5 The ribbon diagram illustrating the crystal structure of Shiga toxin 1.....	41
Fig. 1.6 The structure of globotriaosylceramide, Gb3.....	44
Fig. 1.7 The synthesis pathway of Gb3.....	44
Fig. 1.8 Schematic diagram of the type three secretion system of EHEC O157:H7.....	56

CHAPTER 2

INTRODUCTION

Fig. 2.1 The cell cycle regulation.....	71
Fig. 2.2 Components of the proliferative-differentiative crypt-luminal axis of the colon epithelium.....	74

MATERIALS AND METHODS

Fig. 2.1 Histogram of propidium iodide staining detected by FL-2 corresponding to total DNA content in different phases of the cell cycle in ethanol-fixed cells..	94
Fig. 2.2 Dot plot of propidium iodide fluorescence detected by FL-2 to distinguish single cells from cellular aggregate and debris.....	94

RESULTS

Fig. 2.1 Histograms and mean of fluorescence intensity (MFI) of Gb3 surface expression of different cell lines.....	98
Fig. 2.2 Shiga toxin cytotoxicity plates of immortalised cell lines with different Gb3 surface expression.....	101

Fig. 2.3 Flow cytometry results for Gb3, pancytokeratin and vimentin on bovine primary terminal rectal cells.....	104
Fig. 2.4 Bovine nasal associated lymphoid tissue (NALT) cryosections stained for Gb3 and pancytokeratin.....	107
Fig. 2.5 Bovine colon cryosections stained for Gb3 and pancytokeratin.....	108
Fig. 2.6 Bovine terminal rectal mucosa cryosections stained for Gb3 and pancytokeratin.....	109
Fig. 2.7 Bovine colon cryosections stained for Gb3 and vimentin.....	111
Fig. 2.8 Bovine terminal rectal mucosa cryosections stained for Gb3 and vimentin	112
Fig. 2.9 Bovine colon cryosections stained for Gb3 and major histocompatibility complex class II (MHC II).....	114
Fig. 2.10 Bovine terminal rectal mucosa cryosections stained for Gb3 and major histocompatibility complex class II (MHC II).....	115
Fig. 2.11 DNA staining profile with propidium iodide of cells treated with purified Stx2.....	117
Fig. 2.12 Proliferation cellular nuclear antigen staining of purified Stx2-treated Caco-2 and T84 cells.....	118

CHAPTER 3

INTRODUCTION

Fig. 3.1 The bovine terminal rectal mucosa.....	133
Fig. 3.2 Lymphocytes associated with the lymphoid follicles of the bovine terminal rectal mucosa.....	136

RESULTS

Fig. 3.1 Flow cytometry dot plots of CD3+/CD4+ cells detected from EHEC O157:H7-challenged and unchallenged calves.....	170
Fig. 3.2 Flow cytometry dot plots of CD3+/CD8+ cells detected from EHEC O157:H7-challenged and unchallenged calves.....	171
Fig. 3.3 Flow cytometry dot plots of CD3+/ $\gamma\delta$ + cells detected from EHEC O157:H7-challenged and unchallenged calves.....	172

Fig. 3.4 Flow cytometry dot plots of CD16+/NKp46+ cells detected from EHEC O157:H7-challenged and unchallenged calves.....	173
Fig. 3.5 Flow cytometry dot plots of CD21+ cells detected from EHEC O157:H7-challenged and unchallenged calves.....	174
Fig. 3.6 Flow cytometry dot plots of SiRP- α + cells detected from EHEC O157:H7-challenged and unchallenged calves.....	175
Fig. 3.7 IFN- γ released by bovine terminal rectal cells quantified by ELISA...	179
Fig. 3.8 DNA staining profile with propidium iodide of cells treated with IFN- γ	182
Fig. 3.9 Proliferation cellular nuclear antigen staining of IFN- γ -treated Caco-2 and T84 cells.....	183
Fig. 3.10 Western blot radiograph of lysates from purified Stx2 and IFN- γ -stimulated Caco-2 cells.....	188
Fig. 3.11 Western blot results of Caco-2 cell lysates stimulated with culture supernatants of EHEC O157:H7 EDL 933 or isogenic Stx1-/Stx2- and IFN- γ (i).....	189
Fig. 3.12 Western blot results of Caco-2 cell lysates stimulated with culture supernatants of EHEC O157:H7 EDL 933 or isogenic Stx1-/Stx2- and IFN- γ (ii).....	190
Fig 3.13 Western blot results of Caco-2 cell lysates stimulated with MMC-induced culture supernatants of EHEC O157:H7 EDL 933 or isogenic Stx1-/Stx2- and IFN- γ (iii).....	191

CHAPTER 4

INTRODUCTION

Fig. 4.1 Faecal shedding of EHEC O157:H7 by experimentally infected weaned calves	204
Fig. 4.2 Alignment of the EHEC O157:H7 Strain 9000 (PT21/28) and EHEC O157:H7 Strain 10671 (PT32) genomes to EHEC O157:H7 EC4115 (Φ Stx2a+/ Φ Stx2c+).....	205

RESULTS

Fig. 4.1 Stx production by EHEC O157:H7 in different culture media (bovine-isolated strains)	226
Fig. 4.2 Stx production by EHEC O157:H7 in different culture media (bovine-isolated compared with human-isolated strains).....	228
Fig. 4.3 The toxicity of mucus-cultured EHEC O157:H7 filtered supernatants to Vero cells.....	231
Fig. 4.4 The toxicity of LB-cultured EHEC O157:H7 filtered supernatants to Vero cells.....	233
Fig. 4.5 The toxicity of MMC-induced LB-cultured EHEC O157:H7 filtered supernatants to Vero cells.....	235
Fig. 4.6 Comparison of the toxicity of bovine and human isolated EHEC O157:H7 strains to Vero cells.....	238
Fig. 4.7 Competitive growth assay results between <i>E. coli</i> MG1655NK and <i>E. coli</i> K-12-Sp5 in 10% BTRM.....	241
Fig. 4.8 Competitive growth assay results between <i>E. coli</i> MG1655NK and <i>E. coli</i> K-12-Sp5 <i>stx2A::kan ΔlacZ</i> (<i>E. coli</i> K-12-Sp5) in 10% BTRM.....	242
Fig. 4.9 Competitive growth assay results between EHEC O157:H7 Sakai <i>stx2A::kan</i> and Sakai Δ Sp5 in 10% BTRM.....	245
Fig. 4.10 Competitive growth assay results between EHEC O157:H7 Strain 9000 and EHEC O157:H7 Strain 10671 in 10% BTRM.....	246
Fig. 4.11 Competitive growth assay results between EHEC O157:H7 Strain 9000 and EHEC O157:H7 Strain 9000 $\Delta\Phi$ Stx2a/ Φ Stx2c in 10% BTRM.....	247
Fig. 4.12 EHEC O157:H7 adherence to HeLa cells.....	249
Fig. 4.13 EHEC O157:H7 adherence to EBL cells.....	250
Fig. 4.14 H7 expression in mucus-cultured bovine strains of EHEC O157:H7 examined by fluorescence microscopy.....	252
Fig. 4.15 EspA expression in mucus-cultured bovine strains of EHEC O157:H7 examined by fluorescence microscopy.....	253
Fig. 4.16 Western blot of bacterial cytosolic lysate grown in 10% BTRM.....	254
Fig. 4.17 Western blot of bacterial cytosolic lysate grown under T3SS conditions	255

Fig. 4.18 Survival of <i>G. mellonella</i> larvae challenged with EHEC O157:H7 Strain 9000 strains.....	258
Fig. 4.19 Survival of <i>G. mellonella</i> larvae challenged with EHEC O157:H7 Strain 10671 strains.....	258
Fig. 4.20 Survival of <i>G. mellonella</i> larvae challenged with EHEC O157:H7 Sakai strains	259

List of Tables

CHAPTER 2

MATERIALS AND METHODS

Table 2.1 List of antibodies for Gb3 detection by flow cytometry.....86

Table 2.2 List of antibodies for Gb3 and cell lineage marker detection by fluorescence microscopy.....90

CHAPTER 3

MATERIALS AND METHODS

Table 3.1 List of primary and secondary antibodies used to stain lymphocytes and macrophages/monocytes harvested from bovine terminal rectum.....157

RESULTS

Table 3.1 Statistical analysis of bovine terminal rectal cells immune-labelled and detected for different cell surface marker combination by flow cytometry.....176

Table 3.2 Statistical analysis of CD3+/CD4+ flow cytometry data.....177

Table 3.3 Statistical analysis of DNA staining profile for Caco-2 cells stimulated with IFN- γ184

Table 3.4 Statistical analysis of DNA staining profile for T84 cells stimulated with IFN- γ185

CHAPTER 4

MATERIALS AND METHODS

Table 4.1 List of bacterial strains used in this study.....212

RESULTS

Table 4.1 Statistical analysis of data from competitive growth assay between *E. coli* MG1655NK and *E. coli* K-12-Sp5 in 10% BTRM.....241

Table 4.2 Statistical analysis of data from competitive growth assay between *E. coli* MG1655NK and *E. coli* K-12-Sp5 *stx2A::kan Δ lacZ* (*E. coli* K-12-Sp5) in 10% BTRM.....242

Table 4.3 Statistical analysis of data from competitive growth assay between EHEC O157:H7 Sakai <i>stx2A::kan</i> and Sakai Δ Sp5 in 10% BTRM.....	245
Table 4.4 Statistical analysis of data from competitive growth assay between EHEC O157:H7 Strain 9000 and EHEC O157:H7 Strain 10671 in 10% BTRM.....	246
Table 4.5 Statistical analysis of data from competitive growth assay between EHEC O157:H7 Strain 9000 and EHEC O157:H7 Strain 9000 Δ Φ Stx2a/ Φ Stx2c in 10% BTRM.....	247

Abstract

Shiga toxin (Stx) is a bacteriophage (phage)-encoded virulence factor of the Enterohaemorrhagic *Escherichia coli* (EHEC) O157:H7 implicated in the pathogenesis of renal tissue damage and bloody diarrhoea in human. Cattle are the main asymptomatic reservoir for EHEC O157:H7 with the lymphoid-follicle rich areas of the terminal rectum identified as the primary colonisation site. However, the significance of Stx during bovine intestinal colonisation by EHEC O157:H7 remains unclear with mixed findings described in published studies. The objective of this study was to investigate if Stx and the Stx-encoding phage significantly contribute to EHEC O157:H7 colonisation particularly at the bovine terminal rectum. The expression of Stx receptor, Globotriaosylceramide (Gb3) at the bovine terminal rectum was analysed by fluorescence microscopy, revealing a similar pattern of Gb3 detection in the bovine colon with scattered positive detections limited to sub-epithelial, mesenchymal-associated cells. Purified Stx2 treatment of Gb3+ and Gb3- epithelial cell lines for 6 to 18 hours produced no effect on the cell cycle and proliferation. CD3+/CD8+, CD3+/ $\gamma\delta$ + and CD21+ cells were significantly different between calves infected with EHEC O157:H7 Strain 9000 (Stx2a+/Stx2c+) and the uninfected calves, but not in calves with Strain 10671 (Stx2c+). Stx did not interfere with IFN- γ -activation of the JAK/STAT1 pathway in epithelial cells. Bovine EHEC O157:H7 strains isolated from Scottish cattle farms in the IPRAVE study (Phage type 21/28 and 32) were used for a series of bacterial phenotypic characterisation assays. Total Stx production, Verocytotoxicity, growth in a competitive environment, epithelial cell adherence and *Galleria mellonella* virulence assay were performed to compare the IPRAVE EHEC O157:H7 strains (PT21/28 and PT32) and the isogenic Stx-phage mutants. Stx levels produced by the bovine-originated EHEC O157:H7 strains were significantly lower than that of the human isolated strains. The absence of Gb3 on the bovine terminal rectal epithelium, the non-significant changes in the cell cycle along with the uninterrupted IFN- γ activation of the JAK/STAT1 pathway in intestinal epithelial cells and the minute quantities of Stx generated by EHEC O157:H7 bovine strains suggest that the toxin is not involved in colonisation directly, at least at the intestinal epithelial level. Although future work is required to explain the mechanisms underlying the observed EHEC O157:H7 phenotypic changes particularly in the Stx-phage mutant strains, the work done has proven that the Stx-encoding phage indeed has the ability to exert changes in the bacterial cell leading to changes in bacterial phenotypes, which in turn, might affect the colonisation of the bovine intestine.

Lay Summary

Enterohaemorrhagic *Escherichia coli* O157:H7 (EHEC O157:H7) infection in human is associated with symptoms ranging from mild, watery to bloody diarrhoea accompanied with complications resulting in the loss of kidney functions that could end up being fatal. EHEC O157:H7 resides in the bovine intestine specifically at the terminal rectum and transmission to human is mainly through the food chain. EHEC O157:H7 carries genes of bacterial viruses (termed bacteriophage) enabling the bacteria to produce Shiga toxin (Stx). Stx is the major factor related to the more severe symptoms mentioned. Despite being colonised, cattle remain healthy and act as the source of bacterial cells propagated within the environment. This study aims to investigate how Stx and the Stx-bacteriophages could potentially influence EHEC O157:H7 colonisation at the bovine intestine. The bovine terminal rectum was microscopically examined for the presence of the Stx receptor, Globotriaosylceramide (Gb3). Gb3 was not detected on the cells lining the terminal rectum of cattle. *In vitro* assays testing the effects of Stx on epithelial cell lines proliferation and a vital pathway inside epithelial cells involved in initiating cellular defense against bacterial pathogens did not support the idea for a role for Stx during intestinal colonisation. The total production of Stx and toxicity on Vero cells (Stx-sensitive cells), the competitive growth ability, the capacity to bind to epithelial cell lines and the ability to kill *Galleria mellonella* larvae were compared between the EHEC O157:H7 bovine strains possessing and not (mutant strains unable to produce toxin) possessing the Stx-bacteriophages. Differences were observed as a result of not possessing the Stx-bacteriophages suggesting that the viruses could potentially control the behaviour of the bacteria which may be important during EHEC O157:H7 intestinal colonisation. Interestingly, EHEC O157:H7 strains isolated from cattle produced significantly lower levels of Stx than the human originated EHEC O157:H7 strains. In conclusion, direct involvement of Stx in bacterial colonisation of the bovine terminal rectal cells was not observed, while Stx-bacteriophages did affect certain bacterial traits commonly associated with colonisation. Future study is required to explain the underlying mechanisms of how the Stx-bacteriophages work in influencing the bacteria to behave differently in the presence of different type of Stx-bacteriophage(s).

Chapter 1: Introduction

1.1 *Escherichia coli* (*E. coli*)

Escherichia coli is a diverse species of Gram negative, facultative anaerobic bacteria that was discovered back in 1885 by a German-Austrian paediatrician, Theodor Escherich. He was investigating gastrointestinal infection in children when he came across rod-shaped, fast growing bacteria which he named *Bacillus communis coli* in the faeces of young patients. After his death, the bacterium name was changed to *Escherichia coli* (*E. coli*), to honour his discovery [1].

A single *E. coli* cell is about 0.5 μm in width and up to 2 μm in length. As with other Gram negative bacteria, the outer membrane layer and inner cytoplasmic membrane are separated by a thin peptidoglycan wall (maximum 4 nm) [2]. The peptidoglycan wall of *E. coli* normally maintains a cylindrical shape during exponential growth, while in the stationary phase it changes into a more spherical shape [3, 4]. Serotyping is commonly carried out based on the 'O' antigen that is part of the outer membrane lipopolysaccharide (LPS) and flagellar (H) antigens, while sometimes the capsular (K) and fimbrial (F) antigens are also used to type the strains.

E. coli constitute a minor part of the microbiota along the intestinal tract in mammals and reptiles, and can contribute to the host's resistance to colonisation by incoming pathogens by physically competing for attachment sites on intestinal cells as well as producing bacteriocins. In humans, *E. coli* normally resides within the thick mucus layer of the large intestinal tract, particularly the caecum and colon with approximately 10^7 - 10^9 colony-forming unit (C.F.U.) of *E. coli* present per gram of faeces. The thick mucus layer covering the large intestinal epithelium serves as the nutritional ecological niche, primarily providing gluconate and other mucus-derived sugars to the commensal *E. coli* [5]. In the early hours after birth, *E. coli* are among the first bacteria found to colonise the intestine of newborns, mainly as a result of exposure to maternal faecal bacteria and nurses based at the maternity wards [6, 7]. The population continues to grow until 2 years of age, when it starts to stabilise at 10^8 C.F.U. per gram and then declines as individuals age [8, 9].

1.2 Pathogenic *E. coli*

E. coli can become opportunistic pathogens under certain circumstances such as in immunocompromised hosts or when the intestinal wall becomes perforated, exposing the normally 'sterile' parts of the abdomen to the intestinal contents. A subset of *E. coli* strains are considered pathogenic and these are associated with different types of diseases, sometimes referred to as intestinal or extra-intestinal, depending on the site of infection. Findings of phylogenetic analyses indicate that lateral transfer and acquisition of mobile genetic elements including plasmids and prophages encoding for virulence and colonisation factors or the loss of other sets of genomes to adapt to the colonisation niche in the host are associated with the evolution of *E. coli* pathotypes [10, 11]. Key pathotypes of intestinal *E. coli* include: Enterohaemorrhagic *E. coli* (EHEC) associated with bloody diarrhoea and severe complications including kidney failure [12], Enteropathogenic *E. coli* (EPEC) known for causing watery diarrhoea [13], Enterotoxigenic *E. coli* (ETEC) leading to profuse watery diarrhoea in children predominately an issue in underdeveloped countries [14], Enteroaggregative *E. coli* (EAEC) recently identified as an emerging cause of persistent diarrhoea in malnourished or immunosuppressed children [15], Enteroinvasive *E. coli* (EIEC) causing acute ulcerative intestinal infections [16] and the Diffusively adherent *E. coli* (DAEC) that has the characteristic of diffusive adherence to intestinal epithelium [17]. While Uropathogenic *E. coli* (UPEC) and the sepsis, meningitis-associated *E. coli* (MNEC) are two of the pathotypes involved in infection at extra-intestinal sites [18].

1.3 EHEC as an emerging public health concern

EHEC have been increasingly recognised as an emerging group of enteric pathogens implicated in diseases of humans [19, 20]. Of particular interest is EHEC O157:H7, the most common serotype associated with human cases in Great Britain [21] and is the focus of my thesis. Infection can result in mild to bloody diarrhoea (haemorrhagic colitis) accompanied by severe abdominal cramps which can progress to haemolytic uraemic syndrome (HUS) which is the leading cause of kidney failure in paediatric cases and occurs in about ten to fifteen percent of human EHEC

infections [12, 22]. The incubation period can range between three to eight days, and most patients recover within ten days. However, those that do not recover can progressively deteriorate into HUS defined by a triad of symptoms (haemolysis, anaemia and thrombocytopenia) which could potentially lead to acute kidney failure especially in children [23]. The production and activity of Shiga toxin (Stx), a bacteriophage-encoded virulence factor is implicated in the more severe disease manifestations mentioned and is also the main subject of this thesis (a more in-depth review of Shiga toxin will be discussed later in section 1.7.1). Most individuals without underlying disease or immunosuppression will recover following the course of the disease, while in some other patients, severe renal tissue damage requires the patients to rely on lifetime supportive therapy mainly by dialysis and even blood transfusions [24]. About 90% of HUS cases in Scotland are associated with EHEC O157:H7 infection [25, 26]. EHEC are considered to have a low infectious dose (less than 100 C.F.U.), and possess an array of virulence factors that can lead to this serious and sometimes fatal infection. The lack of preventive measures to limit infections and sole reliance on supportive therapy in human patients means that this *E. coli* pathotype is of high public health importance in particular in countries experiencing outbreaks. These include many countries in the developed world and there is little data available with regard to EHEC epidemiology in many developing countries (further described below in sections 1.5 and 1.6).

1.4 Reservoir and transmission of EHEC to humans

EHEC O157:H7 resides in the intestinal tract of healthy ruminants primarily cattle and to a lesser extent in sheep and goats [27, 28]. A national survey between January 1999 to January 2000 on EHEC O157:H7 prevalence in faeces at slaughter across Great Britain indicated that the annual prevalence was higher in cattle than sheep (4.7% and 1.7% respectively) [29]. The prevalence is even higher in the United States, with 28% of cattle found to be shedding EHEC O157:H7 [30]. Despite being colonised, cattle remain asymptomatic, with the exception of infected newborn calves or immunosuppressed animals [31, 32]. Naylor et al. proposed that the bovine terminal rectum, located from 0-15cm from the recto-anal junction is the principal colonisation site of EHEC O157:H7 in cattle [33]. EHEC O157:H7 tropism towards

the terminal rectum in its bovine host has yet to be fully understood although nutrient factors and adaptation to the environment within the rectal niche are thought to partly explain the affinity to the site. *E. coli*, as any other enteric bacteria, rely heavily on glycogen for internal storage of carbon and energy, with the inability to metabolise internal glycogen directly linked to poor colonisation [34]. As nutrient availability in the large intestine is limited, EHEC O157:H7 and other bacterial strains residing in the rectum are forced to adopt strategies to compete for nutrient and energy. One proposed strategy is that the bacterial strains living within a niche in close proximity may require and utilise different types of nutrients [35]. Additionally, *E. coli* do not produce polysaccharide hydrolase for digestion of complex sugars from mucin (large glycoprotein components of mucus) forcing them to rely on free fragments of monosaccharides and disaccharides, e.g. fucose, released from digestion by hydrolase-producing anaerobic bacterial species (e.g. *Bacteroides thetaiotaomicron*) residing in the same niche as *E. coli* [5, 36]. EHEC O157:H7 may also be more efficient in nutrient utilization than the surrounding commensal or competing strains at the rectum, as previously described for the growth of EHEC O157 strain EDL 933 in bovine small intestinal content, which coincided with stronger induction of genes required for enzymatic degradation of the sugars in EDL 933 than the commensal *E. coli* [37, 38]. The rectum also has relatively lower levels of acetate compared to the anterior parts of the bovine gut. Acetate is a short fatty acid known to inhibit the expression of the locus of enterocyte effacement (LEE) operon encoding the components of a type three secretion system (T3SS; refer below in section 1.7.2). Therefore it may be that the lower levels of acetate at the rectum, rather than the rest of the bovine gut, provides a less restrictive environment for EHEC to express the T3SS leading to stronger adherence at the rectal site [39, 40].

Transmission to humans is via the faecal-oral route, often associated with direct or indirect contact with contaminated faeces [21, 41]. Farm, domestic and wild animals have all been linked to transmission and outbreaks [27, 42]. This also includes visit to petting zoos which has been shown to be related to EHEC O157:H7 infections particularly among children [43]. Apart from contact with contaminated cattle-related products, outbreaks could also be as a result of consuming water,

unpasteurised fruit juice and vegetables contaminated with ruminant faeces [44-47]. Environmental exposure to the bacteria is also another risk factor and mode of transmission [48]. Person-to-person transmission has also been observed, with approximately 20% of outbreaks in Britain, Canada, Ireland, Japan, USA and Scandinavia shown to involve some secondary transmission, with shedding from infected humans lasting for two to three weeks [49].

1.5 Examples of EHEC O157:H7 outbreaks

The first series of outbreak that lead to the recognition of EHEC O157:H7 as a human pathogen occurred in the United States from February through March and May to June, 1982 [50]. A total of forty seven people dining at the restaurants of the same fast food chain in Oregon and Michigan were affected with severe crampy abdominal pain, accompanied with watery diarrhoea that progressed into bloody diarrhoea and the absence of fever. Examination of nine out of twelve stool samples identified for the presence of a non-invasive and non-enterotoxigenic *E. coli* O157:H7, which was considered as a 'rare' serotype to be isolated during that time. This bacterial strain was also isolated from beef patty sampled from the restaurant in Michigan [51]. In 1993, another large outbreak involving a fast food chain of restaurants occurred, this time around seven hundred individuals experienced severe abdominal pains and bloody diarrhoea, four children died and a high percentage of individuals developed HUS [52]. The 1993 multistate outbreak was traced back to undercooked hamburgers served in the restaurants, and EHEC O157 was isolated from patients and frozen beef patties [53]. In the UK, the first EHEC O157:H7 outbreak was thought to have occurred in 1983 in the Wolverhampton area and it was reported to have been associated with an increase in incidence of HUS in children [54]. Another large outbreak involving more than a hundred individuals occurred in West Lothian in 1994 which was associated with contaminated pasteurised milk consumption, while in 1996 in central Scotland, epidemiological investigations identified meat from a butcher as the likely source for an outbreak that lead to 20 deaths, also the highest number of fatalities of all outbreaks recorded [55] until the atypical EHEC infection in North Germany in 2011 [56]. The largest EHEC O157:H7 epidemic to date occurred in July 1996 in Sakai City, Osaka, Japan

involving nearly ten thousand individuals, including several fatalities and similar disease manifestations, with contaminated white radish sprouts as the source of infection [47]. The strain isolated from this outbreak is known as EHEC O157:H7 strain Sakai and is one of the two EHEC O157:H7 strains that were fully sequenced and annotated at the turn of the millennium [57]. The other fully sequenced strain is EDL 933, the EHEC O157:H7 strain isolated from the 1982 Michigan outbreak linked to ground beef [58].

1.6 EHEC O157:H7 Prevalence in Scotland

In Scotland, the most common risk factors associated with human infection includes consumption of meat or other animal-based products and environmental exposure [41, 59]. Visit to farms, direct contact with contaminated faecal material and animal pasture used for recreational activities are among the ways humans can contract the bacteria through the environment [43]. In 2004, Health Protection Scotland and the Health Protection Agency reported that 209 out of 918 confirmed infections in Great Britain occurred in Scotland which makes the rate of infection per hundred thousand consistently higher in Scotland than most places in the rest of the world [60, 61]; other countries with relatively high rates of infections include Argentina and Ireland [62, 63].

Surveys on faecal samples obtained from Scottish farms revealed about one in five of each sampled farm were confirmed positive for EHEC O157:H7 infection [64-66]. The first study sampled 12-30 month-old beef finishing cattle around Scotland identified 7.9% prevalence of O157-shedding animals, with 22.8% of farms estimated to have at least one animal shedding [65]. Prevalence of EHEC O157:H7 was shown to be influenced by seasonality, with more faecal shedding detected during summer which corroborates with an increase in confirmed EHEC O157:H7 clinical cases [29] [67].

Faecal samples obtained at slaughter from cattle and sheep were characterised to be of Phage Type (PT) 2, 8, 21/28 and 4, 32, respectively [29]. Analysis of data

from the Scottish Executive Environment Rural Affairs Department (SEERAD) (March 1998 until May 2000) and the International Partnership Research Award in Veterinary Epidemiology (IPRAVE) (February 2002 to February 2004) identified that over 50% of the positive cattle isolates and human cases, between 1998 to 2004 were EHEC O157:H7 phage type (PT) PT 21/28. EHEC O157:H7 PT32 was detected at much lower levels in both cattle and human isolates (10% and 5%, respectively). EHEC O157:H7 PT21/28 generally contains both Stx2a and Stx2c-encoding prophages, while bovine PT32 predominately contain only a Stx2c-encoding phage. PT 21/28 is also associated with higher risk of developing HUS in Scottish children than other phage types [66, 68]. The more severe clinical outcomes have been associated with Stx2a production [69-71], with PT21/28 strains being capable of expressing this particular Stx2 variant based on the presence of *stx2a* gene (Figure 1.1).

1.7 Virulence factors of EHEC O157:H7

Sequence and trait based analyses have determined that EHEC O157:H7 has evolved from *E. coli* O55:H7, a pathogenic clone isolated from an infant with diarrhoea [72]. Chronologically, *E. coli* O55:H7 began as a *stx1+* strain, with the ability to ferment sorbitol and the presence of the Locus of Enterocyte Effacement (LEE) genes in the chromosome [73]. It then acquired genes to change the somatic 'O' antigen to O157, gained Stx2-encoding bacteriophages, a large virulence plasmid, pO157 and acquired beta (β)-glucuronidase (GUD) activity. The strain eventually loss the ability to ferment sorbitol (sor-). Analysis by pulsed-field gel electrophoresis (PFGE) identified significant diversity among the EHEC O157:H7 isolates with the existence of two distinct lineages; i) lineage I comprising EHEC O157:H7 isolated from both humans and cattle, and ii) lineage II consisting of EHEC O157:H7 isolated mostly from cattle and rarely from humans [74, 75]. Further genomic analyses suggested for the presence of another lineage termed lineage I/II or intermediate lineage, however the host ecology and associated phenotypes of isolates belonging to this lineage remains to be fully characterised [76]. Isolates clustered under lineage I are regarded as human/clinical-based associated with upregulated expression of virulence and colonisation factors and severe disease outcomes with

higher mortality rate compared to the bovine-biased isolates of lineage II [77] [11]. Virulence genes encoding for Stx1 and Stx2 were upregulated in human-isolated strains [78] and more importantly the presence or absence of the *stx2a* gene is regarded as significant determinant in explaining the differential virulence observed between human-biased and bovine-biased isolates [77]. Bovine-biased isolates were identified to contain specific genes associated with niche adaptation, for example higher resistance to acidic environment in the bovine gut, thereby facilitating the survival rate which was estimated to be better than clinical strains [11, 79]. Stx-encoding phages (described below in section 1.7.1.2) are regarded as one of the major factors introducing diversification via lateral gene transfer into the genomes of the ancestral strains leading to the emergence of pathogenic Stx-producing *E. coli* strains [74, 75, 80-82], facilitated by its abundance in the environment [83] and high resistance to disinfectants and extreme conditions (heat treatment and chlorination) [84]. Part of my thesis focuses on the impact of these Stx-encoding phages on EHEC O157:H7 colonisation which will be further explained under section 1.9 below. Much more recent and ongoing analysis of EHEC O157 evolution in the UK has a different order of evolution in relation to the Stx phage acquisition and is summarized with permission of Dr. Tim Dallman (Public Health England) in Figure 1.1.

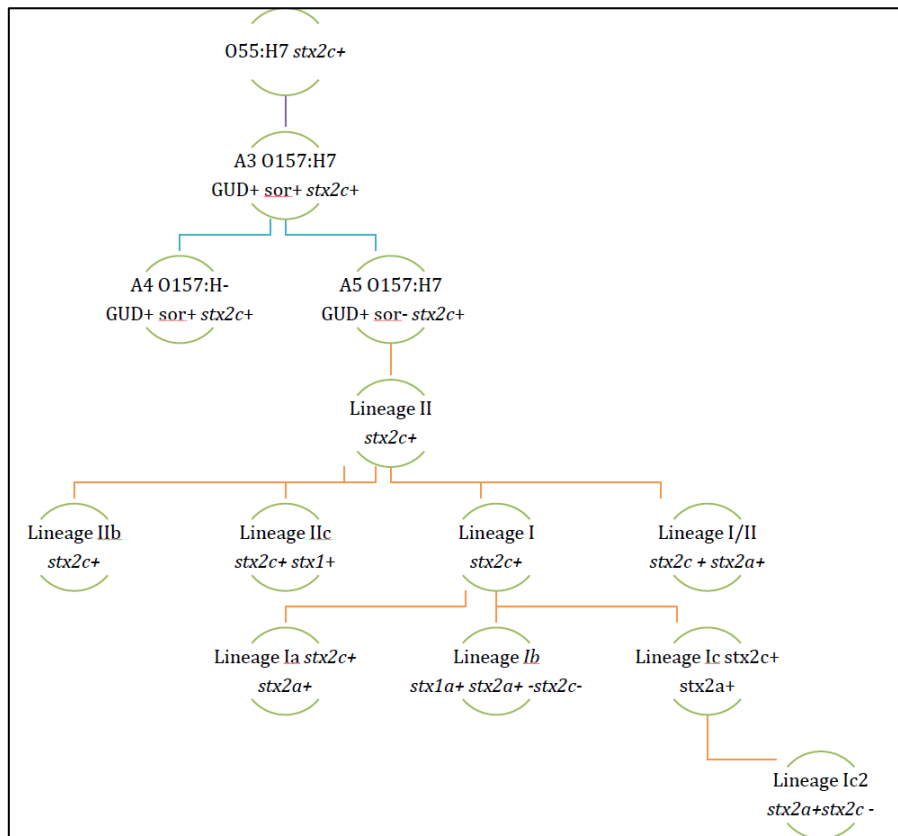


Figure 1.1 The evolution of EHEC O157 in the UK. The new evolutionary model on the origin of the current EHEC O157 strain presented was based on a phylogenetic analysis recently proposed [85]. The stepwise series of events was maintained from *stx2c+* E. coli O55 to the beta-glucuronidase (GUD) positive last common ancestor (A5) that evolved into the contemporary lineage II. Three extant lineages of Lineage II : lineage IIa (ancestral branch), IIb (*stx2c+*) and IIc (acquired *stx1*, *stx2c* retained) were identified. A *stx2c+* lineage I strain and a lineage I/II (*stx2c+* *stx2a+*) evolved from the Lineage II *stx2c+* branch (estimated to occur 125 and 95 years ago, respectively). The lineage I (*stx2c+*) strain then evolved by acquiring the *Stx2a* phage 3 times (lineage Ia, Ib and Ic). Lineage Ib acquired the *Stx1a* phage and at the same time losing the *Stx2c* phage, while the *Stx2c* phage was also removed from the lineage Ic strain. The loss and gain of the *Stx*-encoding phages is believed to be dynamic but with the tendency for the phage(s) to be retained in the cattle. The phage regions were also shown to be the hotspots of DNA exchange.

1.7.1 Shiga toxin

1.7.1.1 The discovery of Shiga toxin (Stx)

In 1897, Kiyoshi Shiga discovered the dysentery bacillus from stools and intestinal walls of infected patients. The aetiological agent which was initially termed as *Bacillus dysenteriae*, now known as *Shigella dysenteriae*, caused acute localised invasive colitis by the act of invading and proliferating inside intestinal epithelial cells and mucosal macrophages. Dr. Shiga also observed the production of toxic factors from the bacteria. Later Gerald T. Keusch discovered an enterotoxin produced by *Shigella dysenteriae* type I, which was later shown to be the same toxin associated with neurotoxic and cytotoxic activities [86, 87] now known as Shiga toxin (Stx) [88]. Stx was often associated with the development of HUS (acute haemolytic anaemia, thrombocytopenia and acute renal failure) in diarrheagenic patients [89, 90]. Similarly, in EHEC O157:H7 infected patients, symptoms such as severe abdominal pain and bloody diarrhoea could then be followed by HUS, especially in children and the elderly. Later it was identified that EHEC O157:H7 expresses similar AB5 toxins termed Shiga-like toxins, or Shiga toxin 1 (Stx1) and 2 (Stx2). The genes encoding for Stx of *S. dysenteriae* are on the chromosome, while the Stx1 and Stx2 of STECs were shown to be encoded by phages with modular and mosaic gene arrangements similar to that of the lambdoid bacteriophages acquired via horizontal gene transfer [91, 92]. Since the role of Stx have been well characterised to be pivotal to the pathogenesis of EHEC O157:H7 in humans, the association of the toxin during colonisation of the cattle intestine by EHEC O157:H7 is still poorly understood and therefore is examined in the current study (refer to section 1.9 below for thesis aims).

1.7.1.2 Shiga toxin-encoding bacteriophages

By definition, Stx-encoding bacteriophages or Stx phages are any bacterial-infecting virus that carries a *stx* operon containing *stx* genes encoding for the A and B subunits of the toxin. Stx phages are morphologically diverse however were characterised to display similar gross appearance as members of the lambdoid phages with icosahedral heads (short or elongated) with long contractile or non-contractile

tails (of varying lengths) or short tails [93-95]. They undergo a temperate phage lifestyle containing two phases; the first is where the phage genes are integrated into the bacterial chromosome and remain ("lysogenisation" of the bacterial host phase) until conditions are in favour for reactivation of the phage resulting in the "lytic" cycle (Fig. 1.2). Lysogeny conversion is when the phage integrates into a strain; in the case of the Stx-phages these can convert a non-harmful bacteria to a potentially pathogenic strain. Phages capable of inducing lysogenic conversion are proposed as significant contributors to the ongoing evolution of pathogenic strains [96].

The genes encoding for Stx can be divided into two types; i) inducible prophages or ii) Stx-prophage remnants which persists as cryptic genes on the bacterial chromosome and lack the ability to induce Stx production, but are most likely able to contribute during recombination of phage genes driving evolution of bacterial strains [97, 98]. The genome size of most Stx phages characterised to date are larger than the typical lambdoid (λ) phages, however the function of the extra set of genes carried by the Stx phages has yet to be fully confirmed. Many studies have suggested that these extra or accessory sequences of the Stx phages are believed to contribute to the survival of not only the phages but also the bacterial host as well, such as that previously described for the *bor* gene of the λ coliphage [99]. This particular gene was expressed during lysogeny and encoded for factors that significantly increased for the survival of the *E. coli* host cell in animal serum.

Stx-encoding bacteriophages persist not only within the bacterial host, but these viruses are also abundant in the extra-intestinal environment, even more so than their STEC hosts [83]. These phages resist several inactivation methods targeted at the bacterial population, thereby increasing their survivability and further potential propagation into other bacterial hosts [84]. The presence of persistent, infectious Stx-phage particles that are readily available in the environment to infect new bacterial hosts may facilitate the capacity for Stx expression into new hosts, as seen in the 2011 STEC outbreak in Germany involving the newly recognised atypical enterohaemorrhagic *E. coli* pathotype, Entero-aggregative Haemorrhagic *E. coli* (EAHEC) [100]. This emergent strain harboured a Stx2a-phage that was shown to be

similar to those present in bovine STEC strains [82]. This illustrates how mobile and adaptable these Stx-encoding phages are to be effectively spread among strains of different host species. Therefore it is important to study these Stx-encoding bacteriophages in order to understand how their lysogeny into the bacterial host chromosome may contribute to EHEC O157:H7 colonisation in the bovine intestinal tract.

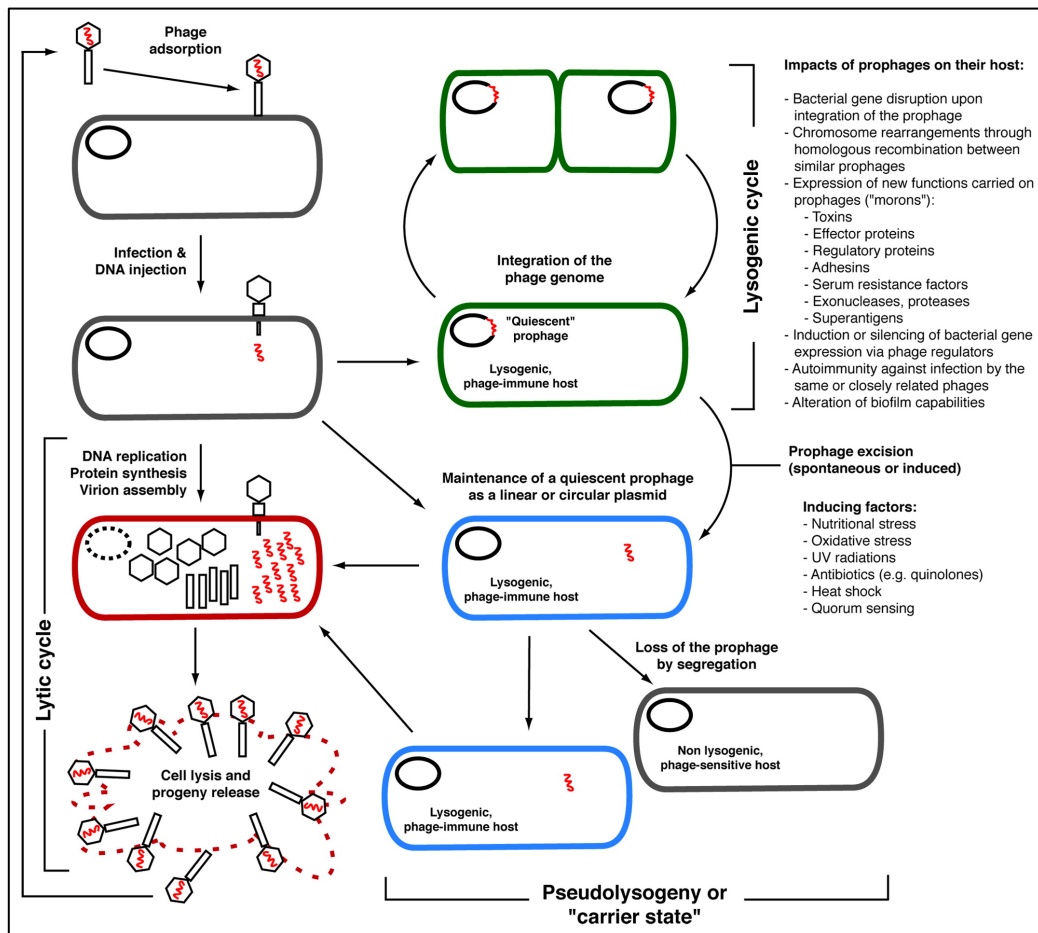


Figure 1.2 Different phases in the life of a phage (taken from Fortier and Sekulovic) [96]. Virulent phages undergoing the lytic lifestyle upon infection of the host will immediately have its DNA replicated leading to lysis at the end of the cycle releasing assembled phage particles ready to infect other bacterial cells. Temperate phages, in contrast have two phases throughout their life cycle; i) Lysogenic cycle where the phage integrates its genome within the host chromosome and remains inactive, with the prophage DNA replicated together with the host cell thereby transmitting prophage DNA to the newly produced progeny cells. ii) Upon induction (e.g. Stressors inducing DNA damage) prophage is excised from the host chromosome switching from lysogeny to the lytic cycle.

1.7.1.3 Shiga toxin expression

The transcription of *stx1* genes could be initiated upon activation of the functional p_{Stx1} promoter, regulated by the iron-dependent Fur transcription repressor [101]. A low iron concentration in the environment will trigger the cleavage and removal of the Fur repressor, which will then activate the p_{Stx1} promoter and the consecutive *stx1* genes, Fig. 1.3 [101]. Whereas Sung et al. had identified for a promoter-like sequence for *stx2* transcription, however the sequence is considered vestigial as it does not contribute to Stx2 production and the presence of the sequence is thought as coincidental to the assimilation of the *stx2AB* genes into the late regulatory genes of the phage [102, 103]. Instead, Stx2 production occurs upon activation of the late phage genes, directed upon triggering of the phage lytic cycle (Fig. 1.4). This phage-directed mechanism of *stx* gene transcription is also evident in the Stx1-encoding phage [104]. The *stx* genes are located within the late region of the phage genome which are only transcribed and translated once the phage is in the lytic phase following induction of the bacterial SOS response in the cell (Fig. 1.4, [105]). The SOS response is triggered by DNA damage and the appearance of single stranded DNA; this allows the formation of activated RecA which in turn catalyses the autocleavage of the LexA repressor governing expression of several SOS induced genes in the bacteria. The activated RecA also catalyses the auto-cleavage of the prophage *cI* repressor leading to expression of the bacteriophage lytic cycle. The toxin release is closely linked to bacterial lysis directed by the late phage genes, allowing efficient release of not only the toxin but also the phage particles, avoiding the need for a secretion system which may require more energy [106]. This does not rule out other induction or release mechanisms, but this is the understood primary route at this time. Moreover *in vitro* experiments comparing the production of Stx1 by STEC O26 Strain H19 in the presence of SOS-inducing agent (Mitomycin C) and low iron medium strongly suggests that despite both conditions induced the production of Stx1, the release of the toxin could only be detected in the supernatant of H19 cells grown in MMC [104]. The medium with low iron concentration stimulated the production of Stx1 but failed to induce lysis leading to accumulation of the Stx1 intracellularly. This mechanism also explains why antibiotic treatments, especially those targeting bacterial DNA, are often contraindicated in patients

infected with STECs as this will exacerbate the condition due to increased bacteriophage and Stx production [107].

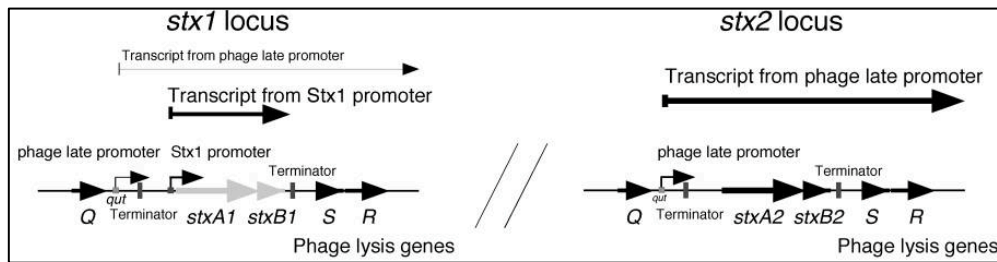


Figure 1.3 The transcription of *stx1* and *stx2* genes, taken from Shimizu et al. [108]. *Stx1* expression could be induced by activation of the functional p_{Stx1} promoter (located directly upstream from the *stx1* gene sequence) regulated by environmental iron concentration via the Fur transcription repressor. In addition, the production of *Stx1* could also be mediated by the phage late promoter, induced upon activation of the phage lytic cycle. Whereas the transcription of the *stx2* genes occur following the induction of the phage lytic cycle, and is transcribed from the phage late promoter.

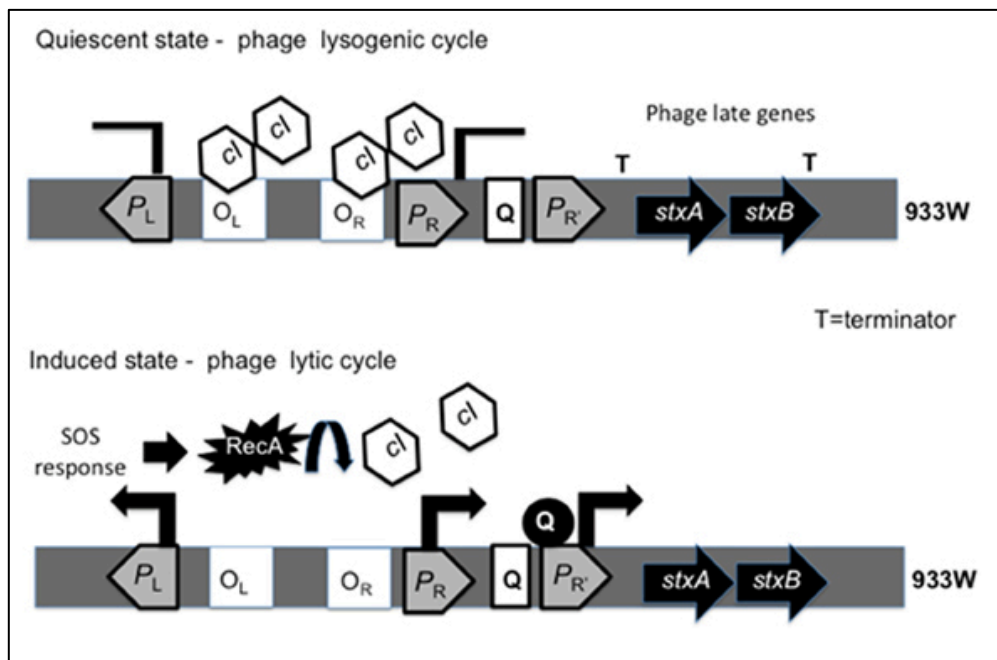


Figure 1.4 Phage-mediated expression of the Shiga toxin 2 genes, taken from Sperandio and Pacheco [105]. In the quiescent state, the expression of phage genes are inhibited by the action of the *cl* repressor that bound to the operator sites, O_L and O_R . The terminator (T) downstream of the late right promoter, $P_{R'}$ prevents the transcription of *stxAB*. The presence of signals inducing SOS response will immediately produce and activate *RecA*, that then promotes cleavage of the *cl* repressor. The depressed P_R then leads to the expression of the anti-terminators *N* and *Q*. The *Q* anti-terminator will bind to $P_{R'}$ and activate the late phage genes including *stxAB*, prior to bacterial lysis that will release *Stx* into the environment. 933W is the *Stx2*-encoding bacteriophage from EHEC O157:H7 Strain 933 originally obtained from G.K. Morris, Centers for Disease Control, Atlanta, Georgia [109].

1.7.1.4 The structure of Shiga toxin

Shiga toxin 1 is 98% homologous to the amino acid sequence of the Stx of *S. dysenteriae* [110]. While Stx2 is quite distinct in its amino acid sequence with less than 60% similarity to the Stx1 [111]. To date, there have been several subtypes of Stx2 identified (Stx2a, Stx2c, Stx2d, Stx2e, Stx2f) [91]. The Stx structure is comprised of two subunits, A (32 kDa) and B pentamer ring (approximately 7.7 kDa per unit) (Fig. 1.5). The A moiety is comprised of two subunits linked by a single disulphide bond; A1 and A2. The former is presumed as the biologically active A subunit, while the latter moiety functions to primarily maintain the structure of the holotoxin and bridges between A1 and the B pentamer ring [112]. The B pentamer interacts with Stx receptor, Globotriaosylceramide (Gb3), surface expressed by Stx sensitive cells, allowing toxin binding and subsequent toxin internalisation by the cell. The A and B moieties are connected at the C-terminus of only three of the B subunits, allowing the A moiety to bend to the side opposite from the three B subunits [113].

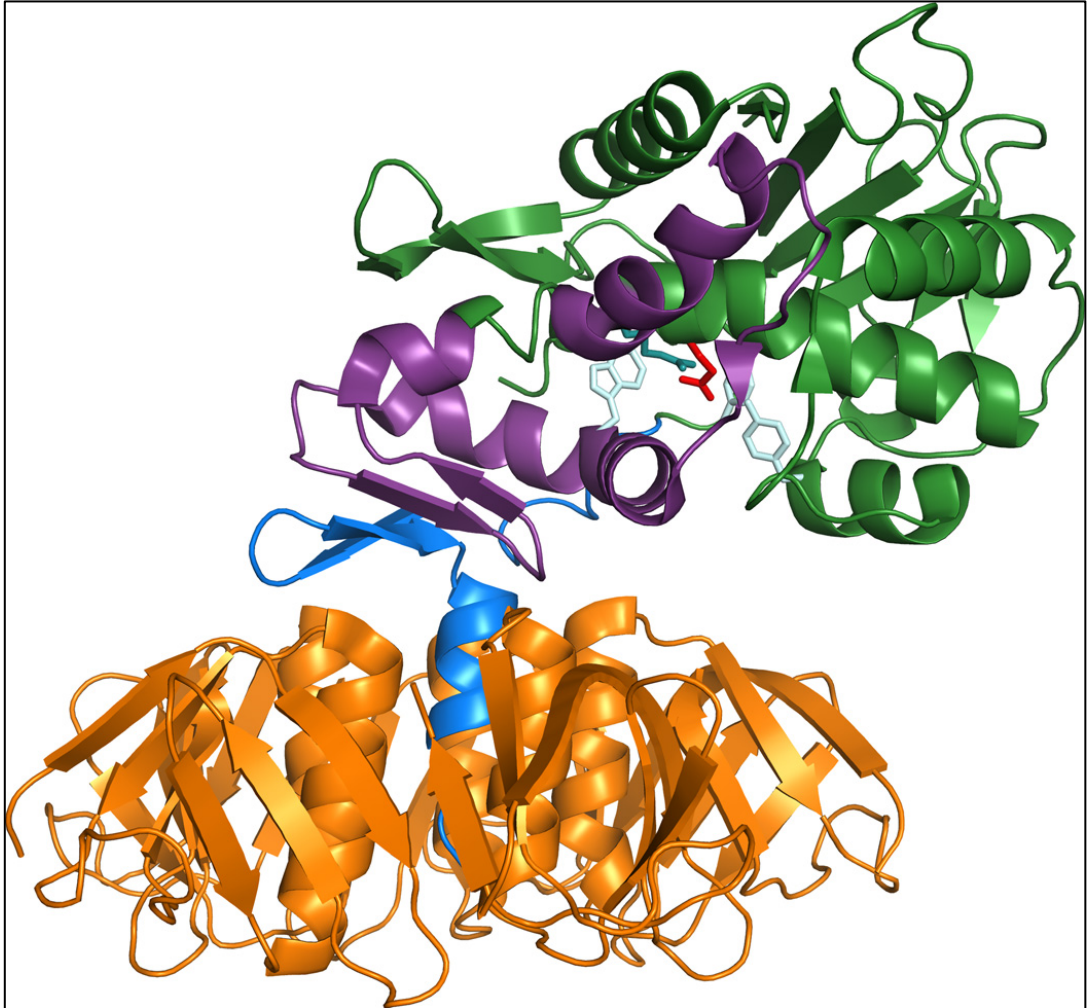


Figure 1.5 The ribbon diagram illustrating the crystal structure of **Shiga toxin 1**. The A1 subunit is depicted in green, with the part of A1 interacting with ribosome shown in purple. The blue ribbon depicts the A2 subunit and the B pentamer is shown in orange. Active-site side chains are indicated in red (active residue 167) and other putative side chain (pale blue). The figure was drawn with PyMOL Molecular Graphics System, Version 1.5.0 Schrödinger, LLC. by Dr. James Vergis and taken from Melton-Celsa, et al [112].

1.7.1.5 Globotriaosylceramide (Gb3) as the receptor for Shiga toxins

The globotriaosylceramide [Gal α (1-4), Gal β (1-4) glucosylceramide or Gb3] (Fig. 1.6) is the receptor for all Stx toxin types except for Stx2e which preferentially binds to the globotetraosylceramide (Gb4) [114, 115]. Gb3 is a variant of glycosphingolipid (GSL), the most abundant and diverse subtype of glycolipid in animals, plants, fungi, bacteria and invertebrates [116]. GSLs have many biological roles including membrane structure, host-pathogen interaction, intercellular communication and membrane protein function modulation. In host-pathogen interactions, GSL function as receptors for a variety of non-enveloped virus such as Norovirus and Rotavirus [117] and bacterial toxins including cholera toxin and Stx [118]. CD19 and Interferon-alpha 2 Receptor (IFNAR2) were among the physiological ligands suggested for Gb3 as it was shown that these two have sequence similarities with that of the Stx B subunit [119-121]. Binding of Gb3 to IFNAR2 will activate several transcription factors and growth inhibition, while interaction with CD19 mediates homotyping of cells which occurs at germinal centres in antigen-induced B cell differentiation [120, 122]. Gb3 has also been reported to be overexpressed on cancerous cell lines and human tumours, with examples including Burkitt's lymphoma, leukemia, astrocytoma, colorectal, ovarian and breast cancers [123-127]. Gb3 expression has also been proposed to be significantly correlated with the metastatic potential of human colon cancer [128].

The α 1,4-galactosyltransferase (*A4GALT*) gene encodes the Gb3 synthase enzyme, which catalyses galactose ceramide transformation to lactosylceramide before the formation of Gb3 (Fig. 1.7) [129, 130]. The ability of the toxin to bind to its receptor is affected by the fatty acid chain length and the degree of unsaturation [131]. Stx1 preferentially binds to Gb3 with fatty acid chain containing more than 20 carbons, while Stx2c has a preference towards shorter fatty acid chains [132]. The presence of unsaturated fatty acids enhances the Stx1 and Stx2c binding to Gb3, possibly associated with an increase in lateral mobility within the lipid bilayer [132]. Although Stx cytotoxicity has been shown to correlate with Gb3 synthase activity and Gb3 content [133], an earlier study argued that cell sensitivity towards the toxins do not entirely depend on total Gb3 concentration [131, 134]. The contradictory

findings may be partially explained by the association of Gb3 with 'lipid rafts', defined as detergent-resistant microdomains of the apical plasma membrane, enriched with clusters of glycolipid-cholesterol assembled with specific membrane proteins and signal transducers [135]. Majority of Gb3 studied were shown to reside within the lipid rafts and this was shown to be necessary for Stx1 binding and translocation across Caco-2 monolayer [111, 136]. Moreover, the clustering of Gb3 within lipid rafts was identified as the main discriminator for pathology *in vivo* as shown by Khan et al. (2009). Despite the high presence of Gb3 within the nephron, the only part that is affected by Stx are the glomeruli since Gb3 are organised within the lipid rafts as compared to Gb3 in other parts of the nephron[135].

Several methods have been used for the analysis of Gb3 expression including flow cytometry, fluorescence microscopy and lipid chromatography while transcription and quantification of Gb3 synthase A4GALT could also be used as an indicator of Gb3 expression as its expression levels have been correlated with Gb3 surface expression [129, 137].

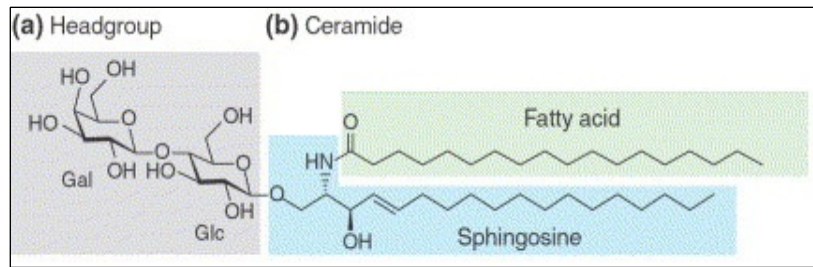


Figure 1.6 The structure of globotriaosylceramide (Gb3) (Adapted from [130]). Gb3 belongs to the globo-series (type 4) GSL core structure. Gb3 is amphiphatic, composed of the hydrophobic ceramide (sphingosine; long chain amino alcohol containing amide linkage to fatty acid) and the hydrophilic carbohydrates (Gal; galactose α 1-4, Glc; glucose β 1-3). The carbohydrates typically lie on the plasma membrane, with the outer surface of carbohydrate chain exposed to the extracellular space and accessible for interaction with ligands including Shiga toxins [117 {Schnaar RL, 2009 #999}].

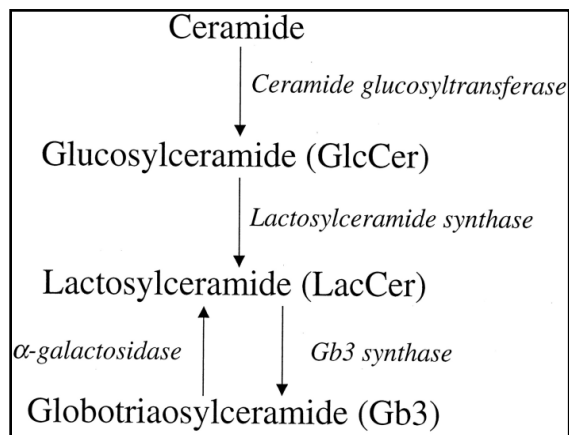


Figure 1.7 The synthesis pathway of globotriaosylceramide (Gb3). (Adapted from [130]). Gb3 is synthesised in the endoplasmic reticulum and Golgi apparatus beginning with sequential addition of individual carbohydrate units to the ceramide (glucose by ceramide glycosyltransferase) to synthesise glucosylceramide (GlcCer) and galactose by lactosylceramide synthase producing lactosylceramide (LacCer). Gb3 synthase then converts LacCer to Gb3 and transported to the cellular surface to incorporate with the plasma membrane [116] [138].

1.7.1.6 Shiga toxin internalisation by eukaryotic cells via retrograde transport

Upon binding of Stx B subunit to the terminal galactose disaccharide moiety of its receptor, the globotriaosylceramide (Gb3) (or globotetraosylceramide, Gb4 for Stx2e) on the cell surface, the toxin-receptor complex is internalized by endocytosis in a clathrin-dependent manner [139]. The endosome containing the toxin is trafficked to the Golgi apparatus through the perinuclear endocytic recycling compartment. From the Golgi apparatus, the toxin follows a retrograde pathway and is translocated to the endoplasmic reticulum [140]. The precise trafficking pathway is unclear but it is believed that the toxin follows the pre-existing route within the cell to reach endoplasmic reticulum (ER). An enhanced intracellular retrograde transport of the endocytosed toxin to the Golgi and endoplasmic reticulum were proven to increase cytotoxicity [141].

For resistant cells that express Gb3, it is considered that Stx will be transported to the lysosome for degradation [142]. Recent studies have elucidated the process of retrograde trafficking of the AB5 toxins with the involvement of ER-associated degradation (ERAD) pathway [143]. Inside ER, the toxin associates to the large multi-chaperone complex causing it to partially unfold. The ER then recognizes the Stx as misfolded protein and excretes the toxin out into cytosol via the ERAD pathway. In normal situations, ERAD will cause the misfolded proteins to undergo proteasome degradation. However, in the absence of lysine residues (as the site of ubiquitination in target protein), Stx escapes the proteosomal degradation process. Following cleavage of the disulphide bond between the A subunits by furin (a calcium-sensitive serine protease) in the *trans*-Golgi network. The A1 and A2 subunits remain linked by a disulfide bond until it reaches the endoplasmic reticulum (ER) where the two subunits get separated allowing the A1 subunit to be translocated across the ER membrane to the cytoplasm before reaching its target, the ribosome to interfere with protein synthesis [144-146]. The A1 subunit has RNA N-glycosidase activity, targeting the adenosine within the 28S ribosomal RNA of the 60S ribosomal unit. This depurination interferes with the translation process, as adenosine is involved at the interaction site with Elongation-factor 2 (EF-2) ternary complex,

producing transfer RNAs that are unable to associate with the ribosomal complex, thereby inhibiting protein synthesis in target cells [113].

1.7.1.7 Shiga toxin early interaction with and translocation across epithelial monolayers

Purified Stx2 introduced intravenously into baboons resulted in glomerular thrombotic microangiopathy, while baboons receiving purified Stx1 showed no blood profile or clinical signs indicating haemorrhagic uraemic syndrome (HUS) [147]. Such findings are in parallel with that of epidemiological studies where patients infected with STECs producing Stx2 as well as animal models treated with Stx2 to be closely associated with HUS [90, 148-150]. However, Stx1 is also able to cause mild damage to the mesangial cells of baboons [151]. Despite differences recorded in the potency of Stx subtypes (Stx2 is 400-fold more toxic than Stx1 in mice [152]), one fact remains that in order to exert renal tissue damage, the toxin must be expressed, transported across the epithelial monolayer of the intestine and remain bioactive until it reaches the target tissue. Stx expression *in vivo* and the consecutive events including crossing mucosal epithelium and entrance into the systemic circulation to reach target organs remain vague. Although one would suspect a receptor-mediated endocytosis by Gb3 to be the simplest way of explaining the translocation process, data from studies had indicated negative Gb3 expression by human colon epithelial and immortalised intestinal cells [153-155]. Furthermore, cells expressing Gb3 are at high risk of succumbing to cytotoxicity [156]. Therefore, mechanism(s) must exist to allow translocation of the toxins from intestinal lumen into the underlying beds of blood capillaries within the lamina propria and submucosal region. The route followed by the toxins must also protect its bioactivity until it reaches the blood and the distal target organs.

Stx1 was shown to travel across Caco-2 epithelial monolayers transcellularly without causing any disruption to the monolayer integrity and the movement being energy dependent [157]. This finding was further supported by another study which discovered that Stx1 were detected in cytoplasmic endosomes of T84 cells and none was present in the paracellular space [154]. Later Stx1 and Stx2 were shown to

translocate Caco-2 cells at a different rate, with 2.9% of Stx1 translocated the monolayer compared to only 0.07% of Stx2 [158]. In the same study, Stx1 was again shown to translocate in an energy-dependent, saturable manner, whilst the movement of Stx2 was not. Stx1 also translocated faster across Gb3-negative T84 cells than Caco-2 cells [159]. The presence of neutrophils promoted the translocation of Stxs across epithelial cells [160], however examination of sections from inflamed intestinal biopsies showed no difference in the binding pattern or translocation of Stx1 and Stx2 when compared to normal intestines [161].

In a more recent publication, Stx1 and Stx2 were observed by confocal microscopy to be present inside the ileal and colonic epithelial cells of EHEC O157:H7-infected human samples [162]. In addition, both toxins were also present within lamina propria as well as within sloughed dead particles in the intestinal lumen. Similar observations were reported in *in vitro* organ culture (IVOC) of paediatric intestinal biopsies but with the absence of Stx binding to the epithelium [159].

A published study reported on Stx1 gaining entrance into T84 cells via macropinocytosis shed more light on Stx translocation [162]. Macropinocytosis is the process of uptaking solutes in extracellular fluid via macropinosomes (formed from ruffling of the cellular membrane via actin-filament dependent process, which later fuses against the other end of the cellular membrane and interacts with cytoplasmic lysosomes to release the contents or degraded via endocytic pathways). The Stx-B subunit was used to study toxin translocation across Gb3-negative T84 epithelial monolayer and revealed that Stx translocation occurred via macropinocytosis mediated by the activation of Src. In addition, the macropinocytosis also increased the rate of transcytosis of the toxin across the cells. Interestingly, this Stx-uptake process was observed to be stimulated by the presence of EHEC colonies at the intestinal epithelium [163]. Other pathogenic enteric bacteria namely *Salmonella* Typhimurium was shown to stimulate macropinocytosis in HeLa and Caco-2 cells thereby gaining direct entrance route into the epithelial cells [164].

Findings provided with regards to Stx interaction with epithelium to date mostly were deduced from experiments carried out under laboratory conditions. To investigate if such findings agree with events taking place *in vivo*, Trans and colleagues employed vertical diffusion chamber system with polarised T84 cells to simulate the microaerobic environment in the human intestine to study Stx expression and translocation during EHEC O157:H7 infection [165]. They reported that EHEC growth and Stx production were downregulated under a microaerobic environment, conditions which are considered to be more appropriate in investigating events occurring *in vivo*, compared to an aerobic environment which has routinely been used in most laboratory experiments. Despite the limited bacterial growth and toxin production, Stx2 of strain EDL 933 translocation was enhanced. Stx2 translocation also relied on the presence of the bacteria since translocation rate of purified Stx2 was downregulated after a 5-hour incubation. Interestingly, it was also shown that Stx translocation occurred in a transcellular manner and not via macropinocytosis, in contrast to a previous report mentioned above [162].

In cattle, purified Stx1 adhered to the epithelial crypts of the jejunum, mid-intestine and caecum sections, but not to the endothelial cells within the submucosa [159]. Purified Stx2 neither bound to the epithelial nor endothelial structures of the bovine intestine. In addition, the crypt cells of bovine colon epithelium bound to and internalised purified Stx1 but remained resistant towards the toxicity as it was degraded via a lysosomal-dependent pathway [142]. Differential Gb3 expression and Stx binding pattern between human and cattle may partially explain the distinguished clinical outcomes (discussed in detail in Chapter 2, Introduction section 2.1).

1.7.1.8 Shiga toxin in EHEC O157:H7 pathogenesis

Haemorrhagic colitis (HC), generally known as bloody diarrhoea is one of the clinical signs reported in most EHEC infections [51, 90, 166]. Prior to the presence of visible blood in the stool, infected individuals were reported to have severe abdominal cramps and watery diarrhoea, which may or may not be accompanied with low grade fever [22]. Blood content in stools varies from streaks of redness to absolute blood [89, 90, 166]. In a 2-year study of routine stools from 10

hospitals in the United States, 0.39% were positively identified for the presence of EHEC O157:H7 [167]. The positive isolation of EHEC O157:H7 is most likely from a bloody stool compared to a stool without visible blood and was also identified as the most common pathogen to be isolated from bloody stools yielding pathogenic enteric bacteria. Some studies also associated HC with a more prolonged shedding of EHEC O157:H7 [168].

It is believed that intimate EHEC adherence to the intestinal epithelium and more importantly, the subsequent Stx translocation to the underlying lamina propria containing small blood vessels initiates the occurrence of HC [22, 162]. Stx2 was shown to induce damage to the human intestinal cells of an *in vitro* organ culture (IVOC) [159]. Furthermore, Stx2 treatment resulted in intestinal epithelial extrusion and the binding of the toxin to the endothelial cells of the lamina propria. The Gb3-enriched surfaces of intestinal microvascular endothelium confers for high sensitivity of the cells towards the action of Stx, particularly Stx2 [159]. Following Stx binding and uptake by the Gb3-positive endothelial cells, the toxin will then be translocated to the Golgi apparatus and nucleus resulting in full cytotoxicity [141, 169]. The dead endothelial cells detach from the microvascular structure, causing leakage of the capillary which may then seep out of the intestinal wall from disrupted intestinal barrier which resulted from the effect of A/E lesion as well as Stx epithelial extrusion [159].

Human colon mounted in an Ussing chamber and treated with Stx positive EHEC strains resulted in interruption in water absorption across the mucosa accompanied with significant morphological changes including epithelial detachment, mononuclear infiltration and loss of mucus-secreting goblet cells [170]. The study showed Stx2 as the bacterial factor responsible for the damage induced, which was augmented in the presence of EHEC. Earlier, Stx2 was shown to inhibit water absorption across human colon *in vitro* and suggested that the toxin may specifically target the mature, absorptive villous enterocytes leading to loss of water absorption [171]. While Creydt et al. (2004) reported on the ability of Stx2 B subunit to inhibit the net fluid absorption across human colon as well as causing fluid

accumulation in rat colon ligated loops [172]. Evidence so far provided indicated that the toxin, particularly Stx2 is highly involved in the pathological events leading to not only HC, but also watery diarrhoea.

Haemorrhagic uraemic syndrome (HUS) is the primary cause of acute renal failure in children infected with STECs [173]. Stx is the virulence factor from STECs associated with HUS following an STEC infection by targeting the endothelial cells of the glomeruli and initiating various dysfunctions of the endothelial cells leading to microangiopathy. Following Stx release from lysed bacterial cells in the intestine, the toxin will be translocated across the intestinal epithelial barrier to reach the underlying blood vessels [157, 165]. Once inside the blood vessel, it is thought that the toxin binds to Gb3-expressing blood cells, as previously observed in a study where the toxin binds to Gb3 on the surface of neutrophils of human and mice [174]. The Stx bound neutrophils will then circulate systemically until the cells reaches the microvascular endothelial cells of the glomeruli in the kidney. Here, the Stx is thought to dissociate from the neutrophil to bound to the Gb3-rich domain on the surface of endothelial cells of the glomeruli [175]. This Stx-endothelial cell association will trigger a pro-inflammatory and pro-thrombotic cascades resulting in thrombotic microangiopathy, characterised by vascular edema with detachment of the endothelial cells exposing the subendothelial matrix and deposition of the dead cells and debris, platelets aggregation and fibrin deposition [176]. Mechanisms underlying the endothelial dysregulation in the kidney of HUS patients is complex. Among the documented evidence includes an increase in the ratio of plasminogen activator inhibitor to the tissue plasminogen activator leading to stabilisation of the fibrin clots [177], higher release of tissue factor from endothelial cells [178], upregulation of the stromal cell-derived factor-1 (SDF-1) from endothelial cells which binds to the CXCR4 receptor leading to enhanced platelet activation and aggregation [179], release of higher levels of the platelet attractant, von Willebrand factor (vWF) [180] and increased secretion of endothelial adhesion molecules [181]. In addition, recent studies have elucidated the complement dysregulation as an important factor in determining the subsequent endothelial damaging consequences during HUS. Stx enhances the release of P-selectin, a cell adhesion molecule from

endothelial cells which triggers the release and activation of C3, an activator of the complement system via the alternative pathway. The presence of excessive C3 further exaggerates the thrombogenic state through activation of the alternative complement pathway[182], which in turn increases the expression of P-selectin.

An increase in the sensitivity of microvascular endothelium and proximal tubule cells in the kidney towards Stx has been suggested for the susceptibility of the renal cells to succumb to Shiga cytotoxicity. The basis for such an increased in sensitivity was shown to be directly related to the high Gb3 synthase and low alpha (α)-galactosidase levels in cultured human proximal tubule cells [183]. Post-diarrhoeal HUS is generally more prevalent in children, presumably as a result of inverse correlation between Gb3 expression and age. This theory however was challenged by a study examining Gb3 expression in renal cryosections of individuals aged between infancy to 85 years old and identified similar Gb3 expression for all samples examined [184]. In addition, 3 hr of treatment with 500 ng/ml of Stx1 resulted in similar binding rate across the frozen sections to both glomeruli and tubular cells, with no significant differences noted amongst the intensity of the anti-Stx1-stained cryosections. Therefore, it is highly possible that the involvement of other factors in addition to Stx-Gb3 is required to explain the pre-dominance of HUS cases among the younger patients. This may include factors such as exposure of the glomeruli and tubular cells to bacterial LPS and cytokines which may potentiate the sensitivity levels towards the toxin [150, 185, 186].

Pathological localisation of STEC infection correlates to the distribution of Gb3. Since the endothelial cells of the cerebrum expresses Gb3, microangiopathic thrombi formation resulting in neurological symptoms could develop in certain individuals where the toxin is able to reach the brain via circulation [187]. Such lesions involving the nervous system could potentially be fatal and therefore early diagnosis of an STEC case is essential to prevent the toxin from reaching the brain. Interleukin-1 (IL-1) and Tumor Necrosis Factor (TNF), two inflammatory cytokines usually present during STEC infection, in synergy are able to upregulate the transcription of enzymes essential for Gb3 synthesis; ceramide glucosyltransferase

(CGT), lactosylceramide synthase (GalT2) and Gb3 synthase (GalT6) in human brain endothelial cells (HBEC) [137]. As a consequence, exacerbation of clinical symptoms follows due to increased sensitivity of the endothelial cells upon Gb3 upregulation, leading to a poor prognosis for the patient.

Microvascular endothelial cells of the human colon are rich in Gb3 content and was shown to be able to bind to both Stx1 and Stx2 *in vitro* [188]. Although Stx1 has a higher affinity to bind to Gb3, Stx2 was more toxic to the transformed human microvascular endothelial cells which correlates with findings from epidemiological studies which associates Stx2 with higher risk of developing HUS [90]. The intestinal epithelial cells, in contrast, were shown to not express Gb3 on the surface [153, 159, 189]. However in a more recent study, the authors detected mRNA of Gb3 synthase from normal human colon tissue sections and human carcinoma cells (HCT-8) [190]. Interestingly, a fraction of these cells do express surface Gb3 as detected by fluorescence microscopy, however the amount of cells readily detected with surface globotetraosylceramide (Gb4) outweighs Gb3 expression. Gb4 is biosynthesised from Gb3, mediated by Gb4 synthase and contains an additional N-Acetylgalactosamine (GalNAc), attached to the Pk trisaccharide of Gb3 [191]. Gb4 is capable of binding to Stx, however the binding is much less efficient than Gb3 and Gb3 except for Stx2e (Stx variant in porcine edema disease) which preferentially binds to Gb4 [114, 115, 191]. Under circumstances where Gb4 predominates the intestinal epithelial surface area more than Gb3, it was suggested that more Stxs (all subtypes except for Stx2e) will have better chances of transcytosing the epithelial monolayer and skip the receptor binding step before entering the blood circulation to reach target organs expressing Gb3 [190]. Finally, it was also reported that Stx1 and Stx2 both bound to Paneth cells present within the crypts of Lieberkuhn in frozen sections of paediatric intestinal biopsies [161].

1.7.2 Type three secretion system (T3SS)

The ability to form attaching and effacement (A/E) lesions on intestinal epithelial cells distinguishes EHEC from many of the other *E. coli* strains that contain Stx-encoding bacteriophages and produce Stx. This phenotype plays a major

role in formation of bacterial microcolonies along the intestine and therefore in facilitating persistence within the host. The type three secretion system (T3SS) is an organelle that can deliver proteins from inside the bacterium into a host eukaryotic cell. The system includes basal structure, translocator and effector proteins, with the injection apparatus and many key delivered effector proteins expressed from a chromosomal pathogenicity island termed the locus of enterocyte effacement (LEE). The actual translocation structure on the surface of the bacterial cell may form before or during contact of the bacterium with the intestinal host epithelial cell, and is comprised of an EscF needle complex onto which is attached a polymerised EspA filament. This filament connects to a pore formed in the host membrane by the EspD and EspB proteins. The full apparatus from basal units to the translocon allow effectors to be secreted between the cells in an ATP hydrolysis-dependent manner. Some of the earliest work in EPEC and EHEC demonstrated that a protein called the translocated intimin receptor (Tir) was transferred into the eukaryotic cell. Intimin which is expressed from the LEE but exported in the standard *sec*-dependent manner into the bacterial outer membrane then binds to Tir that has become integrated into the eukaryotic cell membrane. This interaction initiates Tir clustering followed by signalling events leading to actin polymerisation and pedestal formation.

Multiple other effector proteins are now known to be involved in the re-organisation of the cytoskeleton resulting in ‘intimate’ bacterial attachment [192]. The villi on the apical surface of the intestinal epithelial cells are then lost (effacement) with the bacteria firmly attached to the host cell forming the histopathological feature known as the A/E lesion. T3SS regulation is complex and involves a dynamic between the environment, signalling from nearby bacteria and the regulators itself including the master LEE-encoded regulator, *ler* [193, 194]. The complex nature of LEE regulation has been reviewed relatively recently [40] which encompasses multiple factors from the core regulators namely Ler and the second most important regulator, the global regulator of *ler* activation (GrlA) and repression (GrlR) feedback loop, as well as the bacterial nucleoid associated proteins. In addition, global regulators could be encoded both on the chromosome (such as the by the second T3SS; ETT2 of EDL 933 and Sakai that was suggested to affect bacterial

adherence and regulation genes encoding virulence factors in a yet undefined mechanism) [195] and by horizontally acquired genetic elements (for example homologs of the direct EPEC Ler activator PerC encoded on lambdoid prophages of EHEC O157:H7 required for full virulence [196]). Additionally, control by Hfq, initially identified as a host factor of the QB phage, which functions as an sRNA chaperone and is actively involved in post-transcriptional regulation of the LEE and T3S. Kendall et al. 2011 found that the Hfq regulates LEE expression in a strain-dependent manner as it up-regulates T3SS in EHEC 86-24 but act as a negative regulator of LEE expression in EHEC O157:H7 EDL 933 [197]. Communication between bacterial species via chemical secretions resembling hormones or quorum sensing (QS) have also been described in modulating the LEE activity, for example the QseA transcriptional regulator capable of activating the LEE1 operon [198]. Furthermore, the microbiota residing near the colonisation niche (e.g. *Bacteroides thetaiotaomicron*, refer Section 1.4 above) [199] and nutrient availability/metabolism (e.g. butyrate/acetate, D-serine amino acid and fucose) [39, 200] were also shown to contribute to the regulation of the genes encoded by the LEE operon. An example could be illustrated by LEE regulation by interaction between two two-component systems (TCS); with the i) the fucose sensing kinase and fucose sensing response regulator (FUSKR) system (fucose sensing and metabolism) repressed by the ii) QseBC (flagella and motility) and QsEF (pedestal formation) QS regulatory cascades [201, 202]. The presence of fucose in the EHEC O157:H7 culture caused a complex interaction between the two systems mentioned resulting in a reduction in the expression of LEE [199, 203]. The T3SS is also positively regulated by high levels of bicarbonate ions in the culture medium [204], however this was not observed in a study reporting on an EspA-mediated enhanced EHEC binding to intestinal cells performed under microaerobic conditions to mimic the low oxygen levels in the intestine [205].

The formation of the intimate attachment via the A/E lesion on the intestinal epithelium has been associated with disruption of the tight junctions between the enterocytes and dysregulated absorption of water and ions mediated by the secreted bacterial effector proteins leading to diarrhoea [206]. Previous studies on pathogens

causing disruption of the barrier function were focused more on other bacterial strains possessing the T3SS apparatus namely the EPEC strains and *Citrobacter rodentium*, with only a few papers focusing on EHEC strains [206-209]. EspF, a mitochondrion-targeting effector protein leading to the activation of the mitochondrion death pathway [210], is secreted by the EPEC strains via the T3SS and was determined to be essential in disrupting the tight junctions of the small intestine [208]. The mechanism involved redistribution of one of the tight junction proteins, occludin intracellularly and an increase in the permeability of the epithelial monolayer leading to a significant reduction in the transepithelial electrical resistance (TER). *In vivo* study using A/E mouse model infected with *C. rodentium* indicated for the role of EspF as necessary to significantly disrupt the interepithelial cellular tight junctions with a marked increase in the colon luminal water contents [207]. A study comparing the ability to disrupt the intestinal barrier function between EPEC and EHEC strains suggested for EPEC strains to be more efficient in reducing the TER post-infection in T84 cells, despite similar levels of occluding redistribution by strains of both pathotypes [209]. The study identified that the EspF expressed by EHEC was not able to fully mediate the intestinal barrier disruption, as shown for EPEC. Furthermore the *espF* mutant of EHEC was still able to reduce the TER of the T84 monolayer, suggesting for the presence of other mechanism(s) involved in EHEC to subvert the tight junction barrier. The ability for EHEC to significantly disrupt the intestinal barrier required for the expression of U-EspF, a redundant EspF-like homologue encoded by EHEC. In a more recent study of EPEC and tight junction disruption, the ability of the EspF protein to affect the tight junctions requires for the involvement of two other bacterial effector proteins secreted by the T3SS of EPEC; the mitochondrial-associated protein (MAP) and intimin [211]. Much is still unknown on the exact mechanism(s) and contribution of the T3SS effector proteins of EHEC O157:H7 in causing diarrhoea and further work is required to fully understand the pathophysiology involved.

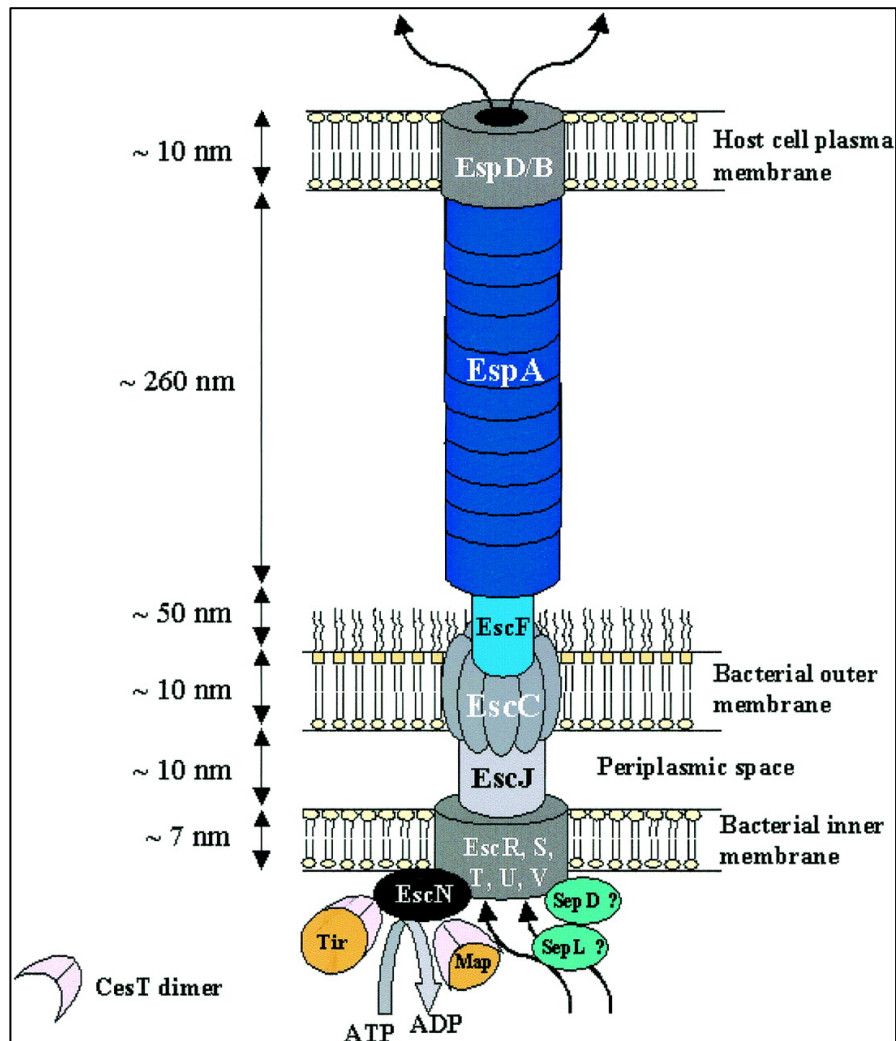


Figure 1.8 Schematic diagram of the type three secretion system of EHEC O157:H7 [212]. The apparatus is mainly comprised of two parts, the basal body (EscC) which connects the inner and outer bacterial membranes and the filament (EscF and polymerised EspA) that bridges the effector proteins from the bacteria into the host cell through the host cell plasma membrane. The basal body (EscC) is positioned in the bacterial outer membrane and is connected to the inner membrane ring structure (containing the EscR, EscS, EscT, EscU, and EscV proteins) via the EscJ lipoprotein. EspB and EspD form the translocation pore in the host cell plasma membrane. The cytoplasmic ATPase EscN provides the energy to the system by hydrolyzing ATP molecules into ADP. SepD and SepL have been represented as cytoplasmic components of the TTSS.

1.7.3 Other bacterial factors involved in adherence

Flagella are primarily composed of the flagellin (FliC) protein in *E. coli* and are known for providing motility to the bacteria by a propeller-like motion which generates additional torque through the presence of the hook structure. It has also been described to influence adherence as well as being an inducer of pro-inflammatory responses in host cells as it is recognised by Toll-like receptor five (TLR-5)[213, 214]. H7 flagella specifically have been shown to play a role in EHEC O157:H7 adherence to bovine epithelial cells [215] and they are an effective target in developmental cattle vaccines to limit EHEC O157:H7 excretion from cattle [216].

Other bacterial factors shown to facilitate bacterial adherence to host cells are fimbriae, hair-like structures projected from the bacterial cell. Most fimbrial genes are encoded on the chromosome. EHEC O157:H7 has been shown to produce haemorrhagic coli pili (HCP) which are associated with the type four pilus type and are implicated in forming connections between the bacteria and host cells via their long, bundled polar structure[217]. In addition, HCP is also a potent inducer of pro-inflammatory cytokines including Interleukin-8 (IL-8) and Tumor Necrosis Factor-alpha (TNF- α), thereby possibly contributing to haemorrhagic colitis [218]. The long polar fimbriae (Lpf) 1 is the EHEC O157:H7 homologue of the Lpf expressed by *Salmonella enterica* serovar *typhimurium*, an adhesin promoting adherence to the human intestine particularly at the Peyer's patch epithelium [219, 220]. Lpf1 has been implicated in promoting EHEC adherence to epithelial cells by interacting with the fibrinogen, collagen IV and laminin of Caco-2 and HeLa cells [221]. Similarly, curli, another adhesin composed of aggregated thin fibers, is also capable of interacting with the extracellular matrix of T84 cells and significantly contributes in EHEC binding to abiotic surfaces and lettuce leaves [220]. There are also the F9 fimbriae and the *E. coli* common pilus (ECP) also known as Mat fimbriae. The F9 fimbriae enhanced EHEC O157:H7 colonisation in the colon of young calves but not to bovine gastrointestinal explant tissue [222]. Mutation in the genes encoding for F9 fimbriae resulted in a reduced shedding of EHEC O157:H7 in calves, but the strain was still able to colonise the rectal epithelium suggesting that the fimbriae is not

implicated in the rectal tissue tropism. On the other hand, ECP is critical for EHEC O157:H7 adherence to HEp-2 and HeLa cells. The expression of ECP is enhanced in a low oxygen, high carbon dioxide environment, similar to that in the intestinal lumen [223]. Interestingly, many of the fimbrial operons present in EHEC O157 appear to contain deletions indicating this serotype has lost the potential to express many common fimbrial types, including functional type 1 fimbriae; this has been proposed to contribute to the specific tropism of the organism in cattle as it may not have the capacity to easily adhere at other sites [13, 224].

1.7.4 Plasmid encoding virulence factors

The large virulence plasmid O157 or pO157 is a 92kb plasmid detected in most EHEC strains [225]. It encodes for EHEC-haemolysin, a type two secretion system (T2SS), catalase-peroxidase and a serine protease. The EHEC haemolysin is thought to contribute to EHEC virulence by providing iron upon interaction with haemoglobin [226]. T2SS contributes to EHEC pathogenicity by promoting adherence, in particular the secreted protein YodA, shown to be important in EHEC adherence to HeLa cells [227]. StcE, a zinc metalloprotease is also secreted via the T2SS and has been shown to remove glycoprotein 340 from the surface of host intestinal epithelial cells, reducing the viscosity and function of the protective mucus layer over the epithelium. This potentially allows intimate attachment of EHEC O157:H7 to the intestinal epithelial cells [228]. KatP, a bifunctional enzyme with catalase and peroxidase activities, is also encoded by pO157 and provides protection of the bacteria from oxidative stress [229]. The extra-cellular serine-protease (EspP), a member of the serine protease autotransporters of Enterobacteriaceae (SPATE) is secreted by EHEC O157:H7 via the plasmid encoded type V secretion system during the early phases of infection [230]. EspP was associated with actin remodelling for the formation of the A/E lesion [231] and recently was shown to target the protocadherin-24 and mucin-2, resulting in EHEC O157:H7 attachment to the intestinal epithelial cells and microvilli effacement in human stem cell-derived colonoids [232]. In human patients, it was reported to be associated with haemorrhagic intestinal mucosa [233] while in calves, EspP may be able to positively influence the intestinal colonisation by EHEC O157:H7 [234].

1.8 Diagnosis of EHEC infection

Sorbitol MacConkey supplemented with Cefixime and Tellurite (CT-SMAC) agar has been routinely used to facilitate the selection for the growth of EHEC O157:H7 colonies which appear as colourless round colonies measuring from 2-3mm in diameter [16]. The suspected EHEC O157:H7 colonies are then confirmed by a Latex agglutination test, where latex beads coated with anti-O157 immunoglobulin are used. In instances where the nature of the sample prevents sufficient amount of colonies to be isolated, the sample can be first cultured in enrichment broth and immuno-magnetic separation (IMS) carried out using magnetic beads coated with antibody to increase the chances of detection [235, 236]. This can then be followed up by plate-based detection as above. Another phenotype that can be assessed is the ability to produce Shiga toxins (Stxs), the primary virulence factors associated with EHEC O157 pathology in humans. Shiga toxin (Stx) can be semi-quantified by Enzyme-Linked Immuno-Assay (ELISA) kits or testing the supernatants from a bacterial culture on African Green Monkey Kidney (Vero) cells, known to be highly sensitive to the toxic activity of Stx [237]. Epidemiological studies often adopt phage typing to group EHEC O157:H7 based on the sensitivity of the isolates to a standardised group of bacteriophages designated with numbers, resulting in a particular isolate being sensitive to a certain phage type classified as PT, followed by the group number of bacteriophage that the isolate is sensitive to. Pulse Field Gel Electrophoresis (PFGE) is also used to confirm for the presence of EHEC O157:H7 in the samples, however recent advances in pathogen detection had allowed for a more accurate, reliable molecular-based analyses such as microarray assays, Next Generation Sequencing and Whole Genome Sequencing [238, 239].

1.9 Aims of the thesis

1.9.1 Shiga toxin in EHEC O157:H7 colonisation of the intestine

It is already well established that Stx is the cardinal virulence factor expressed by EHEC O157:H7 that is implicated in the more severe disease manifestations in humans [240]. Moreover the presence of *stx2* gene distinguishes the virulence levels particularly between EHEC O157:H7 isolates recovered from humans and cattle [11, 77]. The presence and persistence of EHEC O157:H7 were also correlated to lineage type with better colonisation observed in human-biased isolates (lineage I), which was enhanced in the presence of Stx2 [78, 241, 242]. It was also identified that the two lineages contained differences in the Q anti-terminator gene found upstream of the *stx2* operon [10], however it is unknown if this is the primary factor triggering different levels of virulence between strains belonging to the two lineages. The role of Stx during EHEC O157:H7 colonisation of the asymptomatic bovine intestine however remains ambiguous [241, 243-245] and forms the first aim of this thesis to investigate the role of Stx at the bovine terminal rectal epithelium the during EHEC O157:H7 colonisation. To achieve this, Chapter 2 attempted to fill the knowledge gap in the Gb3 status at the bovine terminal rectum, followed by *in vitro* assays employing intestinal epithelial cells to investigate the effect of Stx on epithelial cell growth and proliferation. This is based on previous findings that the synthesis of Gb3 is regulated by the eukaryotic cell cycle and other published articles suggesting that the toxin interrupts the viability and proliferative aspects of intestinal epithelial cells [246-249]. An arrest at certain phases of the cell cycle may provide an advantage to EHEC as this could potentially extend the life span of the differentiated, matured enterocytes residing at the tip of the rectal crypts colonised by the bacteria. The importance of surface Gb3 expression and other factors in mediating cytotoxicity towards Stx are also discussed.

The next main aspect of my study shifted the focus to a broader view by investigating the consequences of an O157:H7 infection to several subtypes of immune cell populations within the bovine terminal rectal mucosa [250]. It is not

known how these sub-populations that lie closely under the epithelial mucosa specifically respond to EHEC O157:H7 colonisation at the rectal site. This set up the aims for the third chapter of this thesis; to compare bovine terminal rectal mucosal immune response between calves challenged with different EHEC O157:H7 types expressing different combination of Stx, against samples from unchallenged, control animals. Chapter three presents results derived from post-mortem samples of calves challenged with two different bovine EHEC O157:H7 strains, EHEC O157:H7 Strain 9000 (PT21/28) and EHEC O157:H7 Strain 10671 (PT32), with the former strain possessing an extra Stx2a phage in addition to Stx2c phage (also present in PT32), associated with very high levels of shedding from the bovine host [60, 251]. It was anticipated that there will be different levels of immune responses between non-infected and infected animals based on previous studies reporting for Stx1-mediated immuno-modulation in cattle [252, 253]. The presence of increased interferon-gamma (IFN- γ), a predominant cytokine indicative of a cellular response to EHEC O157:H7 colonisation led to *in vitro* assays examining if IFN- γ is able to interrupt intestinal epithelial cells proliferation, which was shown to occur in the intestinal crypt cells in rats [254]. The findings could contribute to a better understanding of the interactions that occur among the intestinal epithelial cells and the underlying immune cells residing within the lamina propria at the principal site of EHEC O157:H7 colonisation in cattle.

1.9.2 Shiga toxin-encoding bacteriophages and EHEC O157:H7 colonisation of the intestine

The following chapter focused on the bacteriophages encoding for Stx during EHEC O157:H7 colonisation of cattle intestine. Stx phages are major drivers of evolution in the emergence of new pathogenic strains of EHEC O157:H7 [98]. It has been described that Stx phages are involved in regulating virulence levels and colonising capacities according to the niche being occupied, for example the bovine-biased isolates are able to withstand the adverse acidic environment in bovine gut better than human-isolates [11, 79]. Chapter 4 aims **to understand how possession of different Stx phages by EHEC O157:H7 strains could impact on bacterial colonization- and virulence-associated traits.** The availability of bovine associated

strains belonging to PT21/28 (Strain 9000) and PT32 (Strain 10671) with their isogenic Stx-phage mutants allowed assessment of specific phenotypes, namely: competitive growth, total Stx production, epithelial binding and virulence assessed in a larvae model (*Galleria mellonella*). The environment in which the bacteria colonise the bovine terminal rectum is complex with the presence of thick mucus lining to provide early protective barriers against incoming threats. Assays in Chapter 4 utilised mucus harvested from the terminal rectum of calves as a growth medium for EHEC O157:H7 strains, allowing assessment of the bacterial phenotypic traits associated with colonisation and virulence in an environment that is less artificial than the common growth media used routinely in the laboratory. Moreover, the presence of *stx* genes within the chromosome of EHEC O157:H7 next to the genes regulating mucin (large glycoproteins of the mucus with 80% comprising of carbohydrates including N-acetylgalactosamine, N-acetylglucosamine, galactose, fucose, sialic acids, mannose) metabolism suggests an interaction between the genes which might provide growth advantage to the bacteria leading to significant differences between Stx phage+ and Stx phage negative strains [255]. Recent unpublished work [256] has established the growth curves of the same bovine strains in 10% bovine terminal rectal mucus, with evidence that EHEC O157:H7 Strain 9000 (PT21/28) had a faster growth rate than Strain 10671 (PT32). It was anticipated that the observations obtained at the end of Chapter 4 would strongly reflect the type of Stx-phage carried by the strain, with the presence and expression of the *stx2a* genes in Strain 9000 PT21/28 providing growth advantage in the bovine and probably human intestines, enhanced toxicity to epithelial cells and therefore virulence upon transmission into human hosts. This may further clarify why Stx-phages are strongly retained in the bacterial chromosome throughout the evolution of EHEC O157:H7 particularly in successfully propagated, pathogenic strains. Information on the binding of these bovine associated EHEC O157:H7 isolates to epithelial cells would greatly enhance the current understanding on the already complex regulatory network governing bacterial adherence to eukaryotic epithelial cells, particularly in assessing the association between Stx-encoding phages and the T3SS expression. Lysogeny of EHEC O157:H7 was shown to repress LEE expression resulting in reduced ability to bind to host cells [257] which conflicts with

the expectation that Stx-phage possessing strains are superior in colonization which is reflected by the binding capacity. However the LEE repression was observed in artificial laboratory medium compared to the bovine terminal rectal mucus and therefore was tested in the current study. It may be that different combination of Stx-encoding prophages function to control the balance of strategies for the bacterial host to colonise, propagate and transmit to susceptible hosts.

In summary, the early chapters (Chapter 2 and 3) examine the role of Shiga toxin bovine intestinal colonisation, by investigating several components present at the terminal rectum that might be the target for the toxin to enhance bacterial colonisation. Chapter 4 focuses on the Shiga toxin-encoding bacteriophages and how they could influence important colonisation phenotypes of the host, EHEC O157:H7 organism. Chapter 5 provides a general discussion of the main findings and draws some conclusions about the contributions Stx and the phages that encode them to EHEC O157 colonisation of the bovine host.

Chapter 2:

Assessing the significance of Shiga toxin interaction(s) with Gb3 at the bovine intestinal epithelium during EHEC O157:H7 colonisation

Chapter 2

Introduction

2.1 Gb3 distribution in humans and cattle

Following the identification of the bovine terminal rectum as the principal EHEC O157:H7 colonisation site, no literature to date has studied the presence of Gb3 at the bovine terminal rectum. To address this knowledge gap, part of this chapter is aimed at investigating Gb3 expression and localisation among cells at the bovine terminal rectum as this may be one of the factors potentially contributing to the presence and maintenance of EHEC O157:H7 colonisation in cattle. Differential Gb3 distribution between humans and cattle have been postulated as one of the possible reasons why cattle do not show clinical symptoms as those described in EHEC O157:H7-infected humans.

Human renal tissue contains zones rich in Gb3 expression associated with Stx-induced injuries observed in patients with diarrheagenic HUS particularly on microvascular endothelial cells of the glomeruli, as well as the proximal and distal tubular epithelial cells and mesangial cells [7, 258-260]. Extra-renal Gb3 distribution in humans has also been described in the neurons [261] and blood vessels of the central nervous system [262]. Human intestinal epithelial cells do not express Gb3, rather the Stx receptor was detected on the microvascular endothelium of the lamina propria [263] and on intestinal pericryptal myofibroblasts [161]. By comparison, the Gb3 receptor is not present on the murine renal glomeruli [264], but is expressed by the murine epithelial cells of the distal colon [265] and endothelial cells of the brain [266]. Whereas Gb3 is highly expressed by the villous intestinal epithelial cells in rabbits, particularly of more than 16 days of age and correlates to the Stx enterotoxicity in rabbits that is associated with an inhibited sodium ion absorption [267]. Certain human immune cell populations have also been identified to express Gb3, including monocytes, activated platelets and germinal tonsillar B cells [122, 268, 269].

In cattle, Gb3 was not detected in the bovine intestine according to a study [270], while others have reported the presence of Gb3 positive cells associated either with bovine colon epithelial crypts [142] or bovine mesenchymal-derived (non-epithelial) regions [271, 272]. Primary bovine colon epithelial cell cultures harbour a

subset of Gb3-positive cells, however the receptor was identified to not be surface expressed, rather the receptor was shown to be localised intracellularly, conferring resistance against the cytotoxic effects of Stx1 and perturbations in the chemokine expression profile [272]. Diversion in Stx1 trafficking in the cytosol where Stx1 was localised into the lysosomes upon internalisation rather than following the retrograde route to the ribosome via the Golgi apparatus and endoplasmic reticulum were thought to account for the resistance of bovine colonic crypt epithelial cells to Stx1-induced cytotoxicity [142, 273].

Bovine intra-epithelial leukocytes (IEL), B cells and mucosal macrophages are among the non-epithelial, mesenchymal-associated cells shown to express Gb3 [253, 271, 272, 274]. Nearly 15% of bovine distal ileal intra-epithelial leukocytes (IEL) were Gb3-positive, predominantly CD3⁺ CD6⁺ CD8 α ⁺ T lymphocytes along with only a small proportion of CD4⁺ and B cells. Transformation of these cells to large blast cells was halted when exposed to Stx1 [275]. Mucosal macrophages, a term introduced by Stamm et al. (2008) to describe the Gb3 positive cells co-expressing vimentin (mesenchymal cell marker), are present within the lamina propria of the bovine colon and these were shown to succumb to the cytotoxicity effect of Stx1 [272]. Bovine CD8⁺ cells from peripheral blood mononuclear cells (PBMC) were also able to express Gb3 following mitogenic stimulation with phytohaemagglutinin, lipopolysaccharide and pokeweed mitogen [274]. In addition, Stx1 blocked the proliferation of bovine CD8⁺ and CD21⁺ lymphocytes of the PBMC [252].

2.2 Gb3 as a determinant for Stx cytotoxicity

The association between Gb3 presence and Stx cytotoxicity in different immortalised cell lines frequently used in *in vitro* studies were also assessed in this chapter. Although most of the cell lines used in my study have already been investigated for the expression of Gb3, recent findings suggest that these immortalised cell lines could respond differently to the toxin as a result of heterogeneous Gb3 expression across the same cell line in different laboratories [276]. This chapter will present and discuss the findings from different immortalised

cell lines (some of which are routinely used in Chapter 3 and Chapter 4) tested for both Gb3 expression and sensitivity towards Stx. Gb3 is generally regarded as a determinant for eukaryotic cells to succumb to the cytotoxic effects of Stx (Gb3 expression [133] where Gb3 organisation within the plasma membrane of the host cell (e.g. lipid rafts) [135, 136] as well as the composition, length and saturation status of the hydrocarbon and fatty acid chain of Gb3 contributes to the binding and internalisation of the toxin by the cell [131, 132]). Despite this, pre-incubation of cells with Gb3 were shown to not be able to protect Vero cells from Stx2 cytotoxicity which lead them to suggest that Stx potency depends on more than just the presence of Gb3 [112, 191]. This includes the type of host cell (e.g. human microvascular endothelial cells or human macrovascular endothelial cells) [188], Stx subtype [69] and genotype [277], Stx affinity towards Gb3, toxin stability and binding mode [278], the structure of the toxins particularly the A subunit [279], intracellular trafficking of the A subunit [158] and the furin cleavage of the A subunits into A1 and A2 fragments for maximal toxin potency [280].

2.3 The mechanism of actions of Stx-induced cytotoxicity

The death of eukaryotic cells following exposure to Stx is thought to occur following depurination of the 28S rRNA of the ribosomal unit 60S component by the A1 fragment of the A subunit leading to protein synthesis inhibition. Injury to the renal microvascular endothelial cells is believed to be central to the development of HUS pathogenesis however details on the exact mechanism(s) linking protein synthesis inhibition and cellular death in these cells remains ambiguous. Several forms of cellular death have been described including apoptosis, necrosis, autophagy, anoikis and excitotoxicity [281, 282]. Apoptosis, a highly conserved mechanism in eukaryotic cells mediated by a family of cysteine proteases, Caspases, removes unwanted or defective cells via a sequence of events leading to cellular disintegration within an intact membrane plasma [283] and was suggested as the death pathway upon exposure to Stxs [156, 248, 249, 258, 284, 285]. The following paragraphs provide a brief review on Stx and apoptosis in different types of eukaryotic cells.

A study on the cytotoxicity of Stx1 towards human glomerular endothelial cells resulted in a reduction in cell viability particularly among sub-confluent proliferating cells. Enhanced Stx1 toxicity was observed after stimulation of the glomerular endothelial cells with the pro-inflammatory cytokine, tumor necrosis factor-alpha (TNF- α) via upregulation of the toxin receptor, Gb3 [286]. Another study exposed rat primary glomeruli endothelial cells to Stx1 resulting in pathologic changes resembling those observed in human HUS however the lesions described were associated more with changes in the glomerular endothelial cell adhesion to the basement membrane and production of procoagulant vasoconstrictor arachidonic acid metabolites causing a significant increase in cell retraction and gap formation in the monolayer, rather than protein synthesis inhibition or reduction in cell viability [287]. Stx stimulation of primary human umbilical vein endothelial cells (HUVEC) lead to both protein inhibition and apoptosis, however the authors argued that these two events occurred by separate pathways as protein synthesis inhibition by cyclohexamide did not caused apoptosis or enhanced Stx cytotoxicity [285]. Protein synthesis inhibition and apoptosis induction were thought to occur via distinctive pathways since Stx1 was able to inhibit mitogenesis and protein synthesis without affecting the viability of human glomerular mesangial cells.[286].

In non-renal cell types, numerous reports have been published on Stx induction of cellular death via apoptosis. Stx purified from EHEC O157:H7 Strain EDL 933 were inoculated into rabbit ileal loops resulting in death by apoptosis of the mature, differentiated columnar absorptive epithelial cells [288]. Bhattacharjee et al demonstrated that Stx1 was able to mediate apoptosis in HCT116 human colon cancer cells by inducing overexpression of the growth arrest and DNA damage (GADD) family of genes leading to cell cycle arrest at the S phase [289] (refer Figure 2.1 for a brief description on eukaryotic cell cycle). Stx1 incubation of HCT-8 cells (human colon carcinoma cell line) resulted in apoptosis via caspase 3 cleavage and DNA fragmentation [156]. The authors proposed that exposure to Stx1 resulted in ribotoxic stress response accompanied by increased levels of C-X-C chemokines including Interleukin-8 (IL-8), leading to the activation of the c-Jun (NH-2)-Terminal Kinase (JNK)/stress-activated protein kinase (SAPK) and p38 MAPK pathways

which in turn triggered apoptosis [156]. Treatment of HEp-2 cells with Stx1, Stx2 and Stx2c induced apoptosis via activation of caspase-8 which eventually affects the Bcl-2 proteins (family of anti-apoptotic and pro-apoptotic proteins involved in controlling cell concomitant with apoptosis) and activation of caspase-9, resulting in apoptosis [249].

In contrast, purified Stx2 from an EHEC O157:H7 strain prevented the spontaneous apoptosis of human neutrophils, thereby increasing the life span of the neutrophils to exert more damage to the surrounding tissues [290]. These observations suggests that Stx types are able to exert differential effects based on the type of host cell that the toxins encounter.

Apoptosis is also regulated by genes involved in cell cycle progression [291] and it has been suggested that some of the cell cycle regulatory effectors (Figure 2.1) may sensitise the cells to apoptosis, depending on the cellular context [292]. Toxins produced by certain bacteria are able to interrupt the eukaryotic cell cycle [293]. Examples include subtilase cytotoxin of STEC which was shown to degrade BiP (a member of the hsp70 family of stress-regulated proteins) causing downregulation of cyclin D1 leading to cell cycle arrest at G1 in Vero cells [294]. Another example is the cytolethal distending toxin of the sorbitol fermenting EHEC O157:H⁻ which causes irreversible G2/M arrest [295]. It is not known if Stx is able to contribute to EHEC O157:H7 colonisation *in vivo* at the bovine intestine by interfering with the life cycle of the intestinal epithelial cells, although most *in vitro* work described above suggested differential effects of Stx depending on the type of cell that internalises it. The following section introduces the final aspect investigated in this chapter in relation to assessing the effect of Stx on epithelial cell viability via cell cycle and proliferative assays.

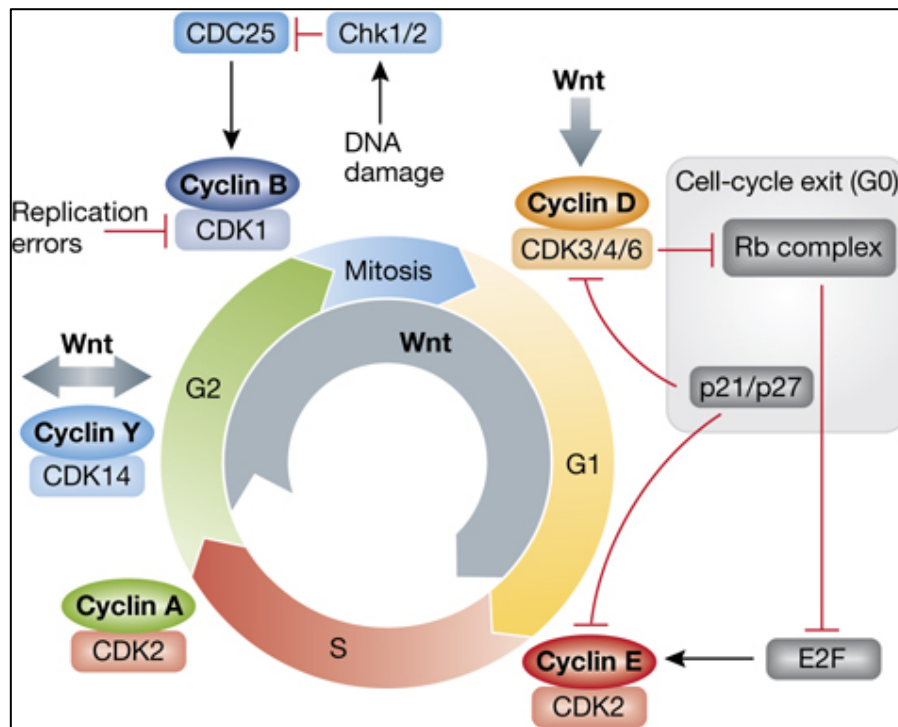


Figure 2.1 The cell cycle regulation, taken from Niehrs and Acebron [296]. The cell cycle is a highly regulated process involving a family of protein kinases named cyclin-dependent kinases (CDKs) [297]. Cyclical changes in CDK levels are mostly under the control of cyclins [298]. Binding of cyclins to specific CDKs forms the cyclin-CDK complex which then activates protein kinase activity and triggers cell-cycle events. CDK activity ends upon cyclin degradation. Cyclin classes are present at these checkpoints: i) G1/S phase-cyclins which commits the cell to DNA replication, ii) S-phase cyclins required for DNA replication initiation and iii) M-phase cyclins which promotes mitosis [292]. In G1, cyclin D initiates Rb complex phosphorylation, which derepresses E2F to induce cyclin E transcription. Components of this complex as well as p21 and p27 oppose these effects and can result in cell-cycle exit to G0. After DNA replication in S phase, different quality controls ensure the integrity of the DNA, while a cyclin B/CDK1 complex orchestrates progression into mitosis. Chromosome abnormalities and DNA damage are reported to this complex via different pathways to delay or stop cell division [296]. Canonical Wnt signalling can regulate the cell cycle at the indicated levels, along with other pathways described in Fig. 2.2.

2.4 Stx and intestinal epithelial cell proliferation

The intestinal stem cells consistently proliferate at a high rate to rapidly restore depleted intestinal cells under normal circumstances or in response to injury and infection [299] (Fig. 2.2). It was estimated that the turnover of bovine terminal rectal epithelial cells is four days before sloughing off [300, 301]. Studies have also indicated that susceptibility of a cell to the toxin is correlated with certain phases of the eukaryotic cell cycle [246, 302]. It was identified that Stx1 bound to Gb3 on Vero cells only between the cell cycle phases of G2 to the telophase in mitosis, which correlated with maximal synthesis and expression of the glycosphingolipid receptor during the two phases mentioned [246]. It seems that Gb3 is surface expressed even before exiting the cell cycle via differentiation. It is most likely that the synthesis of Gb3 is partly dependent on butyrate, a volatile fatty acid normally present in mammalian intestinal lumen which is also a known inducer for cellular differentiation [303]. It is not known whether butyrate availability in bovine gut would have an impact on Gb3 expression *in vivo* during an EHEC O157:H7 presence [246, 304, 305]. Different feeding protocols aiming at reducing the transmission of pathogenic *E. coli* from cattle to humans have been tested, some regimes of which were thought to reduce bacterial survival by altering the intestinal luminal fermentation conditions which directly affects volatile fatty acid concentrations, intestinal lumen pH and microbiota composition, all of which are required by the colonising bacteria [306, 307]. Another strategy to reduce the risk of bacterial survival and transmission to humans is by accelerating the proliferation rate of intestinal epithelial cells by manipulating cattle diet and shown to facilitate the clearance of EHEC O157:H7 from the bovine gut [308]. From one point of view, Stx may be useful to bacterial colonisation if, for some reason, it is capable of halting the cell cycle of the daughter cells progressing up the crypt-luminal axis at the terminal rectum, thereby delaying the expulsion of bacterial-attached cells into the lumen. It has been previously reported that *Salmonella enterica* serovar *Typhimurium* is able to modulate the murine intestinal stem cells niche via its type three secretion system effector, AvrA which activates the beta-catenin/Wnt signalling pathways leading to an increased in cellular proliferative activity, showing that certain bacterial-secreted factors are capable of affecting epithelial layer homeostasis [309].

From a study that supported a role of Stx in positively influencing EHEC O157:H7 colonisation in both HEp-2 cells and mice intestine, the authors showed that the enhanced binding capacity of the bacteria was most probably due to the upregulated presence of Nucleolin following exposure to purified Stx2 at the cellular surface coinciding with bacterial attachment [241]. Nucleolin is the major nucleolar protein of growing eukaryotic cells associated with the intranucleolar chromatin and pre-ribosomal particles. It functions to induce chromatin decondensation and plays a role in pre-rRNA transcription and ribosome assembly. Nucleolin is also ubiquitously distributed in the nucleus and sometimes cytoplasm of eukaryotic cells [310]. The mechanism linking Stx and nucleolin is still unknown, however the authors stressed that both proteins have similar affinity for ribosomal RNA. Secondly, nucleolin could be upregulated at the cellular surfaces of the bacterial bound cells as part of the cellular stress response to intoxication during pre-apoptotic stages. By upregulating nucleolin at the bacterial binding site within the cellular surface, it could also be speculated that Stx could target and manipulate eukaryotic proteins closely associated with the cell cycle machinery to the advantage of EHEC O157:H7 colonisation in the intestine.

DNA staining by propidium iodide (explained further in Chapter 2, Materials and Methods section 2.15) is a commonly used method to check for the distribution of cells across the different phases of the cell cycle [291]. This method was applied to experiments in this chapter on intestinal epithelial cells treated with Stx2, in addition to staining for the proliferating cellular nuclear antigen (PCNA), a commonly used marker for detecting proliferating cells [311].

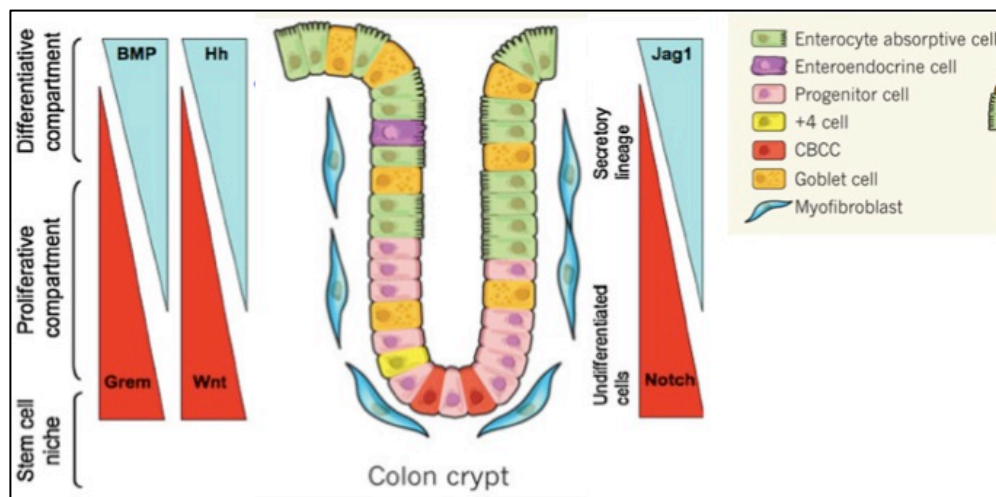


Figure 2.2 Components of the proliferative-differentiative crypt-luminal axis of the colon epithelium, modified from Medema et al. [312] and Kosinski et al [313].

All of the cell lineages of the intestinal epithelium originated from cells of the stem cell niche, the crypt base columnar cells (CBCC) and the +4 stem cells (stem cell markers identified in human and mice). Transiently-proliferating progenitor cells arise from the stem cells that moves up the crypt and differentiate into either: absorptive enterocytes, enteroendocrine cells, mucus-secreting goblet cells, Tuft cells (produce opioids and enzymes for prostaglandin synthesis) [314] in the small intestine and the M cells (reviewed in Chapter 3, Introduction section 3.11). Note the absence of the extended villi structure at the top of the colonic crypt, one of the feature that differentiates between the large and small intestines. Following differentiation, most of the matured cells will move up to the lumen before being shed (estimated around four days in the bovine gut) and expelled. Myofibroblasts are an integral component of the stem cell niche secreting factors that regulate intestinal stem cell function, including those belonging to the proliferation pathways; i) Wnt (Wingless integrated signalling pathway) ligands [315], ii) BMP (bone morphogenetics proteins) antagonists, such as Gremlin 1 and iii) the Notch pathway (proliferation of undifferentiated secretory lineage) proteins [316]. The Wnt protein family and BMP antagonists are expressed in a reciprocal gradient to the pro-differentiative, anti-proliferative bone morphogenetic proteins (BMP, blue circles) and Hedgehog (Hh, yellow squares) protein families along the crypt–villus axis. Hh is expressed by differentiated colonocytes and limits expression of Wnt target genes to the base of the crypts. Activation of Hh increases BMP signalling and inhibits the Wnt pathway. Myofibroblasts are Hh responsive and regulate the patterning of the crypt–villus axis. Inhibition of the Notch pathway leads to the differentiation of stem cells into the secretory lineage. The Notch ligand Jagged-1 is expressed in a reciprocal manner to the Notch-1, -2 and -3 receptors [313, 316]. In the small intestine, the highly specialised epithelial Paneth cells, are present at the bottom of the crypt areas and secretes various antimicrobial peptides and proteins. The Paneth cells also secrete factors involved in modulating the epithelial stem and progenitor cells of the small intestinal epithelium [317].

The questions raised in this chapter as well as the rest of the thesis are important as limited information is available on events taking place during colonisation of the bovine terminal rectum by EHEC O157:H7, particularly the lack of knowledge on the status of Gb3 expression at the principal EHEC O157:H7 colonisation site and Stx production *in vivo* (if produced, at what quantity and how this affects the host and bacterial survival, refer Chapter 4). This chapter also explores other potential roles that could be ascribed to the repertoire of Stx functions in the mammalian gut, particularly on epithelial proliferating homeostasis. The objectives for this chapter were:

1. To examine bovine terminal rectal mucosa for any presence of Gb3 by flow cytometry and fluorescence microscopy. In both methods, co-staining with epithelial or mesenchymal cell markers were undertaken to allow identification of Gb3 expressing cell types from a heterogeneous population
2. To assess the association between Gb3 surface expression on different immortalised cell lines, some of which had or had not been reported for Gb3 presence, and sensitivity towards Stx2
3. To investigate if Stx2 influences the proliferation and subsequently cell cycle of intestinal epithelial cells by
 - a. Comparing the levels of a proliferative marker, Proliferating Cellular Nuclear Antigen (PCNA) following epithelial cell exposure to Stx2
 - b. Comparing the propidium iodide (PI)-DNA staining profiles of intestinal cell lines stimulated with Stx2

Chapter 2

Materials and methods

2.1 Routine cell culture techniques

All of the continuous cell lines used were maintained at 37°C, in an incubator with 5% CO₂. Typically, the cells were revived from the liquid nitrogen-freezers prior to being propagated in the laboratory to check for viability before further use. Upon removing the cryotube containing cell suspension from the -175°C freezer, the cells were quickly thawed in a 37°C water bath before being transferred into a 10 ml Thermo Scientific™ Sterilin™ tube with screw cap containing 9 ml of complete cell culture medium (described below for each cell line). The cells were then centrifuged for 5 min, 260 relative centrifugal force (RCF or x g) (SciQuip, 3K15, Sigma Laboratory Centrifuges) before adding 5 ml of complete cell culture medium and transferred into a 25cm² tissue culture flask. The cells were visually inspected daily for viability and the medium changed every 3 days. Upon reaching full confluence, the cells were washed in phosphate buffered saline (PBS) before being dissociated from the flask using TrypLE™ Express enzyme, (12563029, Life Technologies) for 5 min at 37°C, 5% CO₂ before diluting the enzymatic activity in complete culture medium at least 1:2. The cells were then centrifuged for 5 min, 260 x g and sub-cultured in a ratio of 1:3, with a seeding density of 1x10⁴ cells/ml to 1x10⁵ cells/ml. Cells were counted using the TC20™ Automated Cell Counter (Bio-Rad), with 10 µl of cell suspension diluted in 0.2% Trypan Blue (17-942E, Lonza) added per chamber of the cell counting slide (Bio-Rad).

For long term storage, the cells were pelleted before being slowly re-suspended in cell freezing medium consisting of 70% of the basal medium specific to each cell line (mentioned below), 20% fetal calf serum (FCS) (F0643, Sigma) and 10% Dimethyl sulfoxide (DMSO) Hybri-Max™ (D2650, Sigma), 1 ml per cryotube which were then stored in cryogenic freezing container Mr Frosty™ (Thermo Scientific Nalgene) at -80°C overnight before transferring to the liquid nitrogen containing freezer (-175°C) for long term storage.

2.2 Vero cells

Y.Yasamura and Y.Kawakita of Chiba University, Japan successfully derived Vero cells from the kidney of an adult African green monkey (*Cercopithecus*) in 1962 [318]. These cells are well-characterised and are sensitive to a number of viruses and have successfully been used in development of vaccines, the poliovirus and inactivated rabies vaccines among others. The cells were purchased as Vero-B4 (ACC33) from the DSMZ German Collection of Microorganisms and Cell Culture, Leibniz Institute (Braunschweig, Germany). The cells were maintained in 90% Roswell Park Memorial Institute (RPMI)-1640 with HEPES modification (R5886 Sigma), 10% FCS, 1% Penicillin-Streptomycin (10,000 U/ml, 15140-122, Invitrogen) and 1% Glutamax™ (35050-038, Life Technologies).

2.3 Caco-2 cells

Caco-2 cells are a derivative of a human colon carcinoma. The line has been shown to express Gb3 and is sensitive to Stx and mimics the differentiated cells on the villi of the small intestine [305]. The cells were maintained in 90% Dulbecco's Modified Essential Medium (DMEM) (D5796, Sigma), 10% FCS and 1% Penicillin-Streptomycin and 1% Glutamax™.

2.4 T84 cells

The T84 is a human colon adenocarcinoma-originated cell line which resembles the human adult colonic crypt epithelial cells and therefore has less-developed brush border as compared to the Caco-2 cells. T84 cells were used as the 'Gb3-deficient' cell line in this study [305]. T84 cells were maintained in 50% DMEM, 50% Ham's F-12 Nutrient Mix (21765-037, Invitrogen), 10% FCS, 1% Glutamax™ and 1% Penicillin-Streptomycin.

2.5 HeLa cells

The HeLa cells were derived from the cervical cancer cells of Henrietta Lacks in late 1951 after she passed away [319]. Until present, these cells have been used in numerous studies across the world due to the cells being immortal and easy

to propagate in the laboratory. HeLa cells have been shown to be positive for Gb3 surface expression as the Vero cells in previous studies and have therefore been used in comparative studies of Stx activity [133, 320] These cells were maintained in the same complete culture medium as described above for Caco-2 cells (refer to section 2.3).

2.6 EBL cells

The Embryonic Bovine Lung (EBL) cell line was established from the lung of a 7-month old bovine fetus [321]. Since a well-characterised immortal cell line of the bovine intestine is yet to be established, EBL cells were included in this study owing to its epithelial-like phenotype and that the epithelial lining of the gastrointestinal tract and lungs are both derivatives of the same germ layer, the endoderm [322]. The complete cell culture medium used for the culture of EBL cells is as described above for Caco-2 and HeLa cells (refer to section 2.3).

2.7 Chinese Hamster Ovary (CHO)-K1 cells

The Chinese Hamster Ovary (CHO) cells were derived as a sub-clone from the parental CHO cell line initiated from a biopsy of an ovary of an adult Chinese hamster by T.T.Puck in 1957 . The cells are regularly used as a negative control for Gb3 expression experiments since they do not express Gb3 [323-325]. The cells were provided courtesy of Dr Carla Garcia-Morales, The Roslin Institute. The cells were maintained in 90% Ham's F-12 Nutrient Mix with 10% FCS, 1% GlutaMAX™ supplement (35050-061, Gibco®, Life Technologies) and 1% Penicillin-Streptomycin.

2.8 Bovine primary terminal rectal cell culture

The cells were prepared by Edith Paxton (Roslin Institute) according to the Cellular Microbiology Group standard operating procedures, CMG/SOP/01. Two to three cattle recta with intact anal canal were obtained from a local abattoir on the day of the procedure and were transported on ice in transport medium consisting of Hank's Balanced Salt Solution (HBSS) (55021C, Sigma) containing 25 mg/ml of

Gentamicin (G1396, Sigma) to the post-mortem room at the Royal (Dick) School of Veterinary Studies. The recta were flushed to remove faecal material within the lumen. A longitudinal dissection was made into the mucosal layer. The terminal rectum, defined as the distal 4 cm part from the recto-anal junction was identified and carefully removed from the underlying connective tissue and immersed in HBBS with 5 µg/ml Fungizone (15290-018, Invitrogen). The tissue samples were then brought into a Containment Level 2 (CL2) laboratory to continue the process. Excess mucus was gently scraped off using the sides of a clean glass slide to expose the epithelial lining of the rectal mucosa layer. A second scraping was then done, this time with more pressure to harvest approximately 15 g of scraped rectal mucosa and collected in 50 ml of HBSS. The tissue suspension was centrifuged at 260 x g for 2 min. After decanting the supernatant, the washing process was repeated until the supernatant was clear, with large tissue pieces remaining in the pellet. In order to release the epithelial cells, particularly the crypts, the tissue was then digested in 25 ml DMEM supplemented with 1% FCS, 1% Penicillin-Streptomycin (P4333, Sigma), 25 µg/ml Gentamicin (G1396, Sigma), 75 U/ml of Collagenase (C2674, Sigma) and 20 µg/ml of Dispase I Neutral Protease, Grade 1 (04942086001, Roche) at 37°C, 200 RPM for 80 min on a shaking incubator (INFORS HT Multitron Standard).

Repeated steps of a differential centrifugation process (260 x g, 2 min) were then carried out in HBSS containing 2% sorbitol to enrich the isolated crypts from large, undigested materials and fibroblasts. At the end of the process, crypts have been visualized microscopically from the pellet and re-suspended in early culture medium (97.5% DMEM, 2.5% FCS, 0.25U Insulin, 10 ng/ml Epidermal growth factor (EGF), 25 µg/ml Gentamicin) to approximately 1000 crypts/ml. 800 µl of early culture medium with approximately 500-700 crypts was added to each collagen-coated well of a 24-well-plate and 2 ml with approximately 1200-1400 crypts were added to the wells of a 6-well-plate. The cells were incubated at 37°C, at 5% CO₂. Twenty four hours post-seeding, the medium was replaced with complete culture medium (Minimum Essential Medium Eagle's (MEM)-D-valine (M3795, Sigma) containing 1% FCS, 0.25U Insulin, 10 ng/ml EGF and 25 µg/ml of

Gentamicin). The cells were monitored on a daily basis via observation under the light microscope, ensuring zero percent of contamination (bacteria, yeast) and minimal presence of fibroblast. The cells were cultured to about 60 - 70% of confluence level (approximately 3 days post-seeding), before proceeding with experiments.

2.9 Shiga toxin

The purified Shiga toxin 1 (PStx1) and purified Shiga toxin 2 (PStx2) were purchased from Toxin Technology, Inc., Sarasota, Florida (STX-1, lot # 110308V1, STX-2, lot # 111108V2). Both purified toxins were reported to have toxicity of greater than 10^7 Units per milligram (mg) and purity level of approximately 50% confirmed by sodium dodecyl sulphate polyacrylamide gel electrophoresis (SDS-PAGE). Upon arrival (delivery was under a strict process as Stx is under Schedule 5 regulations), the toxins were dissolved in PBS to produce laboratory stock solution of 10 µg/ml in PBS and stored at -80°C in a locked freezer.

2.10 Shiga toxin cytotoxicity assay

To assess the sensitivity levels of the continuous cell lines used in this study towards purified Stx variants, cytotoxicity assays were conducted. Vero, Caco-2, CHO, EBL, T84 and HeLa cells were cultured in flat-bottomed, 96-well-plate with approximately 1×10^5 cells per well and incubated as described above. Once a confluent layer has been formed, the culture medium was removed and replaced with serum-free medium containing either purified Stx1 or purified Stx2 (Toxin Technology, Inc.) diluted at 50 ng/ml, 100 ng/ml, 200 ng/ml and 400 ng/ml, with the exception of HeLa cells. Due to limited availability of the purified Shiga toxins, HeLa cells were treated with filtered lysates of bovine EHEC O157:H7 isolate Strain 9000 (possessing phages encoding for Stx2a/Stx2c) and its isogenic Stx2a and Stx2c-encoding phage mutant. A more detailed description on phenotypic characterisation and bacterial lysate preparation of these two EHEC bovine isolates are described in Chapter four (refer to Chapter 4, Materials and methods section 4.1 - 4.7). In brief, both EHEC O157:H7 Strain 9000 and its Stx2-phage negative mutant strain were grown in LB, for 18 h at 37°C, 200 R.P.M. The overnight cultures were then diluted

1:100 in fresh LB and left to grow until the optical density (O.D.) 600nm reading reached 0.2-0.25. 10 µg/ml of Mitomycin C (MMC) was added into the cultures to induce crosslinking of the deoxyribonucleic acid (DNA) of the bacterial cells thereby maximising the levels of Stx production and release from lysed bacterial cells (lysate). The MMC-supplemented cultures were further incubated overnight and filter-sterilised (Millex® GV-syringe filter unit membrane, pore size 0.22 µm, Merck Millipore) to collect cell-free lysate containing Stx (for EHEC O157:H7 Strain 9000). The filtered-lysates of Strain 9000 (Stx positive) and Strain 9000 $\Delta\Phi\text{Stx2a}/\Phi\text{Stx2c}$ (Stx negative) were then diluted in DMEM (1:100) before being added to HeLa cells. Negative control cells received serum-free media (or LB in serum-free media for HeLa cells) while positive control cells were treated with 0.1% Triton™ X-100 (T8787, Sigma). The cells were placed in the incubator at 37°C, 5% CO₂ for a maximum of 72 h. Daily checks of the cells were performed by observing the cells under light microscopy to determine if the cells were already responding to the toxin. After 72 h, the toxin containing serum-free media was discarded and the cells were gently washed in pre-warmed PBS (37°C) once.

65 µl of 2% formalin in PBS was added to each well for 1 min at room temperature to fix the cells. The fixative was replaced with 65 µl/well of crystal violet tissue culture stain (52 ml of 0.5% crystal violet (Sigma), 10 ml of absolute ethanol, 10.8 ml of 37% formaldehyde and 127.2 ml of PBS) and incubated at room temperature for 24 h. The fixed cells were then washed gently with distilled water until the water appeared clear and were air-dried. The plate was scanned for visual record. 100 µl of 10% acetic acid was added per well and the plate was placed on an orbital shaker for 15 min at room temperature to dissolve the crystal violet stain. The values of absorption at O.D. 595nm were obtained using a plate-reader (FLUOstar OPTIMA, BMG Lab technologies) and analysed within Microsoft® Excel.

2.11 Flow cytometry

2.11.1 Flow cytometry buffer

The buffer consists of 2% FCS in PBS prepared fresh prior to the start of each experiment.

2.11.2 Immuno-staining

In general, upon cell harvesting, the cells were centrifuged at 260x *g* (SciQuip model 3K15, Sigma Laboratory Centrifuges) for 5 min and suspended in flow cytometry buffer (volume depends on the size of pellet obtained, could range from 2 ml to 10 ml). The cells were then distributed accordingly into wells of a 'v'-bottom shaped, 96-well-plate. The cells were washed again at 1200 R.P.M. (Jouan BR4i Multifunction Centrifuge, Thermo Electron Cooperation) for 2 min; the supernatants were removed and re-suspended in primary antibody solutions or flow cytometry buffer, at the appropriate concentrations. The cells were kept at 4°C for 30 min, covered with aluminium foil if the primary antibody used were directly conjugated with fluorochrome. This was followed by two washes in flow cytometry buffer as described before incubating the cells with the appropriate conjugated secondary antibody(s) for 20 min at 4°C, protected from direct light. The cells were then washed as described for at least three times before adding 100 µl of the buffer into each well and transferring the cells into a labelled flow cytometry tube containing 400 µl of flow cytometry buffer.

For intracellular staining which required the cells to be permeabilised, cells were added with BD Cytotfix/CytoPerm™ reagent (554722, BD Biosciences) and incubated at 4°C for 20 min, protected from light before washing twice with BDPerm/Wash™ buffer (554723, BD Biosciences) (diluted 1:10 in distilled water). This was followed by the similar procedure for antibody staining as described above, with the exception of the buffer used to dilute the antibody(s). The antibody(s) were diluted in 1x BDPerm/Wash™ buffer, at the appropriate concentrations. All of the washes were also done using the 1x BDPerm/Wash™ buffer to maintain the cell

membrane in a permeabilised state. For instrumental settings of the flow cytometry machine, three types of controls were routinely used. This includes unstained cells, single stained cells of all the antibodies being used and cells that were stained with only the secondary antibody(s). The unstained cells were washed or suspended in flow cytometry buffer throughout the whole cell immune-staining procedure.

2.11.3 Data acquisition and analyses

The stained cells were acquired through the BD FACSCalibur™ (BD Biosciences) according to the general protocol of running the machine. The instrument settings were adjusted by its ampere and voltage gain so as to bring the population of cells of interest to be in the middle of the Forward Scatter (FSC)-Side Scatter (SSC) dot plot. Histograms of the appropriate channel for each fluorochrome-conjugated-antibody(s) and two-colour dot plots were also plotted to perform compensation later on if necessary. Typically, 10,000 events within the gated region were collected across all samples. In the event of fewer cells available, as experienced when running bovine primary rectal cells, the total events acquired within the gated region was reduced to 5,000 cells. All acquired data were saved onto the network drive before analysis with FlowJo software (Treestar, Inc.).

The antibodies (Table 2.1) were tested on cell lines that were either already established to be positive for cell surface Gb3 expression: Vero, Caco-2, T84, CHO, EBL and HeLa cells (Vero, Caco-2 and HeLa cells were previously regarded as Gb3 positive cells, while T84 and CHO cells are regarded as the Gb3-negative cell lines) [131, 276, 305, 320, 323, 326, 327]. After the specificity and optimum concentrations of the antibodies were confirmed, a similar protocol was applied to the bovine terminal rectal cell cultures.

The primary cells were used at day 3 to day 5 post-seeding from collagen-coated 6-well-plates, with prior inspection of the morphology of the cells under light microscope to ensure that the cells in the culture were healthy and not overgrown by fibroblasts. The bovine primary terminal rectal cells were double stained with the epithelial cell marker; pan-cytokeratin (PCK) and the mesenchymal cell marker;

Vimentin [272]. This was done to selectively detect Gb3 positive cells, either of epithelial (double stained Gb3+/PCK+ cells) or mesenchymal origin (double stained Gb3+/Vimentin+) since the cells were derived from a highly heterogenous cell population from the bovine terminal rectum [272].

Table 2.1 List of antibodies for Gb3 detection by flow cytometry.

Antibody	Clone	Isotype	Concentration	Source
Rat anti-Gb3	38-13	IgM	1:50 1:100	AbD Serotec (MCA 579)
Mouse anti-pancytokeratin (PCK)	C-11 PCK-26 CY-90 KS-1A3 M20 A53-B/A2	IgG1	1:50	Sigma (C2562)
Mouse anti-vimentin-FITC	V9	IgG1	1:50	Sigma (V6630)
Goat anti-rat IgM-PE	-	-	1:50	AbD Serotec (302009)
Rabbit anti-mouse-IgG-FITC	-	-	1:100	Sigma (F2012)

2.12 Tissue section harvest and cryosection production

The aim of these experiments was to detect Gb3 expression at the primary site of EHEC O157:H7 colonisation as this has not been previously investigated (in detail) in cattle. The tissue sections were obtained from the rectum of one calf involved in a separate study and were acquired by collaborators at the Moredun Research Institute (Pentlands Science Park, Midlothian, UK). The calf was previously screened to be free of EHEC O157:H7 infection by the Immuno-magnetic Separation (IMS) test and was one of the animals serving as a non-infected control in a study involving other infected calves. At the end of the study, the calf was humanely euthanised to allow *post-mortem* examination and sample extraction. The rectum was immediately acquired and processed where tissue strips of size 0.5 cm (width) x 4cm (length) were cut out of the terminal rectal area transversely (following the circular muscle orientation). To serve as comparison and tissue staining control, similar tissue sections were cut out of the colon mucosa as well as from the nasal mucosa. Colon mucosa has previously been shown to express Gb3 in random areas [272] as well as within the crypts [328] while the nasal mucosa is thought to include some of the Gb3-positive cells within its associated lymphoid tissue, since certain follicular B cell populations expresses Gb3 [122]. The tissue strips were rolled up to form a circular ring and were placed on individual cork discs. Then, the tissues were covered with Tissue-Tek™ CRYO-Optimum Cutting Temperature (OCT) Compound (14373-65, Andwin Scientific) before dipping into liquid nitrogen to flash freeze and stored at -80°C freezer until use. The tissues were then sent to the Shared University Research Facilities (SuRF) at the Queen Margaret Research Institute (QMRI), University of Edinburgh to produce cryo-sections of 5 µm thickness that were immediately fixed in cold ethanol (-20°C) and stored at -80°C before continuing the procedure for immuno-staining described below.

2.13 Immuno-fluorescent staining of bovine cryo-sections

The bovine cryo-sections were thawed at room temperature for approximately 5 min. Using a hydrophobic wax pen, a border was drawn around the sections on each slide and the wax was left to dry (1 - 2 min). At this point, the sections were transferred into a moist humidified chamber (slide staining tray with lid, #11968004, Fisherbrand®,) filled up with distilled water (DH₂O) to prevent the tissue sections from drying. Approximately 100 µl (depending on the size of the sections, could vary between 100 µl to 200 µl) of PBS was carefully dropped onto the edge of each section to re-hydrate the tissue for 30 min at room temperature. This was then followed by a blocking step to avoid non-specific binding of the antibodies. Tissue sections were incubated in blocking buffer consisting of 1% bovine serum albumin (BSA) (A2153, Sigma), 2% normal goat serum (G9023, Sigma) and 0.125% Tween 20-PBS (PBS-T) for 1 h at room temperature. Sections were then incubated in iT Signal Enhancer buffer (I36933, Life Technologies) for 30 min at room temperature, washed in 0.125% PBS-Tween 20 once before primary antibody incubation (all primary antibodies are indicated in Table 2.2, were diluted in staining buffer containing 1% BSA, 2% normal goat serum in 0.125% PBS-T, overnight, 4°C). The sections were washed in washing buffer (1% BSA in 0.125% PBS-T) once for 30 seconds, followed by 3 x 5 min washes. Excess liquid was wiped and the sections were transferred back into the humidity chamber to continue with secondary antibody (Table 2.2) incubation in staining buffer at room temperature for 30 min, protected from light. Unstained control slide was left in staining buffer (1% BSA in PBS-T) throughout the staining under similar conditions with the rest of the slides. No primary antibody and rat IgM isotype controls were also included. The sections were washed in washing buffer as above. 12 µl of ProLong® Gold anti-fade mountant with DAPI (4',6-diamidino-2-phenylindole) (P-36931, Molecular Probes®, Life Technologies) was added on each cover slip before mounting the slides onto it, avoiding formation of air bubbles that might interfere with the microscopy examination further on. The mounted sections were kept in the slide holder box overnight, in dark conditions to adequately dry the mounting media. From then on the slides were either kept at 4°C or examined under fluorescence microscope (Leica DMLB) and images were taken with the Image processing and analysis in Java

(Image J) programme (Rasband, W.S., U. S. National Institutes of Health, Bethesda, Maryland).

Table 2.2 List of antibodies for Gb3 and cell lineage marker detection by fluorescence microscopy.

Antibody	Clone	Isotype	Concentration	Source
Rat anti-human Gb3-IgM	38-13	IgM	1:20	AbD Serotec (MCA579)
Rabbit anti-human Pancytokeratin	Polyclonal	IgG	1:50	abcam® (ab9377)
Mouse anti-human Vimentin	V9	1gG1	1:100	abcam® (ab8069)
Mouse anti bovine MHC Class II DQ	CC158	IgG2a	1:50	AbD Serotec (MCA5655)
Goat anti-rat IgM (μ) Alexa Fluor® 594	-	-	1:800	Molecular Probes® (A-21213)
Purified rat IgM isotype control	-	-	1:20	Biolegend (400801)
Goat anti-rabbit (IgG) Alexa Fluor® 488	-	-	1:800	Molecular Probes® (A-11034)
Donkey anti-mouse (IgG) Alexa Fluor® 488	-	-	1:800	Molecular Probes® (A21202)

2.14 Haematoxylin and Eosin staining of cryo-sections

The fixed bovine cryo-sections were thawed for 5 min at room temperature before inserting the sections into glass slide racks and loading into the Leica Autostainer XL V2.01 automated slide stainer. Briefly, the sections were dipped in Haematoxylin for 3 min, followed by two washes in water for 3 min, then in the blueing reagent, Scott's tap water substitute (Leica Biosystems) for 2 min and then rinsed in water for 3 min. The sections were then transferred to the tank with Eosin (2 min), water for 45 seconds and dehydrated in 95% ethanol twice for 30 seconds and 100% ethanol for 1 min, twice. Next was a mixture of ethanol and xylene for 1 min before completing the process with clearing in xylene (to minimise light diffraction and promotes nearly optically perfect images since xylene has a similar refractive index with the suffused fixed protein) twice for 1 min and a final dip in xylene. The glass slide racks were removed from the autostainer before adding ClearVue™ mountant (Thermo Scientific) onto individual cover slips to which the glass slides were mounted to. The finished H&E stained slides were dried on a flat surface, at room temperature, overnight to settle the mountant before examining the slides and taking images with an upright light microscope (Nikon Instruments Europe B.V.) and analysed using ZEN blue edition (Carl Zeiss Microscopy GmbH).

2.15 Stx and cell cycle/proliferation

2.15.1 DNA staining solution

1 ml of DNA staining solution (to stain one sample in a FACS tube) contains 2 µl of Propidium iodide (PI, 1mg/ml, Biotium), 0.5 mg/ml of DNase free-ribonuclease A (RNase A) from bovine pancreas (stock 10 mg/ml, Sigma) and 948 µl of PBS. The DNase-free RNase A was prepared according to the manufacturer's instructions.

2.15.2 Cell counting and fixation

At the end of each stimulation time point, cells were washed twice with sterile PBS and harvested with 1x TrypLE™ Express (600 µl of TrypLE™ Express

per well, incubated at 37°C for 5 min before stopping its action by diluting in 1 ml of PBS). The cells were pelleted at 260 x g for 5 min and re-suspended in 300 µl of PBS. 20 µl of cell suspension were added into equal volume of 0.2% Trypan Blue Stain (15250-061, Invitrogen) and left for 5 min at room temperature. 10 µl of the mixture was loaded into the counting chamber slides for cell counting using the TC20™ (Bio-Rad) automated cell counter. The cell concentration was then adjusted with PBS to obtain at least 1×10^5 cells in 300 µl per tube before adding 700 µl of 100% ethanol (ice-cold) to fix the cells. The fixed cells were stored at 4°C for at least 24 h before resuming with DNA staining.

2.15.3 Shiga toxin cell stimulation

Caco-2 and T84 cells were maintained in T75 cell culture flasks at 37°C, 5% CO₂ until a confluence level of 50% were achieved. These cells were sub-cultured and maintained under similar conditions until reaching 50% confluence for at least one cycle before the cells were sub-cultured into 6-well-plates at a low seeding density of 6×10^3 cells/cm² and incubated for 40 h. The purified Stx2 (Toxin Technology, Inc.) was diluted in normal cell medium to obtain a concentration of 100 ng/ml. Control cells received normal culture medium. The cells were incubated at 37°C, 5% CO₂ for either 6 h or 24 h.

2.15.4 DNA staining and flow cytometry

After incubation of the ethanol-fixed cells at 4°C for 24 h, the cells were stained with DNA staining solution (details mentioned in 2.15.1). Prior to staining, the cells were centrifuged to wash off the ethanol at 5000 R.P.M., 5 min at 18°C. The supernatant (ethanol) was removed by tipping the tube downwards onto paper towels to absorb the ethanol. This prevents losing the cell pellet from the bottom of the tube. The cells were then re-suspended in 0.5% BSA in PBS, 1 ml per tube and centrifuged again as before. The BSA was added to promote the cells to pellet as they tend to float within the supernatant due to their size and weight. The supernatants were removed in similar manner as the ethanol. 1 ml of DNA staining solution was added into each tube with approximately 1×10^5 cells and incubated at 4°C for at least 24 h before acquiring data on a BD FACSCalibur™ machine.

2.15.5 Data acquisition and DNA content analysis by flow cytometry

DNA content of ethanol-fixed cells were analysed by detecting signal of propidium iodide staining under fluorescence channel-2 (FL-2). 10,000 events were collected with low flow rate to obtain better resolution of the DNA-PI histogram peaks for every sample with BD CELLQUEST™ (BD Biosciences). The presence of doublets or aggregates of cells upon crossing the laser beam during acquisition will result in the presence of extra peaks in the FL-2 (total fluorescence signal of PI) histogram, as opposed to the typical three peaks corresponding to DNA content in different phases of the cell cycle (Figure 2.1). An additional step was performed to exclude cell aggregates and debris by plotting an FL2-Width against FL2-Area dot plot (Fig. 2.2). Gating was then applied on the single cell population to derive the FL-2/PI histogram for analysis of total DNA content. The boundaries were manually set for G1, S and G2/M (with the guidance of an expert in cell cycle analysis by flow cytometry, Robert Fleming of the Bio-Imaging and Flow Cytometry facilities at Roslin Institute, UK), based on the typical histogram shape (Fig. 2.1) producing peaks corresponding to the proportion of cells within each phase of the cell cycle (G1, S, G2/M), based on the DNA content (refer to Fig. 2.1 and Fig. 2.2). Statistical analyses of the proportion of cells within each phase were performed in GraphPad Prism Version 6 (GraphPad, Inc.) with multiple t-test using Holm-Sidak method, alpha at 5.00%, without assuming similar standard deviation (S.D.) values to compare the proportion values between IFN- γ treated Caco-2 and T84 cell with the untreated controls.

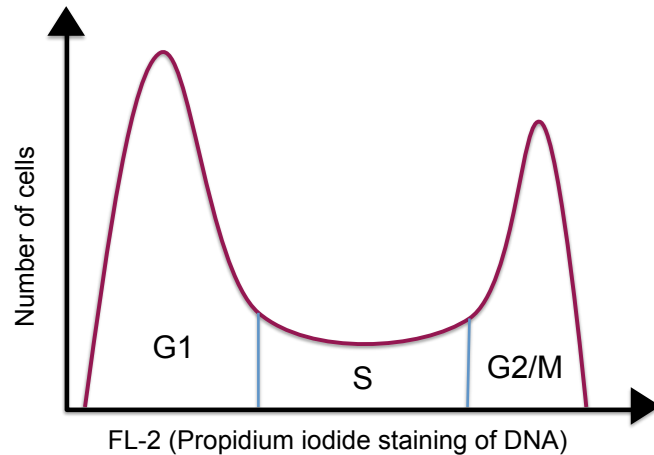


Figure 2.1 Histogram of propidium iodide (PI) staining detected by fluorescence channel 2 (FL-2) corresponding to total DNA content in different phases of the cell cycle in ethanol-fixed cells. The amount of DNA in phases of the cell cycle is reflected by total fluorescence of PI-stained nuclei. Quiescent, non-replicating cells contain single copies of the DNA, compared to the mitotic cells of G2/M phase with two copies of DNA (double fluorescence intensity). Cells in the S-phase contains intermediate amount of DNA, between the G1 and G2/M phases.

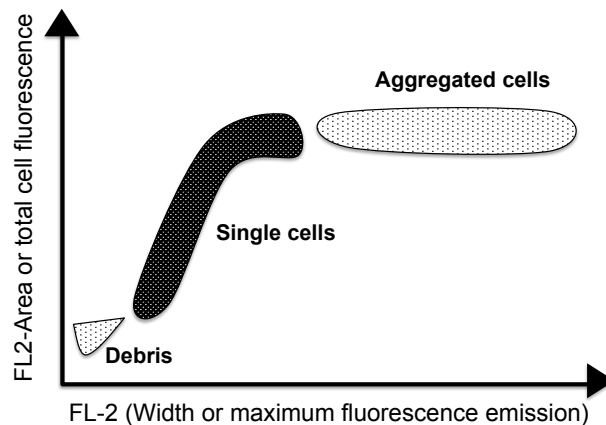


Figure 2.2 Dot plot of propidium iodide fluorescence detected by FL-2 to distinguish single cells from cellular aggregates and debris (adapted from Cell Cycle Basics, Lerner Research Institute, Cleveland Clinic, Ohio, United States). The single cell population will have a recognisable pattern on the FL-2/Width versus FL-2/Area dot plot, with the values of maximum fluorescence emission and total cell fluorescence to be in lower than the doublets or aggregated cells, but higher than cellular debris. DNA analysis of the selected single cell population will result in a histogram with better resolution of the DNA peaks (seen in Fig. 2.1).

2.15.6 Detection of proliferating cells

Caco-2 and T84 cells were stimulated with PStx2 for 6 and 24 h and cell culture were prepared as described above. At the end of the PStx2 treatment, the cells were washed in PBS and fixed following the same fixation protocol as for PI staining of cellular DNA (refer to 2.15.4). The fixed cells were stained with mouse anti-human Proliferating Cell Nuclear Antigen (anti-PCNA, Clone PC10, Phycoerythrin (PE)-conjugated, sc-56-PE, Insight Biotechnology), diluted in flow cytometry buffer at 1:100 in 500 µl of sample per tube. The cells were left at 4°C for 30 min before washed in flow cytometry buffer twice. The PCNA-labelled cells were detected by flow cytometry according to the procedure described above with FL-2 as the fluorochrome detection channel.

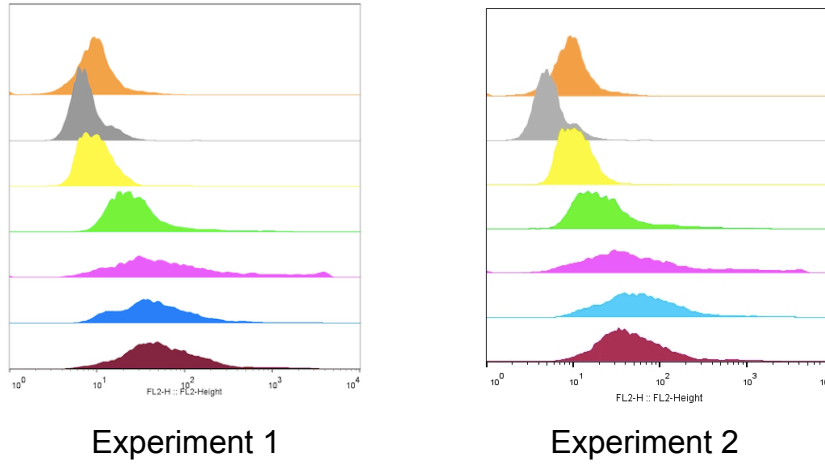
Chapter 2

Results

2.1 Gb3 expression on different immortalised cell lines

Vero cells have been established to be highly positive for Gb3 expression [131]. Therefore for the purpose of testing and optimising antibodies for detection of Gb3 expression at the bovine terminal rectum, Vero cells were used as a positive control. In contrast, Chinese hamster ovary (CHO) cells have been previously demonstrated to be deficient of Gb3 cell surface expression [123, 329] therefore these cells were used as a negative Gb3 expression control. In addition, human Caco-2 and T84 cells were investigated for Gb3 expression due their intestinal origin and epithelial phenotype. Bovine EBL cells were used as reference cells for the bovine system. In a first set of experiments, the Gb3 surface expression of all cell lines was investigated by flow cytometry analysis.

Figure 2.1 presents the flow cytometry results shown as compilation of all histograms for the cell lines analysed for Gb3 surface expression. Data analysis was done in Flowjo programme to produce median of fluorescence intensity (MFI) values to enable comparison of the FL2-channel signals among the different cell lines relative to the control (secondary antibody only stained cells). Cell lines with MFI values of more than that for the secondary antibody staining only control were assumed to be positive for Gb3 staining. On average, the MFI values for Gb3 detection on Vero, HeLa and Caco-2 cells from the two experiments were approximately 4.5 - 5.8 times more than that of the secondary antibody only control value, indicating that the three cell lines had similar Gb3 expression. Gb3 expression on T84 cells were relatively 2 - 2.6 times more than the control MFI, while CHO cells, as predicted had MFI values of less than the control MFI.



Peak (Cell line/Staining for control)	Median of Fluorescence Intensity (MFI) Experiment 1	Median of Fluorescence Intensity (MFI) Experiment 2
Secondary antibody staining	9.47	9.45
Chinese Hamster Ovary (CHO)	7.23	5.23
Embryonic Bovine Lung (EBL)	9.47	10.5
T84	24.6	19.8
HeLa	42.9	55.2
Caco-2	52.8	42.9
Vero	50.9	42.9

Figure 2.1 Histograms and median of fluorescence intensity (MFI) of Gb3 surface expression on different cell lines. The cells (Vero in red, Caco-2 in blue, HeLa in magenta, T84 in green, Embryonic Bovine Lung (EBL) in yellow and Chinese Hamster Ovary (CHO) in dark grey) were stained for surface Gb3 and acquired on a BD FACS Calibur™ instrument. 10,000 events were collected for each cell line. Data were analysed with Flowjo software (Treestar Inc., City, USA) by placing a gate to exclude cellular debris, followed by setting the cut-off point for positive staining based on cells stained with only the secondary antibody (Goat anti-Rat IgM PE-conjugated) before calculating the median of fluorescence intensity (MFI) values from the statistical toolbar. The histogram plots were then overlaid and set for half offset display producing above plots, each plot indicates a different set of replicate for the experiment.

2.2 Sensitivity of different immortalised cell lines towards Shiga toxins

To investigate the influence of Shiga toxin treatment on Gb3 expression levels, the cell lines were treated with purified Stx1 and purified Stx2. The aim of these experiments was to confirm the expression of Gb3 and to analyse the functionality of Gb3 as a Stx receptor, since sensitivity towards Stx is correlated with Gb3 expression on the surface of the cells [132, 330]. Shiga toxin cytotoxicity assays were done for all cell lines using purified Stx1 and Stx2 (Fig. 2.2), except for HeLa cells due to the limited availability of purified toxins at later stages of my thesis work. To overcome this issue, sensitivity of HeLa cells to the toxin was instead tested with filtered lysates of Mitomycin C-induced EHEC O157:H7 Strain 9000. Strain 9000 possesses Stx2a and Stx2c-encoding prophages, therefore the lysate of this strain is expected to contain high levels of Stx2a and Stx2c. On the other hand, MMC-induced culture lysate was also generated for a strain derived from EHEC O157:H7 Strain 9000 with phages encoding for Stx2a and Stx2c deleted. The absence of the two Stx-encoding phages in the isogenic Strain 9000 mutant, in theory would produce Stx-free lysates, serving as negative control for HeLa cytotoxicity, apart from the other negative assay control (serum-free medium) (Fig. 2.2). As expected, Vero cells were the most sensitive cells tested towards the toxicity effect after treatment with both purified Stx1 and purified Stx2. Even at the lowest treatment dose (0.1 ng/ml), nearly 50% of Vero cells were killed post 72 h exposure to the purified toxins. This result is consistent with the flow cytometry results in Fig. 2.1 which showed that Vero cells had high expression levels of Gb3. Caco-2 cells showed a dose-response cytotoxicity effect when treated with purified Stx1, however this effect was not observed when the cells were treated with purified Stx2. T84 cells were resistant to lower doses of both purified toxins but approximately 5% - 20% of the cells succumbed to PStx1 and PStx2 treatment at higher doses (500-1000 ng/ml). EBL cells were neither affected by purified Stx1 nor purified Stx2 treatments at the end of the 72 h incubation, while only less than 5% of CHO cells were sensitive to both toxins.

Incubation of HeLa cells with filtered supernatants of LB-grown EHEC O157:H7 Strain 9000 and its isogenic Stx phage deficient cultures for 72 h revealed that the HeLa cells were sensitive to the treatment of the Stx-positive supernatant. The HeLa cells receiving supernatant of the Stx phage mutant remained as viable as the negative control cells (DMEM medium with LB diluted 1:100).

No statistical analyses were done on the Shiga toxin-cytotoxicity assay data since values obtained were mean of technical repeats (ranging from three or six or nine wells per treatment). Due to the limited amount of purified Stx2 available and time constraint, independent repeats of the cytotoxicity assays were not done. However, it was observed that technical replicates of the individual cytotoxicity assays provides similar absorbance values and hence is regarded as a robust assay.

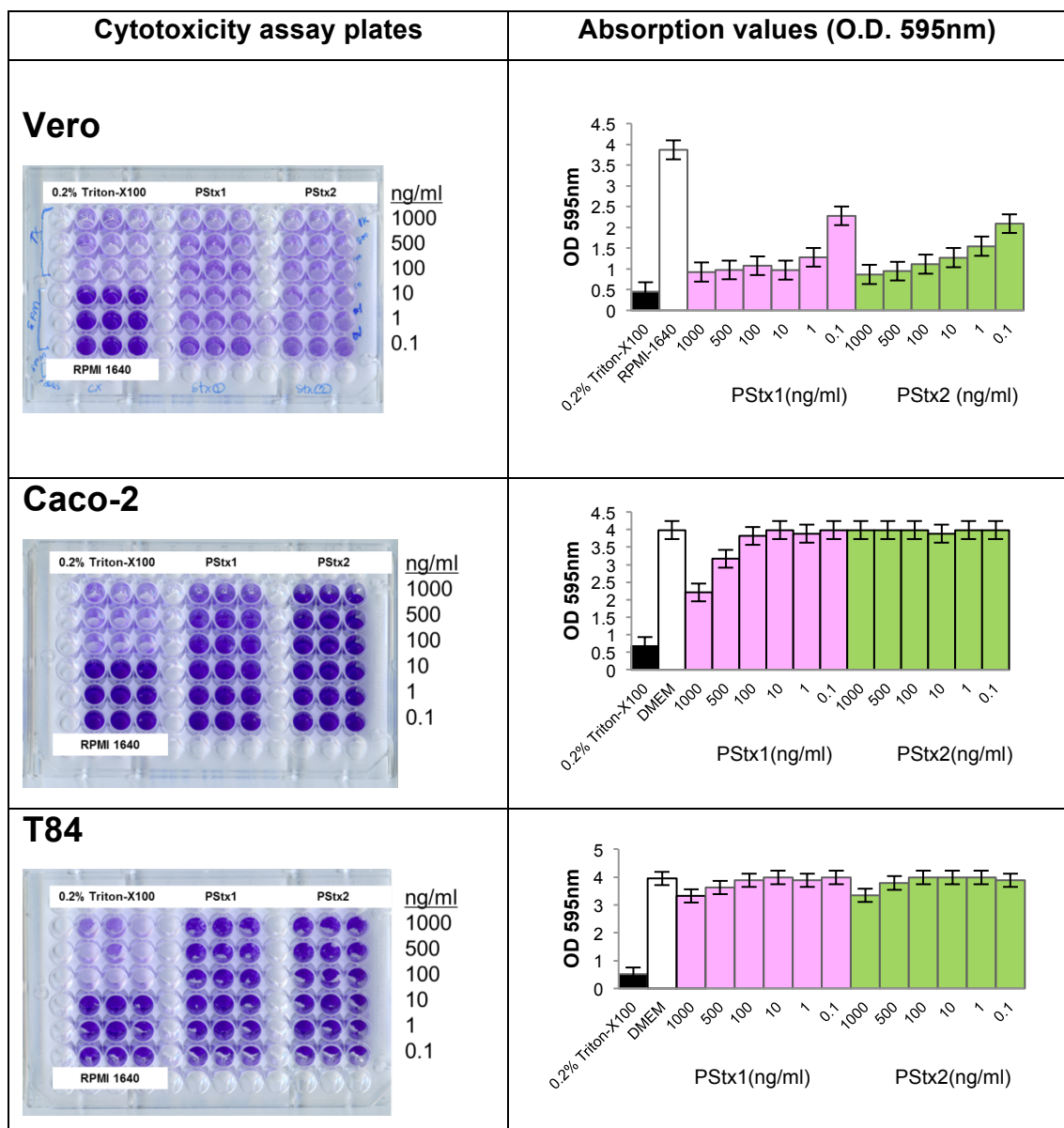


Figure 2.2 Shiga toxin cytotoxicity assay plates of immortalised cell lines with different Gb3 surface expression. Bar plots present the absorption values (O.D. 595 nm) from at least three replicate wells signifying viable cells remaining in the plate post 72 hours incubation with either purified Shiga toxin 1 (PStx1), pink bars; purified Shiga toxin 2 (PStx2), green bars, 0.2% Triton-X100 (positive control), black bar and DMEM (negative control), white bar, at 37°C, 5% CO₂. At the end of incubation, the cells were washed with PBS and fixed in 2% formalin and stained with crystal violet staining solution for 18 hours at room temperature. The fixed cells were washed in distilled water before dissolving the crystal violet stain in 10% acetic acid.

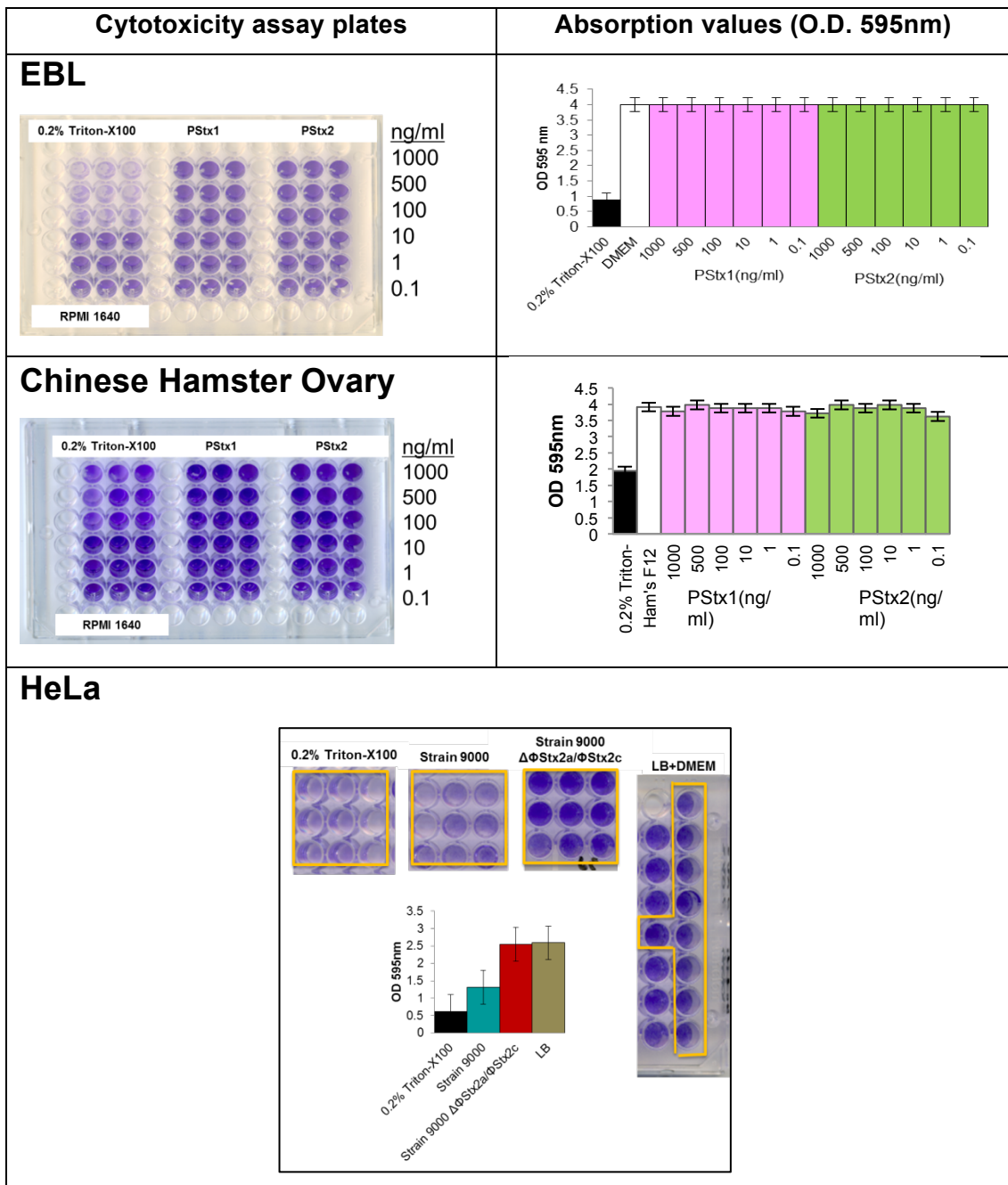


Figure 2.2 Continued. Shiga toxin cytotoxicity assay plates of immortalised cell lines with different Gb3 surface expression status. Bar plots for EBL and CHO cells present the average of absorption values at O.D. 595 nm from at least three replicate wells signifying viable cells remaining in the plate post 72 hours incubation with either purified Shiga toxin 1 (PStx1), pink bars; purified Shiga toxin 2 (PStx2), green bars, 0.2% Triton-X100 (positive control), black bar and DMEM for EBL, Ham's F-12 media for CHO cells (negative control), white bar, at 37°C, 5% CO₂. The bottom bar plot represents the absorption values at O.D. 595 nm for viable HeLa cells after 72 hours under similar incubation conditions as above in filtered lysate of EHEC O157:H7 Strain 9000 (dark green bar), EHEC O157:H7 Strain 10671 (red bar) and LB (brown bar), all diluted in DMEM.

2.3 Gb3 expression by cells of the bovine primary terminal rectal culture

There was a huge difference in the flow cytometry results of Gb3+/PCK+ dot plots from two independent batches of bovine primary terminal rectal cells (Fig. 2.3). The results from the first experiment showed on average 44.2% surface detection for Gb3+/PCK+ cells, while 47.2% of permeabilised cells stained for surface and intracellular Gb3+/PCK+. On the other hand, in the second experiment bovine primary terminal rectal cells showed a much lower staining for Gb3+ and PCK+, both regarding surface and total expression levels (on average 2.80% and 7.81%, respectively). Double staining the cells for Gb3 and vimentin antibodies revealed very low detection in both experiments, with 0.88% of surface and 0.93% of total Gb3+/Vimentin+ cells detected in batch 1, whilst only the second batch provided negligible values of detection for both surface and intracellular Gb3+/Vimentin+ stained cells.

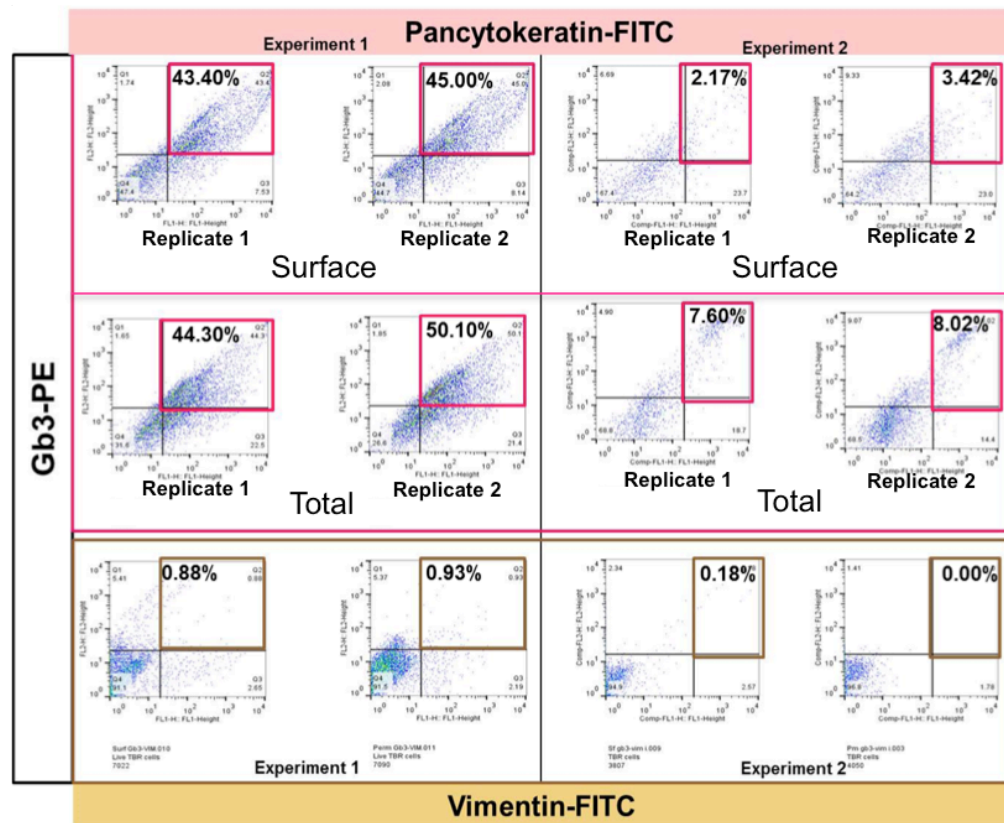


Figure 2.3 Flow cytometry results for Gb3, Pancytokeratin (PCK) (pink boxes) and Vimentin (brown boxes) on bovine primary terminal rectal cells. The dot plots show the output from two different primary terminal rectal cell independent batches, with the plots within the pink boxes as Gb3+/PCK+ populations, surface (all plots in the top row in the pink box) and total (cell permeabilised to obtain signals from both surface and intracellular) (all plots in the bottom row of the pink box) detection. While the four dot plots within the bottom brown boxes are bovine terminal rectal cells stained for Gb3+ and vimentin, surface and total detection. Gb3 antibody staining of the cells were followed by staining with anti-rat-IgM-PE (AbD Serotec) (FL2 channel) and the PCK-stained cells were probed with anti-mouse FITC-conjugated antibody (Sigma) detected by channel FL1. Vimentin staining was done with a FITC-conjugated mouse anti-vimentin antibody (Sigma).

2.4 Gb3 detection on bovine cryosections

Fig. 2.5 - 2.10 shows the bovine cryosections stained for immunofluorescence analysis of Gb3, PCK (epithelial cells), vimentin (non-epithelial/mesenchymal cells), major histocompatibility class II (MHC II) and DAPI (nucleic acid/DNA staining). Fig. 2.4 presents immune-staining control tissue sections, nasal mucosa from the same calf where the rest of the cryosections were obtained from. At least three sections were independently stained for both bovine terminal rectal and colonic mucosae and thoroughly examined ensuring all parts of the sections were analysed by fluorescence microscope. The fluorescence microscopy images presented in this chapter are from the third set of cryosections examined and are representative of the appearance of the cryosections consistently observed in all three independent examinations. Due to limited availability of cryosections and time constraint, Haematoxylin and Eosin (H&E) staining were only done on cryosections from the third set of tissues stained for fluorescence microscopy. H&E staining images are of cryosections that were cut consecutive (before or after) to the fluorescence-stained sections providing information on the histological structures present in the sectioned tissues examined.

2.4.1 Gb3 and Pancytokeratin co-staining

To identify if Gb3 is expressed at the terminal rectum in bovine, the terminal rectal and colonic cryosections were stained with rat anti-Gb3-IgM antibody, followed by the secondary goat anti-rat IgM-AF 594 conjugated antibody. In order to discriminate Gb3 expression on bovine terminal rectal and colonis mucosa, the cryosections were co-stained with one of the two different classes of cellular microfilaments, the Type I and II keratins (cytokeratins) or Type III mesenchymal microfilaments (vimentin) [331, 332].

The anti-PCK antibody comprise of a broad range of monoclonal antibodies that reacts with the cytoplasmic cytokeratins. These cytokeratin intermediate filaments are important in cell structure maintenance by providing mechanical support to the epithelial cells [333, 334]. The PCK antibody also does not react with

non-epithelial normal human tissues, therefore suitably used as the 'epithelial cell marker' [334, 335]. Immunofluorescence analysis of Gb3+/PCK+ staining of bovine terminal rectal cryosections revealed the lack of epithelial-associated Gb3 expression (Fig. 2.9-2.10). However, the appearance of randomised, positive signals from some colonic crypts and within the inter-crypt areas of terminal rectal and colon cryosections (refer to split channels for Gb3 staining in Fig. 2.5) might suggest for actual presence of Gb3. To address this, immunofluorescence analysis of the cryosections were performed with co-staining Gb3 with either vimentin or major histocompatibility class II (MHCII).

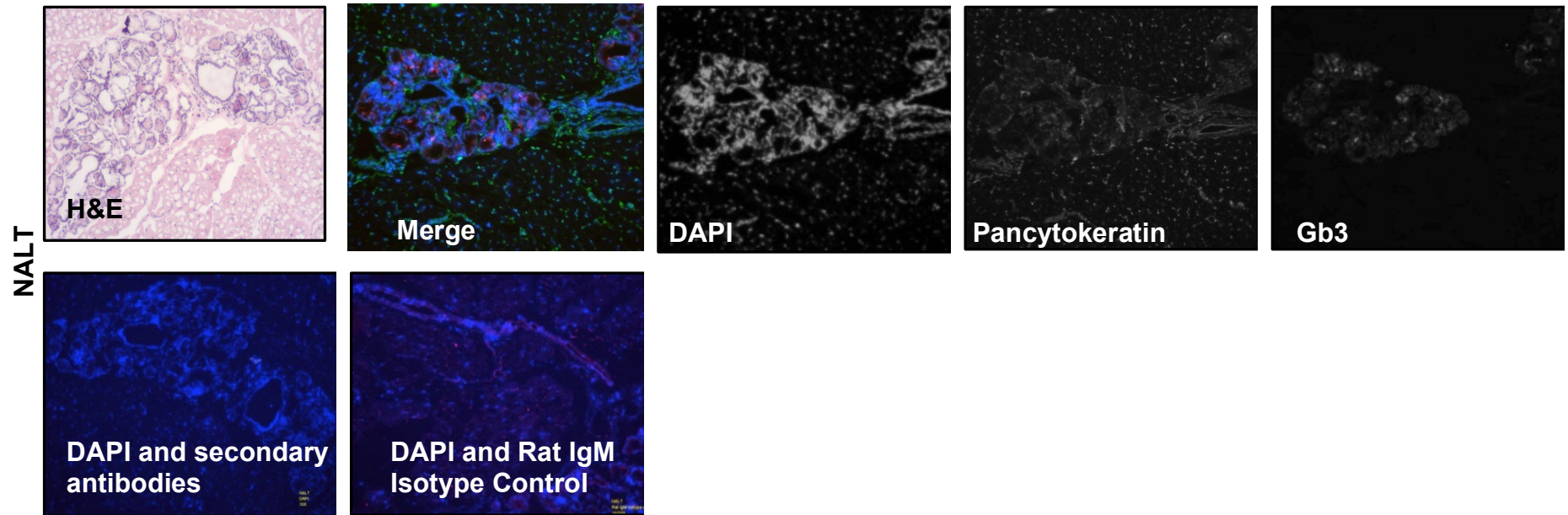


Figure 2.4 Bovine nasal associated lymphoid tissue (NALT) cryosections stained for Gb3 and Pancytokeratin (PCK). DAPI staining of the DNA (blue), PCK staining with secondary goat anti-rabbit conjugated to Alexa Fluor® 488 (green) and Gb3 staining with secondary goat anti-rat IgM conjugated to Alexa Fluor® 594 (red) are shown in colour (merge) and in greyscale (separate channels). Haematoxylin and Eosin (H&E) stained cryosection and DAPI co-stained cryosections with secondary antibodies only and rat IgM isotype are also presented.

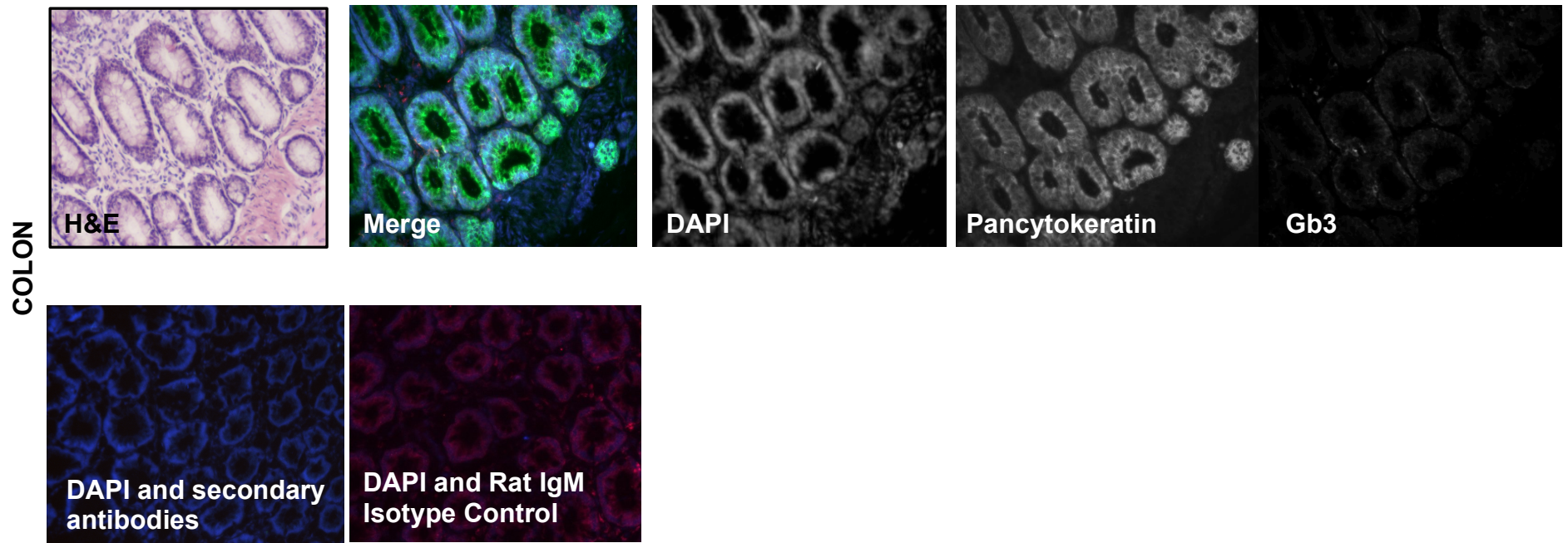


Figure 2.5 Bovine colon mucosa cryosections stained for Gb3 and Pancytokeratin (PCK). DAPI staining of the DNA (blue), PCK staining with secondary goat anti-rabbit conjugated to Alexa Fluor® 488 (green) and Gb3 staining with secondary goat anti-rat IgM conjugated to Alexa Fluor® 594 (red) are shown in colour (merge) and in greyscale (separate channels). Haematoxylin and Eosin (H&E) stained cryosection and DAPI co-stained cryosections with secondary antibodies only and rat IgM isotype are also presented.

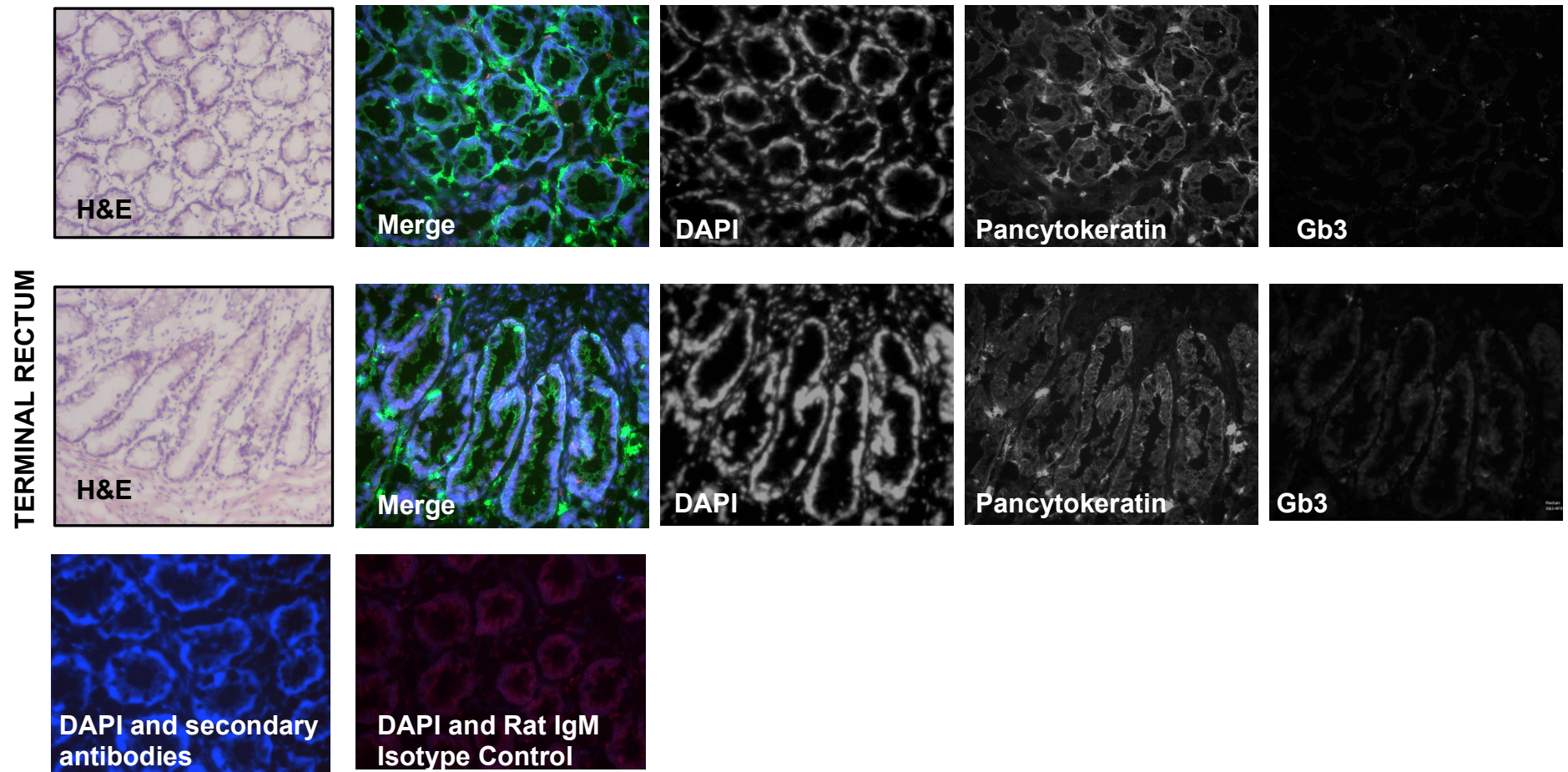


Figure 2.6 Bovine terminal rectal mucosa cryosections stained for Gb3 and Pancytokeratin (PCK). DAPI staining of the DNA (blue), PCK staining with secondary goat anti-rabbit conjugated to Alexa Fluor® 488 (green) and Gb3 staining with secondary goat anti-rat IgM conjugated to Alexa Fluor® 594 (red) are shown in colour (merge) and in greyscale (separate channels). Haematoxylin and Eosin (H&E) stained cryosections and DAPI co-stained cryosections with secondary antibodies only and rat IgM isotype are also presented.

2.4.2 Gb3 and Vimentin co-staining

Vimentin is expressed in a wide range of cell types including fibroblasts, endothelial cells, macrophages, neutrophils, leukocytes, mesangial cells and renal stromal cells, making it as a good marker for non-epithelial cells [336]. Vimentin has also been recognised as the marker for epithelial-mesenchymal transition (EMT), a cellular reprogramming process whereby epithelial cells acquire mesenchymal phenotype with increased mobility [337]. It is also used as the M cell marker present within the intestinal follicle-associated-epithelium (FAE) in rabbits [338]. With regards to this study, positive vimentin staining could represent non-epithelial cells present within the inter-cryptic areas in the terminal rectal and colonic mucosa including fibroblasts, macrophages and neutrophils.

Results for Gb3⁺/Vimentin⁺ immunofluorescence staining are shown in Fig. 2.7-2.8. The strongest signal for mesenchymal-associated Gb3 staining were seen in the terminal rectal cryosection within areas resembling lamina propria, with the presence of structures presumed to be blood vessels based on the H&E staining, distant from the crypts and surface of the terminal rectal mucosa. No evidence of positive Gb3 staining were observed on the terminal rectal crypts. Such findings suggest that the Stx receptor within the terminal rectum might be associated with the lamina propria bearing blood vessels and possibly the deeper part of the sub-mucosal layer, rather than on the epithelium. The presence of areas with positive signals of the Gb3 fluorescence were also observed around structures suspected as blood vessels in several cryosections of the colonic mucosa, further supporting that Gb3, if expressed, is not associated with the epithelium. The connective tissue surrounding blood vessels of the colon were found to be negative for Gb3 staining.

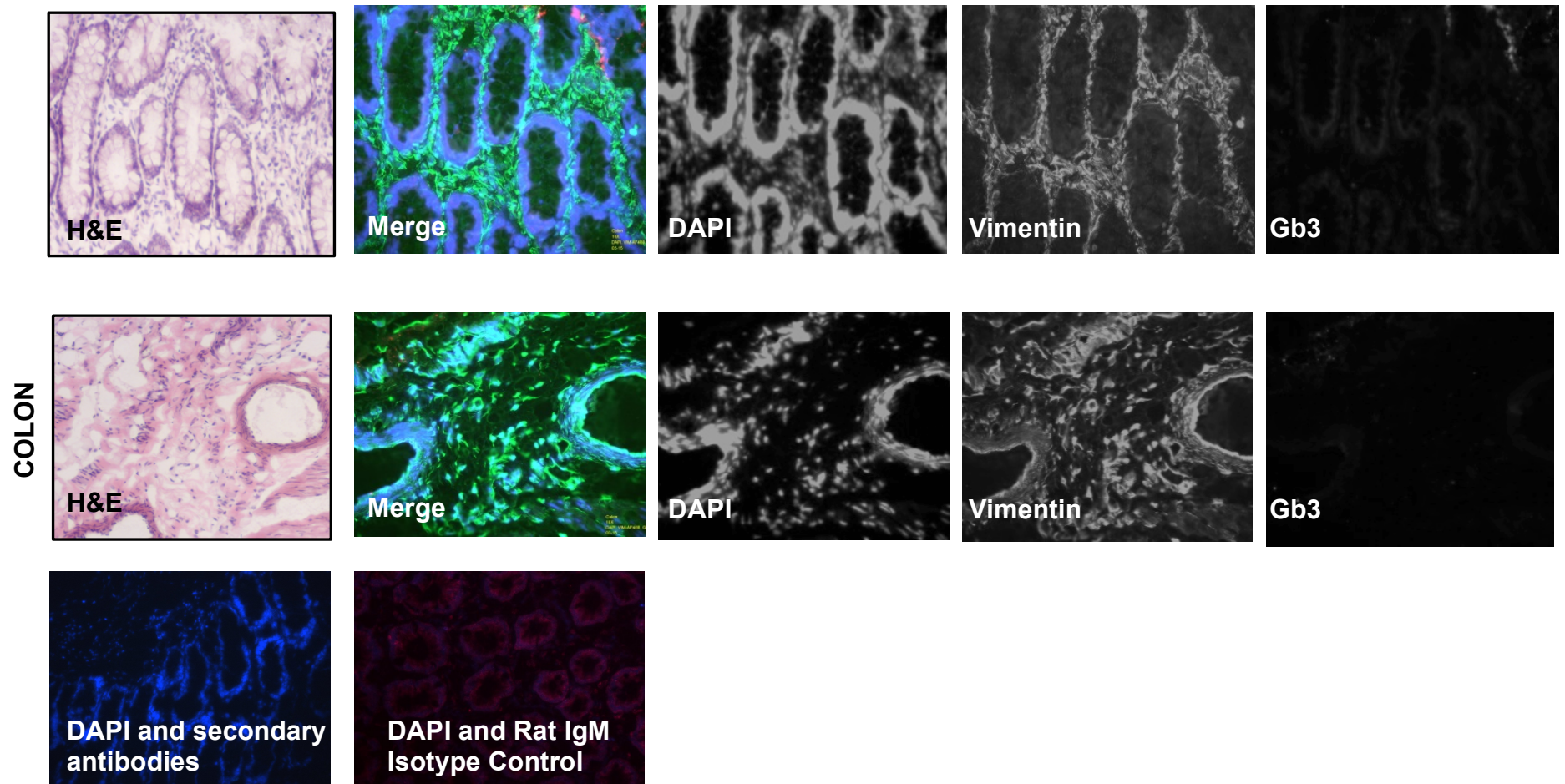


Figure 2.7 Bovine colon cryosections stained for Gb3 and vimentin. DAPI staining of the DNA (blue), vimentin staining with secondary donkey anti-mouse conjugated to Alexa Fluor® 488 (green) and Gb3 staining with secondary goat anti-rat IgM conjugated to Alexa Fluor® 594 (red) are shown in colour (merge) and in greyscale (separate channels). Haematoxylin and Eosin (H&E) stained cryosections and DAPI co-stained cryosections with secondary antibodies only and rat IgM isotype are also presented.

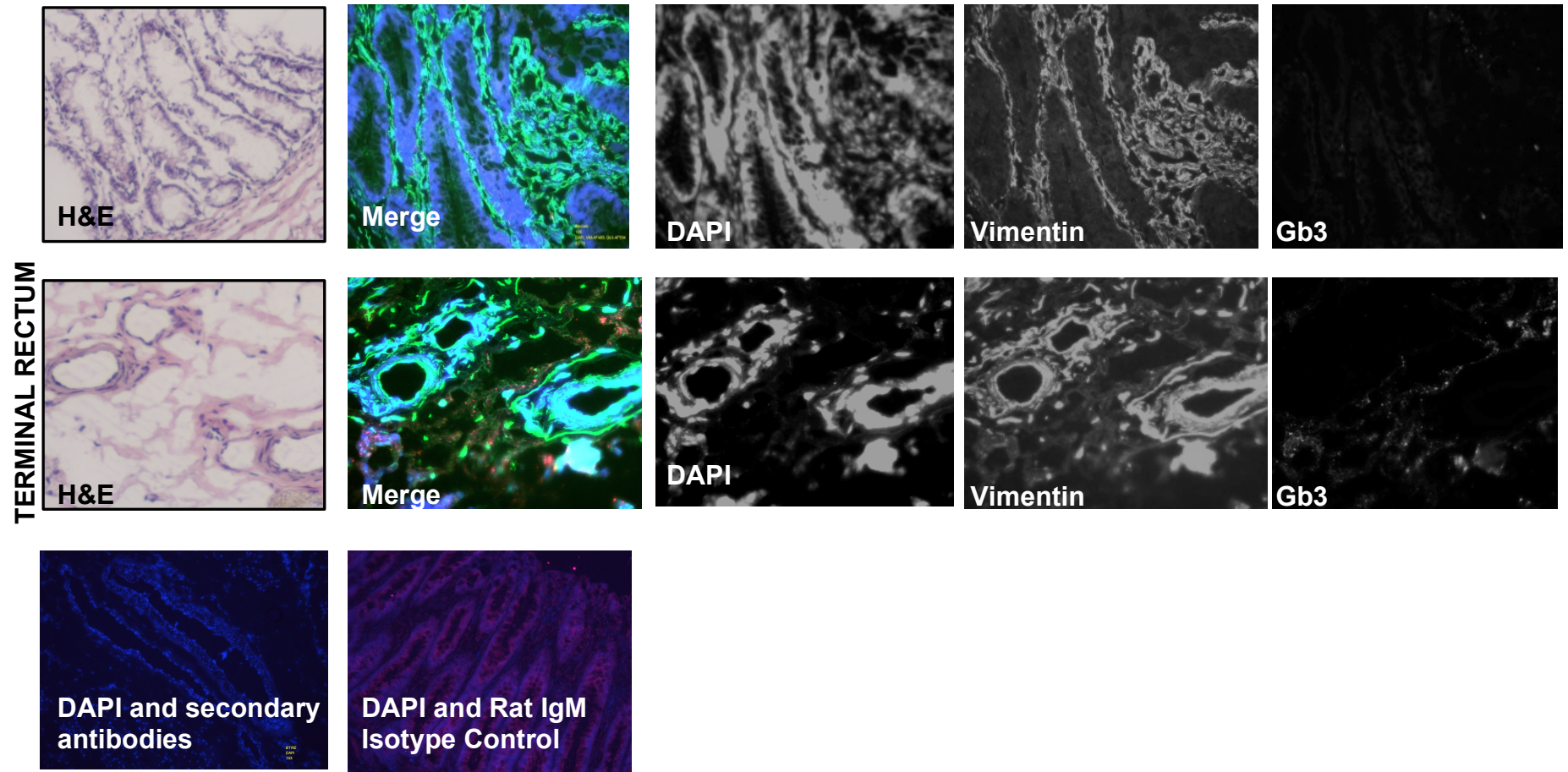


Figure 2.8 Bovine terminal rectal mucosal cryosections stained for Gb3 and vimentin. DAPI staining of the DNA (blue), vimentin staining with secondary donkey anti-mouse conjugated to Alexa Fluor® 488 (green) and Gb3 staining with secondary goat anti-rat IgM conjugated to Alexa Fluor® 594 (red) are shown in colour (merge) and in greyscale (separate channels). Haematoxylin and Eosin (H&E) stained cryosections and DAPI co-stained cryosections with secondary antibodies only and rat IgM isotype are also presented.

2.4.3 Gb3 and Major Histocompatibility Class II (MHC II) co-staining

MHC II is constitutively expressed by professional antigen-presenting cells (APCs) primarily macrophages, dendritic cells and B cells [339], all of which could be present scattered within the crypt areas, particularly at the FAE region. Following the findings in Fig. 2.5-2.8 for positive Gb3 staining within the connective tissue surrounding the crypts and vessels, co-staining with MHC II antibody would help to clarify if the professional APCs, present within the mucosal layer of the intestinal lumen expresses the Stx receptor. The findings for immunofluorescence analysis of Gb3+/MHC II+ co-stained bovine cryosections are presented in Fig. 2.9-2.10. Weak Gb3 staining around areas resembling blood vessels are seen for both terminal rectal and colonic mucosa sections. However, no corroboration for Gb3 and MHC II staining was observed in the two large intestinal parts examined, implying that Gb3 is most likely not expressed by the professional APCs.

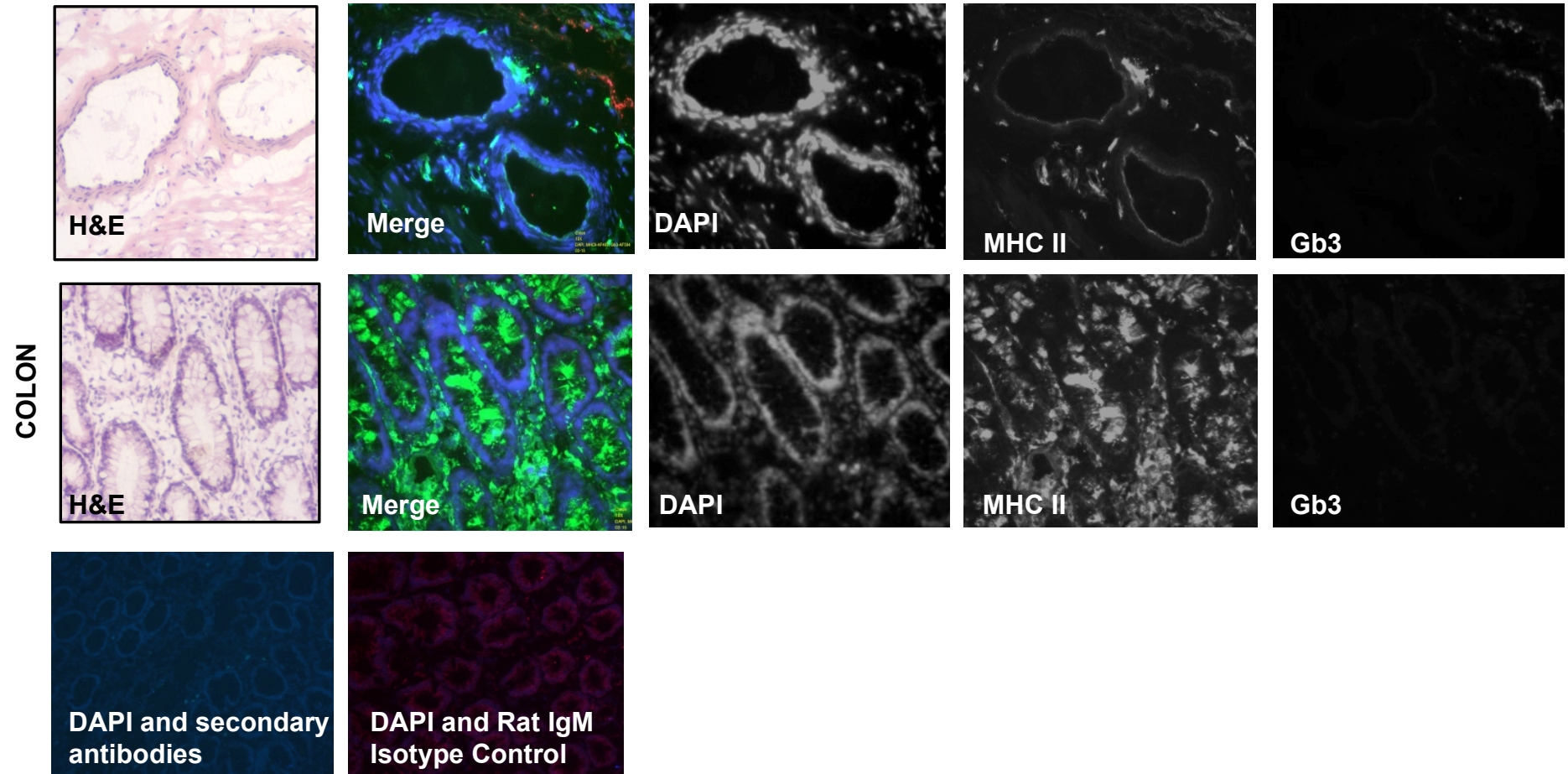


Figure 2.9 Bovine colon mucosa cryosections stained for Gb3 and major histocompatibility complex class II (MHC II). DAPI staining of the DNA (blue), MHC II staining with secondary donkey anti-mouse conjugated to Alexa Fluor® 488 (green) and Gb3 staining with secondary goat anti-rat IgM conjugated to Alexa Fluor® 594 (red) are shown in colour (merge) and in greyscale (separate channels). Haematoxylin and Eosin (H&E) stained cryosections and DAPI co-stained cryosections with secondary antibodies only and rat IgM isotype are also presented.

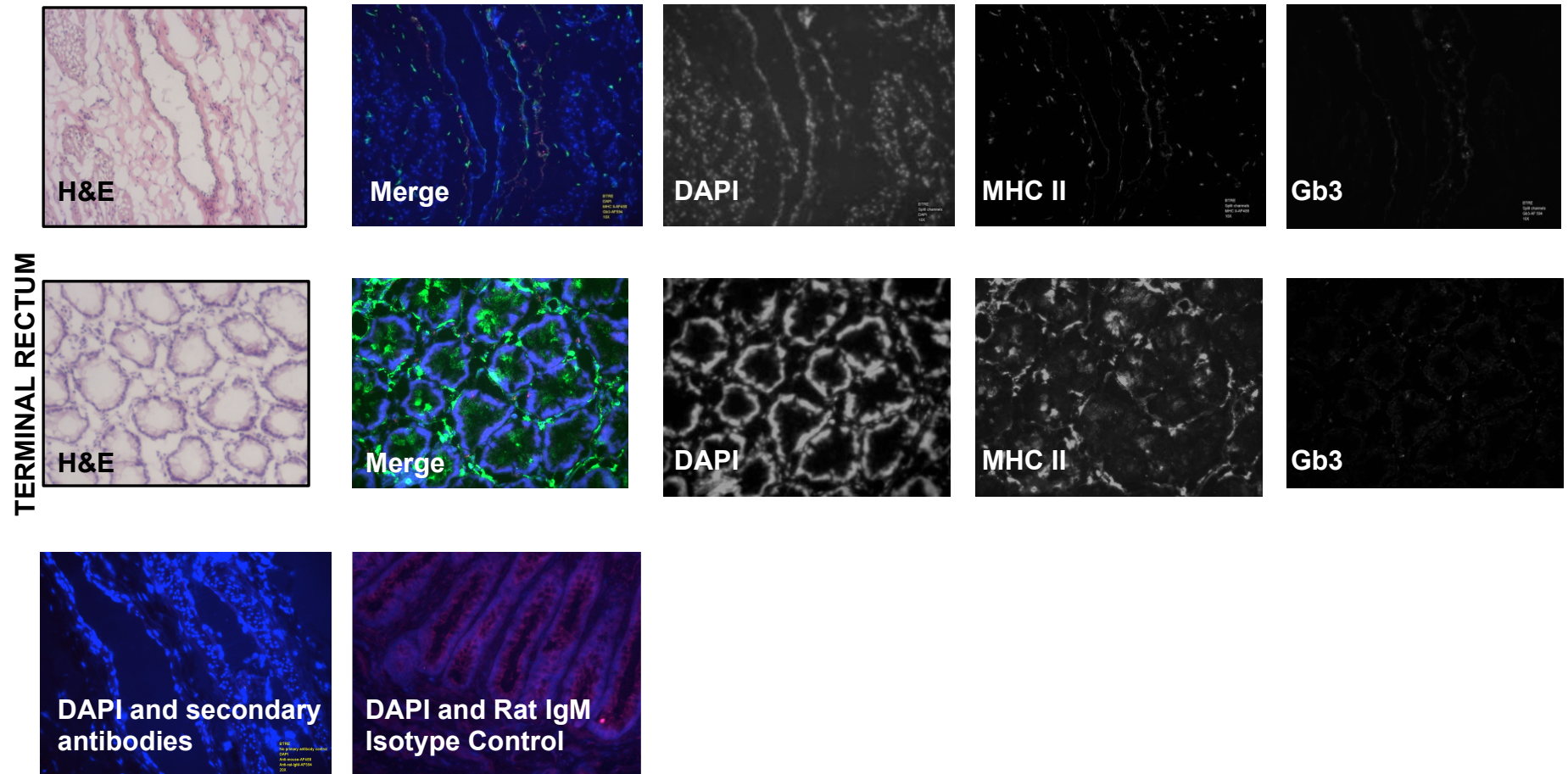


Figure 2.10 Bovine terminal rectal mucosa cryosections stained for Gb3 and major histocompatibility complex class II (MHC II). DAPI staining of the DNA (blue), MHC II staining with secondary donkey anti-mouse conjugated to Alexa Fluor® 488 (green) and Gb3 staining with secondary goat anti-rat IgM conjugated to Alexa Fluor® 594 (red) are shown in colour (merge) and in greyscale (separate channels). Haematoxylin and Eosin (H&E) stained cryosections and DAPI co-stained cryosections with secondary antibodies only and rat IgM isotype are also presented.

2.5 The effect of Stx on intestinal epithelial cell cycle and proliferation

DNA staining with propidium iodide in cells treated with purified Stx2 for 6 h did not cause significant changes of the cell cycle in either Caco-2 or T84 cells, as shown in Fig. 2.11. The average percentages of cells in G1, S and G2/M phases were similar for Caco-2 cells treated with purified Stx2 or not as analysed by multiple t-test with Holm-Sidak method ($\alpha=5\%$) without assuming consistent standard deviations, with G1-phase [$t(4)=0.251$ (p-value=0.814)]; S-phase [$t(4)=0.879$ (p-value=0.429)] and G2/M phase [$t(4)=0.475$ (p-value=0.660)]. T84 cells had a slight increase in the proportion of cells in G1 and S phases, compared to the untreated group. The differences however were not statistically significant when analysed with multiple t-test using the Holm-Sidak method (alpha value of 5%, without assuming consistent standard deviations) with statistical analysis for G1 phase [$t(4)=2.41$ (p-value=0.07)], S-phase [$t(4)=2.78$ (p-value=0.05)] and G2/M-phase [$t(4)=2.72$ (p-value=0.05)].

To analyse specific effects of purified Stx2 on cellular proliferation, cells were stained with antibody against the proliferation cellular nuclear antigen (PCNA). Again, neither Caco-2 nor T84 cells showed a significant different response at 6 and 24 h after treatment when compared to untreated controls (Fig. 2.12). Since this experiment was only performed once, statistical analysis could not be done on the data. However, as no difference was observed between purified Stx2 and untreated cells in DNA staining cell cycle profiles under similar conditions, this suggests that Stx2 has no direct effect on the cell cycle and proliferation rates of both cell lines.

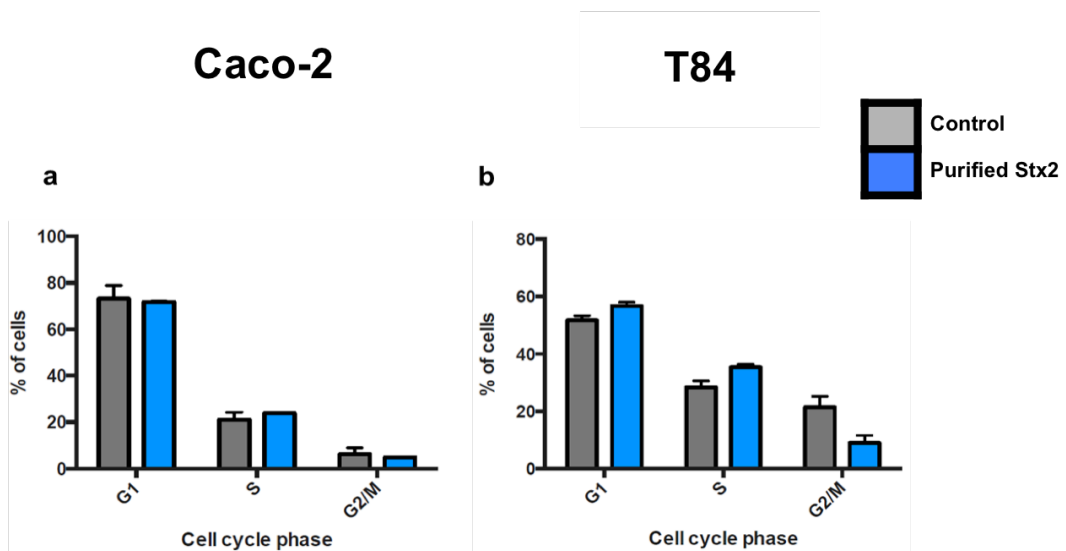


Figure 2.11 DNA staining profile with propidium iodide of cells treated with purified Shiga toxin 2 (PStx2). Bar plots showing the average (n=3) of Caco-2 (Fig. 2.11a) and T84 (Fig. 2.11b) cells present in each cell cycle phase. The cells were incubated in PStx2 (100 ng/ml) or serum-free media for 6 hours at 37°C, 5% CO₂. Data were analysed with multiple t-test corrected for multiple comparison using the Holm-Sidak method, alpha=5%, without assuming a consistent standard deviation. The error bars represent the standard error of mean (S.E.M.).

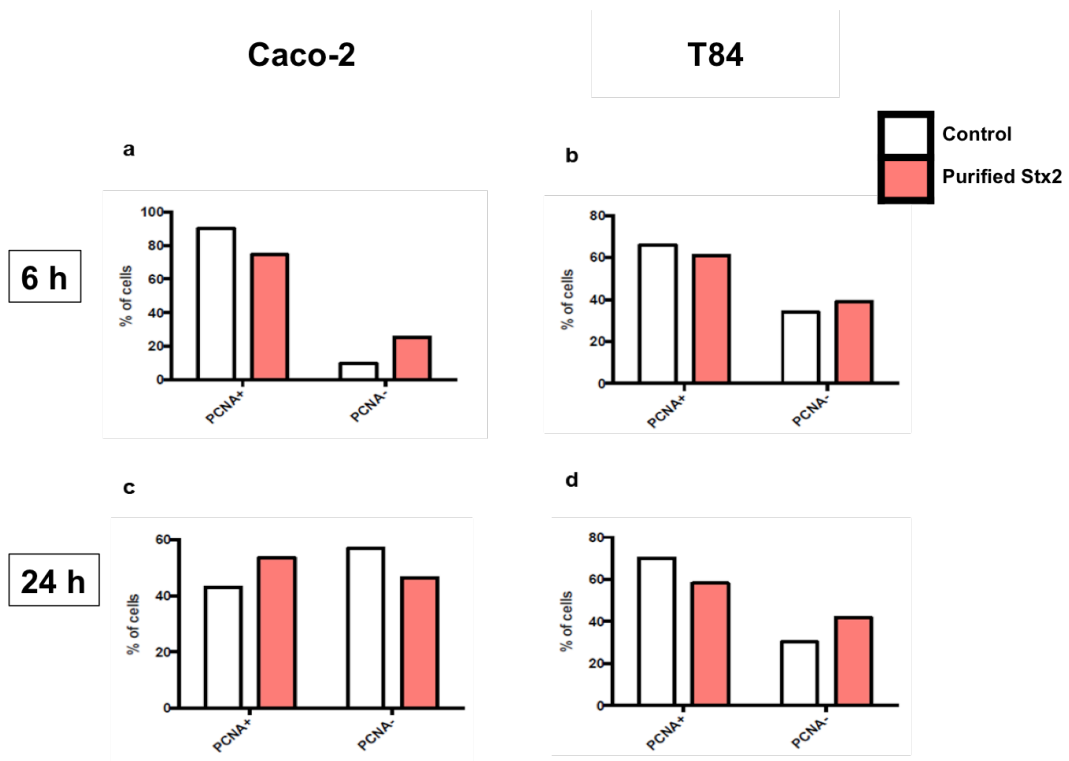


Figure 2.12 Proliferation cellular nuclear antigen staining of purified Shiga toxin 2 (PStx2) treated Caco-2 and T84 cells. Flow cytometry results (n=1) presented in bar plots for Caco-2 and T84 cells stained for proliferating cell nuclear antigen either treated with 100 ng/ml of PStx2 (orange) or serum-free media (white), for 6 hours (Fig. 2.12 a,b) and 24 hours (Fig. 2.12 c,d) at 37°C, 5% CO₂.

Chapter 2

Discussion

Although Stx has been demonstrated to be the causal virulence factor associated with HUS clinical syndromes in human patients, little is still known about its role in bovine intestinal EHEC O157:H7 colonisation. To date, few studies support for the toxin to function in a manner that benefits EHEC O157:H7 adherence by upregulation of the Nucleolin (eukaryotic intimin receptor) [241] or possibly targeting the bovine immune centres at the bovine intestine to modulate the immune response raised against the bacteria to prevent expulsion from cattle [275]. However, certain aspects at the primary colonisation site of EHEC O157:H7 in cattle have yet to be explored. This includes examining the principal colonisation site of the cattle by EHEC O157:H7; the terminal rectum. Previous studies have investigated for the presence of the toxin receptor on bovine colon mucosa which resulted in no significant findings pertaining to Gb3 associated with the surface colonic epithelium [272, 273], rather intracellular Gb3 were detected in the crypt cells of the bovine primary colon cell culture which turned out to be resistant to Stx1 as the toxin was redirected to destruction via lysosomal compartments [142, 328]. Perhaps if Stxs are important for EHEC O157:H7 colonisation at the terminal rectum in cattle, one should expect for higher levels of Gb3 expressed by cells of the primary colonisation site. On the other hand, the receptor may not be required for the toxin to exert effects in facilitating bacterial attachment and persistence at the site since the toxin have been shown to cross the mucosal epithelial border to the lamina propria in a Gb3-independent manner as that described in human intestinal epithelial cells [159, 165]. In another set of experiments in Chapter 2, this study also attempted to answer if Stxs were able to manipulate the proliferation and cell cycle machinery of intestinal epithelial cells, knowing that certain types of cells especially the highly proliferative crypt cells are targeted by effectors and toxins released from bacteria [340]. Interrupting with the host cell cycle or modulating the proliferation machinery could benefit EHEC O157:H7 during intestinal colonisation, for example, by delaying the expulsion of intestinal host cells bounded by the bacteria.

2.1 Gb3 expression in continuous cell lines

The presence of surface Gb3 renders a cell susceptible to Stx1 or Stx2 induced cytotoxicity [133]. Vero, HeLa, T84, and CHO cells responded to the toxins in a presumably Gb3 dependent manner since more cytotoxicity were observed in highly positive cells and vice versa which is in line with published studies [95, 133, 159, 276, 341-343]. An interesting observation was recorded for Caco-2 cells Stx-toxicity assays where the cells responded to Stx1 as anticipated (positive association of Gb3 and cytotoxicity) but not Stx2 despite strongly expressing Gb3. This study has not gone further to investigate the paradoxical resistance of Caco-2 cells to Stx2 although this might be due to a number and combination of factors discussed below.

Several properties of the Shiga toxins could provide arguable explanations on why differential toxicity between Stx1 and Stx2 were observed in Caco-2 cells. The ribosomal phosphoproteins of Caco-2 cells targeted by the A subunits of Stx1 and Stx2 may be different according to Chiou et al. [344]. This may cause the A subunits to go through different ribosomal binding pathways leading to distinctive levels of toxin potency. Furthermore, it has been hypothesised that the difference in potency between Stx1 and Stx2 could be attributed to the binding kinetics and affinity of the B subunits to Gb3 [279]. Different rates of the Stx1 and Stx2 uptake by Caco-2 cells may also be a reason underlying the different toxicity effects observed, as previously reported by Schuller et al. [159]. Conceivably the Stx1 B subunit had higher binding affinity to the Caco-2 cells compared to the Stx2 B subunit leading to higher death of Caco-2 cells. This hypothesis may be plausible as in human renal tissues, Stx1 had a 10-fold higher affinity for Gb3 extracted from human renal tissues [345] and in another study, Stx1 was able to bound and dissociate from the Gb3 faster than Stx2 [346]. The difference in the preferred structure of the Stx B subunit during binding to Gb3 could also result in differential cytotoxicity between the two toxin subtypes. This was based on findings that the Stx1 B subunit is more stringent in binding to Gb3 as it could only interact with Gb3 in stable pentamer structure, as opposed to the Stx2 B subunit which are able to bind to Gb3 even in lower oligomeric states [347]. It may be that absolute toxicity is best

achieved via the Gb3-pentamer B subunit interaction, rather than with the presumably unstable lower oligomeric structures.

Caco-2 cells have been described to spontaneously differentiate upon reaching confluence [348-351]. This could result in differential expression of Gb3 on Caco-2 cells within the same culture, which is dependant on the maturity level of the cells and thus influence the overall Stx toxicity. If the Caco-2 cell culture treated with purified Stx2 in this study were predominantly immature cells not expressing surface Gb3, then this may explain the resistance towards Stx2. However the cells used for Stx1 and Stx2 cytotoxicity assays originated from the same tissue culture flask and sub-cultured at the same time under similar culture conditions, making this hypothesis less likely to explain the different toxicity levels between the two toxin types.

The different levels in potency between Stx1 and Stx2 were only observed in Caco-2 cells, rather than in other Gb3 positive cells including the Vero and HeLa cells. Earlier studies have reported that Gb3 on the cellular membrane does not always correlate with cytotoxicity [136, 286, 325]. Perhaps, differences in the structures and properties of Caco-2 cells in comparison to Vero and HeLa cells may contribute to the observed differences in the response between both cells to Stx1 and Stx2. Furthermore, the presence of Gb3 within lipid rafts on cell membrane was shown to significantly increase cell sensitivity towards Stx. Variations in the lipid raft structures were suggested to affect cellular responses to Stxs [136, 323]. Additionally, different signalling of the Stxs occur between Gb3+ and Gb3- epithelial cells, as reported by Schuller and colleagues where they investigated the intracellular trafficking of Stx1 and Stx2 in Caco-2 and T84 cells [159]. They found that although both Stx1 and 2 were able to reach the endoplasmic reticulum of T84 cells and the A-subunit of both toxins were cleaved in a furin-dependent manner, suggesting for an alternative cellular entrance mechanism taken by the Stxs into the Gb3-deficient cells.

Lastly, instability of the purified Stx2 (PStx2) used may have been a possible factor, although this is unlikely because Vero cells reacted to the same batch of PStx2 as much as they did react to PStx1.

2.2 Gb3 expression at the bovine terminal rectum

Flow cytometry analyses of bovine primary colon epithelial cells [272] identified a small population of Gb3-positive epithelial cells that were able to bind to the B-subunit of the toxin. Despite this the authors were not able to detect Gb3-positive epithelial cells in primary colon culture when investigated further by conventional and confocal microscopy, leading to inconclusion on the Gb3 status in bovine epithelial cells of the colon. Similarly, the results of flow cytometry analyses to detect the expression of Gb3 by primary bovine terminal rectal cells failed to provide a solid evidence as the results were inconsistent. Deriving the primary cells from different individual animals may very well be a major contributor to the observed flow cytometry analyses. Additionally, the uncertainty on the phenotype of the cells present after three or five days in culture posed some difficulty in reaching a solid interpretation. The receptor of interest might either be already expressed on the crypt cells isolated or the receptor was expressed post-seeding upon receiving synthetic cell culture medium or other stimulants. Fibroblast overgrowing within the primary cell culture was also another factor that could influence the outcome of such experiments [272].

To visualise the evidence for the presence or absence of Gb3 on cells of the bovine terminal rectum, this study proceeded with fluorescence microscopy examination of mucosal sections from the terminal rectum of a calf. Fluorescence microscopy images provided no evidence of Gb3 being expressed on both the intestinal epithelial cells (PCK-positive cells) or the underlying lamina propria (vimentin-positive cells). The lack of detection particularly on epithelial cells contradicts the results obtained from the flow cytometry examination of the bovine primary terminal rectal cells in the first batch of cells processed, but similar to what was reported for bovine primary colon epithelial culture cells [272]. In the bovine primary colon epithelial cell culture, there was no evidence on surface expression of

Gb3 which corroborated with the absence of significant anti-Gb3 staining in the histological sections of the epithelial layers of the colon.

Gb3 were reported to be expressed by intra-epithelial leukocytes of the ileum [275] as well as mitogen-stimulated lymphocytes of colon in cattle [271]. These findings may implicate that Shiga toxins preferentially targets the host immune cells than the absorptive epithelial cells as this may result in more beneficial effects to host colonisation by EHEC O157:H7. Furthermore, the Stx1 and Stx2 were found to bind to the Gb3-expressing Paneth cells, in addition to the endothelial cells and myofibroblasts around the crypts of human duodenal mucosa, in contrast to the colonic mucosa [161]. Paneth cells are highly specialised epithelial cells of the small intestine which functions as part of the innate immune response by expressing antimicrobial peptides including lysozyme and alpha-defensins [317]. Taken together my data and others, it is most likely that direct Gb3-Stx interaction does not occur at the bovine terminal rectal mucosa particularly along the epithelial cell layer and that if the toxin does indeed contributes to lesion formation at the site [352], the mechanism would be Gb3-independent.

During the investigation of Gb3 co-expression with PCK and vimentin-positive cells of the bovine terminal rectum, it was also observed for several dispersed areas with positive signals of Gb3-fluorescence near structures which resembled blood vessels. Further staining with anti-MHC class II antibody did revealed co-expression of Gb3+/MHC II+ staining around some, but not all of the blood vessels. This indicates that a specific group of MHC II positive cells do express Gb3, but in low numbers as Gb3+/MHC II+ cells were not consistently observed across all terminal rectal mucosal sections. The lack of time hindered from further phenotyping the Gb3+/MHC II+ cells examined.

Certain factors might limit Gb3 detection from the cryosections, for instance storage condition at -80°C or use of ice-cold absolute ethanol which can potentially cause over-drying of the tissue material thereby disrupting Gb3 structure, which might result in false-negative Gb3 detection. However, this is unlikely since the

positive control for the cryosections (nasal mucosa associated lymphoid tissue of the same animal, containing germinal centres with B cells and antigen presenting cells) had detectable levels of Gb3. The cryosections examined in this study were just sourced from one animal and therefore a different outcome may have been observed if tissues from more animals would have been analysed and compared. It would be useful to examine Gb3 on cryosections from EHEC O157:H7 colonised animals and to compare such results with the data obtained in this study. In addition, the rat-derived anti-Gb3 antibody was derived for specific use on human tissues, however this particular antibody was also shown to react with bovine tissues in a previous study [272]. The anti-Gb3 antibody is also an IgM, an isotype with five binding sites which could easily bound to or trapped within the structures of the mucosal sections, in particular where part of the cryosections, mainly the outmost area, appears to be dry with a loss in structure integrity. These disintegrated areas were easily identified and excluded from examination. A rat IgM-isotype control was also used to ensure that the Gb3+ signals detected were normalised to the isotype control.

2.3 Shiga toxin and epithelial cell cycle/proliferation

Despite the absence of Gb3 expression at the principal colonisation site, the question of whether the growth of intestinal epithelial cells are affected by Stx exposure was investigated. This was based on the belief that Stxs could still translocate across Gb3-negative cells [157-159] and by doing so, may interact with certain components of the epithelial cells that may alter epithelial cell homeostasis, for example epithelial layer integrity [159, 353] and water/ion transport systems [171]. *In vitro* assays testing for cellular proliferation and DNA profiles were performed on both Gb3-positive and Gb3-deficient intestinal epithelial cell lines. Stx2 treatment of both Caco-2 and T84 cells neither showed any evidence which supported the initial hypothesis that the toxin might target and hijack the proliferating machinery of the eukaryotic cell to the benefit of the bacteria, regardless of the Gb3 status of the cells tested. This was opposite to what was observed for Stx1 as it was reported that the Stx1 arrested HCT116 colon cells in the S phase after 24 hours of exposure [289]. In another study, intra-epithelial lymphocytes expressing Gb3 responded to the effect of Stx1 by showing inhibited proliferation [253, 275].

The lack of significant results from both the cell cycle (DNA-Propidium iodide staining plots) and proliferation marker analyses prevented further work to be continued on this subject. Otherwise follow up experiments could have been undertaken with cells synchronised in a particular cell cycle phase to examine which cycle regulator might have been affected by Stx treatment [294, 295].

Although the usage of intestinal cancerous cell lines to study cell cycle seems questionable owing to the erratic/infinite proliferating capacity, these cells have been widely accepted and used as appropriate intestinal epithelial models in a vast number of studies including those involving STEC as well as cell cycle [155, 349, 351, 353-355]. Caco-2 phenotypically resemble epithelial cells as they are polarised and express mature villi whereas the T84 resemble the phenotype of highly proliferating crypts [351, 355]. The different Gb3 status between these two cell lines provided comparison from another angle, in addition to crypt versus differentiated comparison.

The lack of effects on epithelial intestinal cell lines following Stx2 treatment may be due to insufficient stimulation time, which should be stretched further beyond 24 hours, for example, before the toxin could assert perturbations in the cell cycle. Stx2 was used at a sub-lethal dose (100 ng/ml), a dosage which has been commonly used in our laboratory for the Stx-stimulation of eukaryotic cells in immunology-based assays. Therefore, testing Stx on Caco-2 cells for cell cycle based assays performed in this study should be regarded as valid. It is therefore fair to conclude that Stx, at least Stx2, does not target the growth and development of the intestinal epithelial cells both the mature, Gb3 positive cells and the Gb3-deficient, under *in vitro* conditions. Actively proliferating crypt-like cells were observed to still continue proliferating as usual within 6 and 24 hours post-Stx2 treatment.

This study did not detect any profound Gb3 expression at the bovine terminal rectal epithelium which may suggest that: i) Stxs preferentially target the Gb3 positive bovine lymphocytes present in the underlying lamina propria, instead of the intestinal epithelial cells [253]; ii) Stxs are not able to exert cytotoxicity in the

bovine terminal rectal epithelial cells and iii) Stxs may exert effects other than cytotoxicity on the bovine terminal rectal epithelial cells (such as cellular integrity or water/ion channel functions [159, 170]). Cell cycle progression and cellular proliferation were unaffected in Stx2-treated Caco-2 and T84 cells, in contrast to Stx1 which halted the cell cycle progression at the S-phase [289]. It is however acknowledged that results obtained here should be interpreted with caution as further work are needed to support and confirm the findings here, particularly carried out under *in vivo* conditions which could not be realised here due to time and resource limitations. In addition, there is a need to establish continuously dividing intestinal epithelial cells of bovine origin to allow a more relevant system to be used since bovine primary cells, although valuable for its high degree of similarity to the cells present *in situ* in the cattle, have also certain issues to be resolved particularly with regards to consistency between culture batches and fibroblast contamination. Although there was a report on the establishment of a bovine intestinal epithelial cell line [356], the authors are still in the process of characterising the cells and testing for routine use in the laboratory [357]. By employing bovine intestinal epithelial cells, this would provide more confidence in the findings as i) originated from cattle, appropriate species, ii) easier to handle, homogenous cell culture system that will improve consistency between experiments and iii) a more in-depth understanding of events occurring intracellularly as changes in gene and protein expression could be studied with minimal heterogeneity, with the ease of obtaining higher sample amounts (as opposed to sorting primary cells into different types). Furthermore, the *in vitro* system of these continuous cells could be transformed to mimic the conditions *in vivo* by providing other elements such as aerobic/anaerobic conditions [165] or supplementing with different types of nutrients/proteins/others depending on the experiment requirements. Regardless, this chapter provides preliminary information on Gb3 expression at the primary EHEC O157:H7 colonisation site, as well as on the inability of purified Stx2 to interrupt with the intestinal epithelial cell proliferation.

Chapter 3

Assessing immuno-modulation by Shiga toxin at the follicle-associated epithelial mucosa during EHEC O157:H7 colonisation of the bovine intestine

Chapter 3

Introduction

3.1 Overview of the rectum

The rectum is part of the distal large intestine, positioned between the sigmoid colon and the anal canal. It functions as a storage vessel for faeces passed from the descending colon and participates in faecal evacuation through the anus via a series of neuromuscular sphincter mechanisms [358]. In cattle, rectal palpation has been routinely used in procedures such as pregnancy diagnosis, examination of the reproductive organs and artificial insemination.

The outer or serosal layer of the rectal wall is composed of epithelial and connective tissue covered with the mesentery providing blood supply and innervation to the rectum. This is followed by the external muscularis layer consisting of the longitudinal and circular muscular layers. The submucosa layer containing glands and nerve plexuses lies beneath the final layer which makes up the rectal lumen; the mucosal layer. Continuous columnar epithelial cells line the rectal mucosa until the recto-anal junction. This junction is demarcated by a change in the mucosal epithelium from columnar to stratified squamous epithelial cells. The absence of intestinal villi (projections of the mucosal epithelium present in the small intestine up to the ileo-caecal valve and involved in increasing surface for absorption) and the presence of numerous goblet cells are two characteristics typically observed for rectal mucosa. Most water from the faecal content has already been absorbed by the time it reaches the rectum, explaining the absence of villous membrane on the mucosal layer. Lubrication of the faeces is provided by mucus secreted from the goblet cells, with the mucus layer at the rectum observed to be denser among other sections of the intestinal tract [359].

Blood is supplied to the rectum via the superior rectal artery branching from the inferior mesenteric artery, while drainage for the proximal rectum is provided by the superior rectal vein which continues to the inferior mesenteric vein towards the hepatic portal system. The middle and inferior rectal veins carry deoxygenated blood from the terminal rectum to the internal iliac veins. Lymphatic vessels are present within the submucous and subserosa layers of the rectum which drain into the lymphatic vessels present on the outer rectal wall [360].

3.2 Gut-associated lymphoid tissue (GALT)

The mucosal epithelium lines the inner lumen of the intestine, with the lamina propria containing mucosal-associated lymphoid tissue (MALT) interposed between the epithelium and muscularis mucosae. MALT of the intestine also known as gut-associated lymphoid tissue (GALT) is an organized collection of isolated and aggregated lymphoid follicles that serves a critical role as inductive sites for priming the mucosal immune response following antigen recognition and uptake by the follicle-associated-epithelium (FAE) [361-363].

The FAE is identified by the presence of specialised cells named microfold or membranous cells (M cells) (will be discussed further in Introduction Chapter 3, section 3.11) separating the intestinal lumen and the underlying lymphoid follicles of GALT. Parsons et al. (1991) studied GALT of the bovine small intestine and reported the presence of follicles within the lamina propria underneath the dome-shaped FAE consisting of a single layer of homogenous specialised cells (M cells), with the absence of mucus-secreting goblet cell [364]. In the same study, the authors classified aggregation of lymphoid follicles known as Peyer's Patches (PP) into continuous and discrete. Continuous PP were observed only in the ileum of calves with subsets of lymphocytes, particularly B cells (discussed in detail in Introduction Chapter 3, section 3.9) undergoing lymphopoiesis, which involutes as the animal ages, hence proposed to be a primary lymphoid organ in cattle, similar to that of the Bursa of Fabricius in birds [365, 366]. Discrete PP were observed to be present in jejunum, distal ileum, caecum and colon which contained lymphoid follicles mainly associated with mucosal immune reactions, enlarged in older animals and which persist throughout the lifetime as a secondary lymphoid organ [361, 365, 366].

3.3 Recto-anal mucosal associated lymphoid tissue (RAMALT)

It has been estimated that 2.4% of the intestinal wall at the terminal rectum in calves is comprised of GALT [367, 368]. Published studies reported the presence of single lymphoid follicles being more apparent towards the terminal rectum, with a

raised rectal mucosa appearance, adjacent to the anus of calves and cattle [33, 250, 364, 367]. Similarly in humans, the presence of single lymphoid follicles increases in frequency towards the end of the rectum and was shown to correlate with the abundance of microbiota at the site [369]. In addition, small triangular patches of lymphoid tissue were seen to be evenly distributed around the bovine anus [367]. Such patches were also described to be present at the ileo-caecal entrance (continuous with ileal Peyer's Patches and extends to the colon) and proximal colon of calves [367]. Histological examination of the GALT structures at the terminal rectum identified two distinct phenotypes. The first described lymphoid follicles that were scattered within the lamina propria, which was more frequently observed. The other type identified was lymphoid follicles extending from the lamina propria to the muscularis mucosae of the submucosal layer, also known as lymphoglandular complexes. The latter phenotype was associated with older calves raised on conventional farms normally associated with large scale production and confined housing systems [367].

The single and patches of lymphoid follicles present at the terminal rectal or recto-anal area are collectively termed as recto-anal mucosal associated lymphoid tissue (RAMALT) or 'rectal tonsils' [370-372]. In sheep and deer, RAMALT is present as well and is often used to examine for the presence of abnormal prion protein accumulated within the lymphoid tissues in diagnosing transmissible spongiform encephalopathies (González et al., 2006; Wolfe et al., 2007). While in cattle, RAMALT is apparent at the bovine terminal rectum and serves as the primary colonisation site of EHEC O157:H7. Cells cultured from the bovine terminal rectal mucosa are therefore useful for studying EHEC O157:H7 colonisation factors. Epithelial crypts harvested from the rectal mucosa were successfully cultured to produce primary recto-anal epithelial cells [234, 373-375]. Direct application of bacterial colonies at the recto-anal junction of calves has also been previously demonstrated in an EHEC O157:H7 animal colonisation experiment [376].

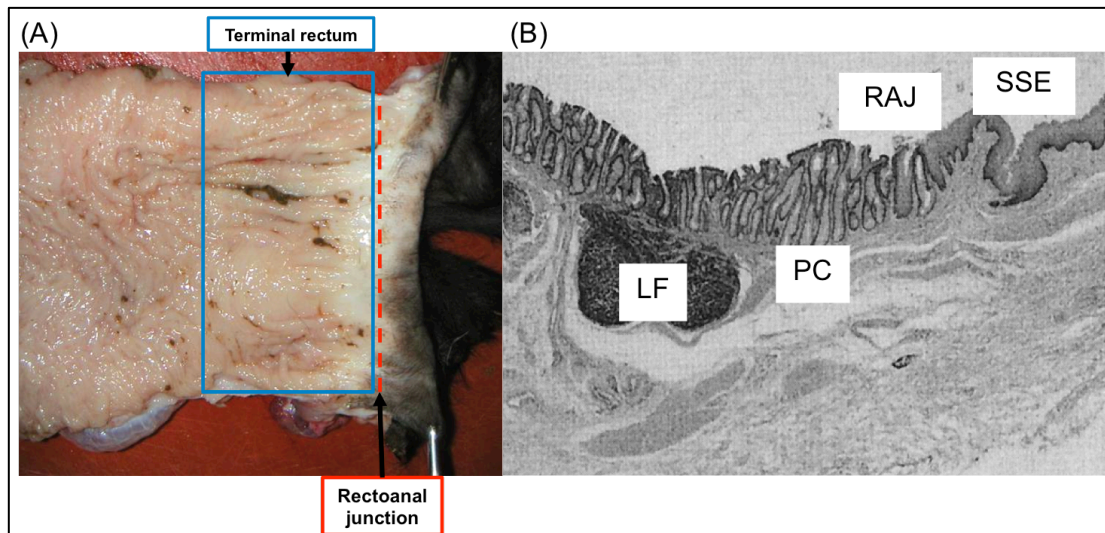


Figure 3.1 The bovine terminal rectal mucosa [Images courtesy of Dr. Arvind Mahajan and [33]]. (A) The anatomical position of the terminal rectum (blue box) and the rectoanal junction (red dotted line) in a calf is shown. **(B)** H&E-stained section of the terminal rectum to the rectoanal junction (RAJ). The RAJ is easily identified by the demarcation between stratified squamous epithelium (SSE) (the beginning of anus) and the columnar epithelium folded into pseudocrypts (PC) (the end of the rectum). The primary colonisation site of EHEC O157:H7 in cattle is at the follicle-associated epithelium overlying the lymphoid follicles (LF).

3.4 Leukocyte composition of the GALT

This section briefly summarises previous findings in published literature on bovine GALT. Further description on the characteristics and activities of different leukocytes mentioned and focused in this study is provided later on (refer Chapter 3 Introduction Sections 3.5 - 3.10).

The composition of the inter-epithelial leukocytes (IELs) differed significantly between the lamina propria and lymphoid patches of the ruminant intestine [377, 378]. The IELs in the bovine small intestine is dominated by T cytotoxic cells (properties further described in Introduction Chapter 3 section 3.6), with fewer B lymphocytes and total T lymphocytes [379]. Whereas the Peyer's Patches contained similar proportions of T cytotoxic, T helper (Introduction Chapter 3, section 3.5), B lymphocytes and monocytes (Introduction Chapter 3, section 3.10) [379]. The Peyer's Patches also contain more major histocompatibility complex (MHC) class II-expressing cells than the lamina propria [379].

T cytotoxic cells detection was limited to only within the interfollicular region of all the intestinal patches and none were observed to be inside the follicles [377]. The large intestinal patches contained 74% of cells expressing the B cell marker, p220, while 25% of the follicular lymphocytes were detected as T helper cells [365, 377]. Major histocompatibility complex (MHC) I is expressed by almost all of the subsets in the patches of the large intestine, while 75% of the cells in the large intestinal patches expresses MHC II [379].

Previous work on characterisation of the leukocytes of bovine RAMALT provided evidence for the presence of main players in mucosal immunity including T helper, T cytotoxic, IEL T $\gamma\delta$ cells, monocytes, dendritic cells, B lymphocytes and Natural Killer cells specifically at this site [250]. In addition, close examination of the histology and phenotype of bovine rectal FAE had identified the presence of specialised cells among the enterocytes overlying the lymphoid follicles, with the capacity to engulf particulates, assigned by the authors as the M-like cells [250]. It has yet to be determined on how the different immune cells present at the terminal

rectal mucosa of EHEC O157:H7-infected calves respond to following a thirty-day challenge with the bacteria and is therefore one of the objective of this chapter. By studying the proportion of different type of immune cells commonly present at the primary colonisation site in EHEC O157:H7 infected calves, we may obtain further understanding of the immune responses taking place *in vivo* and if any of the observations play a significant role for the maintenance of the bacterial colonies in the bovine host. The following section briefly introduces subsets of leukocytes investigated in this chapter.

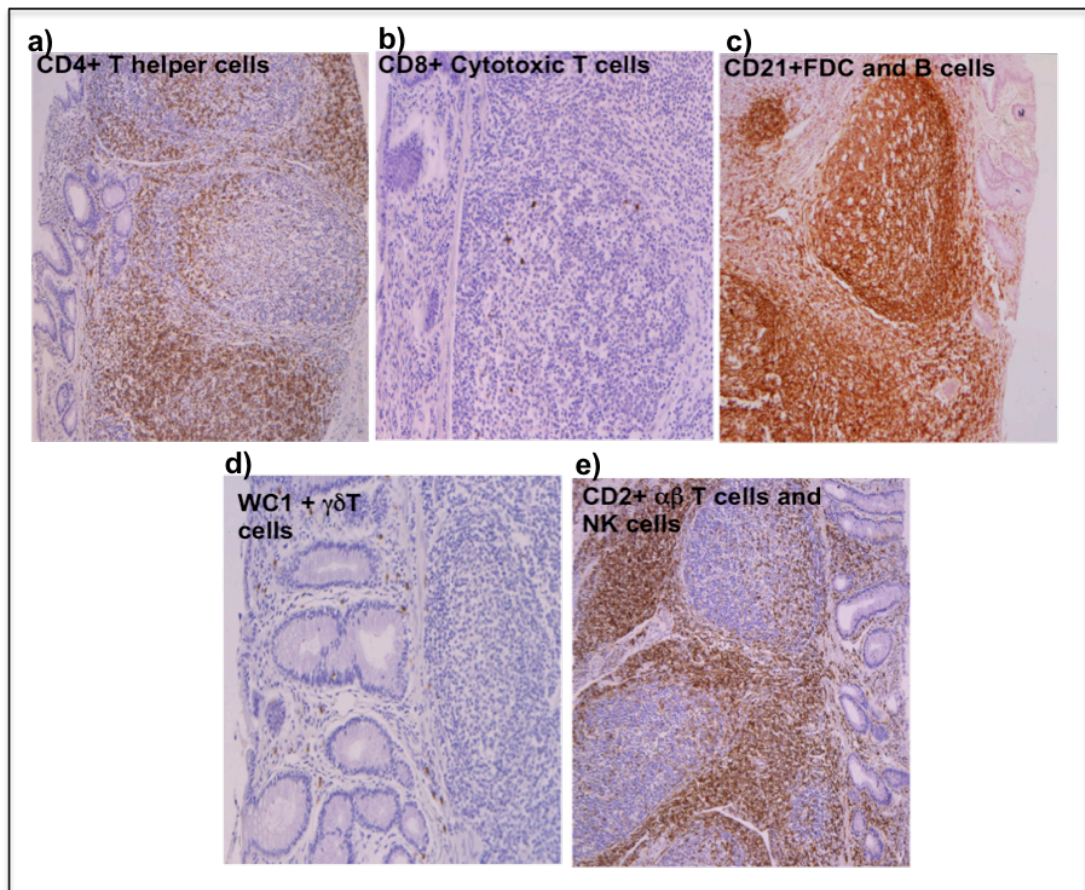


Figure 3.2 Lymphocytes associated with the lymphoid follicles of the bovine terminal rectal mucosa, taken from Mahajan et al. [250]. Immunohistological analysis by the authors identified for the presence of (a) T helper cells (CD4), (b) T cytotoxic cells (CD8), (c) WC1+ $\gamma\delta$ T-cells, (d) $\alpha\beta$ -T cells and natural killer cells (CD2) and (e) mature B-cells and follicular dendritic cells (CD21). The B lymphocytes were mainly found within the follicles, while T lymphocytes were distributed within the parafollicular region.

3.5 T helper lymphocyte (CD3+/CD4+)

CD3 is a complex of protein subunits belonging to the Ig superfamily, expressed on all T cells and is involved in transducing signal upon binding of the major histocompatibility complex (MHC)-antigen complex to the T cell receptors. CD4 is the co-receptor expressed on T helper (Th) cells with the MHC II molecule as the ligand. It is involved in promoting adhesion of the T helper cells to target cells as well as helping in T cell signal transduction [380]. Naive Th cells are activated by antigen-presenting cells (APCs) in peripheral lymphoid tissue, thereby differentiating into two functionally distinct subclasses of effector cells; Th1 or Th2 depending on the nature of antigen presented.

3.5.1 Th1 response

The Th1 response is activated by intracellular microbes leading to naive CD3+/CD4+ cells to differentiate to Th1 cells. Th1 activity is mediated by the master regulator T-bet, involving interleukin-12 (IL-12) and interferon-gamma (IFN- γ) via the Signal Transducer and Activators of Transcription 1 and 4 (STAT 1, STAT 4) pathways [381]. Th1 cells mainly secrete IFN- γ leading to pro-inflammatory responses including upregulation of monocyte and neutrophil production by the bone marrow, stimulation of endothelial cells to express adhesion molecules assisting in leukocyte binding and induction of chemokines to direct leukocyte migration from blood vessel into the infection site [382, 383]. Binding of IFN- γ to the Interferon- γ Receptor (IFNGR) present on macrophages will activate microbicidal action via oxygen radicals and nitric oxide. IFN- γ released from Th1 cells may also activate dendritic cells (DCs) via activation of the CD40 receptor on DCs leading to upregulation of MHC II and IL-12, further enhancing the already activated Th1 response. Th1 cells are also involved in activation of the T cytotoxic and Natural Killer cells in killing tumour and virus infected cells. IFN- γ counteracts the Th2 response via a positive feedback loop further augmenting the Th1 immune response. Recent findings have indicated for *in vivo* activation of the Th1 immune response in calves infected with EHEC O157:H7 [384]. The induction of IFN- γ and T-bet were evident in EHEC O157:H7-infected calves, which peaked at different days post

infection between two groups of calves receiving EHEC O157:H7 strains of different Stx-encoding phage contents. The second half of Chapter 3 (introduced in Introduction Section 3.13) focuses on several potential aspects on the impact of the released IFN- γ and Th1 response induction on the bovine terminal rectal mucosa in EHEC O157:H7 infected animals.

3.5.2 Th2 response

In contrast to the inflammatory-phagocytosis Th1-mediated response targeting intracellular pathogens, Th2 effector cells activate and mediate humoral (antibody) immune response towards extracellular parasites, bacteria, allergens and toxins. GATA binding protein 3 (GATA3) is the master regulator of Th2 differentiation. Exposure to the aforementioned stimuli will activate GATA3 resulting in production of Th2-cytokines including IL-4, IL-5 and IL-13, invoking strong antibody response by B cells leading to expulsion of the extracellular antigens from the host [385-388]. IL-10 is another Th2-cytokine produced with anti-inflammatory characteristics where it inhibits the secretion of pro-inflammatory Th1-cytokines from Th1 cells, macrophages and DCs. In addition, Th2 cells are capable of producing IL-24 and amphoregulin, both of which have anti-tumor properties [389, 390]. Balance between both arms of the Th effector response is crucial to maintain homeostasis and well-being of the host [391].

3.6 T cytotoxic lymphocyte (CD3+/CD8+)

The T cytotoxic lymphocyte co-expressing CD3 and CD8 receptors is the most studied subset among the known CD8+ subsets. The CD3+/CD8+ lymphocytes possess the ability to kill host cells infected with intracellular pathogens or transformed tumor cells thereby protecting the host from further damage. CD3+/CD8+ cells are also major producers of the pro-inflammatory cytokine, Interferon-gamma (IFN- γ) in humans and cattle [392-394]. The naive T cytotoxic lymphocyte travels through lymph nodes scanning for the presence of cognate antigen presented by MHC I molecules on APCs. In addition, the transcription factor eomesodermin (EOMES) has recently been identified as another transcription factor driving human T cytotoxic lymphocyte differentiation [395].

Cytotoxic lymphocytes (CTLs) confer the ability to kill infected and tumor cells via the dual action of perforin and granzymes. Granules containing perforin and granzymes are synthesised in CTLs, which are released via exocytosis into the extracellular space between a CTL and the target cell in a Calcium-dependent manner. Polymerisation of perforin will form polyperforin that functions to create pores in the cellular membrane of infected host cells allowing granzymes to enter the target cell. There have been many groups of granzymes identified, however the best characterised to date is Granzyme B, described to exert strong pro-apoptotic (programmed cellular death) activities. An alternative pathway leading to apoptosis by CTLs is induced by ligation of the Fas ligand (type 2 transmembrane protein of the Tumor Necrosis Factor family) expressed on activated T cells to the Fas receptor, a transmembrane glycoprotein with the structure resembling to the Tumor Necrosis Factor-alpha (TNF- α), present on most lymphoid cells including CTLs [396].

3.7 Natural Killer cell (CD16+/NKp46+)

The Natural Killer (NK) cells are morphologically described as large granular lymphocytes with the capacity to lyse target cells including tumor, viral-infected and allogenic cells. In addition, NK cells are also major producers of IFN- γ thereby contributing to Th1-polarisation of T cells in lymph nodes and mediating immune responses upon interaction with dendritic cells to eliminate infection and non-self marker-expressing cells as well as reducing the spread of cancerous, transformed cells [394, 397-399]. The pathways leading to cytotoxicity are similar to that as described for CD3+/CD8+ cells above. Despite similar mechanisms used to kill target cells, the cytotoxic activities of NK cells are differently induced to that of the CTLs. NK cells rely on normal or self-MHC I recognition by the germline-encoded inhibitory receptor recognition of MHC I, namely the Killer Cell Immunoglobulin-like Receptors (KIR), to arrest tyrosine kinase based activation signals, thereby sparing the normal, MHC I-expressing cells from being killed [400, 401]. Upon encountering non-MHC I expressing cells including tumorigenic (morphologically transformed) and viral-infected (due to the ability of viruses to remove MHC I from infected cells) cells, NK cells are not able to inhibit the tyrosine kinase activating signals triggering the onset of apoptotic pathways [402].

The phenotypic definition of an NK cell in humans and rodents is surface expression of CD56 and CD16 (FC γ RIIIA) from CD3-/TCR- lymphocytes [398, 403]. However, recent studies have proposed for NKp46 (also known as CD335), a type I transmembrane glycoprotein with two extracellular C2-type Immunoglobulin-like domains, as the most definite NK cell marker across many species including cattle [404, 405]. NKp46 is a member of the natural cytotoxicity receptors (NCR) family expressed on tumor cells, transplanted cells derived from a different host (xenogeneic transplantation) as well as viral-encoded ligands [406, 407].

Bovine NK cells are developed in the bone marrow and distributed throughout the spleen, liver, lung and lymph nodes, similar to the distribution in humans and mice [408]. Knowledge at the transcriptional levels of NK cell development, regulation and function is currently limited to mice. 1 to 10% of bovine peripheral blood mononuclear cells and 1.3 - 3.9% of mesenteric lymph node cells express NKp46 [405]. Majority of the NK cells identified in cattle are CD2-/NKp46+ that rapidly proliferates in response to Interleukin-2 and demonstrate cytotoxicity [405, 409, 410]. There was also evidence for CD16 transcribed within the CD2-/NKp46+ population [409]. CD16 is encoded by the low affinity Fc region receptor III-A (FCRIIIA) gene, is a receptor for the Fc portion of ImmunoglobulinG (IgG), able to induce antibody-dependent cellular cytotoxicity (ADCC) upon interacting with target cells coated with IgG [406]. CD16 was found to be expressed on lymphocytes from lymph nodes of healthy calves exhibiting NK cell functions; cytotoxicity and cytokine-production [410]. Therefore in this study, I have utilised co-expression of CD16+/NKp46+ as markers for immuno-phenotyping bovine NK cells from the terminal rectal mucosa.

3.8 T Gamma Delta cell (CD3+/ $\gamma\delta$ +)

Intra-epithelial lymphocytes (IEL), as the name implies, are lymphocytes present in between adjacent epithelial cells, have been identified in the epithelium of the skin, intestinal, genito-urinary and respiratory tracts [411]. The functions of IEL residing locally within the epithelium were described to provide immediate protection to the host from incoming pathogens or malignant cells through its

cytolytic and cytokine-expressing immunoregulatory properties [412]. Interaction between IEL and epithelial cells, particularly that described in the intestine of mice following exposure to *Salmonella*, commensals and microbial antigens leads to the production of the Angiogenin 4 (Ang 4) antimicrobial peptides by Paneth cells [413]. IEL are also able to express fibroblast growth factors (FGF) including keratinocyte growth factor (KGF) to support wound healing in mice, as well as regulating proliferation of enterocytes in monkeys, guinea pigs and mice [414, 415].

A review paper proposed for classification of IEL into Type a and Type b [412]. Type a refers to T cells expressing TCR $\alpha\beta$ +, primarily involved in the adaptive immune system via its MHC I and II recognition with long term memory. The IEL are mainly intestinal IEL scattered within the epithelium of small and large intestine of mice. While Type b IEL are T cells expressing TCR $\alpha\beta$ + CD8 $\alpha\alpha$ + and T cells with TCR $\gamma\delta$. Functionally, the Type b IEL are not restricted by the conventional MHC recognition system and mainly associated with the epithelium of murine skin, vagina and small intestine.

The current study chose to focus on the IEL TCR $\gamma\delta$ cells since in cattle these cells are significantly present in bovine peripheral blood (15-60%) and in the epithelium of the skin and intestinal mucosa [416, 417]. These cells were also detected in significant amounts around the lymph node trabeculae, but sparsely present in B and T cell domains of lymph nodes [416, 418]. Bovine TCR $\gamma\delta$ cells were phenotypically characterised as CD4-/CD8-/TCR $\gamma\delta$ + lymphocytes and recently have been proposed to be a major regulatory T cell subset in bovine immune system [417, 419]. The circulating TCR $\gamma\delta$ cells in bovine peripheral blood are able to spontaneously produce Interleukin-10 (IL-10), a cytokine involved in immunoregulation exerting anti-inflammatory effects [420]. In addition, exposure to mycobacterial products caused significant proliferative activities of T $\gamma\delta$ and Interferon-gamma (IFN- γ) production [418].

3.9 B lymphocytes (CD21+)

The naive and memory B lymphocytes are activated upon contact with specific foreign antigens and antigenic peptides presented by the T helper cells. Stimulation of the resting B lymphocytes leads to proliferation and differentiation of the effector B cells that then mature to become antibody-secreting plasma cells. B cell receptor (BCR) are involved in many B cell biological processes including B cell developmental regulations and transduction and interpretation of signals from the extracellular environment [421]. Among the recognised BCR are CD79 (CD79a and CD79b; both present exclusively on B cells and B cell neoplasms) [422], CD19 (positive regulator of BCR signalling in proliferation and survival of B cells) [423], CD72 (negative regulator of B cell responsiveness) [424] and CD21. CD21 mainly is surface-expressed by mature B cells and was described to be involved in B cell activation and homotypic aggregation of human B lymphocytes [425]. CD21 also binds to IFN- α [426] and serves as a receptor for the Epstein-Barr virus [427]. The anti-bovine CD21 antibody was used in the current study to detect B lymphocytes present in the harvested bovine terminal rectal mucosal tissue since this antibody was shown to react with bovine B cells in a previous study [250]. In addition, a specialised APC, the follicular dendritic cell also expresses CD21 [428].

3.10 Monocytes and macrophages (Signal Regulatory Protein-alpha, SiRP- α + or SiRP-1 α +))

The final group of immune cells to be described in this section are the SiRP-1 α -expressing cells, which includes monocytes, dendritic cells and macrophages. SiRP-1 α or Signal Regulatory Protein-1 alpha is a 55 kDa type I membrane protein and member of the Ig superfamily with three Ig-like domains in its extracellular compartment. Other names for SiRP-1 α includes macrophage fusion receptor, CD172a and MyD-1 antigen. It is implicated in mycobacterial infection in tissue culture particularly in the formation of multinucleated giant cell [429]. The early secretory antigenic target-6 (ESAT-6) and culture filtrate protein-10 (CFP-10) co-secreted by *Mycobacterium tuberculosis* complex mycobacteria together increase the proliferation of SiRP-1 α + cells in bovine peripheral blood with dendritic

cell/macrophage morphology and induces multi-nucleated giant cell formation expressing SiRP-1 α [429]. SiRP-1 α has also been shown to be a better marker for detecting monocytes of the bovine peripheral blood than CD14 [430].

Monocytes are a subset of leukocyte with the ability to differentiate to dendritic cells (DC) or macrophages of different phenotypic and functional subsets. Monocytes develop from the common leukocyte progenitors in the bone marrow and depending on the type of monocyte subset (based on the combination of surface receptors including chemokine CC receptors CCR2 or CCR7, CD14 and CD16 expressed), these monocytes will either function in surveillance throughout the peripheral blood and non-inflamed tissue or emigrate from the bone marrow directly towards the inflamed tissue [431]. Pro-inflammatory cytokines and chemokines released at the inflamed site, along with microbial factors, adhesins and local growth factors influence the fate of the monocytes to either be differentiated into DC or macrophages. In particular, IL-6 and TNF have each been shown to be key players in determining if monocytes from healthy human peripheral blood will differentiate into macrophage or DC, respectively [432, 433]. Under non-inflamed conditions, monocytes differentiate into macrophages in a IL-6 and macrophages-colony stimulating factor (M-CSF) dependent manner [432]. Interaction with bacterial endotoxin and IFN- γ within the microenvironment will activate the classical macrophage activation pathway, pre-dominantly exerting pro-inflammatory effects while in the presence of IL-4 and IL-13, the alternative macrophage activation pathway is activated producing anti-inflammatory effects [434, 435].

3.11 Interaction of bacterial pathogens with the follicle-associated-epithelium (FAE)

Interest towards understanding interactions at the bovine terminal rectum during an EHEC O157:H7 colonisation began once this site was identified as the principal colonisation site of the pathogen [33]. In particular the presence of lymphoid follicles has led to the hypothesis that EHEC O157:H7 might be targeting this niche to interact with host immune cells and further manipulate their responses

as a mean to gain colonisation advantage. Such immune-regulation might result in inducing host tolerance to bacterial factors that could be essential for ensuring persistence. The lymphoid-follicle rich area has been characterised to contain heterogeneous cell populations, with the presence of cells that morphologically and functionally resemble M cells [250]. The authors proposed specific FAE interaction with EHEC O157:H7 during colonisation. They also provided evidence of A/E lesion formation, neutrophil infiltration and induction of specific humoral immune response during EHEC O157:H7 infection at the FAE [352]. *In vitro* organ cultures (IVOC) of human and bovine ileum infected with EHEC O157:H7 strain 85-170 revealed the formation of A/E lesions specifically on FAE [436]. In another study, EPEC O127:H6 diffusely bound to the proximal and distal parts of the small intestine [437]. The authors demonstrated that the type of bacterial intimin expressed (EHEC and EPEC produces intimin- γ and intimin- α , respectively) dictates the preferred site for bacterial localisation and attachment [438].

The M or microfold cells are specialised epithelial cells that differ morphologically and enzymatically from the adjacent absorptive enterocytes. These cells act as entrance portal for luminal antigens and particles before being translocated into the effector sites within the underlying lamina propria for processing and induction or repression of immune responses [439, 440].

The features of a typical M cell include absence of irregular brush border on the apical surface and basolateral cytoplasmic invagination forming pockets containing B and T lymphocytes, macrophages and dendritic cells. The surface glycocalyx and mucus layer appears thinner than the absorptive epithelium, allowing rapid and easy luminal particle and antigen uptake. The beta-integrin (β -integrin) transmembrane receptor is present on the surfaces of M cells allowing binding to the extracellular matrix as well as bacterial strains expressing intimin-gamma (Intimin- γ) [441-443]. M cells lack apical surface glycoproteins including alkaline phosphatase and sucrose-isomaltase, as well as polymeric immunoglobulin (Ig) receptor with low levels of secretory Immunoglobulin A (sIgA) [444]. The capability to translocate intestinal luminal particles or antigens into the FAE makes the M cell a convenient

target for several enteropathogenic bacteria to gain access into the deeper parts of the mucosa before spreading systemically. *Salmonella enterica* serovar Typhimurium, *Yersinia pseudotuberculosis*, *Shigella flexneri* and a rabbit EPEC strain (RDEC-1) are among the pathogens previously shown to exploit M cells in order to cross the intestinal epithelial border [445-448].

One study employed Caco-2 and Burkitt's lymphoma Raji B cells co-culture to generate cells with M cell phenotypes. This was obtained by culturing Caco-2 cells on the apical side of transwells and Burkitt's lymphoma Raji B cells at the basolateral side until Caco-2 cells reached full confluence, spontaneously differentiating and produced Caco-2 cells resembling M cells at the FAE. This *in vitro* co-culture model was used to study EHEC O157:H7 mobility across the FAE, where they successfully demonstrated the ability of EHEC O157:H7 strains to translocate across M cells *in vitro* [449]. The same study also observed EHEC O157:H7 survival, replication and Stx production before inducing apoptosis in THP-1 macrophages. They concluded that following successful translocation across intestinal FAE, some EHEC will interact with the underlying immune cells immediately beneath the FAE. EHEC continues to survive and release Stx into the lamina propria before systemically circulating to renal and brain endothelium.

Despite the encouraging findings from *in vitro* studies linking lymphoid follicles and M cells mentioned above, close examination of tissue sections from EHEC O157:H7-challenged calves did not reveal any evidence to correlate the lymphoid dense area at the terminal rectum and bacterial tropism [352]. Since M cells only cover about 0.01% of the total intestinal epithelial surface [450], it is most likely that the host-bacterial interactions occur at the absorptive intestinal epithelial cells. EHEC O157:H7 tropism towards bovine terminal rectum may reflect non-cellular factors including quorum sensing, nutrient availability and various factors expressed by EHEC O157:H7 including genes for efficient nutrient utilisation or conversion to survive within a highly competitive niche [36, 198, 199, 451].

3.12 Shiga toxin and host immunomodulation

Stx2 was shown to influence bovine cellular immune response as demonstrated in calves challenged with Stx2-producing EHEC O157 Strain 86-24 [452]. In the study, the calves were intra-rumenally challenged with either EHEC O157 Strain 86-24 (Stx2+), Stx-2 negative O157 or non-pathogenic *E. coli* and observed for three weeks before re-infecting all animals with EHEC O157 Strain 86-24. Significant suppression in the proliferation of concanvalin A (conA)-stimulated peripheral blood mononuclear cells (PBMC) of animals in the group that was twice challenged with EHEC Strain 86-24 (Stx2+) were reported, with the proliferative rates reported to be similar to the PBMC from animals challenged with the non-pathogenic strain. In contrast, a significant increase was observed in the proliferative activity of the PBMC isolated from the animals initially inoculated with the Stx negative strain. The humoral responses were similar in all three groups, with comparable levels of anti-O157 antibodies were detected in all animals. These results are in accord with the *in vitro* experimental findings for which a Stx1-expressing EHEC O157:H7 strain reduced the proportion of bovine phytohaemagglutinin (PHA)-stimulated CD8+ T lymphocytes, but not CD4+ T while LPS-stimulated CD21+ B lymphocytes which were only slightly affected [252, 453]. Stx1 inhibited the activation of LPS and conA stimulated-PBMC, as indicated by the absence of CD71 (transferin receptor, co-expressed with CD25 on activated lymphocytes) expression, further supporting Stx-dependent immune-regulating mechanism in the host. In addition, activated bovine PBMC CD8+ T and B lymphocytes expresses Gb3 rendering these cells susceptible to the effects of Stx compared to other subpopulations of the PBMC [271].

Earlier studies of differentiated human monocytes revealed that while resistant to the toxic effect of purified Stx1 and Stx2e, monocyte-derived macrophages were stimulated to express pro-inflammatory cytokines including TNF- α and IL-1 β [186, 268, 454]. TNF- α and IL-1 β released by macrophages during inflammation could enhance the expression of enzymes involved in Gb3 synthesis (ceramide glucosyltransferase, lactosylceramide synthase and Gb3 synthase) on microvascular endothelial cells of the brain and kidney, leading to increased Stx binding and exacerbation of inflammation [137, 186, 455-457].

In contrast to human microvascular endothelial cells, the sensitivity to Stx1 of Gb3+ bovine lymphocytes (CD8+ T) from PBMC is not dependent on TNF- α , IFN- α and IL-2 [253]. While Stx1 stimulation of bovine ileal IELs resulted in 40% of cells responding by secreting IFN- γ , with a small proportion (less than 10%) produced either IL-4 or tumour growth factor-beta 1 (TGF- β 1) [458]. The mRNA and production of pro-inflammatory IL-8, growth-regulated oncogene-alpha (GRO- α), monocyte-chemoattractant protein-1 (MCP-1) and Regulated on Activation, Normal T Expressed and Secreted (RANTES) were significantly increased upon treatment of bovine colon mesenchymal cells with Stx1. Conversely, bovine primary colon epithelial cells were resistant and non-responsive to Stx1 [272].

In a Gb3-deficient human intestinal epithelial cell line (T84 cells), the phosphatidylinositol 3-kinase/Akt/Nuclear factor kappa B (PI3K/Akt/NF κ B) pathway was strongly enhanced after treatment with EHEC O157:H7 Strain EDL 933 Δ stx1/stx2 (Stx-), but was only weakly induced in cells infected with wild type Strain EDL 933 (Stx+) [459]. Results from their study suggests that EHEC infection weakly activate NF κ B pathway in T84 cells, however the consecutive signalling pathways will be inhibited upon Stx1/Stx2 expression. This, with the studies described above indicates that EHEC strains do manipulate immune responses in specific types of cells in a Stx-dependent manner to potentially promote their persistence in the bovine host following colonisation.

This chapter aims to investigate the consequences of Stx presence on the mucosal immune response in bovine terminal rectum following exposure to EHEC O157:H7 strains in an attempt to investigate if Stx influences the colonisation process. Bovine terminal rectal tissues were obtained from cattle slaughtered after a thirty-day challenge experiment with either EHEC O157:H7 Strain 9000 (PT21/28) or Strain 10671 (PT32) performed by collaborators at the Moredun Research Institute (Pentlands Science Park, UK). These two most commonly isolated strains from cattle farms in Scotland differ in Stx-prophage carriage, providing an opportunity not only to examine differences between infected and non-infected tissue samples, but also between samples of animals challenged with strains varying in Stx subtypes [60].

Different subsets of immune cells present at the FAE of bovine terminal rectum previously characterised [250] were immunophenotyped and compared among the calves to determine the impact of EHEC O157:H7 presence on mucosal immune responses at the colonisation site.

3.13 Interferon-gamma (IFN- γ) and EHEC O157:H7 colonisation

A common feature shared amongst the immunophenotyped cells in this chapter is the ability to either express or be responsive to the pleiotropic type II Interferon, IFN- γ . IFN- γ is one of the key mediators of immunity and inflammation. It plays significant roles in regulating the mechanisms and balance in an array of diverse biological processes. Macrophages, fibroblast and epithelial cells have been shown to respond to IFN- γ . The most common properties of IFN- γ described are anti-proliferative, anti-viral, anti-tumour and roles in immunosurveillance [460].

IFN- γ is predominantly produced by activated Th1 CD4⁺ cells upon interaction with antigens presented by major histocompatibility complex (MHC) class II, while antigens presented by MHC class I are able to induce IFN- γ in CD3⁺/CD8⁺ cytotoxic T lymphocytes [461]. Other sources of IFN- γ includes natural killer (NK) cells, natural killer T (NKT) cells and T cell receptor gamma delta (TCR $\gamma\delta$ ⁺) cells [462-464].

Among the roles of this cytokine include activating macrophage and Natural Killer (NK) cells, enhancing CD3/CD8 cell cytotoxicity, upregulating the expression of Major Histocompatibility Complex (MHC) I and II in macrophages, tumour cell surveillance and inhibiting growth of non-haematopoietic cell types including epithelial (further explained in the following in Section 3.14), endothelial cells and fibroblast [465, 466]. IFN- γ could also be involved in regulatory functions to limit tissue damage following inflammation for example in skeletal muscle cells [467], as well as modulating Th1 [468] and regulatory T (Treg) differentiation [469].

The main intracellular transduction pathway activated by IFN- γ is via the Janus kinase (JAK) and signal transducer and activator of transcription (STAT) transduction pathways, before activating the transcription of IFN- γ activated genes involved the transcription of various cytokines and growth factors. The major STAT protein activated by IFN- γ is STAT1 [470]. Interaction between the IFN- γ and the heterodimeric Interferon-gamma receptor (IFNGR) induces conformational change in the receptor, which then activates the Janus protein tyrosine kinase (Jak) 2, followed by transphosphorylation of Jak1 [471]. The activated Jak1 then phosphorylates the critical tyrosine residue 440 on each IFNGR chain to form docking sites for STAT1 [472]. Phosphorylation of two STAT1 proteins leads to dissociation of the STAT1 homodimer from the IFNGR that will then translocate into the nucleus, to bind to the promoters of the IFN- γ transcription factors (gamma activating site or GAS) initiating or suppressing the many IFN- γ regulated genes [465]. During the early phase of activation, Stat1 is also phosphorylated on serine 727 by a process involving phosphatidylinositol 3-kinase (PI3K) and Akt that is required for maximal transcriptional activity [460, 473, 474]. *Stat1*-deficient mice showed normal development but were highly susceptible to bacterial and viral infection [475, 476]. The repertoire of regulated genes in eukaryotic cells that are IFN- γ -JAK/STAT1 pathway-dependent is large. This includes genes that activate macrophage during the later stages of inflammation such as monocyte chemo-attractant protein-1 (MCP-1) and macrophage inflammatory protein-1 (MIP-1) [477]. In addition, IFN- γ activates the suppressor of cytokine signalling-1 (*SOCS-1*) gene providing negative feedback to cytokine production [478]. The genes coding for the anti-viral resistance property of IFN- γ , conferred by the T cell specific GTPase (TGTP) is also regulated via the JAK/STAT1 pathway [479].

Multiple Shiga toxin-expressing *E. coli* strains were able to interfere with the activation of JAK/STAT1 pathway, most probably due to involvement of Stx [480-483]. Therefore, it was investigated if culture supernatants of EHEC O157:H7 strain EDL 933 are able to inhibit the JAK/STAT1 signal transductions in Caco-2 cells. If the outcomes are in agreement with the published findings, further experiments could be performed on bovine intestinal cells and bovine-adapted strains to check if this

phenotype is common across different strains of EHEC O157:H7. Furthermore, it is anticipated that implications following EHEC O157:H7 inhibition of an important intracellular pathway involved in various downstream effects including immune responses and epithelial functions would profoundly affect the colonisation process, particularly directed towards the survival of the pathogenic bacteria.

3.14 IFN- γ and epithelial cell proliferation/cell cycle

Epithelial cell proliferation is an important part of innate immunity, ensuring continuous supply of new cells to refill gaps along the intestinal lining left by cell removal from the tip following programmed cell death at the intestinal villi surface. Many genes regulating cell growth, differentiation and apoptosis are activated by the IFN- γ pathway including *MYC* [484] and caspase 1, apoptosis-related cysteine peptidase (*CASP1*) [485], as well as cyclin-dependent kinase inhibitor-encoding genes in regulating cell cycle, for example p21, a kinase inhibitor arresting the cell cycle at G1-S phase [298, 486, 487]. It was shown that IFN- γ inhibited the proliferation of rat intestinal crypt cells *in vitro* [254]. STAT1 induction following IFN- γ or epidermal growth factor (EGF) binding to the IFNGR inhibited the growth of cells via activation of cyclin-dependent kinase inhibitor (CDK) p21 WAF1/CIP1, but not in a STAT1-deficient cell line, U3A (human epithelial fibrosarcoma cell line) [488]. Epithelial cell growth could also be regulated by IFN- γ in the presence of TNF- α during inflammation in a STAT1-independent pathway by converging the AKT- β -catenin and Wnt- β -catenin pathways resulting in changes to cellular proliferation and induction of apoptosis [489].

To investigate the effects of IFN- γ on the proliferation of intestinal epithelial cells, the two widely used immortalized epithelial cell lines T84 and Caco-2 were used in my research. Both cell lines were exposed to both IFN- γ and Stx to examine if the toxin could further increase or suppress the anti-proliferative effect of the cytokine. As cellular proliferation is closely associated with the cell cycle, simultaneous assays examining the effect of IFN- γ treatment on the intestinal epithelial cells were carried out. Any significant departure from the normal cell cycle pattern (based on DNA staining by propidium iodide) exposure to IFN- γ warrants

further investigation in identifying the possible cell cycle regulatory proteins affected and the specific mechanisms or pathways involved. A recent published article highlighted the involvement of IFN- γ in a novel mechanism of host immunomodulation of epithelial homeostasis following exposure to *Citrobacter rodentium* in mice [490]. Significant depletion in the number of mucus-secreting goblet cells of infected murine colon were observed. Further examination revealed that *C. rodentium* preferred to colonise at the non-hyperplastic crypts, rich in goblet cells rather than on the highly proliferative, goblet cell-depleted epithelium. Presumably as a response to protect from damage by the *C. rodentium* in the host intestine, a reduction in the numbers of goblet cells is modulated by IFN- γ signalling pathways causing depletion of anchoring sites for attachment by the bacteria [490].

To investigate if Stx plays a role in EHEC O157:H7 colonisation at the bovine terminal rectum, the objectives addressed in Chapter 3 were:

1. To examine by flow cytometry, mucosal immune cells previously characterised [250] to be present at the follicle-associated-epithelium of bovine terminal rectum and to determine whether EHEC O157:H7 infection alters the proportions of these sub-populations at the colonisation site.
2. To compare the expression of IFN- γ by bovine terminal rectal mucosal cells between EHEC O157-challenged and control calves.
3. To examine and verify the potential effect of Stx on the IFN- γ activated JAK/STAT1 signalling pathway in intestinal epithelial cell lines.
4. To assess direct interaction between intestinal epithelial cells and IFN- γ potentially affecting intestinal epithelial cell proliferation and growth.

Chapter 3

Materials and methods

3.1 Harvest of terminal rectal mucosal cells

To study the impact of EHEC O157:H7 colonisation specifically towards the mucosal cells of the bovine terminal rectum, immunophenotyping of selected cell surface markers was performed on tissues from colonised and control cattle. *Post-mortem* samples of terminal rectal tissue (defined as part of the rectum at 4 cm distal to the recto-anal junction) were kindly provided by Dr. Tom McNeilly and Alexander Corbishley of the Moredun Research Institute (MRI, Pentlands Science Park, Midlothian, UK) as part of a study assessing immune response in EHEC O157:H7-challenged calves [384]. Two groups of six male dairy (Holstein-Friesian or Ayrshire breeds) calves with an average age of 12 ± 2 weeks were randomly assigned to separate rooms in the MRI High Security Unit (HSU). Two calves were housed in conventional pens, while five additional age-matched calves previously used as control in other studies were used as sources of additional lymph node and rectal mucosal samples. All calves were confirmed negative for EHEC O157:H7 from faecal samples cultured on Cefixime-Tellurite Sorbitol MacConkey (CT-SMAC) agar plates. Non-sorbitol fermenters (colourless colonies) were further tested with the immune-magnetic separation (IMS) technique, a week prior to the commencement of the experiment. Four calves in one HSU room were orally challenged by orogastric intubation with 500 ml PBS containing 10 ml of an overnight LB culture of EHEC O157:H7 Strain 9000 (ϕ Stx2a/ ϕ Stx2c) and its naturally derived Naladixic (Nal)-resistant variant. Four calves in the other HSU room were challenged in the same manner with EHEC O157:H7 Strain 10671 (ϕ Stx2c). The other two calves (sentinels) in each HSU room received 500 ml PBS only. Faecal samples were collected on a daily basis in the first 2 weeks of the experiment and every other day from then on for enumeration of colony forming units (C.F.U.) to produce bacterial shedding curves. Rectal tissue biopsies were also obtained on a weekly basis for gene expression studies. All animals were killed at the end of the trial (31-33 days) by intravenous pentobarbital (60 ml) before *post-mortem* examination was performed. Rectal, mesenteric and pre-scapular lymph nodes were collected for *ex-vivo* restimulation (concanavalin A and LPS) experiments. For immunophenotyping experiments presented in this chapter, the rectal mucosal layer were collected and immersed in Polymyxin B sulfate (Sigma), diluted 2 mg/ml in

normal saline for 30 min in a 150 ml polystyrene straight-sided metal cap container (Starlab) before transported to the Roslin Institute according to biosafety regulations.

The rectal tissues were cut into approximately 1 cm x 2-2.5 cm (length x width) in size in a petri dish and transferred into a 50 ml Falcon™ tube (Fisher Scientific) pre-filled with 10 ml of digestion medium base [Dulbecco's Modified Eagle's Medium (DMEM) (Life Technologies), 1% fetal calf serum (FCS) (Sigma), 1% Penicillin-Streptomycin (10,000 U/ml, Invitrogen) and 25 µg/ml Gentamicin (Sigma)]. More digestion medium was added to a final volume of 25 ml, followed by the enzymes required for tissue digestion, 250 µl of Collagenase (75 U/ml, Sigma) and 250 µl of Dispase I Neutral Protease, Grade 1 (20 µg/ml, Roche). Tubes were manually agitated for five times before being placed in a shaker incubator (INFORS HT Multitron Standard, Company) for 90 min at 37°C, 200 R.P.M. At the end of digestion, tissues appeared to be disintegrated, physically characterised by a liquefied, coagulated appearance as opposed to an intact tissue. This is accompanied by a much darker colour of the digestion medium (change from red to dark red or brown). The tubes were again manually agitated, vigorously for approximately five times to separate the disintegrated and coagulated fibrous tissue materials allowing mucosal cells to be further released into the medium, before centrifuging the tubes at 260 x g for 5 min. Supernatants were filtered through individual cell strainers (pore size of 0.22 µm, Millipore) into a 50 ml Falcon™ tube. Both tubes (supernatant- and digested tissue-containing tubes) were added with 50 ml of lymphocyte medium [80% RPMI-1640 medium (R0883, Sigma), 10% FCS (Sigma), 1% L-glutamine (Invitrogen), 4 µl of β -Mercaptoethanol (Sigma) and 1 ml of Penicillin-Streptomycin (10,000 U/ml) (Invitrogen)] and centrifuged again under the same conditions described above. The differential centrifugation steps were repeated until the supernatants appeared clear (characterised by a pale red colour, with the absence of tissue material) and the cell pellet size resembles to that of a pellet containing approximately 1 x 10⁶ cells/ml. Cells were stained with 0.2% Trypan Blue solution (Invitrogen) in PBS. 10 µl of the stained cells were transferred onto Neubauer Chamber Slide (Marienfeld) for cell counting.

3.2 Immunostaining bovine terminal rectal mucosal cells for flow cytometry

Cells were transferred into a Nunc® 96-Well Polystyrene Conical Bottom Microwell™ plate (Thermo Scientific) at a density of 1×10^6 cells/ml and washed once in flow cytometry buffer (2% FCS in PBS), centrifuged at 1200 R.P.M. for 5 min before staining with primary antibodies obtained in-house from Timothy Connelley's laboratory of The Roslin Institute and Alexander Corbishley (Table 3.1) raised against different combination of established bovine cell surface markers. Nagi and Babiuk (1987) were among the earliest researchers to publish on techniques for extracting and characterising leukocytes from the epithelium and lamina propria of the bovine small intestine [378]. They were able to identify surface immune cell markers of the T helper (CD3+/CD4+) and cytotoxic T cells (CD3+/CD8+) by immunofluorescent characterisation using mouse monoclonal antibodies on lymphocytes of the bovine small intestinal intra-epithelium, lamina propria and Peyer's Patches. While intraepithelial Gamma Delta T cells (CD3+/ $\gamma\delta$ +), first described in cattle in 1989 [491], were detected in my study with a Pan TCR $\gamma\delta$ antibody, GB21a [492, 493]. Detection of CD16+/NkP46+ co-expressing cells represents the Natural Killer (NK) cells [401, 405, 409], while B cells and follicular dendritic cells were detected with anti-CD21 antibody (CD21) [364, 494]. Monocytes, monocyte-derived macrophages and dendritic cells were identified with the antibody against Sirp-1- α (CD172a) [430] for 30 min at 4°C.

The cells were washed three times in flow cytometry buffer (2 min at 1200 R.P.M.) followed by staining with undiluted secondary antibodies (anti-mouse IgG1 Alexa Fluor® 647-conjugated, anti-mouse IgG2 α Pycoerythrin-conjugated, anti-mouse IgG2 β Alexa Fluor® 488-conjugated, Timothy Connelley, The Roslin Institute, Edinburgh, UK), 100 μ l/well. After 20 min of incubation at 4°C protected from light, the cells were washed as described above three times for 2 min and finally re-suspended in 450 μ l of flow cytometry buffer for data acquisition with BD FACSCalibur™ machine.

3.3 Flow cytometry data acquisition and analyses

Data on fluorescence detection of immune-stained cells was acquired by BD FACSCALIBUR™ flow cytometry machine according to the standard operating procedure. Briefly, 10,000 events were collected during acquisition with the BD CELLQUEST™ (BD Biosciences) and saved in the Unix Executable File format for analyses in FlowJo software (Treestar, Inc.). Cells labelled with goat anti-mouse conjugated to Alexa Fluor® 488 were detected by green or fluorescence channel 1 (FL-1), goat anti-mouse conjugated to Pycoerythrin by the yellow or fluorescence channel 2 (FL-2) and goat-anti mouse conjugated to Alexa Fluor® 647 in fluorescence red or channel 4 (FL-4). Compensation between FL-1 and FL-2 was performed before acquisition of data from all samples. Since no viable staining was used prior to loading the samples into the flow cytometry machine, cells were visually assessed from the forward scatter (FSC) versus side scatter (SSC) dot plots to exclude potential cellular debris (typically characterised by the presence of a small group in the bottom left quarter of the dot plot with low FSC and SSC values), therefore selecting presumably ‘viable’ cells in the next steps of analyses. Gating on ‘viable’ cells was also based on typical pattern of lymphocytes in an FSC-SSC dot plot, with the help and technical advice from an experienced immunologist. Double fluorescence staining populations were derived from the ‘viable’ cell population to obtain the proportion of cells in the sample with the select cell surface markers and used for statistical analyses in GraphPad Prism version 6 (GraphPad Software Inc.). Proportion values were log-transformed (log₁₀) before analysed with One-way ANOVA (p-value at 0.05) corrected for multiple comparisons (Dunnett’s test) between EHEC O157:H7 challenged animals (EHEC O157:H7 Strain 9000 or Strain 10671) with the control (unexposed) group. To validate the ANOVA results, Brown-Forsythe test on standard deviation (S.D.) among data were assessed to meet one of the assumption in ANOVA that data were sampled from populations with the same S.D. or variance. All combination of select cell surface markers met this assumption except for CD3⁺/CD4⁺, therefore Kruskal-Wallis test was used to analyse the median values instead for comparison of CD3⁺/CD4⁺ proportions between each challenged groups and the control group.

Table 3.1 List of primary and secondary antibodies used to stain lymphocytes and macrophages/monocytes harvested from bovine terminal rectum.

Antigen	Clone	Isotype	Source	Concentration
CD3	MM1A	IgG1	Tim Connelley [384, 495]	1:4
CD4	ILA12	IgG2a	Tim Connelley [384, 495]	1:4
CD8	ILA105	IgG2a	Tim Connelley [384, 496, 497]	1:4
Gamma delta	GB21A	IgG2b	Alexander Corbishley [377, 384]	1:20
CD16	KD1	IgG2a	Tim Connelley [384, 410]	1:4

Table 3.1 Continued. List of primary and secondary* antibodies used to stain lymphocytes and macrophages/monocytes harvested from bovine terminal rectum.

Antigen	Clone	Isotype	Source	Concentration
NKp46	AKS6	IgG2b	Tim Connelley [384, 405]	1:4
CD21	CC21	IgG1	Dr.Yolanda Corripio-Miyar [250, 384]	1:400
SiRP-1- α	ILA24	IgG1	Tim Connelley [250, 384]	1:4
IgG1-Alexa Fluor® 647 (AF 647)*	Tim Connelley [384]			Undiluted
IgG2a-Pycoerythrin (PE)*				
IgG2b-Alexa Fluor® 488 (AF 488)*				

3.4 Measurement of IFN- γ levels released by bovine terminal rectal mucosal cells

Mucosal cells of the bovine terminal rectal tissue (from the same set of tissue samples of the immunophenotyping procedure as described above in Section 3.1) were cultured at 1×10^5 cells/ml in lymphocyte medium in a Nunc® 96-Well Polystyrene Round Bottom Microwell™ Plate (Thermo Scientific) at 37°C, 5% CO₂ for 48 h. At the end of the 48-h incubation, supernatants were transferred into Greiner 96-Well Polystyrene Flat Bottom Microwell plate (Sigma) for quantitation of IFN- γ released by the cells using the Bovine IFN- γ VetSet ELISA development kit (VS0257B-002, Kingfisher Biotech, Inc.). Bar plot of the mean with standard error of IFN- γ released from the cells of non-infected control calves, EHEC O157:H7 Strain 9000 or Strain 10671-exposed calves were plotted and shown in the results section (Fig. 3.7).

3.5 Interferon- γ stimulation of intestinal epithelial cell lines

To ensure the cells stimulated with IFN- γ were in a proliferating state, a low density cell culture maintenance protocol was adapted from Natoli et al. [350]. The authors have shown that Caco-2 cells cultured at a low density had higher proportions of cells within the S and G2/M phases of the cell cycle as compared to cells in high density culture. Briefly, Caco-2 and T84 cells were seeded at 6.2×10^3 cells/cm² and sub-cultured upon reaching 50% confluence. Caco-2 and T84 cells of this low density culture were then sub-cultured into 6-well-plates (Corning® Costar®, Sigma) at a seeding rate of 1×10^4 cells/ml and incubated at 37°C, 5% CO₂ for 40 h. At the end of incubation, the cells received cell culture medium supplemented with 1000 U/ml of Recombinant human IFN- γ (Merck Millipore), 2 ml per well, while control cells received Caco-2 or T84 cell culture medium. The cells were incubated at 37°C, 5% CO₂ for either 30 min, 6 h or 24 h.

3.6 Cell fixation for propidium iodide staining of DNA

Following IFN- γ stimulation of intestinal epithelial continuous cell lines (described above in Materials and Methods Section 3.4), cells were washed twice with sterile PBS and incubated in 600 μ l of undiluted TrypLE™ Express (Sigma) at 37°C for 5 min to dissociate the cells from the tissue culture flask surface. 500 μ l of cell culture medium was added to each well to stop the trypsinisation of cells by TrypLE™ Express. The dissociated cells were transferred into a sterile 30 ml Polystyrene Universal Container (Starlab Group) for washing (centrifuged at 1500 R.P.M., 5 min) and re-suspended in 300 μ l of PBS. 10 μ l of cell suspension was added into 10 μ l of 0.2% (in PBS) Trypan Blue solution (Invitrogen) and gently mixed. 10 μ l of the mixture was then loaded into the counting chamber slides for cell counting (Bio-Rad) using the TC20™ automated cell counter (Bio-Rad). Cell concentration was adjusted to obtain at least 1×10^5 cells in 300 μ l of PBS per tube (15 ml Falcon™ tube). To fix the cells, 700 μ l of 100% ethanol (ice-cold) was added to each tube followed by incubation at 4°C for 24 h before proceeding with propidium iodide (PI) staining of the DNA.

3.7 DNA staining by propidium iodide for flow cytometry analysis

Prior to staining, the cells were washed by centrifuging at 5000 R.P.M., 5 min, 18°C. Supernatants were gently removed before re-suspending the cells in 0.5% bovine serum albumin (BSA) (Sigma) in PBS to promote the fixed cells to sediment after centrifuging. Cells were washed again as described above before adding 1 ml of DNA staining solution to approximately 1×10^5 cells per tube and incubated at 4°C for 24 h before acquiring data with BD FACSCalibur™ flow cytometry machine. The DNA staining solution consisted of 0.2% propidium iodide (1 mg/ml, Biotium) and 5% RNase A (1 mg/ml) (Sigma) in PBS.

3.8 Data acquisition and DNA content analysis by flow cytometry

Acquisition was performed as described above in Chapter 2, Materials and Methods Section 2.15.5.

3.9 Detection of proliferating cells

Caco-2 and T84 cells were cultured into 6-well plates as described above and stimulated with recombinant human IFN- γ (1000 U/ml) for 6 and 24 h. At the end of stimulation, the cells were washed (1500 R.P.M., 5 min) in PBS once and fixed according to the protocol described above for propidium iodide (PI) staining of DNA. The fixed cells were stained with a mouse anti-human Proliferating Cell Nuclear Antigen antibody (anti-PCNA, Clone PC10, Pycoerythrin (PE)-conjugated, sc-56-PE, Insight Biotechnology), diluted in flow cytometry buffer (2% FCS in PBS) at 1:100 in 500 μ l of sample per tube. The cells were incubated at 4°C for 30 min followed by two steps of washing (as above). The PCNA-labelled cells were detected by BD FACSCALIBUR™ flow cytometry machine with FL-2 as the fluorochrome detection channel. 10,000 cells were collected for each sample with BD CELLQUEST™ (BD Biosciences) software and saved before analysis with FlowJo (Treestar, Inc). A forward scatter versus side scatter (FSC-SSC) dot plot was produced to derive the ‘viable’ cell population, as described in Materials and Methods Section 3.3. Histograms of PCNA-labelled cells were plotted from cells within the ‘viable’ population, with positive staining determined based on the histograms of the unstained cells. Percentages of PCNA-positive cells were compared across different IFN- γ treatment time (6 and 24 h). No statistical test was performed on data as the experiment was not repeated.

3.10 Caco-2 cell stimulation with purified Shiga toxin 2 or culture supernatants from Stx-producing strains and IFN- γ

Caco-2 cells were seeded at a density rate of 1.5×10^4 cells/ml in complete culture medium in 6-well-plates and incubated at 37°C, 5% CO₂ until they reached 100% cell confluence. The cells were treated with purified Shiga toxin 2 (Stx2,

Toxin Technology, Inc.), diluted in Caco-2 culture medium at 100 ng/ml for 6 h at 37°C, 5% CO₂. Control cells received Caco-2 cell culture medium. At the end of the 6-h IFN- γ stimulation, the spent medium was replaced with Caco-2 cell medium containing 250 U/ml or 62.5 ng/ml of recombinant human IFN- γ (Merck Millipore) and incubated at 37°C, 5% CO₂ for either 15 or 30 min. To study the effect of secreted Shiga toxins from EHEC O157:H7 on IFN- γ activated JAK/STAT1 pathway, similar experiment was performed with filtered non-induced and Mitomycin C (MMC) induced culture supernatants of EHEC O157:H7 strain EDL933 and EDL 933 $\Delta\Phi$ Stx1/ Φ Stx2 to treat Caco-2 cells. EHEC O157:H7 Strain EDL 933 was isolated in 1982 from ground beef associated with human clinical cases of severe abdominal pain and haemorrhagic colitis with little or no fever [51]. The outbreak occurred in Oregon and Michigan involving restaurants of the same fast food chain serving hamburgers, among others, which was incriminated as the vehicle of transmission. Strain EDL 933 possesses two Stx-encoding bacteriophages, 933J and 933W encoding for Stx1 and Stx2 expression, respectively [109]. Two to three single colonies of EHEC O157:H7 EDL 933 and its isogenic strain were transferred from an LB agar plate and cultured in minimum essential medium (MEM with L-glutamine, Invitrogen) for 24 h, 37°C, 200 R.P.M. At the end of incubation, the cultures were filtered (0.22 μ m) through filtration membrane units (Millipore) and stored at -20°C until used (non-induced culture supernatants). To produce MMC induced-culture supernatants, both bacterial strains were cultured as mentioned above for non-induced cultures with additional steps. Following the 24-h incubation, cultures were diluted 1:100 in MEM and incubated at 37°C, 200 R.P.M. until the optical density (O.D.) 600 nm readings reached 0.25 before further incubating the cultures in MEM with 5 μ g/ml of MMC (Tocris), 37°C, 200 R.P.M., 18 h. Induced cultures were filtered and stored as mentioned for non-induced culture supernatants. The filtered bacterial culture supernatants were used undiluted on Caco-2 cells.

3.11 Cell lysate collection and storage

At the end of the 6-h treatment period with PStx2 or bacterial culture supernatants, Caco-2 cells were lysed. The 6-well-plates were placed on ice for this procedure to prevent protein denaturation. The spent media were removed and the

cells were washed twice in ice-cold PBS before adding 700 µl of cell lysis buffer [3% Triton™X-100 (Sigma), 1X Halt Protease Inhibitor Cocktail (Thermo Scientific) and 1X Halt Phosphatase Inhibitor Cocktail (Thermo Scientific)] across three wells of a 6-well-plate for 30 seconds. The cells were observed under light microscope for visual signs of cell lysis (visualised as dissociation from the plate surface, loss of cell membrane structure and cell-to-cell contact). Corning® Cell scrapers (Corning Life Sciences) were used to maximise the amount of cell lysate harvested by manually dissociating lysates from the wells before transferring into ice-cold 1.5 ml Eppendorf Tubes® (Eppendorf). The process was repeated for other wells before the lysates were centrifuged at 13,000 R.P.M.) for 5 min. The supernatant harbouring protein mixture were then carefully transferred into sterile micro-centrifuge tubes and immediately stored at -20°C until use.

3.12 Estimation of total protein content in cell lysate

To determine the total protein concentration in cell lysates, the Direct Detect® Spectrometer (Millipore) was used. This spectrometer measures amide bond absorbance of the electromagnetic radiation of the mid-Infrared spectrum. Amide bond is present within a protein structure as it serves to link the building blocks of protein, amino acids. Therefore, measurement of amide bond absorbance of the electromagnetic radiation provides a direct quantification of the total protein present in the sample as compared to BCA or Bradford Assay which measures the product of secondary reactions [498].

To quantify the amount of protein present in cell lysates from Materials and Methods Section 3.11, for every sample, 2 µl of lysate was dispensed on the Direct Detect™ Assay-free Sample Card and left to dry at room temperature. Instrument settings of the Direct Detect™ Spectrometer were set according to sample type (protein) and the internal standard curve (NIST BSA method I) settings, based on the reagents present in the cell lysis buffer (refer to section 3.11). Once the circle on the card containing the lysate sample appeared opaque (an indication of properly dried card), the card was ready inserted into the machine to obtain measurements of protein concentration in mg/ml. The amount of cell lysate and sample buffer to be

loaded into the wells of the Sodium Dodecyl Sulfate-Polyacrylamide Gel Electrophoresis (SDS-PAGE) gel was calculated based on the quantified total protein.

3.13 Separation of protein bands by Sodium Dodecyl Sulfate-Polyacrylamide Electrophoresis (SDS-PAGE)

Equal volumes of Laemmli Sample Buffer (Sigma) were mixed with cell lysate samples from Section 3.12 before heated at 95°C for 5 min. The tubes containing the mixture were immediately placed on ice while samples were loaded onto the handcast SDS-PAGE gel (12% resolving gel, 4% stacking gel, 1 mm). 15 µg of protein sample was loaded into each well before the gel was assembled to the components of the Mini-PROTEAN® Tetra Cell (Bio-Rad) electrophoresis kit. A loading guide was used to position the 100 µl pipette tip direction to ensure that the samples were properly loaded into the wells while avoiding mixture of samples from the neighbouring wells. The first well from the left was always loaded with the molecular weight marker (Precision Plus Protein™ Dual Colour Standards, 161-0374, Bio-Rad) for every group of samples. The clamping frame with the glass plates holding the gels were placed accordingly inside the running chamber. 1X electrode buffer was poured into the space inside the running chamber up to the appropriate levels indicated on the tank (2 or 4 gels) and the tank was closed. The colour-coded electrodes were fixed into the power supply and electrophoresis to resolve proteins within cell lysate was set at 150 Volt (V) for 1 to 1.5 h.

3.14 Semi-dry membrane transfer of proteins from SDS-PAGE gel to nitrocellulose membrane

Nitrocellulose membrane (Amersham Hybond ECL Nitrocellulose Membrane, GE Healthcare Life Sciences), SDS-PAGE gels (from Section 3.13) and thick blot papers (Bio-Rad) were soaked for 15 min in transfer buffer [1 litre (L) of transfer buffer contains 5.82 g of Tris, 2.93 g of glycine and 0.375 g of SDS in deionised water with 200 ml of methanol, pH adjusted to 9.2 before adding more deionised water to 1 L]. The soaked components were then placed on the Trans-

Blot® SD Semi-Dry Electrophoretic Transfer Cell (Bio-Rad) with the nitrocellulose membrane and electrophoresis gel placed in between two thick blot papers. To prevent the presence of air bubbles, a wet and clean plastic tube was used to press and flatten the layers to remove air. The semi-dry membrane transfer unit was set at 15 V, limit 0.6 for 40 min. At the end of the run, protein transfer from SDS-PAGE gels to the nitrocellulose membranes were checked by immersing the nitrocellulose membranes in Ponceau S (Sigma) protein stain for 3 min. The presence of red bands on the nitrocellulose membrane indicates the presence of protein and successful protein transfer. Distilled water was used to wash the Ponceau S stain from the membranes before proceeding to the procedure described in Section 3.15 below.

3.15 Immuno-staining of proteins on nitrocellulose membrane

The nitrocellulose membranes were blocked in 5% BSA in PBS, on an orbital shaker at 4°C, overnight or at room temperature for 1 h. The membranes were washed in Tris-Buffered-Saline with 0.1% Tween®20 (TBST) with two time quick rinse followed by a 20 min incubation (orbital shaker) and two times 5 min washes (orbital shaker) at room temperature. The nitrocellulose membranes were incubated in primary antibodies (rabbit anti-human STAT1, rabbit anti-human phosphorylated STAT1 and rabbit anti-human β -actin, all from Cell Signalling, used at 1:1000) diluted in TBST for 18 h at 4°C, orbital shaker. The membranes were washed as described above and incubated in secondary antibodies at room temperature for 1 h on an orbital shaker. At the end of the secondary antibody incubation, the membranes were washed again with TBST buffer as described above with an addition of two more extra washing steps (four times 5 min washes).

3.16 Protein band detection

An equal amount of the Supersignal West Pico Chemiluminescent substrates (Thermo Scientific) was added to the nitrocellulose membranes (approximately 1 ml per 8 cm x 15 cm membrane), incubated at room temperature for 5 min. Excess detection reagent was drained off and the nitrocellulose membranes were carefully

placed in between two acetate sheets, avoiding air bubble formation. Detection of protein bands was performed with both radiograph developer and G-box Chemiluminescence Detection System (Syngene).

3.17 Nitrocellulose membrane reprobing

Following film exposure, the rabbit anti-human STAT1 was stripped of the nitrocellulose membrane for the first two repeats of Western blotting to allow reprobing with rabbit anti-human phosphorylated STAT1 and rabbit anti-human β -actin. The nitrocellulose membrane was washed for four times in washing buffer (TBST), 5 min per wash. This was followed by an incubation step in protein stripping buffer (100 mL of stripping buffer consists of 6.25 ml of 1M Tris-HCl pH 6.8, 10 mL of 20% SDS, 700 μ L β -mercaptoethanol and deionized water added to 100 mL) for 30 min, at room temperature. The membrane was washed again for six times (5 min per wash) in TBST. To confirm for the removal of the original signal probed, the membrane was incubated again with the secondary antibody against the initial signal detected followed by the steps described above for detection by film exposure to x-ray, which should reveal no signal from the membrane to signify a successful membrane stripping procedure. The membrane was washed again in TBST for four times, 5 min per wash before reprobing the membrane with the rest of the antibodies.

Chapter 3

Results

3.1 Immuno-phenotyping select mucosal terminal rectal cells

EHEC O157:H7 has been demonstrated to show a tropism towards the terminal rectum in colonised cattle [33]. One particular characteristic of the terminal rectum observed is the presence and abundance of lymphoid follicles on the mucosa [352]. This chapter attempts to compare how certain groups of immune cells previously shown to be present at the site respond in calves exposed to EHEC O157:H7 [250]. Therefore, rectal mucosal cells were phenotyped to examine expression of a combination of cell markers from calves of different EHEC O157:H7-exposure status.

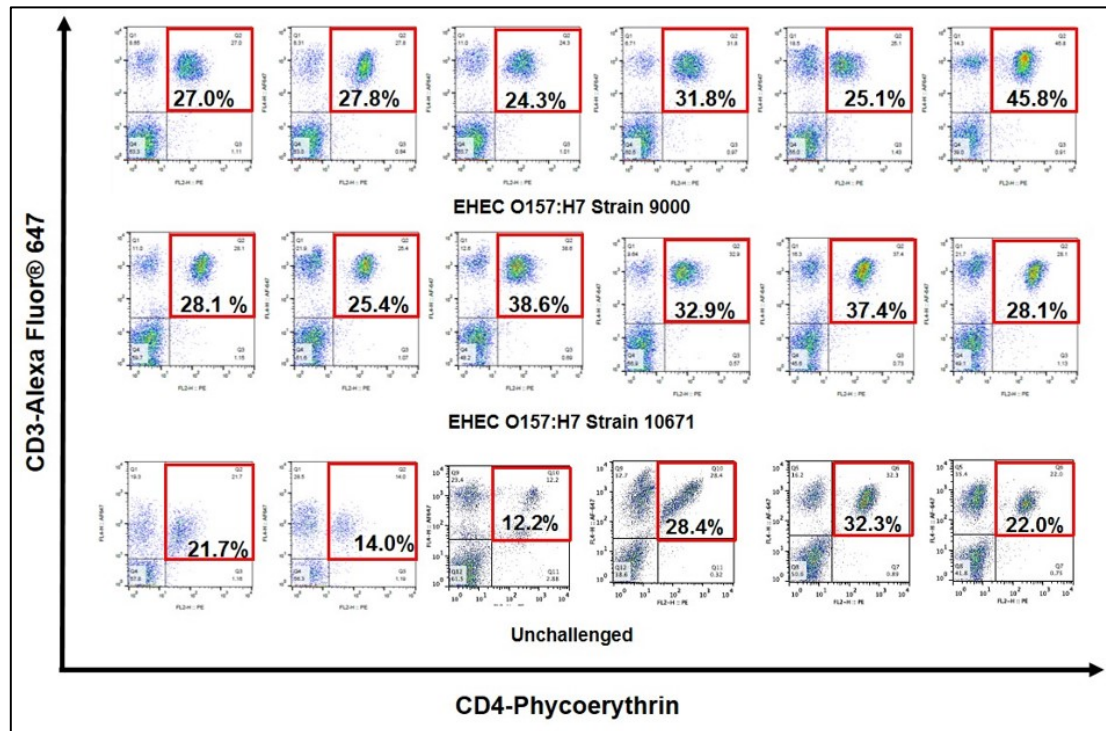
Figures 3.1 to 3.6 present the results obtained from all three groups (calves challenged with EHEC O157:H7 Strain 9000 (Φ Stx2a+/ Φ Stx2c+) or Strain 10671 (Φ Stx2c+) and unchallenged calves serving as controls) for T helper cells (CD3+/CD4+), T Cytotoxic cells (CD3+/CD8+), IEL $\gamma\delta$ T cells (CD3+/ $\gamma\delta$ +), NK cells (CD16+/NKp46+), B cells and follicular dendritic cells (CD21+) and monocytes/macrophages (SiRP-1- α +).

Analysis with 1-way ANOVA in comparing the percentages of the immune cells detected among the three different groups of calves showed statistically significant differences for CD3+/CD8+ (Fig. 3.2) [F (2, 15) = 7.19, p-value=0.0065], CD3+/ $\gamma\delta$ + (Fig. 3.3.) [F (2, 15) = 4.37, p-value=0.032] and CD21 (Fig. 3.5) [F (2, 15) = 4.23, p-value=0.035]. The proportion of T helper cells, NK cells and monocytes/macrophages among the three groups were not significantly different from each other as seen in Fig. 3.1, 3.4 and 3.6.

Post-hoc Dunnett's multiple comparison tests (α =5.00%) to identify which pairwise comparison against the unchallenged control calves were statistically significant indicated differences of the CD3+/CD8+ and CD3+/ $\gamma\delta$ + expressing cells in the EHEC O157:H7 Strain 9000-infected calves compared to the control group [mean differences of 0.3513 (p-value=0.004) and 0.3624 (p-value=0.02), respectively] (Table 3.1). On the other hand, CD21+ expressing cells were

significantly increased in the terminal rectal cells of calves exposed to EHEC O157:H7 Strain 9000 compared to the control calves [mean difference of -0.2763, p-value=0.037] (Table 3.1).

A)



B)

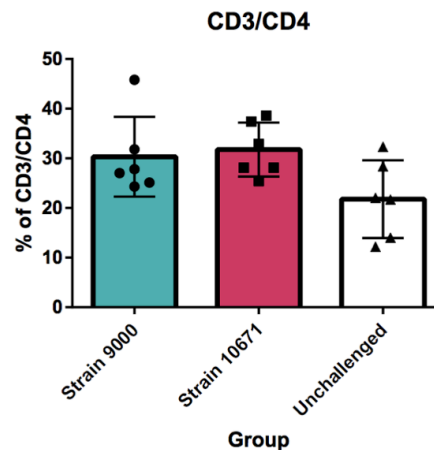


Figure 3.1 Flow cytometry dot plots of CD3+/CD4+ cells detected from EHEC O157:H7-challenged and unchallenged calves. (A) Dot plots with total CD3+/CD4+ population (shown in the red upper right quarter) derived from the 'viable' population of immune-labeled terminal rectal mucosal cells of calves challenged with EHEC O157:H7 Strain 9000 or EHEC O157:H7 Strain 10671 and unchallenged control calves (six individual animals per group). (B) Bar plot presents the mean \pm standard deviation for each group and individual values (total CD3+/CD4+ per total 'viable' terminal rectal cells, %).

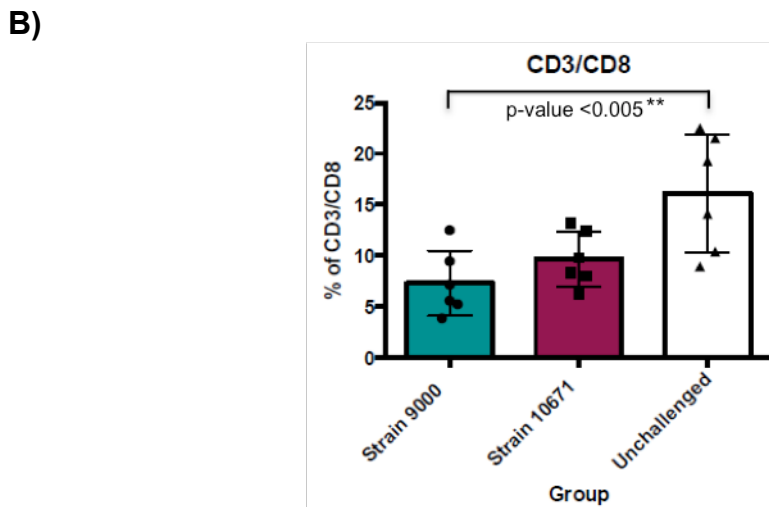
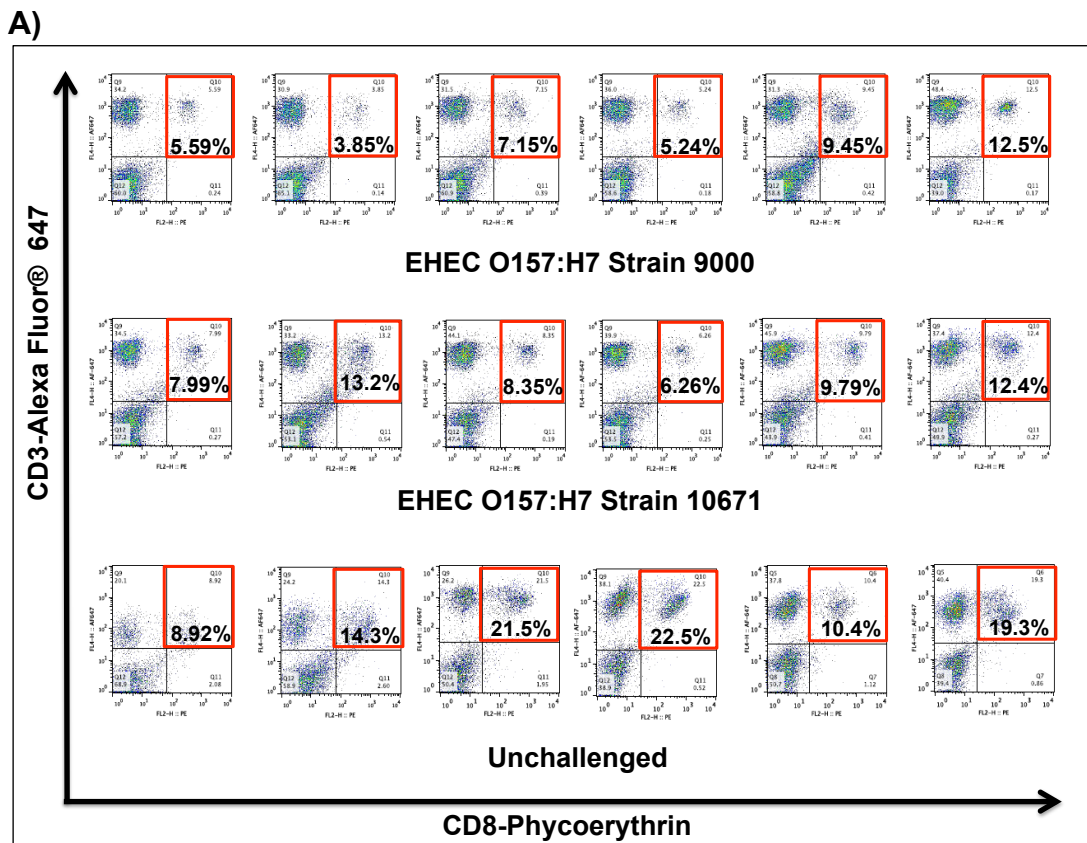


Figure 3.2 Flow cytometry dot plots of CD3+/CD8+ cells detected from EHEC O157:H7-challenged and unchallenged calves. (A) Dot plots with total CD3+/CD8+ population (shown in the red upper right quarter) derived from the 'viable' population of immune-labeled terminal rectal mucosal cells of calves challenged with EHEC O157:H7 Strain 9000 or EHEC O157:H7 Strain 10671 and unchallenged control calves (six individual animals per group). (B) Bar plot presents the mean \pm standard deviation for each group and individual values (total CD3+/CD8+ per total 'viable' terminal rectal cells, %).

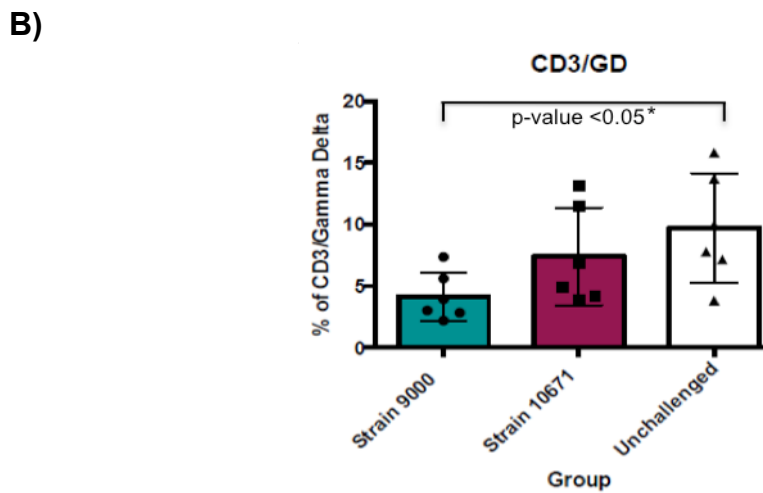
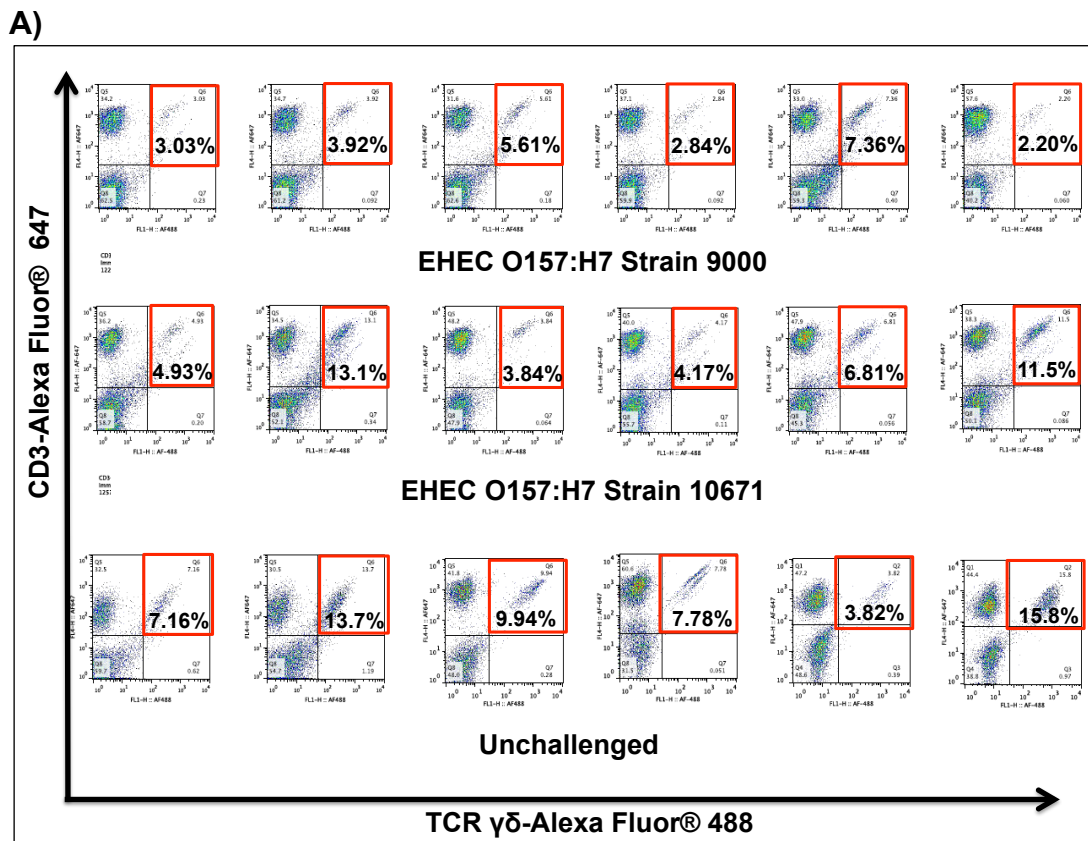
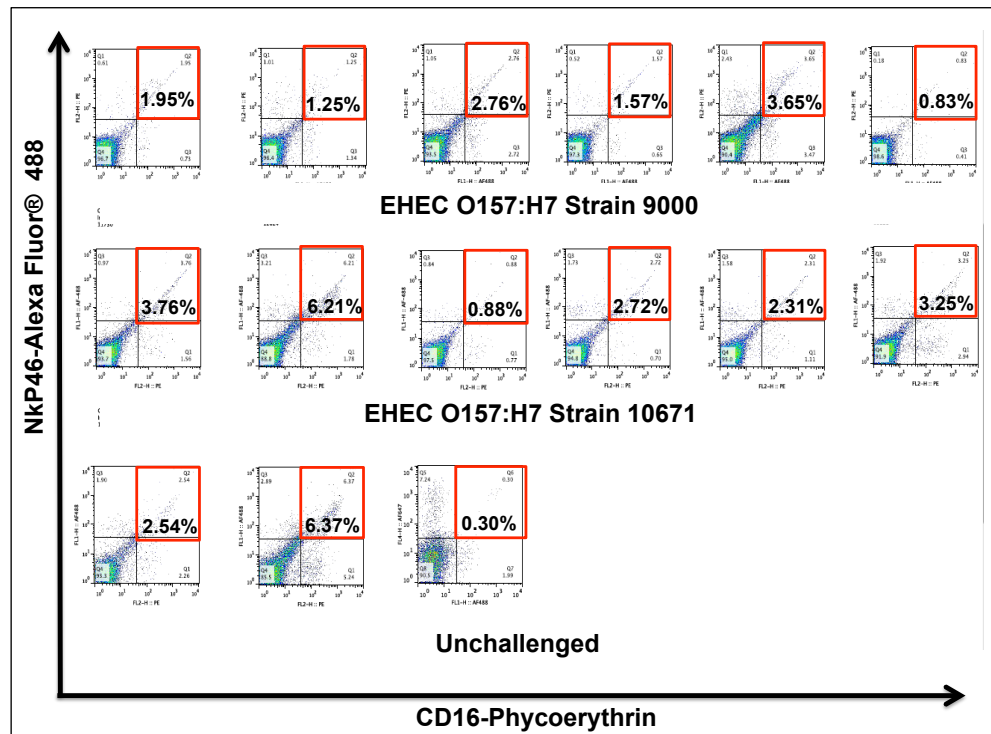


Figure 3.3 Flow cytometry dot plots of CD3+/ $\gamma\delta$ + cells detected from EHEC O157:H7-challenged and unchallenged calves. (A) Dot plots with the CD3+/ $\gamma\delta$ + population (shown in the red upper right quarter) derived from the 'viable' population of immune-labeled terminal rectal mucosal cells of calves challenged with EHEC O157:H7 Strain 9000 or EHEC O157:H7 Strain 10671 and unchallenged control calves (six individual animals per group). (B) Bar plot presents the mean \pm standard deviation for each group and individual values (total CD3+/ $\gamma\delta$ + per total 'viable' terminal rectal cells, %).

A)



B)

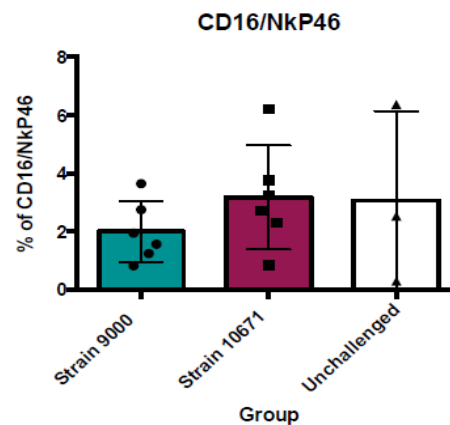
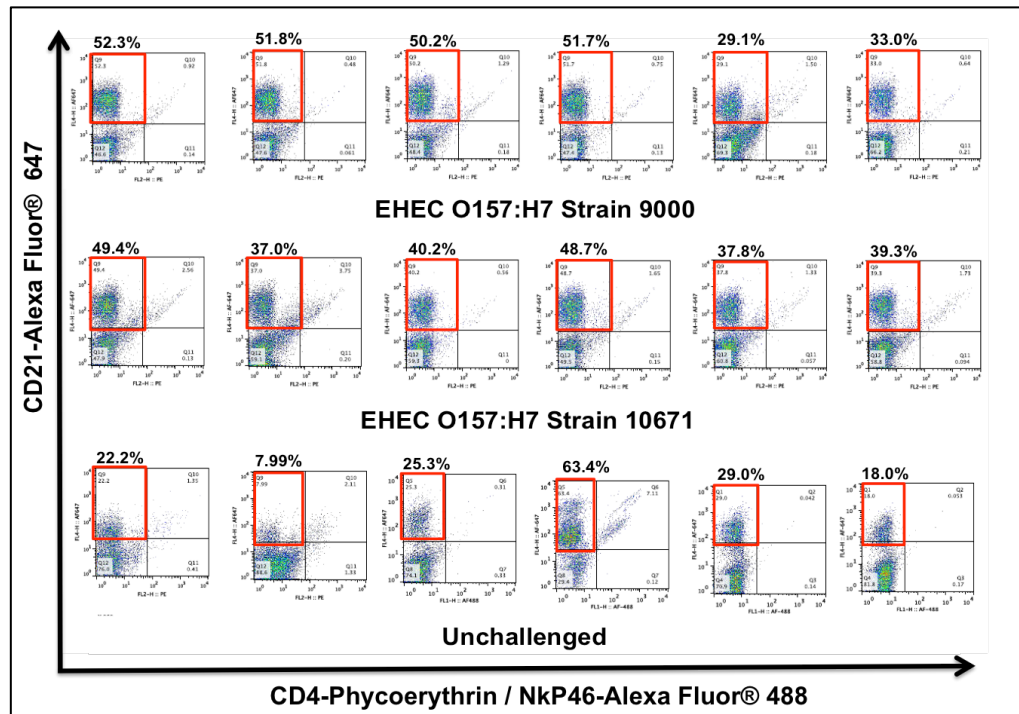


Figure 3.4 Flow cytometry dot plots of CD16⁺/NkP46⁺ cells detected from EHEC O157:H7-challenged and unchallenged calves. (A) Dot plots with the CD16⁺/NkP46⁺ population (shown in the red upper right quarter) derived from the ‘viable’ population of immune-labeled terminal rectal mucosal cells of calves challenged with EHEC O157:H7 Strain 9000 or EHEC O157:H7 Strain 10671 and unchallenged control calves (six individual animals per group except for unchallenged group). (B) Bar plot presents the mean \pm standard deviation for each group and individual values (total CD16⁺/NkP46⁺ per total ‘viable’ terminal rectal cells, %).

A)



B)

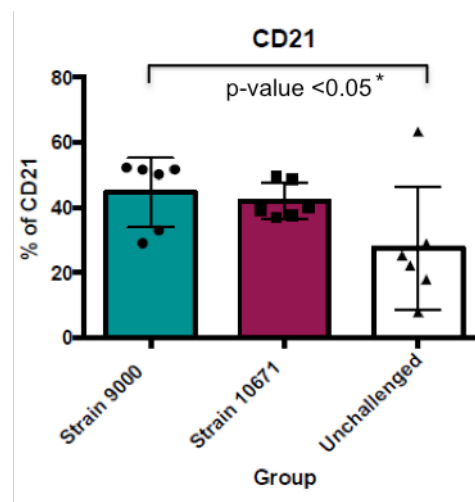


Figure 3.5 Flow cytometry dot plots of CD21+ cells detected from EHEC O157:H7-challenged and unchallenged calves. (A) Dot plots with the CD21+ population (shown in the red upper right quarter) derived from the ‘viable’ population of immune-labeled terminal rectal mucosal cells of calves challenged with EHEC O157:H7 Strain 9000 or EHEC O157:H7 Strain 10671 and unchallenged control calves (six individual animals per group). (B) Bar plot presents the mean \pm standard deviation for each group and individual values (total CD21+ per total ‘viable’ terminal rectal cells, %).

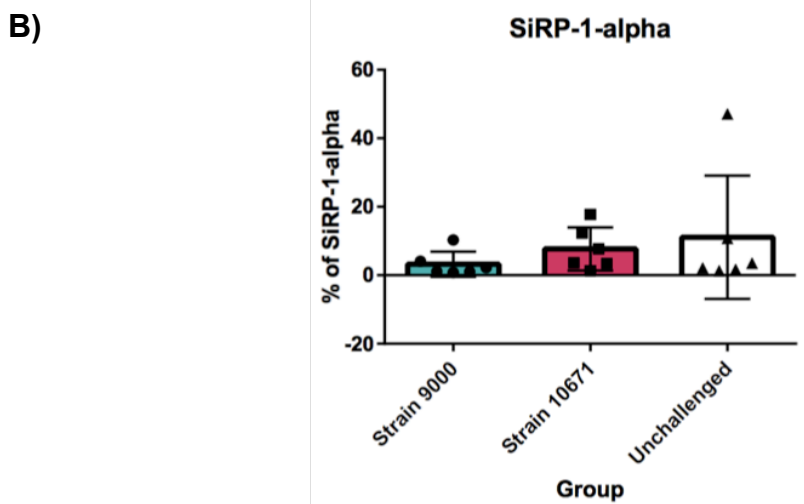
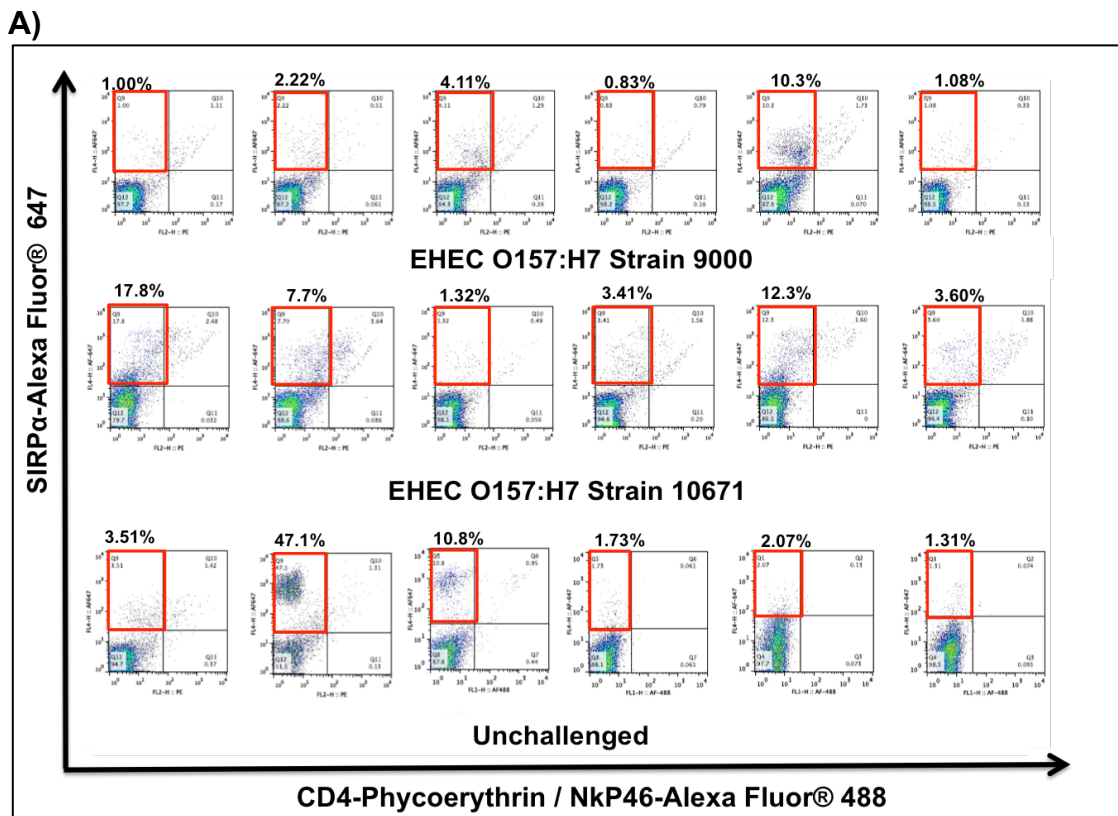


Figure 3.6 Flow cytometry dot plots of SIRP- α (SIRP- α)⁺ cells detected from EHEC O157:H7-challenged and unchallenged calves. (A) Dot plots with the SIRP- α ⁺ population (shown in the red upper right quarter) derived from the ‘viable’ population of immune-labeled terminal rectal mucosal cells of calves challenged with EHEC O157:H7 Strain 9000 or EHEC O157:H7 Strain 10671 and unchallenged control calves (six individual animals per group). (B) Bar plot presents the mean \pm standard deviation for each group and individual values (total SIRP- α ⁺ per total ‘viable’ terminal rectal cells, %).

Table 3.1. Statistical analysis of bovine terminal rectal cells immune-labelled and detected for different cell surface marker combinations by flow cytometry. Percentages of cells with selected cell surface marker combinations from FlowJo analysis were log10-transformed to obtain a Gaussian distribution before performing one-way Analysis of Variance to compare the means of samples from three groups (calves exposed to EHEC-O157:H7 Strain 9000, Strain 10671 and unchallenged control calves). Post-hoc Dunnett's multiple comparison test was used to compare each EHEC O157:H7-challenged groups against the unchallenged control calves. Validity of the ANOVA results was checked with Brown-Forsythe test to ensure equal standard deviation (S.D.) among data. All data complied with the assumption of equal S.D. except for CD3+/CD4+ data (refer Table 3.2).

Surface marker	Group	n	Mean	S.D.	F (1-way ANOVA)	P-value	Post-hoc multiple comparison test	Dunnett's	Mean Difference	P-value	
CD3+/CD8+	Strain 9000	6	7.297	3.186	7.187	0.007**	Unchallenged vs Strain 9000	Dunnett's	0.351	0.004**	
	Strain 10671	6	9.665	2.688					Unchallenged vs Strain 10671	0.210	0.071
	Unchallenged	6	16.12	5.803							
CD3+/γδ+	Strain 9000	6	4.16	1.963	4.368	0.032*	Unchallenged vs Strain 9000	Dunnett's	0.362	0.020*	
	Strain 10671	6	7.392	3.971					Unchallenged vs Strain 10671	0.125	0.513
	Unchallenged	6	9.700	4.427							
CD16+/NkP46+	Strain 9000	6	2.002	1.041	0.493	0.627	Unchallenged vs Strain 9000	Dunnett's	-0.022	0.995	
	Strain 10671	6	3.183	1.784					Unchallenged vs Strain 10671	-0.206	0.652
	Unchallenged	3	3.070	3.070							
CD21+	Strain 9000	6	44.68	10.66	4.225	0.035*	Unchallenged vs Strain 9000	Dunnett's	-0.276	0.037*	
	Strain 10671	6	42.07	5.528					Unchallenged vs Strain 10671	-0.259	0.051
	Unchallenged	6	27.65	18.95							

Table 3.2. Statistical analysis of CD3+/CD4+ and SiRP-1-alpha flow cytometry data. Data was analysed by Kruskal-Wallis test and post-hoc Dunn's multiple comparisons test to compare the mean ranks between the EHEC O157:H7-challenged and unchallenged groups.

Surface marker	Group	n	Mean	S.D.	Kruskal-Wallis statistic	P-value	Post-hoc Dunn's multiple comparison test	Mean Rank Difference	P-value
CD3+/CD4+	Strain 9000	6	30.30	8.03	4.72	0.09	Unchallenged vs Strain 9000	-3.833	0.427
	Strain 10671	6	31.75	5.43			Unchallenged vs Strain 10671	-6.667	0.061
	Unchallenged	6	21.77	7.83					
SiRP-α	Strain 9000	6	3.26	3.664	2.89	0.248	Unchallenged vs Strain 9000	3.333	0.559
	Strain 10671	6	7.688	6.310			Unchallenged vs Strain 10671	-1.833	>0.999
	Unchallenged	6	11.09	17.99					

3.2 ELISA measurement of IFN- γ release by cultured terminal rectum mucosal cells

To analyse production of the pro-inflammatory cytokine, IFN- γ which has been previously reported to affect EHEC O157:H7 colonisation [481, 482, 499] release was measured from the cultured terminal rectal mucosal cells harvested from EHEC O157:H7 challenged and control calves. Total IFN- γ quantified from supernatants of the 48-h cultured cells, after normalising to the blank controls, with a standard curve fitted are shown in Fig. 3.7. IFN- γ released from terminal rectal mucosal cells of calves exposed to EHEC O157 :H7 Strain 10671 was 1.07 ng/ml, 0.59 ng/ml from cells of the EHEC O157 Strain 9000-exposed group and 0.09 ng/ml from the cells of the non-infected control group. The results could not be supported by statistics as the experiment was done only once due to the lack of terminal rectal cells to be used for further repeats of the assay.

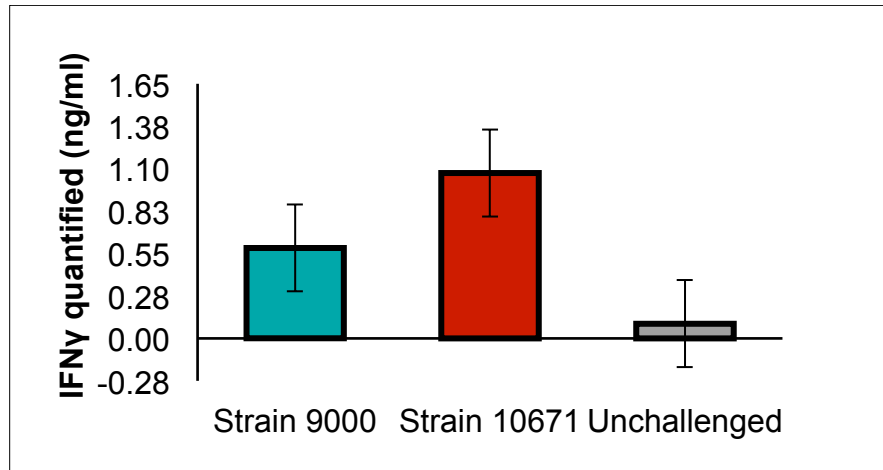


Figure 3.7 IFN- γ released by bovine terminal rectal cells quantified by ELISA. Bar plot showing levels of quantified Interferon- γ (IFN- γ) measured from supernatant of the isolated cells cultured in lymphocyte medium for 48 h, 37°C, 5% CO₂. Error bars indicate standard error of mean (S.E.M.) for calves exposed to EHEC O157:H7 Strain 9000 and Strain 10671 (both n=6) and unchallenged, non-infected control calves (n=2).

3.3 The effect of Interferon- γ on the cell cycle of epithelial cell lines

The next question asked was how does the epithelial barrier of the terminal rectum respond to the presence of IFN- γ in the event of an EHEC O157:H7 colonisation (Fig. 3.7). The current study focused on the effect of IFN- γ on the epithelial cell cycle. IFN- γ have been shown to act as a modulator of epithelial homeostasis by interfering with the epithelial barrier renewal process [489]. Furthermore, the cytokine was reported to block the proliferation of a rat intestinal crypt cell line, IEC-6 [254]. It was therefore hypothesised that during the early stages of EHEC O157:H7 colonisation at the terminal rectal mucosa, immune cells at the immediate epithelial surface (for example IEL TCR $\gamma\delta$ cells) and cells of the lamina propria (T helper, T cytotoxic and NK cells) were stimulated to release IFN- γ . The released IFN- γ will bind to surface IFN- γ receptor, presumably present on intestinal epithelial surface (since IFNGR is expressed by Caco-2 and T84 cells) [500, 501] and exert its anti-proliferative effect.

However, IFN- γ stimulation at 1000 U/ml of both Caco-2 and T84 cells at all three time-points tested (30 min, 6 h and 24 h) did not cause any apparent perturbation in the DNA-propidium iodide (P.I.) staining profile (Fig. 3.8). Statistical analyses as shown in Table 3.3 and Table 3.4 of the data shows that there was no significant difference between the IFN- γ stimulated and non-stimulated Caco-2 and T84 cells at each analysed cell cycle phase (multiple t-tests comparison corrected for multiple comparison using the Holm-Sidak method, with $\alpha=5.00\%$).

The specific effect of IFN- γ on Caco-2 and T84 cellular proliferation was investigated by PCNA staining (Fig. 3.9). This experiment was performed only once, therefore not allowing statistical analyses of the data. Regardless of the intestinal epithelial cell line (Caco-2 resembles the matured epithelial cells at the villi, while T84 resembles the intestinal crypt cells) and the Gb3 surface expression (more on Caco-2 than T84, refer to Fig. 2.1 in Chapter 2), no difference was observed in proliferation after IFN- γ treatment for either 6 or 24 h. Although there seems to be a

slight decrease in the total cells stained positive for PCNA after 24 h of stimulation with IFN- γ in both cell lines, there was not enough evidence for further investigation of this area, so any potential cell cycle effects induced by IFN- γ were not explored further.

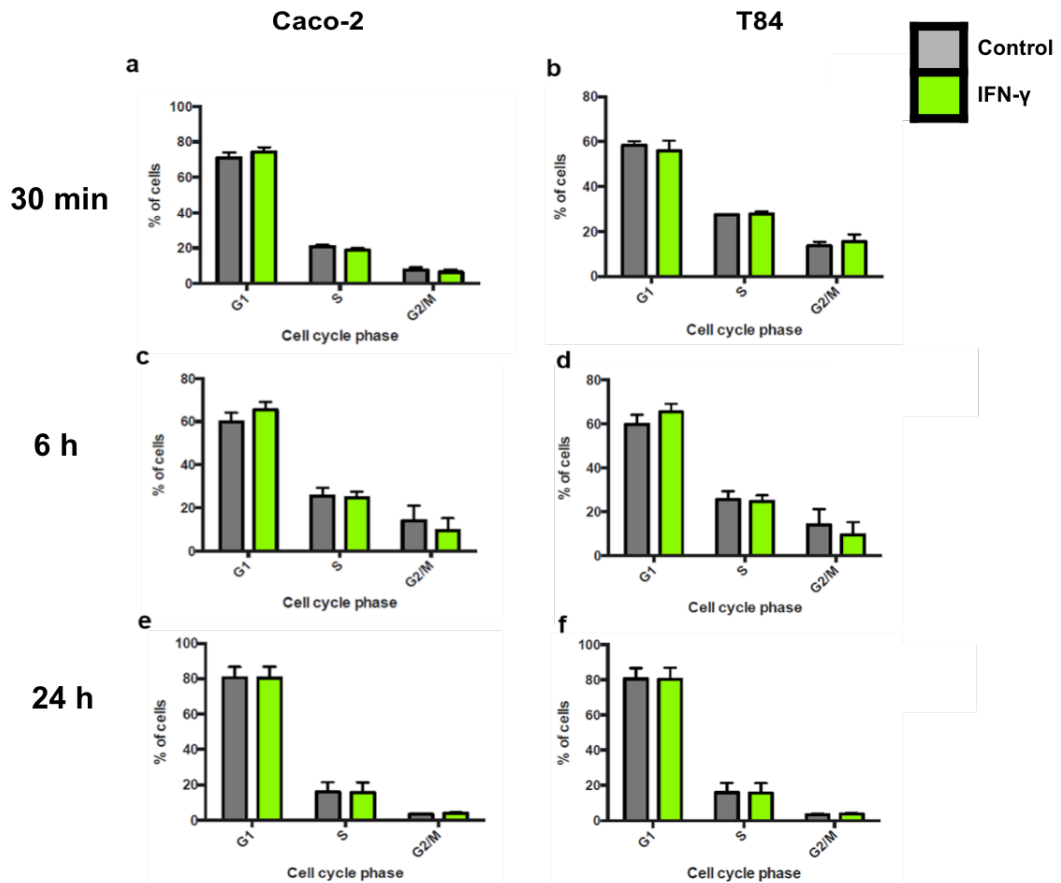


Figure 3.8 DNA staining profile with propidium iodide of cells treated with Interferon- γ (IFN- γ). Bar plots showing the average of Caco-2 and T84 cells in each cell cycle phase after IFN- γ (1000 U/ml) treatment (green) for a, b) 30 min (n=3), c, d) 6 h (n=3) and e, f) 24 h (n=2) at 37°C, 5% CO₂. The gray bars represent DNA staining profile of cells receiving cell culture medium only (control). Data were analysed with multiple t-tests corrected for multiple comparison using the Holm-Sidak method, alpha=5.00%, without assuming a consistent standard deviation. The error bars represent the standard error of mean (S.E.M.).

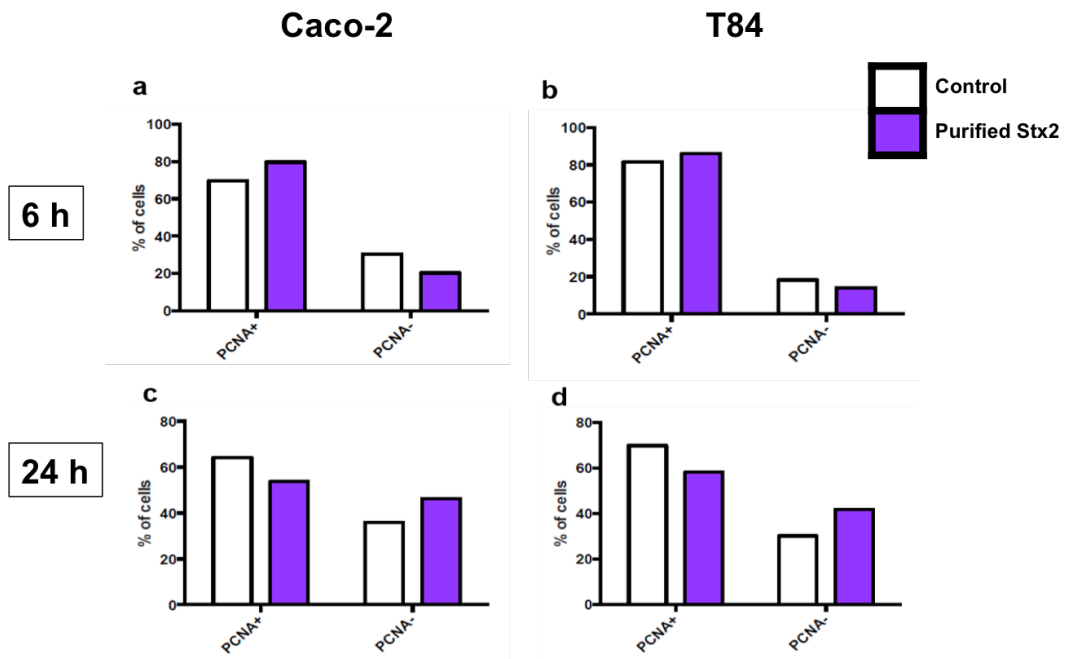


Figure 3.9 Proliferation cellular nuclear antigen staining of Interferon- γ (IFN- γ) treated Caco-2 and T84 cells. Flow cytometry results (n=1) presented in bar plots for Caco-2 and T84 cells stained for proliferating cell nuclear antigen either treated with 1000 U/ml of IFN- γ (purple) or serum-free media (white), for 6 h (a,b) and 24 h (c,d) at 37°C, 5% CO₂.

Table 3.3. Statistical analysis of DNA staining profile for Caco-2 cells stimulated with IFN- γ . Mean of total cells in each cell cycle phase (per 100 cells) were compared between IFN- γ stimulated (1000 U/ml) and unstimulated control cells. Data was analysed with multiple t-test using Holm-Sidak method ($\alpha=5.00\%$) without assuming consistent standard deviation (S.D.) in GraphPad Prism version 6.

Cell line	Treatment	Phase	n	Mean	S.E.M.	t ratio (Control vs. IFN- γ treated)	df	P-value		
Caco-2	Control	G1	3	71.07	2.91	0.791	4	0.473		
		S	3	20.87	1.18		4		0.285	
		G2/M	3	7.56	1.64		4		0.650	
	IFN- γ (30 mins)	G1	3	74.23	2.74	0.345				
		S	3	18.83	1.17					
		G2/M	3	6.47	1.49					
	Control	Control	G1	3	64.18	3.97	0.816	4	0.460	
			S	3	24.86	0.81		4		0.200
			G2/M	3	10.31	3.06		4		0.747
		IFN- γ (6 h)	G1	3	70.72	6.96	0.345			
			S	3	20.09	3.00				
			G2/M	3	8.64	3.74				
Control	Control	G1	3	80.47	3.38	0.632	2	0.592		
		S	3	16.93	2.35		2		0.713	
		G2/M	3	2.36	0.91		2		0.270	
	IFN- γ (24 h)	G1	3	84.05	4.56	0.632				
		S	3	14.85	4.33					
		G2/M	3	0.97	0.16					

Table 3.4. Statistical analysis of DNA staining profile for T84 cells stimulated with IFN- γ . Mean of total cells in each cell cycle phase (per 100 cells) were compared between IFN- γ stimulated (1000 U/ml) and unstimulated control cells. Data was analysed with multiple t-test using Holm-Sidak method ($\alpha=5.00\%$) without assuming consistent standard deviation (S.D.) in GraphPad Prism version 6.

Cell line	Treatment	Phase	n	Mean	S.E.M.	t ratio (Control vs. IFN- γ treated)	df	P-value
T84	Control	G1	3	58.32	1.87	0.493	4	0.648
		S	3	27.46	0.20	0.323	4	0.763
		G2/M	3	13.54	1.85	0.500	4	0.644
	IFN- γ (30 mins)	G1	3	55.9	4.52			
		S	3	27.82	1.09			
		G2/M	3	15.42	3.30			
	Control	G1	3	59.83	4.26	0.995	4	0.376
		S	3	25.34	3.90	0.142	4	0.894
		G2/M	3	13.98	6.97	0.510	4	0.637
	IFN- γ (6 h)	G1	3	65.46	3.73			
		S	3	24.67	2.72			
		G2/M	3	9.4	5.67			
	Control	G1	3	80.5	6.18	0.013	4	0.990
		S	3	15.93	5.55	0.043	4	0.968
		G2/M	3	3.41	0.57	0.548	4	0.613
	IFN- γ (24 h)	G1	3	80.39	6.39			
		S	3	15.59	5.74			
		G2/M	3	3.83	0.60			

3.4 The effect of Shiga toxin on IFN- γ -activated JAK/STAT1 pathway

Published studies had suggested a role for Shiga toxin in supporting *E. coli* colonisation by interfering with intracellular epithelial signalling pathways as mentioned in Chapter 3 Introduction section 3.4. To examine this EHEC O157:H7 strain EDL 933 supernatant (presumed to contain Stx1 and Stx2) [109] as well as purified Stx2 were added to IFN- γ stimulated Caco-2 cells and the lysates examined by Western blotting to detect activated or phosphorylated STAT1 (pY-STAT1) and total STAT1.

Treatment of Caco-2 cells with purified Shiga toxin 2 (PStx2) for 6 h before exposing the cells to IFN- γ for either 15 min or 30 min failed to inhibit STAT1 activation (Fig. 3.10). Further sets of experiments were then carried out by substituting PStx2 with two independent sets of EHEC O157:H7 Strain EDL 933 culture supernatants; with or without MMC induction as the inhibiting effect proposed earlier [502] requires the toxin to be freshly generated from bacterial lysate as opposed to PStx2 (Fig. 3.11 and 3.12). In the first experiment (Fig. 3.11), STAT1 activation was evident in all lysates receiving IFN- γ treatment with the exception of Caco-2 cells exposed to MMC-induced culture supernatant of Strain EDL 933, a finding that is anticipated and parallels the findings in previous publications [483]. The presence of a weak band for phosphorylated STAT1 could be observed for the lane with Caco-2 lysate treated with MMC-induced Stx-negative isogenic EDL 933 (Stx1-/Stx2-) on the same blot (Fig. 3.11). This was unexpected since inhibition of STAT1 activation was only anticipated to be present in samples treated with Stx-positive filtrate. In addition, the presence of this weak band may also be as a result of overloading the gel. To clarify this, the pY-STAT1 band for Caco-2 lysate receiving supernatant filtrate of the Stx-negative Strain EDL 933 culture was compared against the total STAT1 and β -actin bands. It was concluded that the weak detection was most probably the result of a much lower amount of sample loaded into that particular well than the other lanes, leading to a relatively smaller band size.

Findings from the first experiment prompted another experimental repeat to be carried out to verify inhibition of STAT1 activation in Caco-2 cells upon treatment with Stx-positive filtrate (Fig. 3.12). Results of the second experiment (Fig. 3.12) however did not match the first (Fig. 3.11). No differences in the levels of STAT1 activation were observed for all samples tested, which contrasted with the results from the previous blot (Fig. 3.11) in particular for the Caco-2 lysates treated with induced culture supernatants. Another repeat of experiment using a new batch of MMC-induced culture supernatants was performed (Fig. 3.13), supporting the results obtained in the second experiment (Fig. 3.12). Taken together, there was insufficient evidence to support the inhibition of JAK/STAT1 pathway by purified Stx2 or Shiga toxins of filtered EDL 933 culture supernatants.

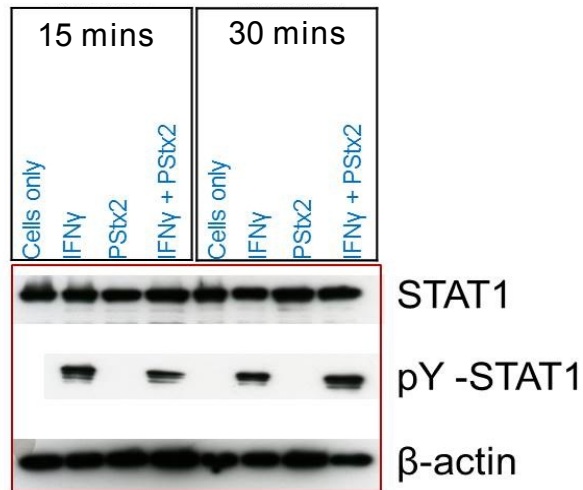


Figure 3.10 Western blot results of Caco-2 cell lysates stimulated with Purified Shiga toxin 2 (PStx2) and Interferon- γ (IFN- γ). Caco-2 cells received PStx2 (100 ng/ml) for 6 h before stimulated with IFN- γ (250 U/ml) for either 15 min or 30 min at 37°C, 5% CO₂. Immunoblotting detection for total STAT1 (91kDa) and activated STAT1 (phosphorylated-STAT1 or pY-STAT1) (91kDa) are shown in the radiograph image. The signals were separately detected from the same membrane following membrane stripping and reprobing procedure. All signals detected following each reprobing steps were compiled in this figure for the purpose of visual comparison only and does not reflect the actual position (molecular weight). β -actin (45kDa) was used as sample loading control.

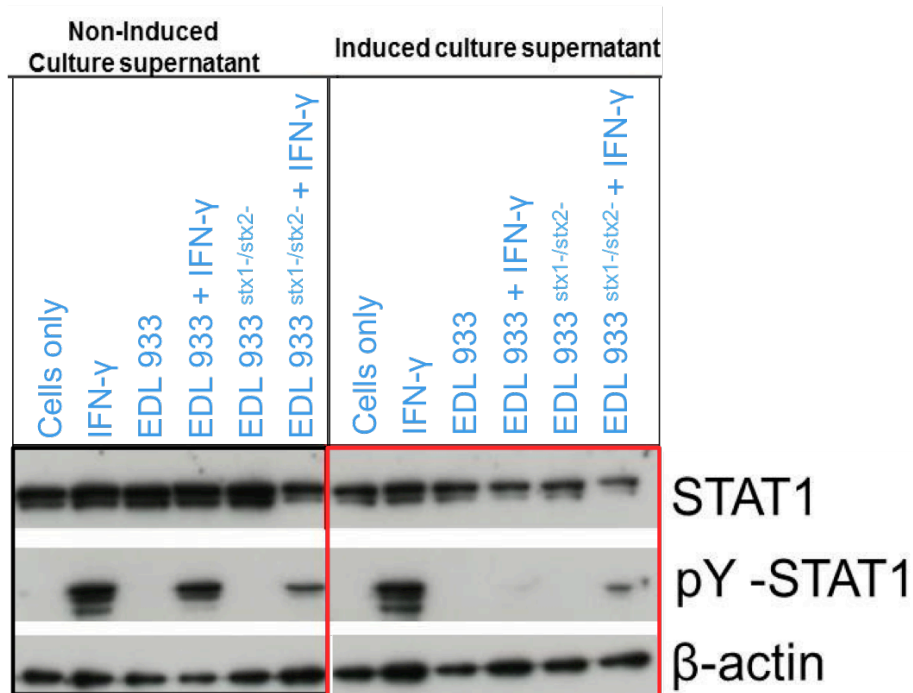


Figure 3.11 Western blot results of Caco-2 cell lysates stimulated with culture supernatants of EHEC O157:H7 strain EDL 933 or isogenic Stx1-/Stx2- and Interferon- γ (IFN- γ) (i). Caco-2 cells received non-induced or Mitomycin C-induced culture supernatants of EHEC O157:H7 strain EDL 933 or isogenic strain EDL 933 Stx1-/Stx2- for 6 h before stimulated with IFN- γ (250U/ml) for 30 min at 37°C, 5% CO₂. Immunoblotting detection for total STAT1 (91 kda) and activated STAT1 (phosphorylated-STAT1 or pY-STAT1) (91 kda) are shown. The signals were separately detected from the same membrane following membrane stripping and reprobing procedure. All signals detected following each reprobing steps were compiled in this figure for the purpose of visual comparison only and does not reflect the actual position (molecular weight). β -actin (45 kda) was used as sample loading control.

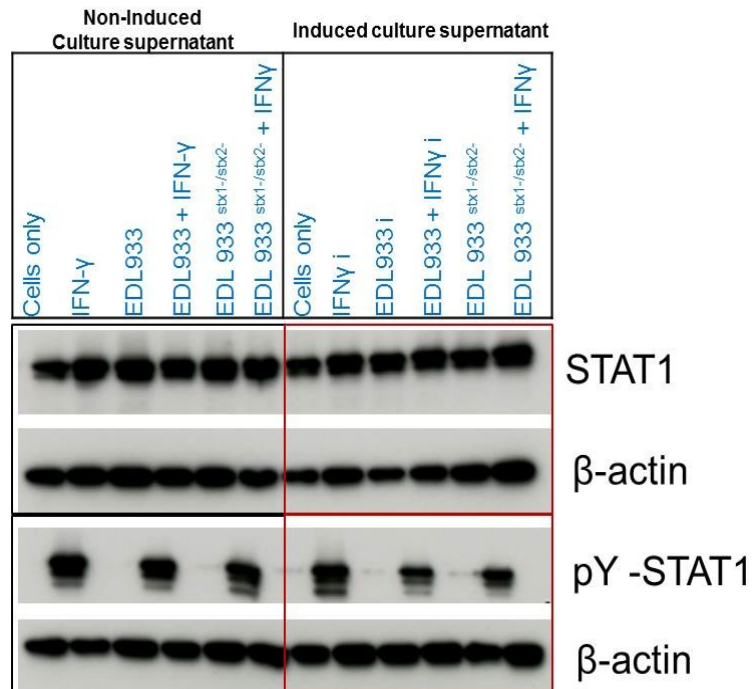


Figure 3.12 Western blot results of Caco-2 cell lysates stimulated with culture supernatants of EHEC O157:H7 strain EDL 933 or isogenic Stx1-/Stx2- and Interferon- γ (IFN- γ) (ii). Caco-2 cells received non-induced or Mitomycin C-induced culture supernatants of EHEC O157:H7 strain EDL 933 or isogenic strain EDL 933 Stx1-/Stx2- for 6 h before stimulated with IFN- γ (250U/ml) for 30 min at 37°C, 5% CO₂. Immunoblotting detection for total STAT1 (91 kda) and activated STAT1 (phosphorylated-STAT1 or pY-STAT1) (91 kda) are shown. Nitrocellulose membranes for detecting STAT1 and pY-STAT1 were each cut into half horizontally for detection of β -actin (45 kda) as sample loading control. Images compiled in this figure are for the purpose of visual comparison only and do not reflect the actual distance on the membrane.

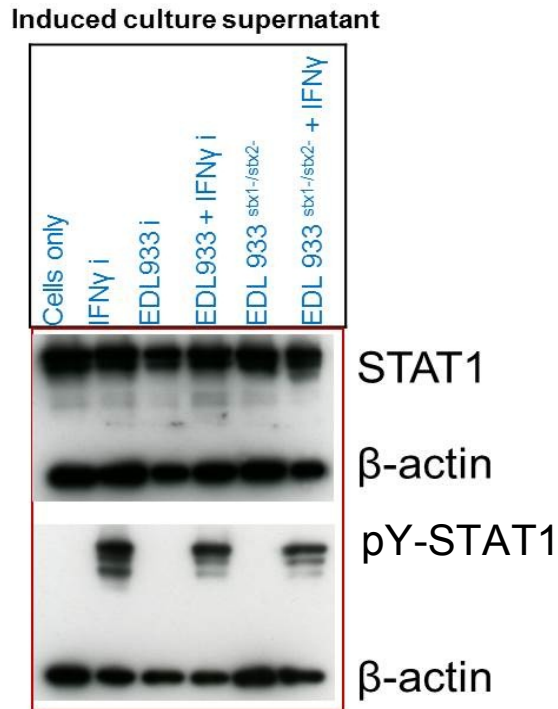


Figure 3.13 Western blot results of Caco-2 cell lysates stimulated with Mitomycin C-induced culture supernatants of EHEC O157:H7 strain EDL 933 or isogenic Stx1-/Stx2- and Interferon- γ (IFN γ) (iii). Caco-2 cells received Mitomycin C-induced culture supernatants of EHEC O157:H7 strain EDL 933 or isogenic strain EDL 933 Stx1-/Stx2- for 6 h before stimulated with IFN γ (250U/ml) for 30 min at 37°C, 5% CO₂. Immunoblotting detection for total STAT1 (91 kda) and activated STAT1 (phosphorylated-STAT1 or pY-STAT1) (91 kda) are shown. Nitrocellulose membranes for detecting STAT1 and pY-STAT1 were each cut into half horizontally for detection of β -actin (45 kda) as sample loading control. Images compiled in this figure are for the purpose of visual comparison only and do not reflect the actual distance on the membrane.

Chapter 3

Discussion

3.1 Cell surface marker expression and Interferon-gamma (IFN- γ) quantified from cells harvested from the bovine terminal rectal mucosa

The main difference known to date between Strain 9000 and Strain 10671 is the type of Stx-encoding phage(s) possessed and with potentially different Stx type(s) expressed [251]. Since the ability to produce Stxs is an important trait rendering virulence to the bacteria, it is anticipated that these highly conserved virulence components (phage and Stx) may play a role in modulating the bovine host immune response. Concurrent data from collaborators [384] had confirmed the presence of a strain-dependent response from the same group of animals of which the bovine terminal rectal tissue used in this chapter were sampled from. Rectal lymph nodes stimulated *ex vivo* with T3SS proteins caused significant increase in the proliferation of CD4+ cells of Strain 9000-challenged group, NK cells of Strain 10671-infected animals, as well as CD8+ and T $\gamma\delta$ cells, implying the involvement of a strain-dependent response in the host [384].

Overall, the proportion of immune cell subpopulations based on surface markers expression appeared similar between infected or exposed and non-exposed animals with the exception of three immune cell subsets from EHEC O157:H7 Strain 9000-infected group. Statistically significant differences between EHEC O157:H7 Strain 9000-exposed and non-exposed controls were determined for the CD3+/CD8+, CD3+/ $\gamma\delta$ + and CD21+ cells. The proportion of CD3+/CD8+ and CD3+/ $\gamma\delta$ + cells were significantly lower in animals challenged with Strain 9000 in comparison to the unchallenged control group. While the expression of CD21+ cells were statistically higher in animals receiving Strain 9000 than the unchallenged calves. It remains uncertain if these observations reflect the actual proportions occurring within the tissues from calves of the two groups (Strain 9000 and unchallenged control). The downregulation of the host immune response, particularly the cellular mediated immunity (CMI) by Stx+ EHEC O157 strain have been described by previous studies using both *in vitro* and *in vivo* assays. Stx1 is able to inhibit the activation of CD8+ cells of bovine PBMC [252] while the bovine

intraepithelial lymphocytes in a gut-loop intestinal infection model were shown to be sensitive to the anti-proliferative effect of purified Stx1 [453]. The proliferation of PBMC from cattle infected with Stx2+ EHEC O157 strain were reported to be significantly reduced when compared with a group infected with a non-pathogenic *E. coli* strain [503].

Since the total number of cells sampled and analysed is unknown, relative comparison of the percentages between the groups becomes impossible. The percentages presented for each immune cells phenotyped were based on the number of cells within the positive quarters of the surface marker (or surface marker combinations) derived from cells within the 'viable/live' cells gated during acquisition of the 10,000 events. During the acquisition, the assumption was that each event corresponded to a single cell. Although the position of the gate used to include 'viable/live' cells across all samples was constant, the total number of cells within the 'viable/live' gates were different. To overcome this, the number of cells positive for the phenotype stained were converted into percentages, with the total 'live' cells as the denominator. These percentages were then used for statistical analysis. In future experiments, it is suggested that the flow cytometry analysis to be done by gating on a constant number of known 'live' cells. To achieve this, an additional step of staining for the DNA or special staining of viable cells could be done prior to processing the samples for flow cytometry analysis of the immune cell populations. By performing this extra step, the data obtained could be improved as all the cellular debris or aggregates are excluded. During acquisition of the 'live' cells, setting the acquisition to 10,000 events within the cells positive for DNA staining will ensure that each event counted is considered a 'live' cell. Flow cytometry analysis of FACS-sorted viable cells (pre-stained with for example propidium iodide) into known total number of cells will improve the accuracy of the data produced.

In addition, the lack of animals infected with a Stx2 negative strain and the absence of serological assays or mucosal IgA measurement hindered from reaching a biologically relevant and sound conclusion. Review of published literature indicated

low, if not absence, levels of Stx-specific antibodies being generated by the bovine host. Serological anti-Stx1 but not anti-Stx2, were detected in experimentally EHEC O157-infected cattle [452, 504]. Newborn calves also lack maternal and acquired Stx-specific antibodies in the serum, providing no protection against STEC infection upon first encounter with the bacteria [505]. In naturally infected calves, maternal and acquired anti-Stx1 antibodies were present only in a small proportion of calves, while no specific antibody against Stx2 were generated [505]. An exception to the lack of strong specific Stx antibodies was described in a study employing dams immunised during pregnancy against inactivated, purified Stx2. The dams were able to generate significant titres of anti-Stx2 and transfer passive immunity to their calves via colostrum [506].

Perhaps, the generation of bovine antibodies directed against Stx-phages and Stx is not a priority to the host as that previously described for other bacterial factors. In a study where calves were experimentally-infected with EHEC O157:H7, the authors detected increased levels of mucosal IgA production against H7 flagellin, as well as IgA which recognized type III secretion-dependent proteins (Esp A, B and D), O157 lipopolysaccharide, and outer membrane porin C (OmpC) [507]. Another study identified low titres of IgG and IgA against the O157 LPS in the faeces of orally challenged adult cattle [508]. In addition, serological findings from EHEC O157-infected cattle detected antibodies against the O157 LPS, intimin and secretory proteins of the T3SS [452]. Animals vaccinated with anti-T3SS proteins were shown to develop IgG and resulted in decreased shedding [216, 509, 510]. *In vitro* study on bovine PBMC detected only a minor influence of Stx1 on CD21+ cells, as compared to significantly suppressed T cytotoxic CD8+ cells [252]. The lack of data on the presence of Stx-phage components and Stx production in the bovine intestine further complicates the interpretation of the data obtained (further work in determining Stx production by Strain 9000 and Strain 10671 is presented in Chapter 4).

Ex vivo stimulation of rectal lymph node cells with EHEC type III secreting proteins and LPS revealed lower levels of IFN- γ in Strain 10671-infected calves than the Strain 9000-exposed animals [384]. Correlations were observed between the

Th1-master regulator (T-bet) induction and IFN- γ expression from rectal lymph node cells, which peaked in parallel to bacterial shedding curves, at day seven post-challenge in animals exposed to Strain 10671, and day twenty-one post-infection for Strain 9000-infected calves [384]. Despite observing the presence of IFN- γ indicating pro-inflammatory cells to be stimulated by the presence of EHEC O157:H7, data from the IFN- γ quantitation assay unfortunately remains inconclusive due to the lack of statistical data. Additionally, there was no significant difference detected between both infected groups and the unchallenged calves with regards to the expression of CD3+/CD4+, the main T lymphocytes involved in a Th1-biased response, although these results still require additional repeats of the immunophenotyping experiment with known total number of cells analysed. In addition, intracellular IFN- γ expression in immune cells by flow cytometry, immunoblotting or mRNA transcriptome analysis would provide a stronger and clearer evidence in discussing IFN- γ production by the bovine terminal rectal cells. Since tissue sample and time were limited, such experiments were not carried out in this study.

Since the terminal rectal cells were obtained at *post-mortem*, certain handling conditions and subsequent procedures performed might cause perturbations in the morphology and ability of the cells to express cytokines, as a result of changes in stimuli (cell culture medium and laboratory growth conditions). This work also did not further investigate the transcriptional levels of important regulators associated with IFN- γ expression since the initial goal was to identify and compare the different immune subsets present in EHEC O157:H7-challenged and control calves; determining the mechanisms causing differential cytokine expression would require more samples than those available at that time of this study. There was no examination of the rectal lymph nodes on similar immune subsets as those immunophenotyped at the FAE of the terminal rectum, which if performed would have provided proper comparison for the EHEC O157:H7 infected animals.

3.2 The effect of IFN- γ on epithelial cell proliferation

Since IFN- γ was shown to interrupt cell division in both macrophages and rat intestinal crypt cells (IEC-6), the potential growth inhibiting effect of this cytokine was studied on Caco-2 and T84 cells [460]. IFN- γ mediated cell cycle arrest could occur since IFN- γ is able to induce the expression of cyclin-kinase inhibitor p21WAF, suppressing cellular proliferation at mid-G1 phase [488]. The aim was to investigate if IFN- γ produced in response to EHEC O157:H7 presence affects the intestinal epithelial cells proliferating capacity. Based on the DNA-propidium iodide labelling across cell cycle phases and PCNA staining, it was concluded that neither Caco-2 nor T84 cells proliferation was changed upon exposure to IFN- γ .

Results obtained suggest that the intestinal epithelial cells are not sensitive to the anti-proliferative effect of IFN- γ , at least as observed under *in vitro* conditions on human intestinal cell lines. Despite the rat intestinal epithelial crypt cells shown to be sensitive to the anti-proliferative effect of IFN- γ , T84 cells with crypt-like features were resistant under the assay conditions. This could be related to diminished expression of IFN- γ signalling components in the T84 cell line as compared to other primary cells that have been used previously to assess effects of IFN- γ .

3.3 Shiga toxin and IFN- γ influence on epithelial signalling of the JAK/STAT1 pathway

Initial evidence provided by a research group proposed that Stx of EHEC O157:H7 interferes with the activation of the JAK/STAT1 pathway [483, 511]. However, results obtained in my study have not been able to provide strong evidence of inhibition of STAT1 activation following IFN- γ stimulation and treatment with either purified Stx2 or Stx+ EHEC O157:H7 EDL 933 culture supernatant and lysate. Consecutive work published by the same authors claimed that Stx interrupts STAT1 phosphorylation and showed that the inhibition effect of signal transduction following IFN- γ exposure required another unknown bacterial factor besides Stx [483]. The study proposed that this might be YodA, a type two secretion protein, to act in synergy with Stx to block STAT1 activation. Further attempts in this study to

provide convincing evidence for such inhibitory activities remained inconclusive. The lack of consistent evidence seen in my study with regards to blocking IFN- γ transduction suggests that Stx do not primarily target disruption of the JAK/STAT1 signalling pathway in intestinal epithelial cells. The reason underlying the different outcomes in the current study and by the published work [483] was not investigated. However factors that may contribute to the disparate observations may be due to the different culture conditions for the growth of Strain EDL 933 used. The current study directly cultured bacterial colonies from an LB agar, into MEM before preparing the filtered supernatant of the culture. Whereas in the published study, the authors pre-cultured the bacteria in Penassay broth prior to adding the bacterial cells in MEM. Growth conditions may be very important in determining the transcriptome and phenotype induced type in the bacterial cells, as that determined for optimum T3SS expression by EHEC O157:H7 in MEM-HEPES [257] and in *Salmonella enterica* Serovar Typhimurium [512]. It may be that under the growth conditions adopted by my study hindered the expression of the necessary bacterial factors (for example YodA) required for the inhibition of STAT1 activation is observed.

Conclusion

At present, the known differences between Strain 9000 and Strain 10671 is in the carriage of different combination/types of Stx-prophages and the shedding abilities with Strain 9000 described as the more successful strain due to the super-shedding phenomena [64] and possession of the Stx2a-prophage. Thus, it was thought for these factors to be closely associated to each other. However, based on the findings of this chapter, there was insufficient evidence to implicate the involvement of Stx-phages and Stx in host immunomodulation by EHEC O157:H7 strains. Results obtained are preliminary and requires more experiments to be performed with the suggested additional protocol (Chapter Four, Discussion section 3.1) to confirm if there is any significant suppression in the CD3⁺/CD8⁺ and CD3⁺/ $\gamma\delta$ ⁺ cells and upregulation of the B cells and follicular dendritic cells (CD21⁺) of the Strain 9000-infected calves than the control animals.

Attempts to directly associate the interaction of EHEC O157:H7 and enterocytes to be mediated by either IFN- γ or Stx also produced no evidence to support the hypothesis tested. The intestinal epithelial cells remain viable with no signs of cell proliferation halted despite exposure to IFN- γ (1000 U/ml) for 6 or 24 h. Stx2 and filtered lysate of EHEC O157:H7 did not interfere with the JAK/STAT1 intracellular signal transduction in epithelial cells. The latter most likely remain important as the site for bacterial anchor in establishing colonisation and maintaining intestinal barrier integrity, with its proliferating activity remain undisturbed. The JAK/STAT1 pathway however is just one of the numerous signalling pathways in which Stx-IFN- γ cross signalling might occur, therefore this study shall not limit the conclusion based on results obtained. Studies on the toll-like receptors (TLRs) particularly on bovine intestinal epithelial cells recently reported TLR4 expression by primary bovine colonocytes [513]. Bovine intestinal epithelial cells derived from fetal bovine intestinal epithelial cells were also confirmed to strongly express TLR4 by real time-quantitative polymerase chain reaction (RT-qPCR) and immunofluorescence staining. TLR1, 3 and 6 were also significantly expressed by the bovine intestinal epithelial cells [514]. TLR4 is mainly associated with detection of Gram negative bacteria and initiation of inflammation by the NF κ B signalling pathway, activated by mitogen-activated protein kinase (MAPK) proteins [515]. Further insight on EHEC O157:H7 and TLR4 signalling particularly focusing on Stx might be worth considered when studying intestinal epithelial cells response. Chapter 4 will follow with more information and discussion specifically focusing on Stx and Stx-encoding phages of the two bovine strains used in this chapter, in an attempt to associate these determinants with bovine terminal rectal colonisation.

Chapter 4: *Shiga toxin-encoding bacteriophages and EHEC O157:H7 colonisation of the bovine intestine*

Chapter 4

Introduction

The significance of EHEC O157:H7 colonisation at the recto-anal junction was linked to super-shedders as these animals, identified to be colonised at the terminal rectum, tend to have prolonged colonisation and higher excretion [60, 516, 517]. The concept of super-shedding for EHEC O157 as described in the discussion of the Naylor et al (2003) manuscript on the rectal localization of the organism: ‘One hypothesis is that among an *E. coli* O157:H7-positive group of animals there are a small number of "supershedders" that greatly enhance transmission and persistence within a herd’ [33]. A "supershedder" refers to an animal that excretes more than 10^4 C.F.U. per gram of faeces, a phenomenon observed not only in cattle, but in sheep as well [60]. This concept of "supershedders" for EHEC O157:H7 colonisation was analysed in a model with findings indicating that the "supershedders" are more likely to be associated with PT21/28 strains of EHEC O157:H7, while strains of PT32 were more likely to be associated with "non-super-shedders" [64]. Another implication from the same study was that preventive measures specifically targeting the "supershedders" could most likely reduce the risk of transmission to humans [518].

In a more recent publication by collaborators working on experimental EHEC O157:H7 colonisation of calves (as described in Chapter 3, Materials and Methods section 3.1), the shedding curves from two groups of animals receiving or exposed to either EHEC O157:H7 Strain PT21/28 or PT32 (Figure 4.1) were established [384]. All of the orally-challenged animals were able to shed at a high rate ($>10^3$ C.F.U./gram of faeces). However, the animals orally challenged with Strain 9000 PT21/28 maintained a longer shedding period (3 to 10 days post-challenge) of $>10^3$ C.F.U./gram than Strain 10671 PT32 (day 3 to 8 days post-challenge). Sentinel animals of the PT21/28 group maintained shedding at higher numbers ($>10^3$ C.F.U./gram) throughout the shedding period (10 days), with the highest colony count between day 6 and 8. From two of the sentinel animals of group exposed to PT32-challenged calves, shedding never exceeded 10^3 C.F.U./gram in one calf while the other sentinel calf shed at $>10^3$ CFU/gram only on day 8. These observations showed that although both strains were able to effectively colonise the intestine of all calves, the calves receiving Strain PT21/28 were able to consistently shed higher bacterial counts ($>10^3$ C.F.U./gram) within a longer time frame than the PT32-

challenged group. Initial genome sequence screening of Strain 9000 PT21/28 and Strain 10671 PT32 showed that these two strains are genetically very similar except for the Stx-encoding prophage types possessed. PT21/28 strains usually contain both an Stx2a-encoding bacteriophage (Φ Stx2a) and an Stx2c-encoding bacteriophage (Φ Stx2c), while the PT32 strains were predominately Φ Stx2c+ only. Although further work is needed to fully characterise these Stx-encoding phages, it may be that the different Stx prophage contents of PT21/28 and PT32 cattle strains significantly contribute to the variations observed in the shedding pattern mentioned above. This is supported by further epidemiological analysis [257]. Therefore, the aim of Chapter 4 is to characterise the colonisation-associated phenotypes of bovine isolated EHEC O157:H7 strains (Strain 9000 PT21/28 and Strain 10671 PT32) in order to understand the contribution of different Stx-encoding prophages (and combination of Stx-prophages) to enhanced colonisation/excretion levels in/from cattle.

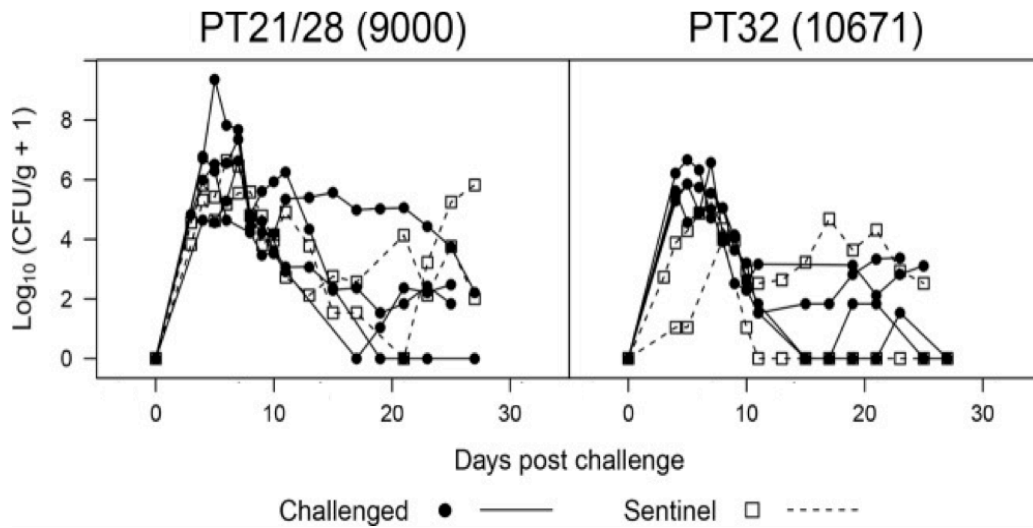


Figure 4.1 Faecal shedding of EHEC O157:H7 by experimentally infected weaned calves, taken from Corbishley et al., 2014 [384]. Each group had six calves housed in two separate rooms, four calves in each group were orally challenged with EHEC O157:H7 Strain 9000 or Strain 10671. Two calves were assigned as sentinels received PBS. Each curves represents an individual animal.

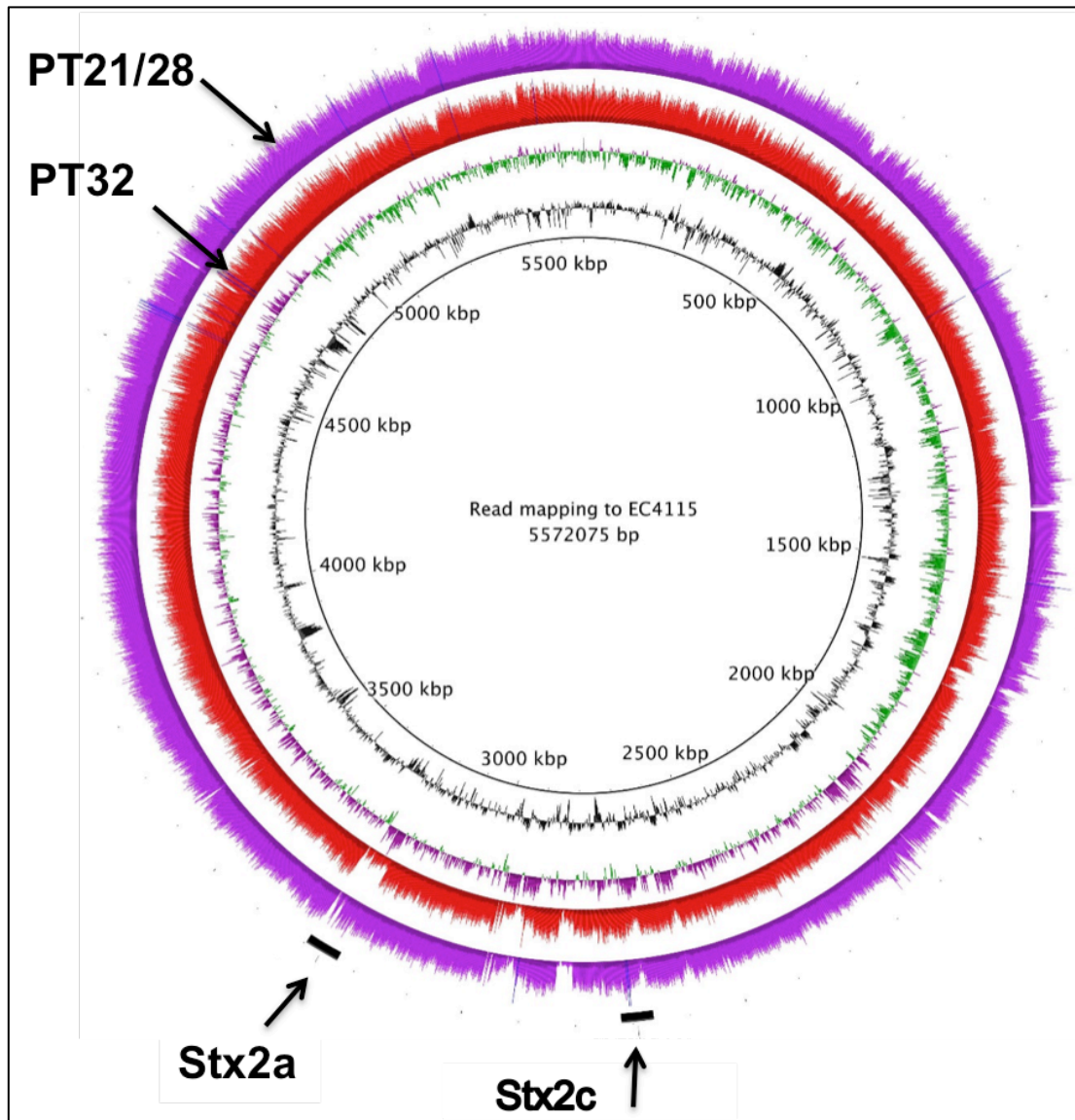


Figure 4.2 Alignment of the EHEC O157:H7 Strain 9000 (PT21/28) and EHEC O157:H7 Strain 10671 (PT32) genomes to EHEC O157:H7 EC4115 (Φ Stx2a+/ Φ Stx2c+) [Image courtesy of Prof. Dr. David Gally, University of Edinburgh]. The main difference between PT21/28 and PT32 is the presence of Stx2a and Stx2c-encoding genes in PT21/28, while PT32 only contains the Stx2c-encoding gene.

4.1 Shiga toxin production and cytotoxicity of bovine and human associated EHEC O157:H7 strains

It will also be important, given one of the overall aims of this thesis research (to assign any role of the toxin in bovine intestinal colonisation) to identify if Stx production differs between strains with different Stx-prophage repertoires. Epidemiological studies strongly suggest that the amount of Stx produced during colonisation in the intestine is an important factor for disease severity [107]. Expression of Stx2a is considered a key factor associated with more virulent EHEC strains, leading to HUS and other severe clinical complications in humans [277]. Therefore Stx2a maybe associated with both increased excretion from cattle and increased pathology in humans. In the long run, this would provide better survivability of PT21/28 and continued propagation as compared to other EHEC O157:H7 strains. The relative contribution of the Stx toxin type to other genes encoded on the prophages is unknown. Similarly, the levels of Stx in colonised animals and even in human patients remains ambiguous, although Stx has been quantified from faecal samples of STEC-infected mice, which ranged between 25-1000 ng/gram of faeces [519]. Efforts to accurately quantify the total Stx produced *in vivo* is regarded as technically impossible at this moment due to the complex nature of the intestine. The presence of Stx-encoding prophage combinations within a strain [520] is regarded as the main determinant for Stx production, however other factors present within the intestine are able to modulate the levels of toxin production such as phage sensitive or phage resistant commensal *E. coli* strains [519, 521] and Shiga toxin neutralising strains (healthy human isolates of *E. coli* serogroup O107, O117) [522] .

4.2 The growth and fitness of EHEC O157:H7 in bovine terminal rectal mucus

The first hypothesis tested in this chapter is that the extra Stx-encoding bacteriophage (Φ Stx2a) possessed by the EHEC O157:H7 strains of PT21/28 group would be able to increase the bacterial fitness and survival at the bovine terminal rectum, thereby increasing the rates of shedding and transmission to other animals, as compared to the strain with a single Stx-encoding phage, Strain PT32 (Φ Stx2c) [256] [61, 66]. Part of this hypothesis was based on preliminary evidence from comparison of the growth curves of EHEC O157:H7 Strain 9000 PT21/28, Strain 10671 PT32 and the Stx-phage negative strain, Walla 3 which suggested a shorter doubling time for the PT21/28 strain [256]. The presence of the Stx2a-prophage in PT21/28 strain is the only known difference that distinguishes PT21/28 and PT32 according to the data from initial genome sequencing of these strains and that PT21/28 were shed at a higher numbers with an extended time period compared to PT32, led this study to speculate for an association to exist between the possession of Stx2a-phage and 'superior' colonisation-associated traits. This, in addition to the ability to encode two Stx types including the most potent Stx type, Stx2a [69, 78, 240, 523] may confer further advantage to the PT21/28 strain based on previous findings with regards to Stx-nucleolin upregulation [241].

Moreover, a thorough review on bacterial sialic acid metabolism questioned the presence of *nanS* genes within the Stx-prophage and prophage remnants of *S. dysenteriae* and certain EHEC O157:H7 strains [524]. NanS is an O-acetyl esterase, an enzyme required for utilisation of sialic acid that is present in the mucus and was shown to be utilised by *E. coli* [255]. One hypothesis is that certain Stx-prophages may result in more efficient use of mucin as an energy substrate by the host bacterium; if this was the case then this would provide another example of how Stx-encoding phages could alter the bacterial host phenotype in order to maintain its presence within the genome, which in turn, benefits host survivability. These findings and hypotheses justify the use of bovine terminal rectal mucus as growth media for EHEC O157:H7 strains in this chapter. Pairwise competition in 10%

bovine terminal rectal mucus allows direct quantification and comparison in order to identify whether a strain is 'fitter' in this environment compared to another. This has to take into account factors such as phage infection/transfer between the competed populations [525]. Previously it was shown that the lambda phages of *E. coli* were able to kill competitor strains within the same environment, however this may only remain within the first ten generations. Following that, lysogenisation of the susceptible strains would cancel out the advantage of possessing the lambda phage as 'biological weapon' [526].

4.3 The binding capacity of EHEC O157:H7 strains possessing different Stx-prophages

Prior to establishing attachment to the host intestinal epithelial cells, EHEC O157:H7 has to overcome the two layers of mucus at the intestine; the thick, loose outer layer and the thinner, dense inner layer [527, 528]. Moreover EHEC O157:H7 also needs to compete with the commensal species already residing in the outer mucus layer. StcE, a zinc metalloprotease secreted by EHEC O157:H7, was shown to act as a mucin-degrading enzyme thereby facilitating contact and adherence of the bacterial cell to the epithelium [529]. As observed by Naylor/Low et al., cattle colonised with EHEC O157:H7 generate micro-colonies on the terminal rectal mucosa that include actin re-arrangements and condensation associated with typical A&E lesions extensively documented for LEE-encoding EPEC and EHEC strains [33, 530]. Despite being described as non-invasive, recently it has been shown that the terminal rectal epithelial cells can contain EHEC O157:H7 cells intracellularly [373]. Intimate bacterial adherence with attaching and effacement lesion on the intestinal epithelial cell is a hallmark for the LEE-encoded proteins in establishing and maintaining successful colonisation. Other bacterial products could also enhance bacterial attachment to the host cells including Shiga toxin 2 [241]. The study reported that Stx2 treatment of HEp-2 cells upregulated nucleolin to the site of bacterial attachment which resulted in a stronger and more efficient colonisation with the nucleolin functioning as another receptor for intimin [241] (as introduced in Chapter 2, section 2.4). Whereas lysogenisation of the Stx2-phage in a PT21/28 strain repressed the T3SS resulting in a reduced ability to form the A/E lesion via

intimate attachment [257]. Furthermore, unpublished findings indicated that the PT21/28 strain adhered better than the PT32 and Walla 3 strains, which again indicates that the bovine-associated strains of the PT21/28 cluster are viewed as 'superior' compared to other strains missing the Stx2a-prophage. Preliminary data from studies with Stx2-producing strains on the binding capacity lead the current study to re-examine the adherence of Strain 9000 (PT21/28), Strain 10671 (PT32) and in addition, analysis of the adherence of isogenic Stx2-phage mutants to eukaryotic cells. Results obtained from the binding assays could then be compared with the shedding data (Fig. 4.1) to assess if better adherence leads to higher shedding numbers.

4.4 Assessing the effect of Stx-prophages on the virulence of EHEC O157:H7 in a *Galleria mellonella* infection model

Ideally, competition of strains in host colonization could be analysed in cattle challenge experiments with mixed inocula and in humans for effects on virulence. The former is very expensive and is limited to very specific questions, while the latter is ethically not possible. As such some type of *in vivo* system/model is desirable to examine effects of altering the prophage content with regard to host-pathogen interactions. Recently, *Galleria mellonella*, generally known as 'waxworms', has been described as a good model to study pathogenesis as an alternative to experiments in mammals [531, 532]. *G. mellonella* larvae possess cellular (phagocytosis, nodulisation and encapsulation) and humoral (melanisation, haemolymph clotting and antimicrobial peptides) immune defense mechanisms [531]. This larvae infection model has been used to study aspects of virulence and innate immune responses following infection with different species of bacteria (*Pseudomonas aeruginosa*, *Listeria monocytogenes*, *Burkholderia pseudomallei*) and fungi (*Candida albicans*, *Cryptococcus neoformans*, and *Aspergillus fumigatus*) [533]. Advantages of this infection model includes incubation at 37°C resembling normal body temperature, the ease of administering the infection dose, better statistical power of the data as large numbers of larvae can be used at a relatively low cost of maintenance. There are relatively simple assays available to assess the outcome of infection. Examples are the melanisation of the larvae which is the

darkening of the body in response to the infection and/or larvae survival. By comparing isogenic pairs of strains with and without Stx-encoding prophages derived from Strain 9000 (PT21/28) and Strain 10671 (PT32), this assay could provide insights into whether the Stx-phages modulate pathways involved in bacterial virulence.

This chapter focuses on Stx-encoding bacteriophages and EHEC O157:H7 colonisation and pathogenesis and it should complement the findings from part one of this thesis on Shiga toxin activity towards a combined understanding of how strain lysogeny with an Stx2-encoding bacteriophage can impact on bacterial growth, colonisation and pathogenesis. One could hypothesise that by harbouring both Stx2a- and Stx2c-encoding prophages, several advantages are gained, for example strains grouped under the PT21/28 cluster could be better colonisers, higher excretion and increased virulence following transmission into human hosts. The specific objectives for this chapter are:

1. To quantify and compare total Shiga toxin production across EHEC O157:H7 strains of bovine and human origin possessing different Stx-phage types.
2. To examine the activity of Stx expressed by EHEC O157:H7 strains containing different repertoires of Stx-phages (wildtype and natural excision variants) under normal and induced conditions.
3. To investigate if Stx-encoding bacteriophages provide any fitness or survival advantage when competed in 10% bovine terminal rectal mucus.
4. To observe if Stx-encoding bacteriophages influence EHEC O157:H7 binding to eukaryotic cells.
5. To study if Stx-encoding bacteriophage positive strains are altered for virulence compared to their isogenic Stx-phage deletion strains in the *G. mellonella* larvae infection model.

Chapter 4

Materials and Methods

Table 4.1 List of bacterial strains used in this study

Strain name used in this study	Strain	Details
Strain 9000 PT21/28 (Φ Stx2a/ Φ Stx2c)	<i>Escherichia coli</i> (<i>E. coli</i>) O157:H7	Bovine isolate from the IPRAVE study [64], Phage Type 21/28. Isolate code WS009000S01E.
Strain 9000 PT21/28 $\Delta\Phi$ Stx2c	<i>E. coli</i> O157:H7	Generated from WS009000S01E by partial deletion of phage in <i>sbcB</i> (RH junction present). Laboratory stock generated by Sean McAteer.
Strain 9000 PT21/28 $\Delta\Phi$ Stx2a	<i>E. coli</i> O157:H7	Generated from WS009000S01E by entire deletion of phage in <i>argW</i> . Laboratory stock generated by Sean McAteer.
Strain 9000 PT21/28 $\Delta\Phi$ Stx2a/ Φ Stx2c	<i>E. coli</i> O157:H7	Generated from <i>E. coli</i> serotype O157:H7 Strain 9000 $\Delta\Phi$ Stx2a by the entire deletion of phage in <i>argW</i> . Laboratory stock generated by Sean McAteer.
Strain 10671 PT32 (Φ Stx2c)	<i>E. coli</i> O157:H7	Bovine isolate from the IPRAVE study [64], Phage Type 32. Isolate code WS0010671S01E.
Strain 10671 PT32 $\Delta\Phi$ Stx2c	<i>E. coli</i> O157:H7	Generated from <i>E. coli</i> serotype O157:H7 Strain 10671 (WS0010671S01E) by the entire deletion of phage in <i>sbcB</i> . Laboratory stock generated by Sean McAteer.

Table 4.1 List of bacterial strains used in this study (Continued).

Strain name used in this study	Strain	Details
Human Strain 1 PT21/28 (Φ Stx2a/ Φ Stx2c)	<i>E. coli</i> O157:H7	Human isolate of <i>E. coli</i> O157:H7 provided by Public Health England (Strain number 122900512). Phage Type 21/28.
Human Strain 2 PT21/28 (Φ Stx2a/ Φ Stx2c)	<i>E. coli</i> O157:H7	Human isolate of <i>E. coli</i> O157:H7 provided by Public Health England (Strain number 132020426). Phage Type 21/28.
Sakai <i>stx2A::kan</i> (Sakai)	<i>E. coli</i> O157:H7	<i>E. coli</i> O157:H7 outbreak strain containing Sp5 phage, with the <i>stx2A</i> toxin gene replaced by a kanamycin cassette rendering a defunct Stx production. Laboratory stock generated by Sean McAteer.
Sakai Δ Sp5	<i>E. coli</i> O157:H7	Derivative of the Sakai outbreak strain with the Stx2a-encoding phage, Sp5 removed. Laboratory stock generated by Sean McAteer.
MG1655 Nal ^R (MG1655N)	<i>E. coli</i> K-12	Laboratory strain made resistant towards Naladixic acid.
K-12-Sp5 <i>stx2A::kan</i> Δ <i>lacZ</i> (K-12-Sp5)	<i>E. coli</i> K-12	Generated by transduction from Sakai <i>stx2A::kan</i> , contains Sp5 phage and with deletion of the <i>lacZ</i> gene. Laboratory stock generated by Sean McAteer.
MG1655 Nal ^R Kan ^R (MG1655NK)	<i>E. coli</i> K-12	Spontaneous Kan ^R derivative from <i>E. coli</i> K-12 MG1655 (Nal ^R).

All of the work on Shiga-toxin producing *Escherichia coli* (STEC) strains was carried out in a Containment Level 3 (CL3) laboratory suite according to the guidelines. Subsequent steps of experiments using Shiga-toxigenic filtrates were undertaken in Containment Level 2 (CL2) laboratory once the filtrates were verified for the absence of live bacteria. Strains were typically cultured overnight at 37°C, with shaking (200 R.P.M.) in different culture media as described below for specific experiments.

4.1 Production of culture supernatants

Single colonies were inoculated into 5 ml of lysogeny broth (LB) broth and were incubated for 18 h at 37°C in a shaker incubator at 200 R.P.M. (Innova™ 4000 Incubator Shaker, New Brunswick Scientific). For CL3 bacterial strains, to prevent spillage if the tube breaks during incubation, the culture tubes were placed in a leak-proof container (similar to the container used to transport bacterial culture), cushioned with paper towels to absorb spillage, if any were to occur. All culture tubes and direct manipulation procedures of the bacterial cultures were within a microbiology safety cabinet unit in the CL3 facility.

The overnight cultures were pelleted at maximum speed, 4°C for 10 min (Heraeus Instruments Megafuge 1.0R). Individual culture tubes were placed in bucket of suitable size within the microbiology safety cabinet unit and sealed with the bucket cover that was then disinfected with 70% ethanol before transferring the buckets into the centrifuge. At the end of the spin, the buckets were carefully lifted out from the rotor and carried into the microbiology safety cabinet unit for further procedure. Supernatants were filter-sterilised (Millex® GV-syringe filter unit membrane, pore size 0.22 µm, Merck Millipore) and a loopful of it was spread onto an LB agar plate for verification of 'zero live bacterial cell' presence inside the filtered-supernatant. The filtered-supernatants were stored at -20°C for at least 24 h (i.e. the time frame to observe any growth on the incubated LB agar plate) or until use.

The same protocol was adopted for bacterial strains grown in 10% bovine terminal rectal mucus to produce Stx-containing filtrates in mucus. Mucus samples

were obtained from five calves used as control animals in an animal challenge experiment at the Moredun Research Institute (MRI). Briefly, terminal rectal tissue was obtained from the animals during *post-mortem* at the MRI, immersed in Polymyxin B sulfate (Sigma), diluted 2 mg/ml in normal saline for 30 min in a 150 ml polystyrene straight-sided metal cap container (Starlab) and transferred to the *post-mortem* room at the Royal (Dick) Veterinary School, Easter Bush campus. The mucus layer was then scraped using glass slide into a clean, labelled 50 mL polystyrene tube with screw cap before stored in a -20°C freezer at the Roslin Institute. Prior to use, the mucus samples were thawed at room temperature before preparing the diluted form (10% mucus in sterile distilled water) for further use in the experiments in this chapter.

To generate Mitomycin C (MMC)-induced bacterial lysates in LB broth, 50 µl of the overnight culture was diluted in 5 ml of sterile LB broth and incubated at 37°C, 200 R.P.M. until the optical density (O.D.) 600nm readings (Ultraspec 10 Cell Density Meter, Amersham Biosciences) reached 0.2 - 0.25. 10 µg/ml of MMC was added into each bacterial culture and was further incubated in the dark at 37°C, 200 R.P.M. for 18 h. The overnight MMC-induced lysate were then filter-sterilised as described for the non-induced cultures.

4.2 Shiga toxin ELISA

The total Shiga toxin (Stx) present in the culture supernatants and lysates were measured using a commercial ELISA kit according to the manufacturer's instructions (RIDASCREEN® Verotoxin ELISA, R-Biopharm AG, Darmstadt, Germany). Samples were used for ELISA prior to the Verocytotoxicity assay to verify the presence of Stx in samples. Inactivated Stxs serve as the positive control for this assay which was supplied by the manufacturer. The negative controls used were either 10% bovine terminal rectal mucus or LB, depending on sample type (mucus or LB-grown bacterial culture). The results were read at O.D. 450nm and were plotted as bar graphs.

4.3 Verocytotoxicity assay

The African green monkey cells also known as the Vero cells express the Stx receptor, Globotriaosylceramide (Gb3) and therefore have been widely used to test the toxic effects of Stx. Vero cells used in this work were obtained from the Leibniz Institute DSMZ-German Collection of Microorganisms and Cell Cultures (Braunschweig, Germany). The cells were seeded in 96-multi-well plates at a rate of 1×10^5 cells/well and incubated at 37°C with 5% CO₂ until confluent. On the day of challenge, the spent media were removed from the wells and the EHEC O157:H7-filter-sterilised culture supernatants, diluted 1:100 in Roswell Park Memorial Institute (RPMI) 1640 medium were added to the Vero cells. 0.2% Triton™X-100 (Sigma-Aldrich) and LB broth both diluted in RPMI 1640 served as positive and negative controls respectively. Another set of Vero cells received RPMI 1640 only as another negative control. All treatments were carried out in triplicate and the assay was repeated at least three times with different batches of culture supernatants/lysates. The cells were placed in the incubator at 37°C, 5% CO₂ for a maximum of 72 h. Daily checks of the cells were performed by observing the cells under light microscopy to determine if the cells were already responding to the toxin. After 72 h, the toxin containing serum-free media was discarded and the cells were gently washed in pre-warmed PBS (37°C) once.

65 µl of 2% formalin in PBS was added to each well for 1 min at room temperature to fix the cells. The fixative was replaced with 65 µl/well of crystal violet tissue culture stain (52 ml of 0.5% crystal violet (Sigma), 10 ml of absolute ethanol, 10.8 ml of 37% formaldehyde and 127.2 ml of PBS) and incubated at room temperature for 24 h. The fixed cells were then washed gently with distilled water until the water appeared clear and were air-dried. The plate was scanned for visual record. 100 µl of 10% acetic acid was added per well and the plate was placed on an orbital shaker for 15 min at room temperature to dissolve the crystal violet stain. The values of absorption at O.D. 595nm were obtained using a plate-reader (FLUOstar OPTIMA, BMG Lab technologies) and analysed within Microsoft® Excel.

4.4 Growth competition assay

To observe if a strain possessing ϕ Stx2 is more competitive than a strain without the ϕ Stx2, growth competition assays were carried out in 10% bovine terminal rectal mucus (BTRM) diluted in sterile water. This growth medium was chosen to mimic as close as possible the environment from where the bacteria are mainly present in the bovine host, as opposed to growing in an artificial growth media such as LB broth or M9 medium.

Each of the paired EHEC O157:H7 strains to be competed were separately inoculated in 10% BTRM overnight and incubated at 37°C with shaking (200 R.P.M.). One of each pair of competed strains was ensured to be Naladixic acid resistant (Nal^R); either readily available from the ZAP laboratory freezer stock or resistance was generated by growing on LB agar containing Naladixic acid (15 µg/ml) and sub-culturing colonies developing resistance towards Naladixic acid again on LB-Nal agar plates. The overnight cultures of the paired strains to be competed were then diluted 10⁻⁴ together in 1ml of fresh 10% BTRM. The co-cultures were then left at 37°C, 200 R.P.M. for 24 h. At the end of the 24 h, 10 µl of the co-culture was then diluted in 1 ml of fresh 10% BTRM. The 24-hour-co-culture was also diluted in a 10-fold dilution series in PBS before spreading on Cefixime and Tellurite-Sorbitol MacConkey (CT-SMAC) plates. The CT-SMAC plates were incubated at 37°C for 18 h. From the colonies growing on the CT-SMAC plates, 100 single colonies were then picked and patched onto a selective agar plate, Luria-Bertani agar supplemented with 15 µg/ml Naladixic acid (LB-Nal). The LB-Nal plates were then incubated at 37°C overnight before the proportions of each compared strain were counted and compared. This procedure was continued for at least 72 -120 h (with approximately 13 generations of bacteria per 24 h).

The protocol described was similarly used for growth competition assays involving other competed paired strains (*E. coli* MG1655NK and *E. coli* K-12-SP5, *E. coli* O157:H7 strain Sakai *stx2A::kan* and *E. coli* O157:H7 strain Sakai Δ SP5), with the selective LB agar plates supplemented with Kanamycin at (50 µg/ml). In addition, for the competed pairs of *E. coli* K-12 and *E. coli* O157:H7 Sakai, the co-

cultures were initially plated out on LB-Naladixic acid and CT-SMAC agar plates respectively, to prevent background growth of other organisms present in the mucus samples.

For growth competition assays involving *E. coli* MG1655NK and *E. coli* K-12-SP5 strains, the co-culture was initially spread on LB-Naladixic acid to prevent background growth in the mucus sample, and were then picked and patched simultaneously on LB-Kanamycin agar plates and 1% lactose-MacConkey agar plates. The latter agar plate was used to check if any lysogenisation of the susceptible bacterial cells (*E. coli* MG1655NK) by the free Sp5 phage released from lysed *E. coli* K-12-SP5 occurred throughout the co-culture period.

All steps involving Stx positive strains were performed in the CL3 laboratory suite and handling of the CL3 bacterial strains was carried out according to defined rules and regulations, for example placing cultures in a second leak-proof container and proper handling of culture tubes before and after centrifugation.

The results are presented as stacked bar plots across the time of co-culture and statistically analysed in GraphPad Prism 6 (GraphPad Software, Inc., La Jolla, CA, USA) using multiple t-tests for each time point, with Holm-Sidak method, assuming that all rows were sampled from populations with similar scatter.

4.5 Bacterial adherence assay

Gb3 expressing HeLa cells were used to evaluate the binding potential of bacteria to an epithelial cell line, while the Embryonic Bovine Lung (EBL) cells were used to compare the binding potential of different mucus-grown Stx2-phage types-containing EHEC O157:H7 strains to Gb3-negative epithelial-like cells. The cells were seeded at 1×10^5 cells/ml in 24-multi-well plates and incubated at 37°C with 5% CO₂ until reaching full confluence.

EHEC O157:H7 IPRAVE Strain 9000, Strain 10671, Strain 9000 $\Delta\phi$ Stx2a/ ϕ Stx2c and Strain 10671 $\Delta\phi$ Stx2c were inoculated in 10% BTRM at 37°C,

200 R.P.M. for 18 h. The cultures were diluted 1:100 in fresh 10% BTRM and were further incubated for approximately 2.5 h at 37°C, 200 R.P.M. to generate cultures at the exponential phase [256].

Prior to cell infection, the spent cell media were removed from the wells, the cells washed once in PBS before 100 µl/well of 10% BTRM were added to the cells. 450 µl of the exponential-phase bacterial cultures (multiplicity of infection (M.O.I.) of approximately 10 bacteria to 1 epithelial cell) were then added to each well accordingly, in triplicate. Three wells that did not receive any bacterial challenge served as controls to ensure that the eukaryotic cell line remained viable in 10% BTRM throughout the infection period.

Infected cells were incubated at 37°C with 5% CO₂ for 30 min. This 30 min time point was chosen based on the optimisation process by a previous study [256]. Any incubation time beyond 30 min will kill most of the epithelial cells in the culture. The plates were covered with an adhesive plate seal with pores before placing the plate cover on top and to prevent spillage of the bacterial cultures during transporting the plate to and from the microbiology safety unit, the plate was then placed into a leak-proof container (polystyrene container of appropriate size).

At the end of challenge time, the 10% BTRM with bacteria were removed and the cells were washed in PBS twice. Then, 250 µl of 0.2% of TritonTMX-100 (Sigma-Aldrich) in PBS were added to all wells and incubated at 37°C, 5% CO₂ for 10 min to dissociate the bacterial-bound cells from the surface of the wells. To harvest the bacterial-bound cells, another 250 µl of 0.2% TritonTMX-100 (Sigma-Aldrich) were added to the set of triplicates and using a pipette tip, the bottom of the wells were scratched to remove the cells from the wells, avoiding froth formation. The cell suspension was transferred from the first well to the second and to the third well cumulatively before collecting all in a 1.5 ml screw-cap tube.

The pooled bacterial-bound cell suspensions were serially diluted (10-fold) and the appropriate dilutions were then plated out on LB agar plates. The plates were

incubated at 37°C for 18 h before counting the colonies present on the plate. Results are presented as individual dot plots, each dot represents the percentage of binding, normalised to the total number of bacteria added from independently repeated experiments with technical replicates of three and analysed in GraphPad Prism 6 (GraphPad Software, Inc. USA). The normalised percentage of binding were analysed using the Friedman test of repeated one-way ANOVA.

4.6 Immunofluorescence staining for H7 and EspA (T3SS effectors)

Bacterial strains were grown as described for bacterial binding assay and fixed in 4% (volume/volume) paraformaldehyde (PFA). After verifying no live bacterial cell present, the fixed cultures were given to Dr. Amin Tahoun to be processed for immunofluorescence staining with primary antibodies [mouse monoclonal anti-O157 IgG (Mast Assure), 1:100, rabbit polyclonal anti-H7 IgG (Abcam) 1:1000 and mouse monoclonal anti-EspA [534], 1:100], and secondary conjugated antibodies [anti-mouse IgG-Alexa Fluor® 568 (Molecular Probes), anti-rabbit IgG-FITC (R&D Systems) and anti-mouse IgG-FITC (R&D Systems); all 1:1000]. Examination of the cultures by confocal microscope were performed by Dr. Amin Tahoun and he has given his consent to show the images in the Results section. These immuno-stained bacterial cells will help determine if there is any significant difference in the expression of the bacterial factors potentially playing a role in binding within the bacterial binding assay time frame.

4.7 Western blotting for H7 and EspD (T3SS effectors)

EHEC O157:H7 IPRAVE strains 9000, 10671 and their Stx2-phage mutants were grown under the same conditions as described above in the experimental method for bacterial adherence assay. Another tube containing the same volume of 10% mucus was also incubated under the same conditions to serve as a background control. At the end of the 2.5 h incubation at 37°C with shaking at 200 R.P.M., the cultures were pelleted at high speed (4300 R.C.F) for 10 min at 4°C before decanting the supernatant and re-suspending the bacterial pellet in 1 ml of PBS. The lysate was

centrifuged again before gently pipetting out the PBS-supernatant, ensuring the pellet was left undisturbed. The pellet was again re-suspended in PBS, the O.D. 600nm measured to ensure similar pellet concentration, centrifuged and re-suspended in 250 μ l of PBS and 250 μ l of sample buffer (Laemmli buffer, Sigma) before incubating it at 100°C for 10 min. The extra washing steps were done to reduce any background proteins that might interfere with the Western blot process, due to the nature of the sample cultured in 10% mucus. The bacterial lysate was then stored at -20°C until completion of the verification step, as described above to ensure no live bacterial cells were present within the lysate since the next steps were carried out in the CL2 laboratory.

Another set of cultures were grown under conditions previously shown by Xu, et al. [257] to induce the expression of the type three secretion system (T3SS) in EHEC O157:H7 strains. Briefly, all of the strains examined were grown in MEM-HEPES for 18 h, 200 R.P.M. at 37°C. The cultures were then diluted 1:100 in fresh MEM-HEPES medium and re-incubated under similar conditions but for 2.5 h until the OD₆₀₀ nm readings reached 0.8. At this point of time, the bacterial cells should be expressing components of the T3SS. The bacterial cultures were then processed to produce filtered bacterial lysate as described above.

Protein concentration was estimated with the Direct Detect™ IR Spectrometer system (Merck Millipore) (described in detail under Section 3.12 in the Materials and Methods section for Chapter 3). Once the amount to be loaded per lane per sample was calculated, samples were loaded into wells of the SDS-PAGE gel (4% stacking gel, 10% resolving gel). The clamping frame with the glass plates holding the gels were placed inside the running chamber. Electrode buffer (1X) was poured into the space inside the running chamber up to the appropriate levels (2 or 4 gels) and the lid was properly placed to close the chamber. The colour-coded electrodes were fixed into the power supply and set to run at 130V, for 80 min. The gels were then soaked in transfer buffer (refer Section 3.14, Materials and Methods section in Chapter 3) as well as the nitrocellulose membrane and thick blot papers for at least 15 min before being placed on the Trans-Blot® SD Semi-Dry Electrophoretic

Transfer Cell (Bio-Rad) in the order of thick blot paper, nitrocellulose membrane, gel and thick blot paper, at 15 V, 0.7 h with limit set at 0.6.

At the end of the transfer process, the nitrocellulose membranes were stained with the reversible Ponceau stain to check for successful protein transfer (visualised as separate lines in lanes corresponding to each lane with protein sample). The membranes were washed with distilled water to remove the stain and immediately placed in blocking buffer (2.5% skimmed milk powder in 0.1% PBS-Tween 20) for an hour, room temperature, shaking (20 Rev/min, Platform Shaker STRG). The nitrocellulose membranes were then washed in 0.1% PBS-T (two quick rinses, one 10 min wash followed by two times of 5 min washes). This was followed with incubation in primary antibody diluted in 5% skimmed milk powder and 0.1% PBS-Tween 20 [mouse anti-RecA (Stressgen/Enzo Life Sciences) at 1:5000 and mouse monoclonal anti-EspD [535] at 1:3000] at 4°C, overnight, on an orbital shaker. The membranes were washed in 0.1% PBS-Tween 20 (two quick rinses, followed by a 30 min wash and two times 5 min washes). Secondary antibody (anti-mouse Horseradish Peroxidase, Dako, Cambridge, United Kingdom) diluted at 1:1000 in 5% skimmed milk powder and 0.1% PBS-Tween20 was added to the membranes for an hour at room temperature, shaking (20 Rev/min). Washing steps were as described following primary antibody incubation with the addition of two more 5 min washes.

An equal amount of the Supersignal West Pico Chemiluminescent substrates (Thermo Scientific) were added onto the surface of the nitrocellulose membranes (approximately 1 ml per 8cm x 15cm membrane), incubated at room temperature for 5 min. The excess detection reagent was drained off and the nitrocellulose membranes were placed in between two acetate sheets. Detection was subsequently done with radiograph developer and the G-box chemiluminescence detection system.

4.8 *Galleria mellonella* larvae killing assay

The *G. mellonella* moth larvae killing assay was used as an infection model to assess the virulence of strains at 37°C. Bacterial strains were grown in LB broth

overnight, at 37°C, shaking at 200 R.P.M. The overnight cultures were then pelleted at speed 4300, 10 min at 4°C and washed twice in PBS. The O.D. 600nm of the cultures were adjusted to 0.1 in Dulbecco's Phosphate Buffer Saline (DPBS, Life Technologies 14190-094). 10 µl of the re-suspended cultures were injected into each larva, directly into the posterior segment of the body using a 10 µl Hamilton Syringe, point style 5, needle 25 gauge. Larvae used weighed between 0.25-0.30 grams and each treatment group contained 20 larvae. The control groups received DPBS or nothing. The larvae were incubated at 37°C, with 5% CO₂. The number of dead larvae was counted at 18, 24, 48, 72, 96 h and for some experiments 120 h post challenge. Survival analyses were plotted and analysed in GraphPad Prism Version 6.0 to compare the trends of different survival curves using the Log-rank (Mantel-Cox) test. For analyses with significantly different survival trends, multiple pairwise comparisons were done with a corrected p-value threshold based on the Bonferroni method;

$$\text{Bonferroni corrected threshold} = \frac{0.05}{K},$$

where K equals to the total number of pairwise comparisons made.

The median and median ratio (with 95% confidence limits) for pairwise comparison of significantly different survival trends were also calculated and presented in the Results section.

Chapter 4

Results

This section presents results obtained from a series of phenotypic assays carried out with EHEC O157:H7 strains of bovine origin (Strain 9000 and Strain 10671), along with isogenic mutants (Strain 9000 $\Delta\Phi\text{Stx}2a$, Strain 9000 $\Delta\Phi\text{Stx}2c$, Strain 9000 $\Delta\Phi\text{Stx}2a/\Phi\text{Stx}2c$, Strain 10671 $\Delta\Phi\text{Stx}2c$). For Shiga toxin ELISA and Verocytotoxicity assays, two human isolates of EHEC O157:H7 belonging to the Phage Type 21/28 (PT21/28) cluster were also tested side by side with the bovine strains. Three types of growth media were used, the first was 10% bovine terminal rectal mucus (BTRM) which should provide the bacteria with nutrients similar to those found at its main colonisation site. The two other laboratory growth conditions were LB and LB supplemented with Mitomycin C (MMC) to induce the bacterial SOS response and lysis, therefore allowing induced levels of Shiga toxin to be assessed.

4.1 Shiga toxin levels detected by ELISA from different growth conditions

4.1.1 Bovine-isolated strains

Overall, the bovine terminal rectal mucus does not provide an environment in favour of Shiga toxin production as seen in Fig. 4.1a. In lysogeny broth (LB)-cultured bacteria, both of the wild type bovine-originating strains produced relatively more toxin than the phage-deleted derivatives (Fig. 4.1b). The difference between the wild type and the Stx-phage-mutant strains was more evident from the results of experiments where the strains were grown in LB, supplemented with Mitomycin C (Fig. 4.1c). An important finding was that the capacity of EHEC O157:H7 strain 9000 $\Delta\Phi\text{Stx}2a$ to produce toxin seemed equivalent to the parental strain. In line with this, EHEC O157:H7 strain 9000 $\Delta\Phi\text{Stx}2c$ failed to produce detectable levels of toxin despite possessing $\Phi\text{Stx}2a$. As anticipated the double Stx phage deletion of strain 9000 had no detectable Stx activity, indicating that all the activity was derived from the $\Phi\text{Stx}2c$. To reaffirm the lack in Stx production by EHEC O157:H7 Strain 9000 $\Delta\Phi\text{Stx}2c$, four clones of this strain were examined for Stx production with similar results, i.e. an absence of Stx production, for all growth conditions tested (Fig. 4.1a-c).

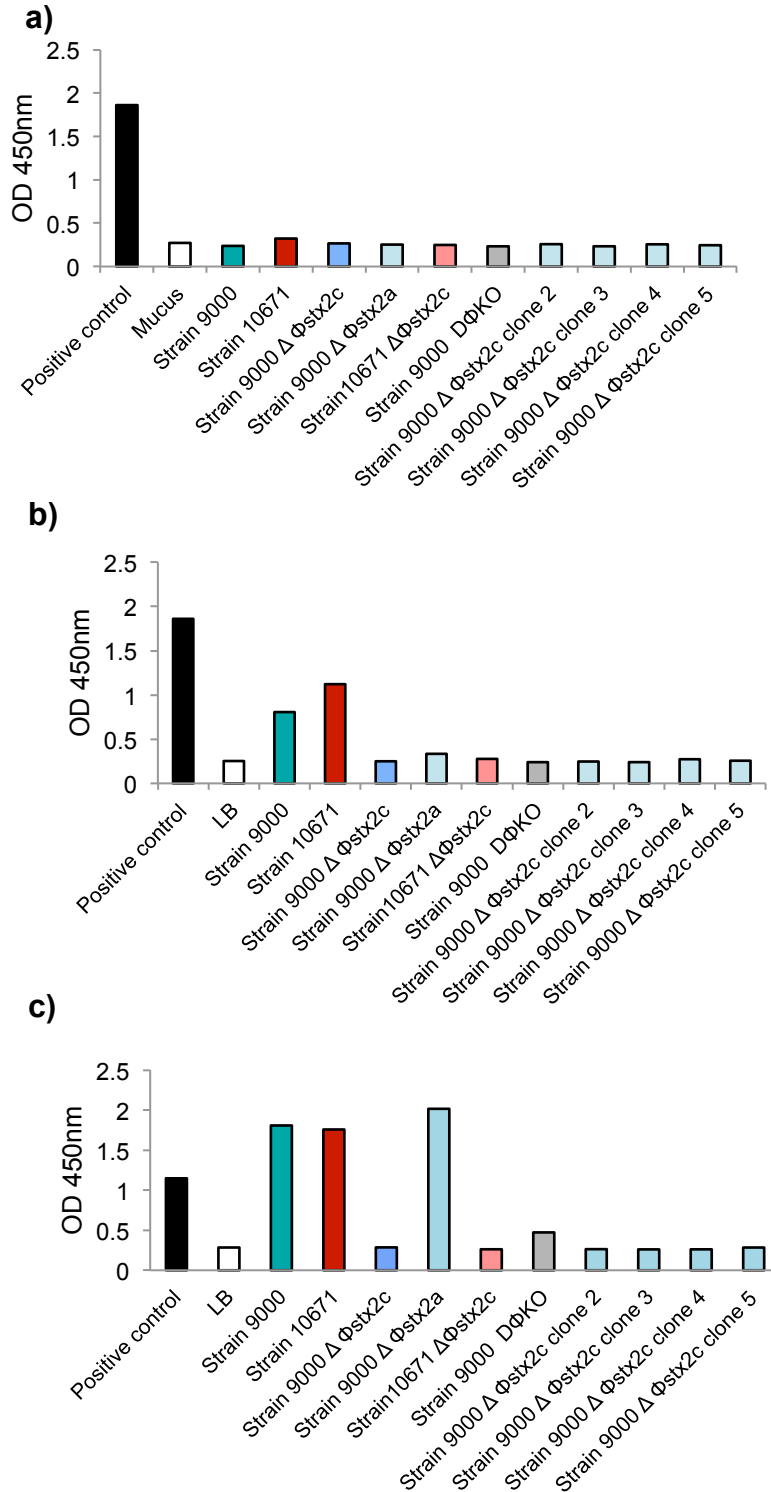


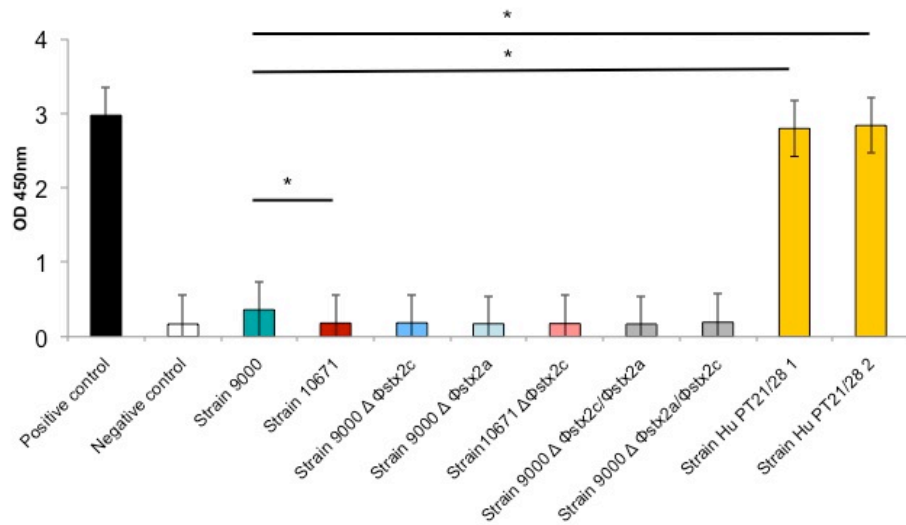
Figure 4.1 ELISA detection of Stx expressed by EHEC O157:H7 in different culture media (bovine-isolated strains). Bar plots represent the absorptive values at O.D. 450nm indicating the levels of Shiga toxin detected in the supernatants of bacterial cultures grown in (a) 10% bovine terminal rectal mucus, (b) LB and (c) LB with MMC (10 μ g/ml). The positive control (black) comprised of inactivated Stxs supplied by the manufacturer of the kit.

4.1.2 Comparison of Stx production between bovine and human-isolated strains

The bovine strains were also compared with two human isolates for production of Stx by ELISA; EHEC O157:H7 Strain number 122900512 (Human Strain 1, Phage Type 21/28) and EHEC O157:H7 Strain number 132020426 (Human Strain 2; Phage Type 21/28) (Fig. 4.2). Fig. 4.2a presents the results for the strains cultured in LB while Fig. 4.2b shows total Stx levels when bacterial strains were cultured in LB with Mitomycin C-induction (10 µg/ml). In both bar plots, the total Stx levels for the human strains were higher (6.5 fold) compared with the bovine EHEC O157:H7 Strain 9000 (belonging to the Phage Type 21/28 cluster). The induced levels for the bovine strains observed in Fig. 4.2b agree with the results from Fig. 4.1c.

One-way ANOVA of LB-cultured strains revealed that the level of total Stx present was statistically significant as a function of bacterial strain with $F(8, 9) = 52.56$, $p\text{-value} < 0.0001$. Post-hoc Sidak's multiple comparison tests identified statistically different levels of Stx between both bovine Strain 9000 and Strain 10671 with the two human isolates (all $p\text{-values} < 0.0001$). Similar analyses were carried out with datasets from the MMC-induced cultures revealing significant differences between the Stx levels of all bacterial strains tested ($F=36.20(8, 9)$, $p\text{-value} < 0.0001$). Multiple comparisons with Sidak's correction found that all strains compared were statistically significant when analysed pairwise ($p\text{-value} < 0.05$) except for comparisons between Strain 9000 and Strain 10671, and Strain 9000 with Strain 9000 $\Delta\Phi\text{Stx}2c$.

a)



b)

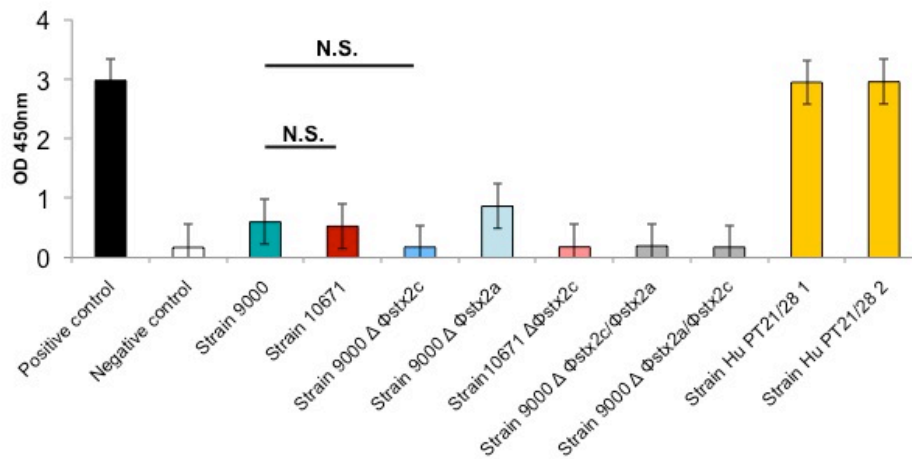


Figure 4.2 ELISA detection of Stx production by EHEC O157:H7 in different culture media (bovine-associated compared with human-isolated strains). Bar plots represent the absorptive values at O.D. 450nm indicating the levels of Shiga toxin detected in the supernatants of bacterial cultures grown in (a) LB and (b) LB with MMC (10 μ g/ml). Error bars indicate the standard error of the mean (S.E.M.) from two experiments. Data were analysed by One-way ANOVA followed by post-hoc multiple comparison (pairwise) with Sidak's correction ($p < 0.05$ *). The positive control (black) comprised of inactivated Stxs supplied by the manufacturer of the kit.

4.2 Verocytotoxicity assay

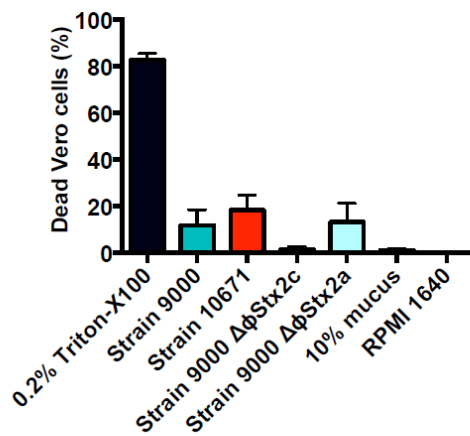
Besides testing bacterial culture supernatants for total Shiga toxin (Stx) by ELISA, the samples were also tested for their toxicity on Vero cells. The extra step of testing the capacity to kill Vero cells was based on previous findings in the laboratory for which it was demonstrated that ELISA is not as sensitive as this activity-based assay. This also provides an opportunity to compare the relative toxicity and Stx production levels among the strains. Vero cells have been routinely used to assess Stx toxicity and are known to be highly sensitive to Stx even at very low levels of the toxin, therefore providing further insight into Stx activity. Results obtained were initially captured in the form of absorption values at O.D. 595nm, based on cell viability and these values were then transformed into a percentage of killed Vero cells based on positive (0.2% Triton-X100) and negative (RPMI 1640 medium) control values.

4.2.1 EHEC O157:H7 strains grown in 10% bovine terminal rectal mucus

Following negative detection of total Stx by ELISA described earlier for cultures grown in 10% BTRM, the toxicity levels on Vero cells compiled from four independent experiments are shown in Fig. 4.3a for EHEC O157:H7 Strain 9000 and two of its single Stx-phage mutants, together with Strain 10671. Differences in the toxicity levels towards Vero cells among the strains tested were observed, with Strain 10671 killing the highest percentage (13.04%) of cells followed by Strain 9000 (6.18%) and Strain 9000 $\Delta\Phi$ Stx2a (5.68%). Strain 9000 $\Delta\Phi$ Stx2c (1.75%) was not toxic for the Vero cells, with values similar to that of the negative control (RPMI 1640 medium) (1.42%). These differences were not statistically significant when the means of different strains were compared by one-way ANOVA [$F(4, 15) = 2.027$, $p\text{-value} = 0.1421$], reflecting the variation between experiments. However, it must be noted that these different levels do agree with the ELISA data (Fig. 4.1a), with strain 10671 producing the highest levels of toxin.

Another Verocytotoxicity assay was carried out for the EHEC O157:H7 strains isolated from cattle, with the testing of four clones of the single Stx2c-phage mutant (Strain 9000 $\Delta\Phi$ Stx2c) to confirm the results obtained in Fig. 4.3a for which this strain did not kill Vero cells raising the possibility that there was no Stx in the mucus culture. The results, as shown in Fig. 4.3b, appeared similar to those observed in Fig. 4.3a. Interestingly, all clones of Strain 9000 $\Delta\Phi$ Stx2c (with the exception of clone 3) failed to induced toxicity on Vero cells beyond the negative control values. Clone 3 of Strain 9000 $\Delta\Phi$ Stx2c and Strain 10671 $\Delta\Phi$ Stx2c both had low percentages of Vero cell killing (8.93% and 8.40%, respectively). EHEC O157:H7 Strain 9000, Strain 10671 and Strain 9000 $\Delta\Phi$ Stx2a all had comparable Verocytotoxicity levels (34.18%, 39.78% and 43.73%, respectively). Statistical analysis was not performed on data in Fig. 4.3b since this experiment was not repeated.

a)



b)

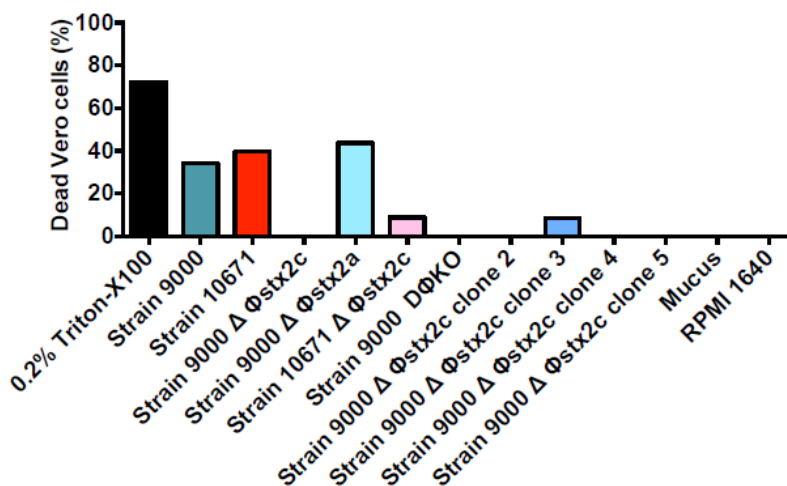


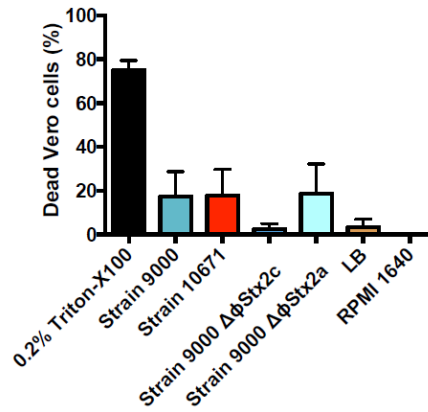
Figure 4.3 The toxicity of mucus-cultured EHEC O157:H7 filtered supernatants to Vero cells. (a) The mean (n=4) and standard error of the mean (S.E.M.) of total dead Vero cells (%) at the end of the 72 h incubation in filtered supernatants of EHEC O157:H7 (diluted 1:100 in RPMI 1640) at 37°C, 5% CO₂. (b) Dead Vero cells (%) of a single verotoxicity assay comparing bovine EHEC O157:H7 isolates with different combinations of isogenic stx phage mutants. All data presented were generated by transforming the absorptive values of the crystal violet staining (viable cells) at O.D. 595nm to percentages of dead cells, based on the positive (0.2% Triton-X100) and negative (RPMI 1640 medium) control values.

4.2.2 Toxicity assays for EHEC O157:H7 strains cultured in lysogeny broth (LB)

In order to compare Shiga toxin (Stx) production in 10% bovine terminal rectal mucus (BTRM) with laboratory growth media, Verocytotoxicity assay were performed with culture supernatants of bovine EHEC O157:H7 strains cultured in LB (37°C, with shaking). The bar plots shown in Fig. 4.4a was generated from results compiled from four independent repeats. Again, the toxicity levels of LB-cultured strains resemble the results obtained for EHEC O157:H7 strains grown in 10% BTRM (Fig. 4.3). One-way ANOVA analysis of the data, however failed to support any significant differences among the mean of all samples compared [$F(4, 15) = 0.7278$, $p\text{-value} = 0.5867$].

The toxicity levels of LB-grown culture supernatants from EHEC O157:H7 bovine strains to Vero cells were tested again as in Fig. 4.4b, with the addition of four clones of EHEC O157:H7 Strain 9000 $\Delta\Phi$ Stx2c. It is apparent that all clones of Strain 9000 $\Delta\Phi$ Stx2c failed to kill the Vero cells with results comparable to that of the Stx-phage negative strains (Strain 9000 $\Delta\Phi$ Stx2a/ Φ Stx2c and Strain 10671 $\Delta\Phi$ Stx2c). Strain 9000, Strain 10671 and Strain 9000 $\Delta\Phi$ Stx2a were all highly toxic to the Vero cells tested. No statistical test was used to analyse this particular dataset since it only contained results from one experiment.

a)



b)

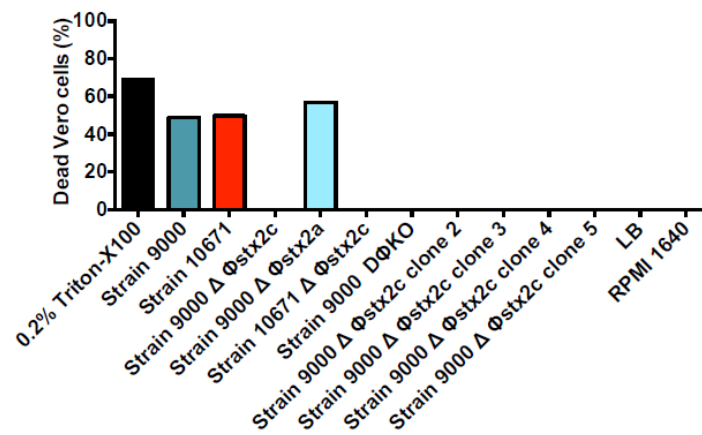


Figure 4.4 The toxicity of LB-cultured EHEC O157:H7 filtered supernatants to Vero cells. (a) The mean (n=4) and standard error of the mean (S.E.M.) of total dead Vero cells (%) at the end of the 72 h incubation in filtered supernatants of EHEC O157:H7 (diluted 1:100 in RPMI 1640) at 37°C, 5% CO₂. (b) Dead Vero cells (%) of a single verotoxicity assay comparing bovine EHEC O157:H7 isolates with different combinations of isogenic stx phage mutants. All data presented were generated by transforming the absorptive values of the crystal violet staining (viable cells) at O.D. 595nm to percentages of dead cells, based on the positive (0.2% Triton-X100) and negative (RPMI 1640 medium) control values.

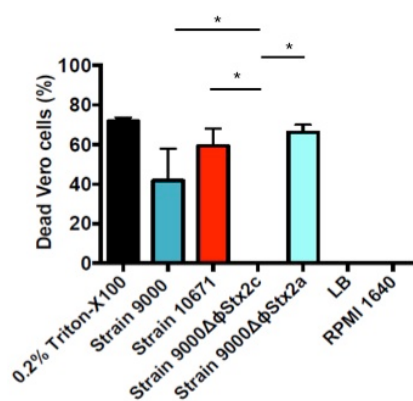
4.2.3 Toxicity of EHEC O157:H7 strains cultured in lysogeny broth (LB) supplemented with Mitomycin C (MMC)

To further assess the maximal capacity for the bovine EHEC O157:H7 strains to produce Shiga toxin, Verocytotoxicity assays were carried out. The bacterial strains were grown overnight in LB, diluted and then supplemented with Mitomycin C to induce DNA damage along with the SOS response in bacterial cells that later leads to a generation and release of Shiga toxins and phage particles.

Fig. 4.5a provides results generated from three independent experiments involving cultures of EHEC O157:H7 Strain 9000, Strain 10671 and the two single Stx-phage isogenic mutants of Strain 9000. Analysis of variance showed that the cytotoxicity effect on Vero cells was dependent on which bacterial strain produces the culture supernatant incubated with the Vero cells, [F(4,10)=14.46, p-value=0.0004]. Post-hoc Tukey's test (p-value 0.05) showed that the toxicity of Strain 9000, Strain 10671 and Strain 9000 $\Delta \Phi$ Stx2c were significantly higher than Strain 9000 $\Delta \Phi$ Stx2c. Strain 9000 $\Delta \Phi$ Stx2a induced the highest toxicity among all strains compared, however statistical analysis did not reveal significant results when compared against Strain 9000 and Strain 10671.

Another Verocytotoxicity assay was carried out with MMC-induced bovine strains, with the addition of four clones of Strain 9000 $\Delta \Phi$ Stx2c (Fig. 4.5b). In this particular experiment, all of the strains with at least one Stx-phage produced very high levels of Shiga toxin, with the exception of all clones of Strain 9000 $\Delta \Phi$ Stx2c. With growth conditions optimised to generate high levels of Stx, the failure to produce toxicity in Vero cells receiving the filtered lysate preparation from Strain 9000 $\Delta \Phi$ Stx2c strongly suggest for the absence of Stx2a production despite the strain possessing a Stx2a-encoding phage in its chromosome.

a)



b)

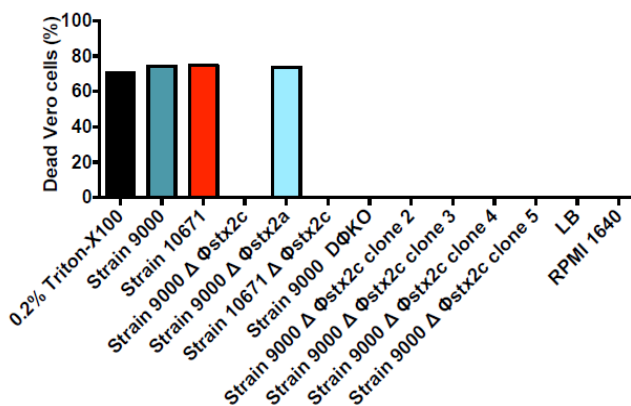


Figure 4.5 The toxicity of MMC-induced LB-cultured EHEC O157:H7 filtered supernatants to Vero cells. (a) The mean (n=4) and standard error of the mean (S.E.M.) of total dead Vero cells (%) at the end of the 72 h incubation in filtered supernatants of EHEC O157:H7 (diluted 1:100 in RPMI 1640) at 37°C, 5% CO₂. (b) Dead Vero cells (%) of a single verotoxicity assay comparing bovine EHEC O157:H7 isolates with different combinations of isogenic stx phage mutants. All data presented were generated by transforming the absorptive values of the crystal violet staining (viable cells) at O.D. 595nm to percentages of dead cells, based on the positive (0.2% Triton-X100) and negative (RPMI 1640 medium) control values.

4.2.4 Verocytotoxicity levels of bovine and human strains of EHEC O157:H7 in lysogeny broth (LB) under non-induced and induced culture conditions

Apart from making comparisons of Shiga toxin production and activity among bovine-originated EHEC O157:H7 strains, Verocytotoxicity levels were also tested for two human isolates of EHEC O157:H7 belonging to the Phage Type 21/28 cluster. All strains were cultured overnight in LB broth with or without Mitomycin C (MMC) induction, before being filtered and added to the Vero cells.

The toxicity level towards Vero cells for EHEC O157:H7 strains grown in LB are as presented in Fig. 4.6a. It is clear that the two human-origin strains were highly toxic to the Vero cells, at levels by comparison to the bovine strains. The mean (n=2) percentage of dead Vero cells for Human PT21/28 (122900512) was 28.47% (S.E. =2.8), Human PT21/28 (132020426) was 17.85% (S.E. =8.6), while bovine Strain 9000 was 0.41% (S.E. =0.41) and the rest of the bovine strains compared did not kill the Vero cells tested. One-way ANOVA of the datasets of Vero cells receiving non-induced cultures (Fig. 4.6a) showed that the toxicity levels on Vero cells were significantly different depending on the strain supernatant used $F(8, 9) = 12.07$ (p-value < 0.001). Holm-Sidak's multiple comparison tests identified significant mean differences when the human isolates were compared to both of the bovine wild-type strains (p-value < 0.05).

Following MMC-induction, the filtered lysates for all strains carrying at least one Stx2-phage were able to kill at least 20% of the Vero cells (Fig. 4.6b). The highest average (n=2) in Vero cell killing was recorded for both of the human isolates, Strain 122900512 (mean=78.8%, S.E. =3.0) and Strain 132020426 (mean=78.7%, S.E. =1.5). EHEC O157:H7 Strain 9000 $\Delta\Phi$ Stx2a killed 62.3% (S.E. =1.9) of the Vero cells receiving its filtered lysate, while the lysate from another isogenic of Strain 9000, the single Stx2c-phage mutant were not toxic. The rest of the strains not possessing any Stx2a or Stx2c-phage were only able to kill less than 7% of Vero cells in the 72-hour treatment. Analysis of the variance for dataset of

induced-cultures (Fig. 4.6b) resulted in highly significant differences among the toxicity levels of all strains compared, $F(8,9)=88.53$ (p-value <0.0001). Post-hoc Holm-Sidak's test strongly suggest significant differences (p-value <0.005) for both of the human isolates than the rest of the strains. Moreover, Strain 9000 $\Delta\Phi$ Stx2a had significantly higher toxic levels than Strain 9000 and Strain 10671 (p-value <0.05). Lysates of strain 10671 were significantly higher than Strain 9000, while Strain 9000 induced significantly higher toxicity than Strain 9000 $\Delta\Phi$ Stx2c and two of its Stx-phage free isogenic strains (p-value <0.05).

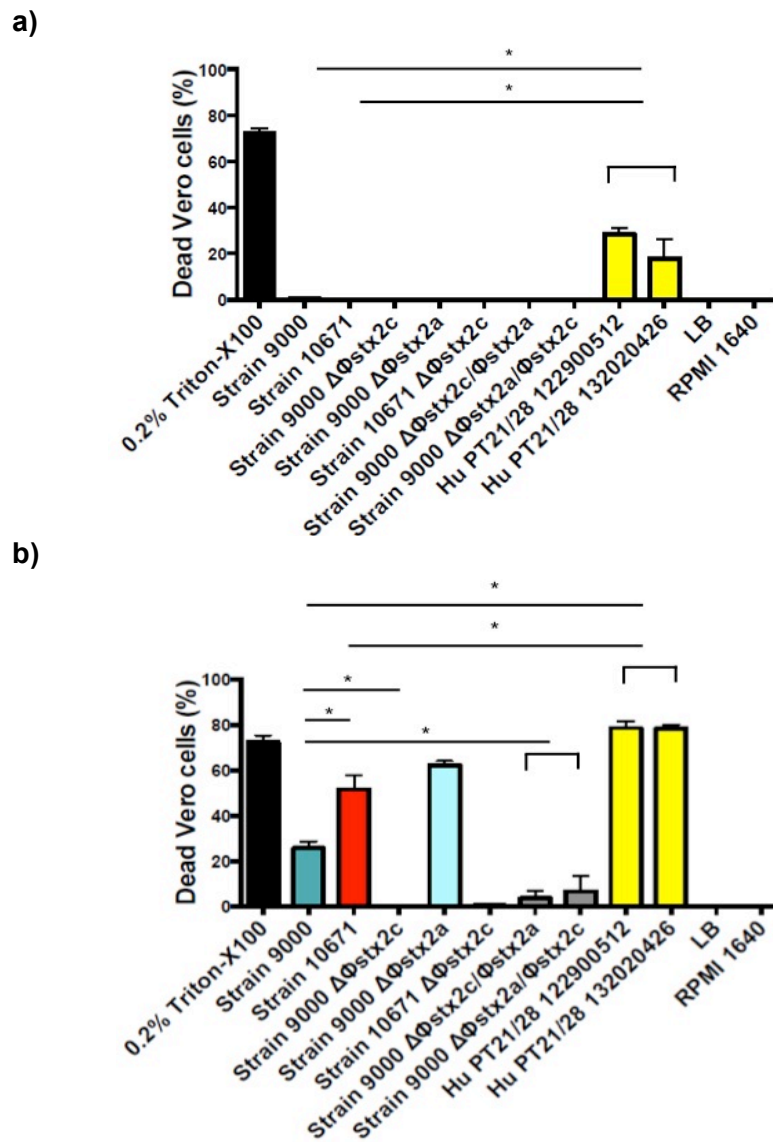


Figure 4.6 Comparison of the toxicity of bovine and human isolated EHEC O157:H7 strains to Vero cells. The mean of the percentage of dead Vero cells at the end of the 72 h incubation in filtered supernatants of (a) LB-cultured and (b) MMC-induced LB culture of EHEC O157:H7 (diluted 1:100 in RPMI 1640 medium) at 37°C, CO₂. The data presented were generated by transforming the absorptive values of the crystal violet staining (viable cells) at O.D. 595nm to percentages of dead cells, based on the positive (0.2% Triton-X100) and negative (RPMI 1640 medium) control values. Error bars indicate the S.E.M. (n=2).

4.3 Growth Competition Assay

4.3.1 Pairwise comparison of *E. coli* strains in 10% bovine terminal rectal mucus (BTRM)

The aim of this series of experiments was to determine if the presence or absence of Stx2-encoding bacteriophages resulted in competitive advantage or disadvantage under the culture conditions used.

4.3.1.1 *E. coli* MG1655NK and *E. coli* K-12-Sp5 *stx2A::kan* (K-12-Sp5)

After 192 h of co-culture, the K-12-Sp5 strain (despite possessing Sp5 phage, this strain is unable to produce Stx as the *stx* genes were removed and replaced with kanamycin resistance cassette) were able to outgrow the Stx phage-susceptible MG1655NK strain (Fig. 4.7, Table 4.1). This was an interesting outcome since the number of K-12-Sp5 cells recorded dropped progressively between 24 to 72 h of the competition. This was then followed by a sudden surge in the K-12-Sp5 population at 96 h co-culture. When the colonies from the selective plate were competed again (120 h- 192 h) the growth advantage was again clearly observed for the K-12 strain containing the Stx2 prophage, Sp5 (K-12-Sp5).

4.3.1.2 *E. coli* MG1655NK and *E. coli* K-12-Sp5 *stx2A::kan ΔlacZ* (K-12-Sp5)

Following the results obtained from competing the MG1655NK and K-12-Sp5 pair, the next step was to see if the rise in the strain possessing Sp5 was due to an increase in the susceptible MG1655NK strain lysogenized with the Sp5 phage. Bacterial co-culture of *E. coli* MG1655NK and K-12-Sp5 was significantly dominated by Sp5-positive cells at all time points following the first 24 h of incubation (Fig. 4.8). All colonies growing on the kanamycin plate (Sp5+) were then tracked for the ability to ferment lactose, with the proportion of lactose-fermenting, kanamycin resistant strains identified as the Sp5-lysogenised MG1655 (MG1655NK-Sp5) cells. However, as presented in Fig. 4.8 and Table 4.2, the results seems to be against this hypothesis. There was no evidence to support lysogenisation of the

susceptible strain as the main reason for the increase in the Sp5 positive colonies observed.

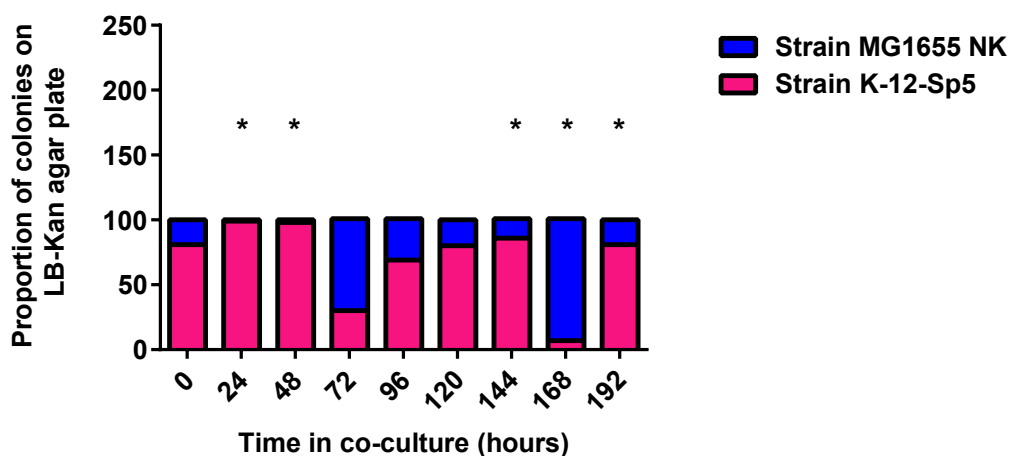


Figure 4.7 Competitive growth assay between *E. coli* MG1655NK and *E. coli* K-12-Sp5 in 10% bovine terminal rectal mucus (BTRM). At every 24-hour time points, co-cultures were serially diluted and spread on LB-Naladixic acid supplemented agar. After overnight incubation, one hundred single colonies were chosen to be placed on LB-Kanamycin agar to select for *E. coli* K-12-Sp5 (pink). The absence of growth was recorded as *E. coli* MG1655NK (blue). Asterisk marks are used for time points with significant differences (Table 4.1) between the strains with respect to the proportion of colonies present in the co-culture.

Time (h)	p-value	MG1655 NK	K-12-Sp5	t ratio	df
0	0.003	19	81	3.40	18
24	< 0.0001*	1	99	5.38	18
48	< 0.0001*	2	98	5.27	18
72	0.037*	71	30	2.25	18
96	0.057	32	69	2.03	18
120	0.004	20	80	3.30	18
144	0.001*	15	86	3.90	18
168	0.0001*	94	7	4.78	18
192	0.003*	19	81	3.40	18

Table 4.1 Statistical analysis of data from competitive growth assay between *E. coli* MG1655NK and *E. coli* K-12-Sp5 in 10% BTRM. Data from two independent experiments were analysed at each time point by multiple t-tests with assumption that all rows of data were sampled from populations of same scatter. Statistical significance was corrected for multiple comparisons using the Holm-Sidak method with alpha value set at 0.05.

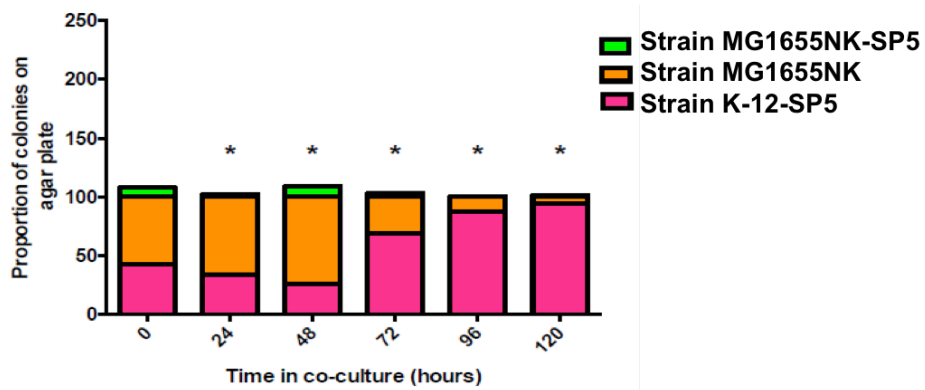


Figure 4.8 Competitive growth assay between *E. coli* MG1655NK and *E. coli* K-12-Sp5 *stx2A::kan ΔlacZ* (*E. coli* K-12-Sp5) in 10% BTRM. At every 24-hour time points, co-cultures were serially diluted and spread on LB-Naladixic acid supplemented agar. After overnight incubation, one hundred single colonies were chosen to be placed on LB-Kanamycin agar plate to select for *E. coli* K-12-Sp5 (pink) with absence of growth recorded as *E. coli* MG1655NK (orange). Simultaneously, single colonies were also placed onto 1% lactose-MacConkey agar to detect any susceptible *E. coli* MG1655NK lysogenized with the Sp5 phage (MG 1655NK-Sp5, green). Asterisks are used to indicate time points with significant differences (Table 4.2) between the *E. coli* MG1655NK (orange) and *E. coli* K-12-Sp5 (pink) strains present in the co-culture.

Time (h)	p-value	MG1655NK	K-12-Sp5	t ratio	df
0	0.112	43	57	1.71	12
24	0.002*	34	67	4.04	12
48	< 0.0001*	26	74	5.88	12
72	< 0.0001*	70	31	4.78	12
96	< 0.0001*	88	13	9.19	12
120	< 0.0001*	95	6	10.90	12

Table 4.2 Statistical analysis of data from competitive growth assay between *E. coli* MG1655NK and *E. coli* K-12-Sp5 in 10% BTRM. Data were analysed at each time point by multiple t-tests with assumption that all rows of data were sampled from populations of same scatter. Statistical significance was corrected for multiple comparisons using the Holm-Sidak method with alpha value set at 0.05.

4.3.1.3 EHEC O157:H7 Sakai *stx2A::kan* and EHEC O157:H7 Sakai Δ Sp5

To further assess if the Stx-phage confers growth advantage to a strain, another growth assay in 10% BTRM was carried out by competing EHEC O157:H7 Strain Sakai *stx2A::kan* which possesses a Stx2a prophage, Sp5, with its isogenic Sp5 mutant Sakai strain. In contrast to the K-12 strains competed earlier, the Sakai *stx2A::kan* and Sakai Δ Sp5 co-culture seemed to be able to maintain an almost 'equal' proportion throughout the entire competition (Fig. 4.9), with the exception at time points 48, 96 and 168 h of co-culture. At these time points, it was determined that the mean differences between the two strains competed were statistically significant (Sakai Sp5 mutant dominating the co-culture), however the extent was not as pronounced as that observed for the K-12 co-culture (Table 4.3).

4.3.1.4 EHEC O157:H7 Strain 9000 and EHEC O157:H7 Strain 10671

Having observed the competition growth assay results for laboratory strain *E. coli* (K-12) and a human outbreak strain (Sakai), this section will present the data obtained from competing pairs of bovine-isolated EHEC O157:H7 strains to compare the behaviour of different strains when co-cultured in 10% BTRM. The first pair to be compared was the IPRAVE EHEC O157:H7 Strain 9000 possessing dual Stx2a/Stx2c-phages and IPRAVE EHEC O157:H7 Strain 10671 with only one Stx-phage, Stx2c. Data compiled from six repeats of this competition experiment showed that having dual Stx2-phage combination in a strain does not seem to provide any growth advantage or make the strain fitter than a strain carrying only one Stx2-phage (Fig. 4.10). If anything the strain might be at a slight disadvantage. Although there were statistically different proportions between the two strains (time points 24 and 96 h), the ratio of the two populations within the culture were around 1:1 (Table 4.4). The results observed is similar to what was observed for the Sakai strains where there was fluctuations in the proportion, each strains was able to compete at a similar rate resulting in a stable alternating fluctuations and that both strains were able to maintain their proportions at a similar rate.

4.3.1.5 EHEC O157:H7 Strain 9000 and EHEC O157:H7 Strain 9000 $\Delta\Phi$ Stx2a/ Φ Stx2c

Since co-culturing both bovine isolates (Strain 9000 and Strain 10671) demonstrated no growth advantages for Strain 9000 despite carrying an extra Stx2a phage gene in its chromosome, the next step was to compete isogenic strains in order to obtain a more appropriate and valid comparison. EHEC O157:H7 Strain 9000 and its isogenic double Stx2a/Stx2c prophage knockout strain were co-cultured for 96 h in 10% BTRM (Fig. 4.11 and Table 4.5). The 'wild-type' Strain 9000 did not have an advantage or disadvantage over its isogenic mutant, despite the absence of Stx2a/Stx2c-phages in the latter strain. Although it should be noted that Strain 9000 did have a statistically higher number of colonies at 96 h of co-culture; this was not maintained or increased when sampled at the subsequent time points (Table 4.5).

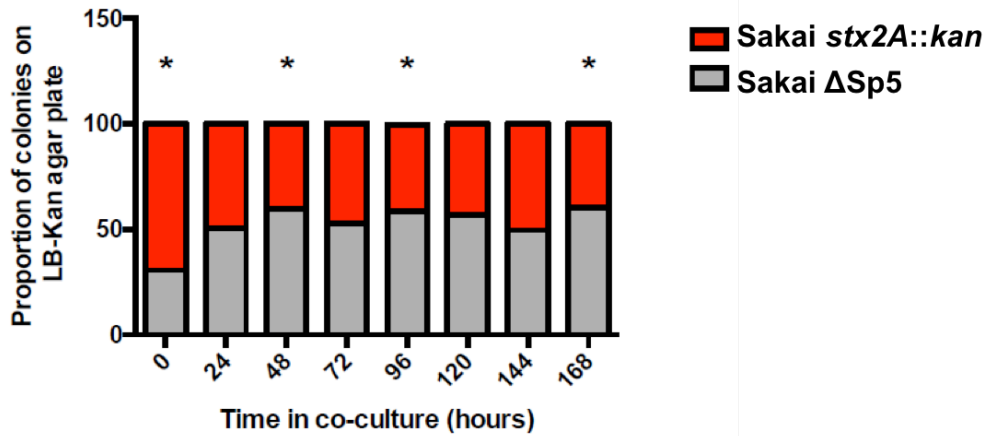


Figure 4.9 Competitive growth assay between EHEC O157:H7 Sakai *stx2A::kan* and Sakai Δ Sp5 in 10% BTRM. At every 24-hour time points, co-cultures were serially diluted and spread on CT-SMAC agar. After overnight incubation, one hundred single colonies were chosen to be placed on LB-Kanamycin agar plate to select for EHEC O157:H7 Sakai *stx2A::kan* (red). The absence of growth was recorded as EHEC O157:H7 Sakai Δ Sp5 (grey). Asterisk marks are used for time point with significant differences (Table 4.3) between both strains.

Time (h)	p-value	Sakai <i>stx2A::kan</i>	Sakai Δ Sp5	t ratio	df
0	< 0.0001*	70	31	7.00	16
24	0.860	50	51	0.18	16
48	0.004*	41	60	3.41	16
72	0.383	48	53	0.90	16
96	0.006*	41	59	3.14	16
120	0.033	44	57	2.33	16
144	0.860	51	50	0.18	16
168	0.002*	40	60	3.59	16

Table 4.3 Statistical analysis of data from competitive growth assay between EHEC O157:H7 Sakai *stx2A::kan* and Sakai Δ Sp5 in 10% BTRM. Data from two independent experiments were analysed at each time point by multiple t-tests with assumption that all rows of data were sampled from populations of same scatter were met. Statistical significance was corrected for multiple comparisons using the Holm-Sidak method with alpha value set at 0.05.

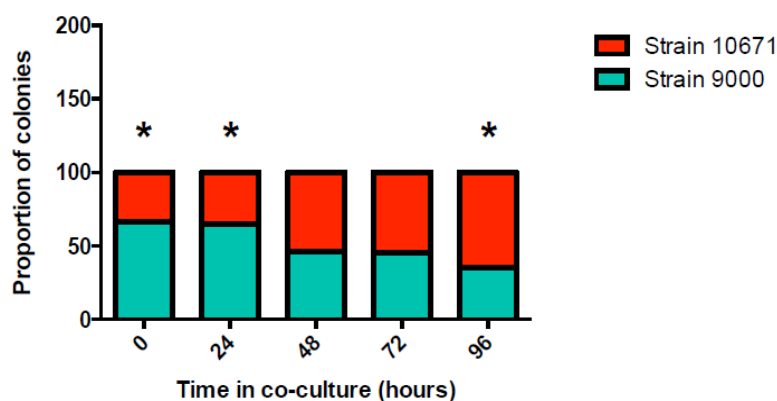


Figure 4.10 Competitive growth assay between EHEC O157:H7 Strain 9000 and EHEC O157:H7 Strain 10671 in 10% BTRM. At every 24-hour time points, co-cultures were serially diluted before plating on CT-SMAC agar. After overnight incubation, one hundred single colonies were chosen to be placed on LB-Naladixic acid supplemented agar to select for EHEC O157:H7 Strain 9000 NaIR. The absence of growth was recorded as EHEC O157:H7 Strain 10671. The experiment was repeated again using EHEC O157:H7 Strain 10671NaIR and EHEC O157:H7 Strain 9000. Asterisk marks for time point with significant differences (Table 4.4) between both strains in the proportion of single colonies present in the co-culture.

Time (h)	p-value	Strain 9000	Strain 10671	t ratio	df
0	0.000*	67	33	4.04	50
24	0.001*	65	35	3.68	50
48	0.357	46	54	0.93	50
72	0.263	45	55	1.13	50
96	0.001*	35	65	3.56	50

Table 4.4 Statistical analysis of data from competitive growth assay between EHEC O157:H7 Strain 9000 and EHEC O157:H7 Strain 10671 in 10% BTRM. Data from the six experiments were analysed at each time point by multiple t-tests with assumption that all rows of data were sampled from populations of same scatter. Statistical significance was corrected for multiple comparisons using the Holm-Sidak method with alpha value set at 0.05.

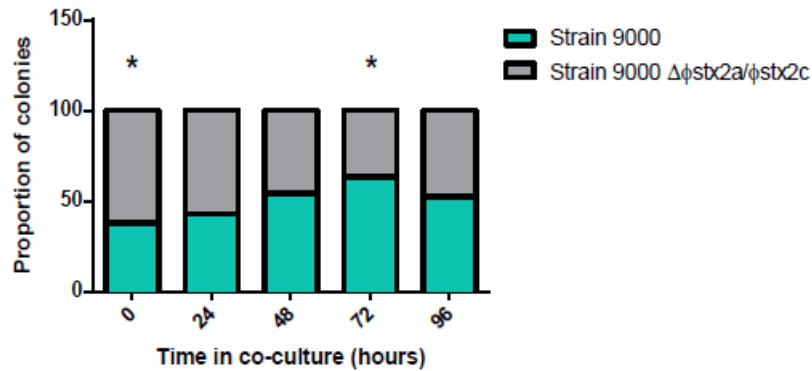


Figure 4.11 Competitive growth assay between EHEC O157:H7 Strain 9000 and EHEC O157:H7 Strain 9000ΔϕStx2a/ϕStx2c in 10% BTRM. At every 24-hour time points, co-cultures were serially diluted before plating on CT-SMAC agar. After overnight incubation, one hundred single colonies were chosen to be placed on LB-Naladixic acid supplemented agar to select for EHEC O157:H7 Strain 9000NaIR. The absence of growth was recorded as EHEC O157:H7 Strain 9000ΔϕStx2a/ϕStx2c. Asterisk marks for time point with significant differences (Table 4.5) between both strains in the proportion of single colonies present in the co-culture.

Time (h)	p-value	Strain 9000	Strain 9000ΔϕStx2a/Stx2c	t ratio	df
0	0.001*	38	62	3.72	20
24	0.039	43	57	2.21	20
48	0.206	54	46	1.31	20
72	0.001*	63	37	3.92	20
96	0.490	52	48	0.70	20

Table 4.5 Statistical analysis of data from competitive growth assay between EHEC O157:H7 Strain 9000 and EHEC O157:H7 Strain 9000ΔϕStx2a/ϕStx2c in 10% BTRM. Data from three experiments were analysed at each time point by multiple t-tests with assumption that all rows of data were sampled from populations of same scatter. Statistical significance was corrected for multiple comparisons using the Holm-Sidak method with alpha value set at 0.05.

4.4 Bacterial adherence to epithelial cells

4.4.1 Bovine EHEC O157:H7 strains binding to HeLa cells

Another bacterial phenotype closely associated with colonisation assessed among the bovine O157:H7 strains was binding to epithelial cells. The objective was to compare the binding capacity of each bovine-isolated strain (Strain 9000 and Strain 10671) with their Stx-phage-free isogenic strains. The first cell line used was HeLa cells, proven to express Gb3 on its surface. 10% BTRM was used as the growth and incubation media for bacterial culture and cell infection. Fig. 4.12 presents the results from three independent experiments showing the percentages of bacterial cells binding to HeLa cells, normalised to the number of total bacteria added. The percentages of total number of bound bacteria per total bacteria added were log-transformed and each isogenic pairs were analysed with an unpaired t-test using Welch's correction without assuming similar standard deviations, with alpha set at 0.05. The HeLa cell binding percentages between Strain 9000 (0.13%) and its isogenic strain (0.58%) was not statistically different [$t(2.5)=1.52$, $p\text{-value}=0.243$]. Similarly there was no significant difference detected between the binding rate of Strain 10671 (0.09%) and its isogenic strain (0.69%).

4.4.2 Bovine EHEC O157:H7 strains binding to EBL cells

Bacterial binding capacity to a Gb3 negative cell line, EBLs, was also assessed under similar experimental conditions as for HeLa cells. The percentage of total cell bound bacteria over total bacterial cell added were log-transformed before analysis with an unpaired t-test using Welch's correction without assuming similar standard deviations, $\alpha=0.05$. There was no difference in the adherence capacities between the wild type strains and the stx-phage negative strains. Statistical analysis for the adherence rate between Strain 9000 (0.84%) and Strain 9000 $\Delta\Phi\text{Stx2a}/\Phi\text{Stx2c}$ (6.41%) revealed no significant difference [$t(2.4)=2.7$, $p\text{-value}=0.09$]. Strain 10671 (1.3%) and its isogenic Stx2c-phage-negative strain (5.92%) also did not differ in their binding rate [$t(2.2)=1.3$, $p\text{-value}=0.310$] to the EBL cells.

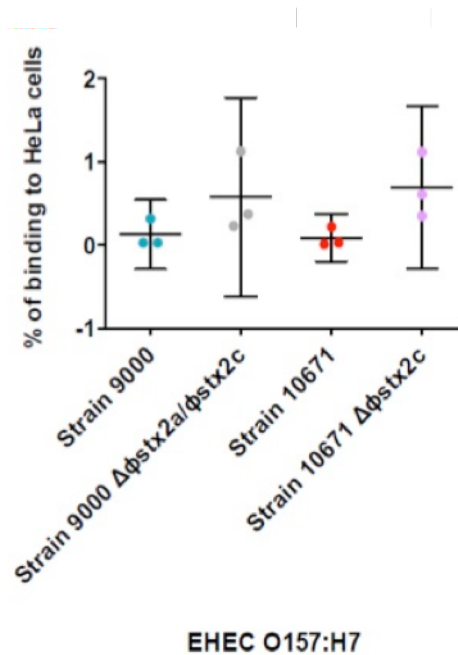


Figure 4.12 EHEC O157:H7 adherence to HeLa cells. Individual dot plot represents the percentage of bacteria bound to HeLa cells over total bacteria added after thirty minutes of incubation at 37°C, 5% CO₂, obtained from three independent experiments. Data were analysed by unpaired two-tailed t-test (with Welch's correction) applied between EHEC O157:H7 Strain 9000 and EHEC O157:H7 Strain 9000 $\Delta\phi\text{Stx2a}/\phi\text{Stx2c}$; and EHEC O157:H7 Strain 10671 and EHEC O157:H7 Strain 10671 $\Delta\phi\text{Stx2c}$, at alpha=0.05. Error bars represents the 95% confidence interval across values per strain.

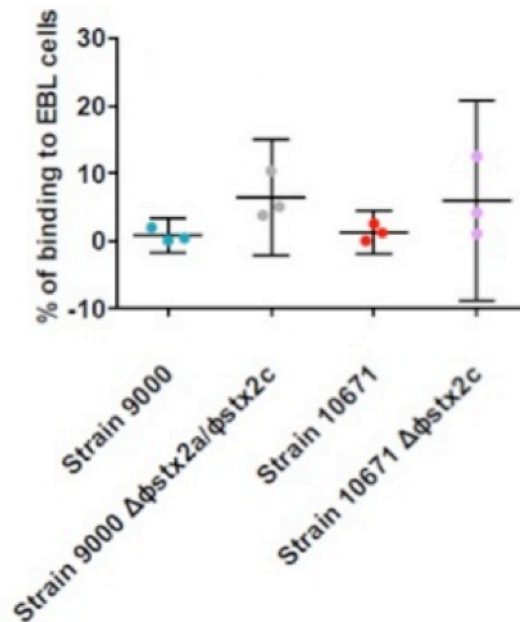


Figure 4.13 EHEC O157:H7 adherence to Embryonic Bovine Lung cells. Individual dot plot represents the percentage of bacteria bound to EBL cells over total bacteria added after thirty minutes of incubation at 37°C, 5% CO₂, obtained from three independent experiments. Data were analysed by unpaired two-tailed t-test (with Welch's correction) applied between EHEC O157:H7 Strain 9000 and EHEC O157:H7 Strain 9000 $\Delta\Phi\text{Stx2a}/\Phi\text{Stx2c}$; and EHEC O157:H7 Strain 10671 and EHEC O157:H7 Strain 10671 $\Delta\Phi\text{Stx2c}$, at alpha=0.05. Error bars represents the 95% confidence interval across values per strain.

4.5 Expression of H7 and EspA (Type Three Secretion) in 10% bovine terminal rectal mucus (BTRM)

Having identified evidence of increased adherence capacity in the Stx-phage free isogenic strains of Strain 9000 and Strain 10671, the next step was to see if the difference was due to differential expression of early attaching factors including flagella and the type three secretion system (T3SS) upon removal of the Stx-phages from the bovine isolates. The strains were grown under similar conditions as for bacterial adherence assay in 10% BTRM and were then processed for immunofluorescence staining to detect for bacterial cell (O157), flagella (H7) or EspA (T3SS). The fluorescence microscopy images in Fig. 4.14 show the mucus-cultured bacterial strains (O157-red) co-stained with H7 (green) antibody, while Fig. 4.15 presents the images for bacterial cells (O157-red) co-stained with anti-EspA (green). There seemed to be an increase in H7 signals in Fig. 4.14 for the stx-phage mutant EHEC O157:H7 strains compared to the isogenic wild type strains. Visual comparison of EspA expression by EHEC O157:H7 strains (Fig. 4.15) indicated more signals of EspA in Stx2c phage mutants of both wild type EHEC O157:H7 strains. However, the presence of fixed mucus on most of the slides examined hindered further conclusion from these results. Therefore, expression of H7 and the T3SS were analysed by Western blotting for all bacterial strains, cultured under the same conditions as for binding assay.

As seen in Fig. 4.16, similar levels of H7 were expressed by all strains regardless of the Stx2-encoding bacteriophage status, while EspD could not be detected. EspD was used rather than EspA since the antibody against EspD was shown to be better for immunoblot detection and gives a better signal than anti-EspA. This indicated that in the mucus the bacteria were generally expressing flagella but not the T3SS. The next step was culturing the bacterial strains under conditions previously shown to promote expression of T3SS proteins [257] and compare the levels of EspD. EHEC O157:H7 Strain 9000 and Strain 10671 were both able to express EspD under T3SS conditions at similar levels, however no EspD could be detected for the isogenic Stx-phage mutant strains (Fig. 4.17).

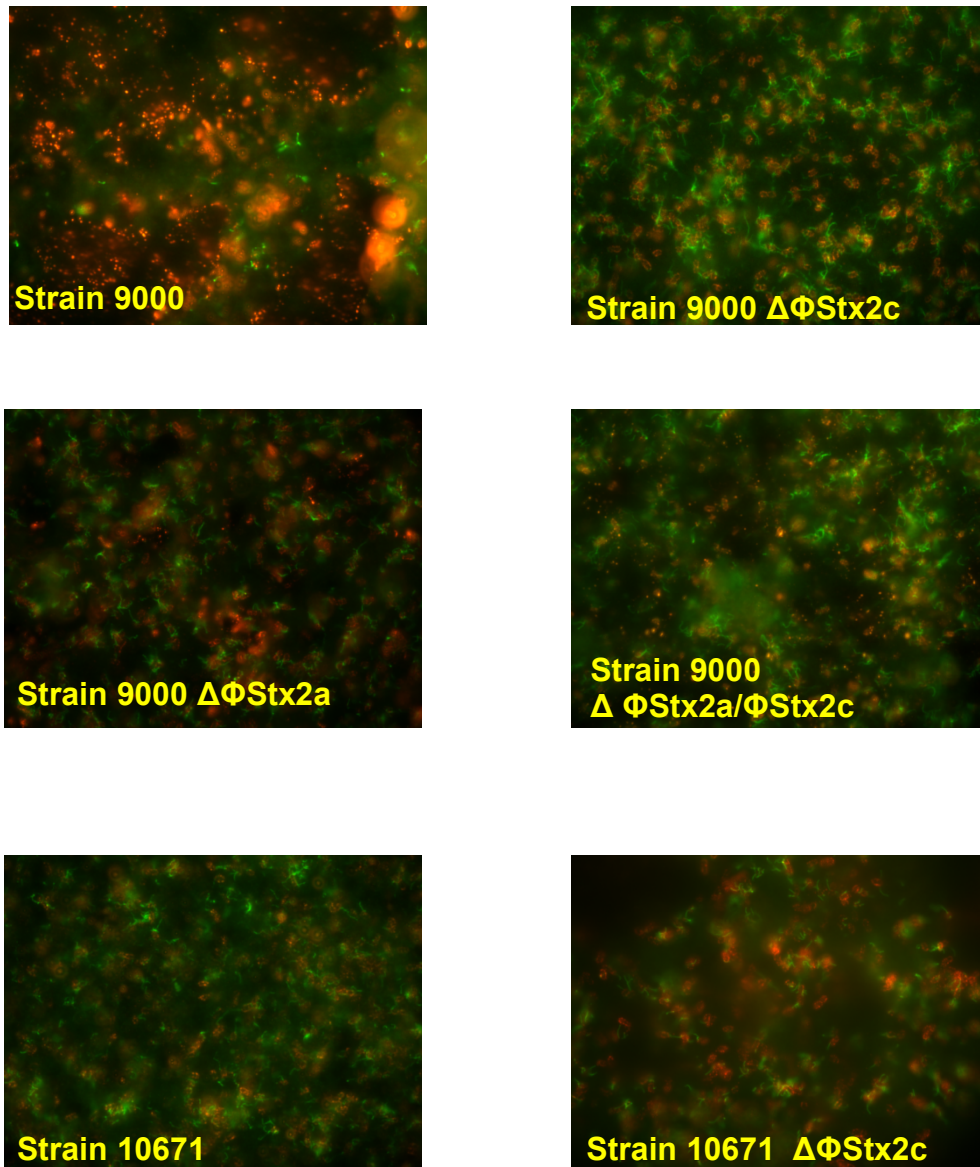


Figure 4.14 H7 expression in mucus-cultured bovine strains of EHEC O157:H7 examined by fluorescence microscopy. EHEC O157:H7 strains were grown in 10% bovine terminal rectal mucus under similar conditions as described for bacterial adherence assay. The mucus culture were then fixed in 4% PFA before immuno-staining procedure performed by Dr. Amin Tahoun. Bacterial cells were labelled with anti-O157-Alexa Fluor® 568 (red) and flagella (H7) with anti-H7-FITC (green). The images were taken with Leica DMLB fluorescence microscope with the help of Dr. Tahoun, before processed and analysed with Image J (U.S. National Institute of Health, Maryland).

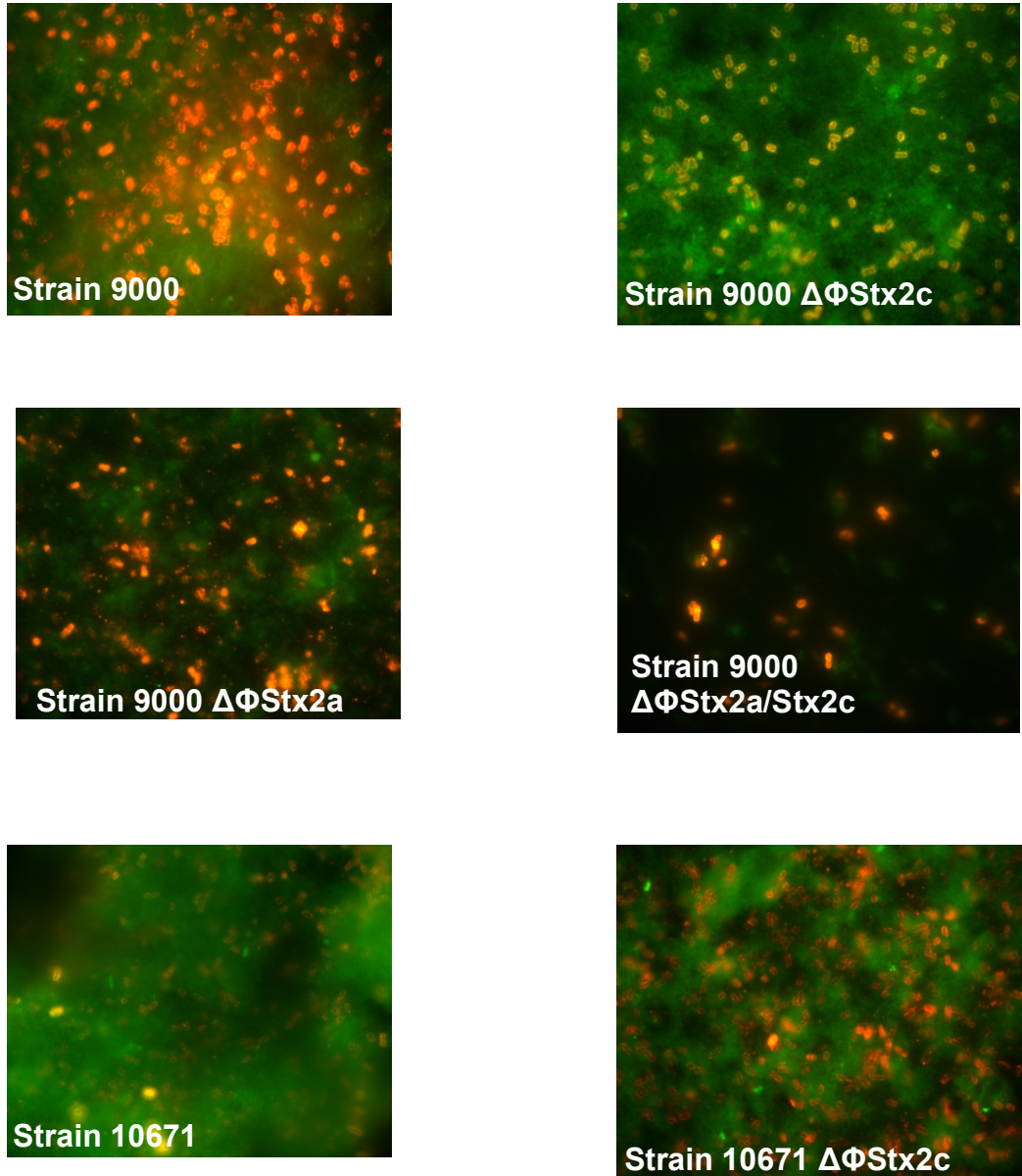


Figure 4.15 EspA expression in mucus-cultured bovine strains of EHEC O157:H7 examined by fluorescence microscopy. EHEC O157:H7 strains were grown in 10% bovine terminal rectal mucus under similar conditions as described for bacterial adherence assay. Bacterial cells were labelled with anti-O157-Alexa Fluor® 568 (red) and anti-EspA-FITC (green). The mucus culture were then fixed in 4% PFA before immuno-staining procedure performed by Dr. Amin Tahoun. The images were taken with Leica DMLB fluorescence microscope with the help of Dr. Tahoun, before processed and analysed with Image J (U.S. National Institute of Health, Maryland).

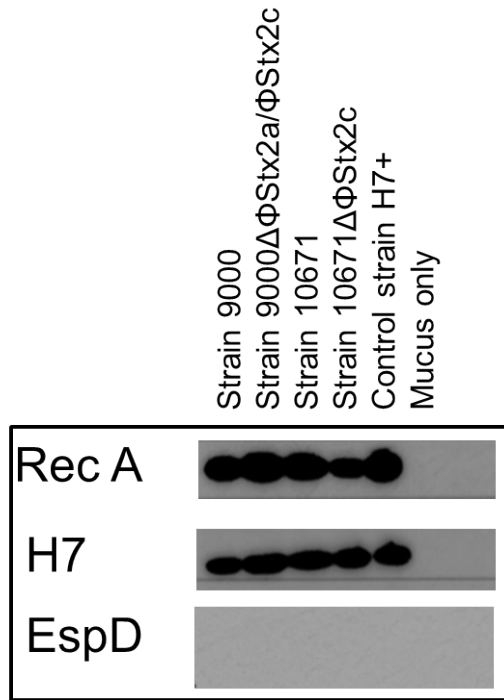


Figure 4.16 Western blot of bacterial cytosolic lysate grown in 10% bovine terminal rectal mucus. Bacterial pellet from EHEC O157:H7 bovine strains grown under similar conditions as described for bacterial adherence assay were checked for H7 and EspD expression levels. RecA served as the loading control. EHEC O157:H7 Strain TUV-0 served as the H7 positive control strain.

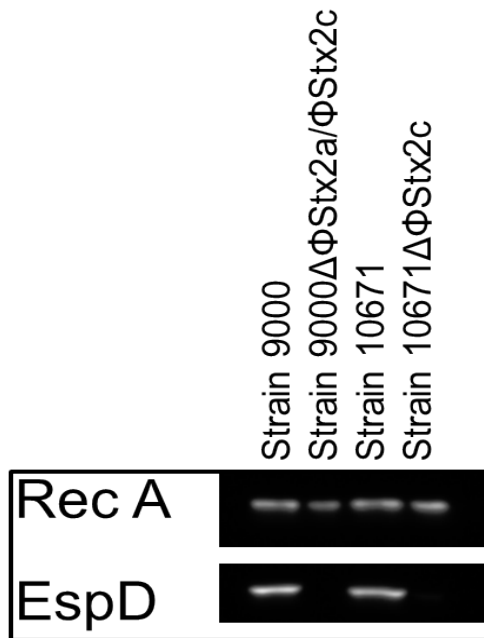


Figure 4.17 Western blot of bacterial cytosolic lysate grown under T3SS conditions. The membranes of four bovine strains of EHEC O157:H7 were probed against EspD antibody (1:3000) to check for the expression of type 3 secretion proteins after cultured under conditions previously shown to enhance T3SS expression. RecA was used to the loading control. Protein were detected by chemiluminescence (G:Box, Syngene).

4.6 *Galleria mellonella* larvae survival upon EHEC O157:H7 challenge

4.6.1 EHEC O157:H7 Strain 9000 and isogenic Stx2-phage mutants

To assess and compare virulence between EHEC O157:H7 Strain 9000 and its isogenic Stx2-phage knock outs, an infection model using *Galleria mellonella* larvae at 37°C, 5% CO₂ was investigated. Data consisted of the number of dead larvae recorded at 18- and 24-hour post-infection, which were then analysed by producing Kaplan-Meier survival plots (Fig. 4.18). The survival curves between all of the larvae groups receiving different strain were significantly different, when analysed with Log-rank Mantel-Cox test, with the alpha=0.0083, based on Bonferroni corrected threshold [Chi square (4)=62.85, p-value <0.0001].

Further pairwise analyses of each isogenic-Stx2-phage mutants to Strain 9000 revealed that the survival curves of the larvae group treated with Strain 9000 were significantly different than the group challenged with Strain 9000 $\Delta\Phi$ Stx2a/ Φ Stx2c [Chi-square (1)=12.15, p-value<0.001]. The median survival time of the larvae receiving Strain 9000 was 48 h and 42 h for Strain 9000 $\Delta\Phi$ Stx2a/ Φ Stx2c challenge, with a ratio of 1.143 (95% C.I. between 0.6435-2.030), while were undefined for larvae groups receiving Strain 9000 $\Delta\Phi$ Stx2a or Strain 9000 $\Delta\Phi$ Stx2c.

4.6.2 EHEC O157:H7 Strain 10671 and Strain 10671 $\Delta\Phi$ Stx2c

EHEC Strain 10671 and its Stx2c-phage mutant isogenic strain were injected into the larvae and similarly as described above for Strain 9000, the number of deaths recorded at every 18 and 24 h. The Kaplan-Meier survival plot are shown in Fig. 4.19. Survival analysis revealed that the survival curves for the group challenged with the Strain 10671 and Strain 10671 $\Delta\Phi$ Stx2c were not statistically different when analysed with Log-ran Mantel-Cox test [Chi square(1)=0.1260, p-value=0.723]. Median survival time for larvae challenged with Strain 10671 was 42 h and for Strain 10671 $\Delta\Phi$ Stx2c, 48h, with a ratio of 0.875 (95% C.I. between 0.5359-1.429).

4.6.3 EHEC O157:H7 Sakai and Sakai Δ Sp5

Virulence in *G. mellonella* larvae was also assessed for EHEC O157:H7 Sakai and its Stx2-phage mutant isogenic strain. Number of larvae deaths were recorded and analysed as mentioned for the other EHEC O157:H7 strains revealing a Kaplan-Meier plot as presented in Fig. 4.20. Survival analysis by Log-rank Mantel-Cox test identified statistically different survival curves between the two larvae group receiving the wild-type Sakai and the Sakai Δ Sp5 mutant [Chi square (1)=7.04, p-value=0.008]. Median survival time for Sakai Δ Sp5 infection in larvae was 48 h but undefined for those infected with the Sakai strain since there were still more than 50% larvae alive at the end of the experiment.

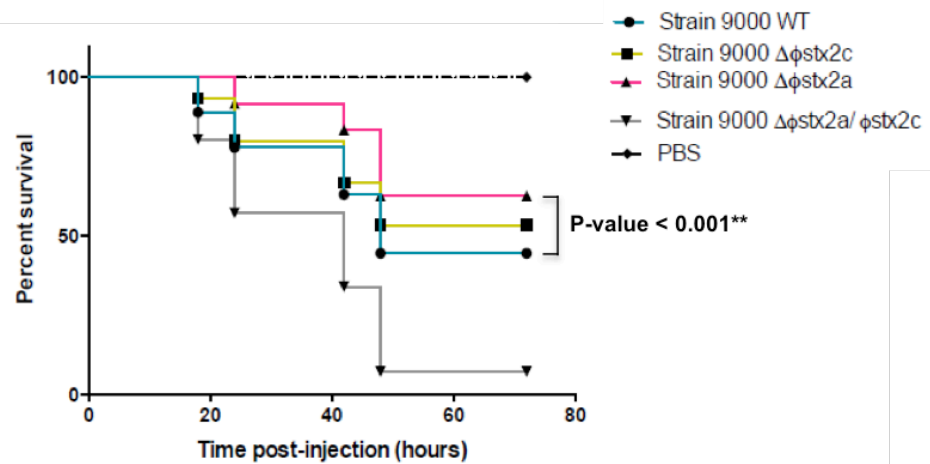


Figure 4.18 Survival of *G. mellonella* larvae challenged with EHEC O157:H7 Strain 9000 strains. At each time point (marked by symbol), the number of dead larvae were recorded and transformed into survival rate (%), as shown in this Kaplan-Meier plot. Each line denotes the bacterial strain used to infect the group, with larvae receiving PBS serves as assay control. Survival analysis was done using the Log-rank Mantel-Cox test in Graph Pad Prism version 6.

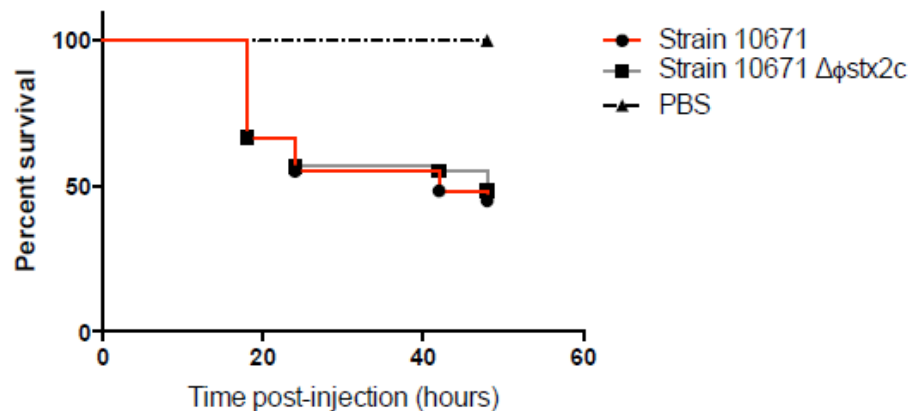


Figure 4.19 Survival of *G. mellonella* larvae challenged with EHEC O157:H7 Strain 10671 strains. At each time point (marked by symbol), the number of dead larvae were recorded and transformed into survival rate (%), as shown in this Kaplan-Meier plot. Each line denotes the bacterial strain used to infect the group, with larvae receiving PBS serves as assay control. Survival analysis was done using the Log-rank Mantel-Cox test in Graph Pad Prism version 6.

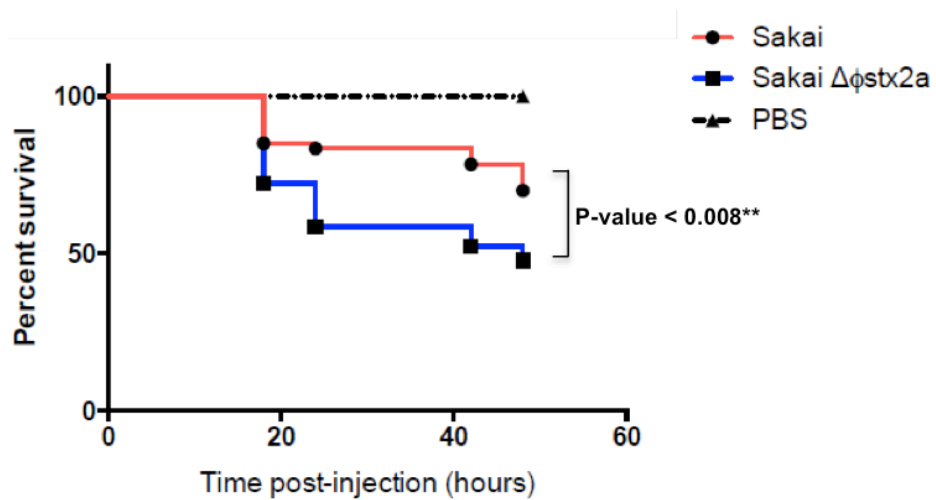


Figure 4.20 Survival of *G. mellonella* larvae challenged with EHEC O157:H7 Sakai strains. At each time point (marked by symbol), the number of dead larvae were recorded and transformed into survival rate (%), as shown in this Kaplan-Meier plot. Each line denotes the bacterial strain used to infect the group, with larvae receiving PBS serves as assay control. Survival analysis was done using the Log-rank Mantel-Cox test in Graph Pad Prism version 6.

Chapter 4

Discussion

Epidemiological studies indicate that EHEC O157:H7 PT21/28 strains are more likely to be associated with higher excretion levels from cattle than many other phage types, including PT32. In addition PT21/28 strains are implicated with severe disease symptoms in human patients. Among the Scottish cattle O157:H7 strains isolated, the PT21/28 strains are more likely to contain a Stx2a-encoding prophage in addition to a Stx2c-encoding prophage which is generally present in both phage types. PT32 strains can contain both Stx2-encoding phages but this combination appears more common in certain other European countries and we have no information on how this then relates to excretion levels of the strains from cattle.

Recent research in collaboration with scientists at the Moredun Research Institute and Scottish Rural College (SRUC), has orally challenged calves with two strains originally isolated in the Wellcome Trust-funded IPRAVE study that fitted the epidemiological profile of the phage types. In two different experiments the PT21/28 strain was excreted at higher levels from the calves than the PT32 strain (Figure 4.1, Chapter 4 Introduction). This validated the choice of these strains for comparative studies. In addition, the T3SS expression was shown to be significantly higher in the PT32 strain compared to PT21/28 [257].

Our group has also sequenced and analysed differences between the genomes of these two strains. While minor differences do exist, the main difference between the two is the Stx2a prophage in the PT21/28 strain. To support this, Stx2a and Stx2c phages were individually removed from the PT21/28 strain. Phage typing of these isogenic mutants of PT21/28 revealed that the PT21/28 $\Delta\Phi\text{Stx2c}$ remains in the PT21/28 cluster, whereas the isogenic PT21/28 $\Delta\Phi\text{Stx2a}$ switched to the PT32 cluster. This is in line with recent evolutionary analysis of EHEC O157 strains in the UK (Dallman et al submitted to PloS Pathogens) indicating that PT21/28 strains have evolved from PT32 strains. Again this information indicates that the higher shedding is most likely to be associated with the Stx2a prophage. This chapter has investigated different *in vitro* phenotypes in an attempt to understand how the phage insertion may contribute to super-shedding.

4.1 Shiga toxin production and potency on Vero cells

As part of the STEC grouping, presumably these bovine EHEC O157:H7 strains should be able to express Stx of the Stx type demonstrated to be present by the genotyping method. Three different growth media were used routinely to generate culture lysates to assay for toxin production and toxicity: i) LB (artificial, laboratory media), ii) LB supplemented with Mitomycin C (to assess the full potential of tested strains to produce Stx) and iii) 10% bovine terminal rectal mucus (to provide growth media that resembles the *in vivo* situation). Overall, under normal laboratory (LB) and lysis-induction (LB + MMC) growth conditions, most of the strains behaved as expected according to their Stx-phage status with the exception of Strain 9000 $\Delta\phi$ Stx2c. It was interesting that 10% BTRM did not provide a permissive environment for Stx production for all the bovine strains compared. In some respects the absence of Stx production under these conditions corroborates the findings in Chapter 2 and Chapter 3 of this thesis where it was suggested that direct Stx interactions with the intestinal epithelium during EHEC O157:H7 colonisation in the bovine rectum is unlikely to result in significant changes with regard to bacterial persistence. There was no clear cellular target for the toxin in terms of the Gb3 receptor and no robust data to indicate an involvement of the toxin in modulating direct epithelial interactions. If negligible levels of Stx are being produced at the bovine terminal rectum *in vivo*, then this indicates that bovine-adapted strains may not be relying on Stx to impose a direct effect on the rectal epithelium for establishing successful colonisation and a high shedding profile. This does not rule out other effects in a more subtle manner, such as immuno-modulation.

Strain 9000 $\Delta\phi$ Stx2c and all of this strain's four clones (saved during the selection protocol for removal of the prophage) failed to produce any detectable levels of Stx or toxicity on Vero cells. It was assumed that by removing Stx2c-phage from Strain 9000, that these strains would still express Stx2a with a potent effect on Vero cells, however this was clearly not observed. Very recently, we have obtained Pacific Biosciences sequence data for a number of the cattle EHEC O157 strains. These have been provisionally analysed by Sharif Shaaban (a PhD student in our research group) and it is clear that Strain 9000 contains an insertion sequence (ISec8)

in the A subunit gene of the Stx2a-encoding gene. Clearly, this is very likely to account for the lack of Stx2a expression in this strain. It was not something we were able to discern from the Illumina-based (short read) sequencing and highlights the value of the long read sequencing technology. Insertion sequences (IS) are the smallest and most abundant transposable elements in prokaryotes [536]. IS have been implicated as significantly contributing to the evolution and diversity of prokaryotes by promoting gene inactivation and chromosomal rearrangements [537]. Further experiments and analyses by the group is ongoing to provide more evidence in order to understand the mechanisms and regulation of IS insertion resulting in such phenotypes. This specific finding has obvious implications for both the *in vivo* and *in vitro* studies, including the likelihood that the increased excretion of strain 9000 is not likely to be due to Stx2a toxin and in fact may be more related to the impact of the remaining prophage, in line with the experiments conducted in this chapter.

Human isolated strains of PT21/28 produced significantly higher levels of Stx compared to the bovine-associated strains, which is in agreement with the findings from a previous study comparing Stx production from HUS-associated and bovine isolated STEC strains [242]. This seems to coincide with the pathology differences between the susceptible humans and the reservoir host, indicating strain adaptability depending on its host. Vero cell killing was relatively higher for both human strains, however the two bovine adapted strains in particular Strain 9000 $\Delta\phi$ Stx2a showed comparable levels of toxicity despite producing less Stx (determined by ELISA) than the human-associated strains, suggesting that the Stx2c produced was potent enough to kill Vero cells despite being produced at potentially lower amounts than from the human isolates. Strain 9000 $\Delta\phi$ Stx2a, when compared against its parental Strain 9000 and PT32 Strain 10671, at times was shown to produce higher Stx levels. It might be that the presence of two Stx-encoding phages in Strain 9000 results in interactions resulting in repression rather than synergy in total Stx production. The Stx2a-phage of Strain 9000 may suppress the production of Stx2c in the parental strain.

Toxin production in this assay was measured relatively based on detection by the immuno-assay kit. The ELISA kit however does not distinguish between the

different Stx types and variants, therefore it is not known which Stx is actually present in each lysate preparation and only presumed based on the genotype. This is especially an important point to be considered when detecting total Stx from Strain 9000 (PT21/28). Quantitative real-time polymerase chain reaction (qRT-PCR) to assess the copies of each toxin type present in the supernatant/lysate preparation would be valuable as this will accurately measure and assign the contribution to each Stx-type and phage. Measuring Shiga toxin levels and toxicity from the human strains in 10% mucus from human colon, for example, might shed some light on how much toxin is produced *in vivo*. It would be interesting to compare toxicity of more human and bovine strains and to study the interactions between Stx-encoding prophages in terms of final Stx production and toxicity.

4.2 Growth of EHEC O157:H7 in competitive environments

It has been observed that bacterial interaction with intestinal epithelial cells surrounded in mucus most likely contains very low, if not negative, levels of Stx and that there was preliminary evidence of control by Stx-phages in determining how much Stx is produced by the strains. Owing to its complex structure and contents, mucus not only protects the intestinal epithelium as part of the innate defense, but also provides nutrients for the colonising bacteria, commensals and pathogens alike. Certain EHEC O157:H7 strains were shown to have different preference over commensals concerning preferred mucin content and carbon resources [36, 199]. The position of *nanS* adjacent to *stx* genes might indicate a role for Stx-encoding phages in increasing the fitness of EHEC O157:H7 to survive in a complex ecosystem in the bovine intestine [255]. Bacteriophages were also suggested to have the power in controlling diversity of a steady state bacterial community indicating the manipulative side of these infectious particles [538]. Based on this, it was then hypothesised that the parental strains harbouring Stx2-phages would perform better in a competition setting with prophage deleted derivatives or strains with a different complement of Stx phages. At the simplest level this might account for the increased excretion of Strain 9000 compared to Strain 10671. The data from the competition assays however is complicated and it is difficult to reach a simple conclusion about prophage contribution. Strain 9000 (PT21/28) with two Stx-encoding phages did not

significantly provide growth advantage over the Strain 10671 (PT32) strain. This inter-strain competition (PT21/28 and PT32) indicates that both are equivalent in terms of fitness and survival, despite the presence of different Stx2-phages in the co-culture. No benefit was conferred to the bacteria by the presence of Stx-phages as the proportion of each paired strains maintained minor fluctuations enabling the paired strains to grow and replicate at similar levels, at least within the time frame of the assays performed.

To further assess the interactions occurring in the co-culture, the laboratory *E. coli* strain K-12 and its derivative strains were further employed for similar growth competition assays. In the early phase of co-culture, the naive K-12 strain were able to dominate over the SP5-lysogenised K-12 strain until day four, where there was a surge in the K-12-SP5+ population making up approximately 90% of the co-culture. This was observed again when the strains were re-competed in fresh culture. Initially it was suspected that the observations occurred as a result of lysogenisation of the naive K-12 SP5 mutants. Incorporation of the prophage into the susceptible host genome would consequently give rise to SP5 phage-resistant population in the formerly susceptible strain, thereby explaining the sudden increase in the SP5+ culture on day 4. However this theory seems to be less likely to explain the fluctuations observed as results of sub-culturing the kanamycin-resistant (SP5+) colonies on lactose-MacConkey agar to check for lysogenised 'naive' K-12 strain revealed otherwise, with the lack of such colonies (marked by the ability to ferment lactose and appear pinkish on the lactose MacConkey agar) on day 4 of co-culture. An alternative explanation for the observed fluctuations would be that initially the total K-12 SP5+ levels dropped due to spontaneous lysis (possibly stressors present in the competitive environment such as waste products or competing over the same nutrient source) or that the SP5 phage-bearing K-12 cells indeed had a slower growth rate than the isogenic SP5 mutant. However, the remaining fraction of the K-12 SP5+ cells would then continue to replicate and vertically transfer the SP5+ genome into the daughter cells. Some of these SP5+ cells then undergo lysis due to stressful conditions in the co-culture (e.g. starvation), releasing infective phages that quickly infect the already vast susceptible K-12 cells present at day 4 of co-culture,

resembling the 'predator-prey' relationships and oscillations [539]. As a consequence, majority of the non-resistant, infected naive K-12 cells were killed, possibly explaining the sudden plunge in the isogenic SP5 mutant cells. This could be viewed as a strategy used by the prophage-bearing strains to outcompete the competitors in the same environment, where the phages were manipulated to the advantage of the strain [526]. A computer simulation of bacterial strain replacement in the presence of phages predicts that the strain that is able to use the most abundant nutrient or metabolise more than one substrate is the preferentially target for phage to attack, resulting in selection against the fitter strain and establishing a fluctuating density of bacterial strains competed around stable levels [539]. This description fits well in terms of explaining the fluctuations observed in the co-cultures.

Competition of the Sakai pair, although showed some oscillations but the peaks were much less pronounced as that observed for the K-12 pair. Although the exact reason is unknown, the findings for the Sakai pair seems similar to that observed in the Strain 9000-double Stx-phage mutants competition. One factor that could lead to this outcome is the fact that the isogenic Stx-phage negative strains were derived from Stx-phage positive strains (Strain 9000), and have some resistance from phage infection conferred by the original phage. While the co-culture bearing Strain 9000 and Strain 10671 failed to produce dramatic peaks as that seen in the K-12 pairs, despite the presumption that Strain 10671 is 'naive' to the Stx2a (and probably Stx2c) phage(s) of Strain 9000. The findings observed could also not explain the different shedding profiles of the two strains (Chapter 4, Introduction Fig. 4.1). Further experiments on determining the sensitivity or resistance of Strain 9000 and Strain 10671 to each of the possessed Stx-encoding phages would facilitate our understanding of the competition growth assays presented.

More valuable insight could be gained by competing the strains on a longer time scale, for hundreds or thousands of generations, to see if the fluctuations observed stabilised. Had there been more inputs to serve as variables such as lysis rate and burst size, it would be of interest to predict the dynamics displayed by the paired competing strains over time, by constructing a simulation model. Recently, it

was observed that EHEC strains deleted of AgvB, an sRNA present in two Lambda-like bacteriophage regions in the EHEC genome and identified as an antagonist sRNA to GcvB (core genome regulator), decreased the competitiveness of the strains in 10% bovine terminal rectal mucus, but not M9 or LB media [540]. AgvB also interacts with Hfq, a post-transcriptional regulator involved in bacterial virulence and stress response [541]. Such evidence implicates the involvement of phage factors in regulating important bacterial growth phenotypes, with the outcome dependent on the strain and environment.

4.3 EHEC O157:H7 adherence to epithelial cell lines

There was no significant difference found in the initial binding rates between Strain 9000 (PT21/28) and Strain 10671 (PT32), despite data from unpublished work [256] which identified that Strain 9000 (PT21/28) bound better than Strain 10671 (PT32) to bovine primary terminal rectal epithelial cells in 10% BTRM. The expression of two bacterial virulence factors closely associated with host cell attachment, flagella and the T3SS were also studied. Ensuring that the bacteria were grown under similar conditions as when prepared for the epithelial binding assays, flagella (H7) and T3SS (EspA/D) expression was examined by confocal microscopy along with Western blotting. Flagella are considered to be involved in the early phases of bacterial attachment and are able to bind to freshly isolated bovine mucus and to mucin components [213, 375]. T3SS was assessed since it is established as an important system for intimate cellular attachment although its role in the early phase (30 min) interactions with epithelial cells is less clear. By confocal microscopy, there seemed to be a higher H7 expression in all of the stx phage mutant EHEC O157:H7 strains and higher EspA in Stx2c phage mutants of Strain 9000 and Strain 10671. However the presence of mucus remnants visualised on most of the slides hindered full view of the bacterial cells trapped within or underneath the mucus. The study then proceeded with immuno-blotting to further compare the levels of H7 and EspA expression in the wild type and stx-phage mutant strains. It was then clear that the H7 levels were similar for all bovine EHEC O157:H7 strains regardless of Stx2-phage status, while there were no signs of T3SS expression which agreed with the timeline of the assay, assessing early adherence rather than a long term binding.

Since H7 levels were similar between strains of different Stx-phage status, the involvement of other potential bacterial factors acting as adhesins expressed in the early phases of attachment may explain the non-significant variations in the binding percentages. Examples include the outer membrane protein A (ompA) shown to be important in EHEC O157:H7 86-24 binding to HeLa and Caco-2 cells [542], enterohaemolysin (Iha) implicated in binding of K-12 to HeLa cells [543], the highly aggregated fibres known as Curli [544] or the F9 fimbriae [545], the Lpf1 [219], the laminin binding fimbriae (YcbQ) [546] or even the zinc metalloprotease (StcE) [228, 529]. Future work will examine the complete gene expression profiles of the isogenic strains to identify the full complement of genes, including adhesins, that might be controlled by Stx2-phage insertion.

The strains were also grown in conditions shown to promote T3SS expression [257] which revealed detectable levels of EspD. These were shown to be similar for both Strain 9000 and Strain 10671, but was absent in their Stx-phage free isogenic strains. This is though in line with findings that T3SS is not expressed in the bovine rectal mucus and not relevant in the early interactions with cells since the expression of T3SS is initiated once the bacterial population reaches the stationary phase [194]. The findings are contrary to those found in an earlier study by our group which demonstrated that T3SS is repressed in the presence of Stx2a-encoding phages in EHEC O157:H7 PT21/28 strains and was up-regulated the $\Delta \phi$ Stx2a strains [257]. The EspD levels of PT32 was also determined to be significantly higher than that of PT21/28. It was determined at that time that following Stx2 lysogenisation, the expression of the cII regulatory protein (transcription activator of genes involved in regulating the fate of the phage to enter either the lysogeny or lytic pathway) was detected and resulted in the repression of Ler (LEE genes regulator) activities which coincided with repressed EspD secretion. Deletion of the cII protein from the Stx2-phage significantly ($p < 0.001$) increased the activation of Ler. Contrasting results at the translational level of T3SS components observed by Xu et al. (2012) and the current study highlights the fact that the behaviour of the strains even within the same PT cluster could be differentially regulated depending on the prophage type leading to varied phenotypes [257]. To clarify why the Stx-phage mutant strains

failed to express EspD requires further specific examination at both the transcriptional and translational levels.

There are some drawbacks with the methods used in the bacterial adherence assay. The epithelial cells were cultured in 10% bovine terminal rectal mucus which prevented longer infection time as the eukaryotic cells start to die in 10% BTRM. If possible, it would be good to prolong bacterial and epithelial cell interactions to analyse A&E lesion formation by the strains with the different Stx-phage composition. Another point to consider is the use of total plate counts as the output to assess adherence of bacteria to epithelial cells. There was also considerable levels of experimental variations leading to a range of total bacterial count across different repeats. If the bacterial cells are not properly removed during washing after the 30 min infection period then this would definitely lead to false positive results, or vice versa if the trypsinising agent added might have adverse effects on the adherent bacteria, possibly killing the bacterial cells. To improve the findings, further work should incorporate more efficient methods such as flow cytometry to accurately count total bacteria bound to cells and also determine the number of bacterial cells attached to each individual eukaryotic cells. This microscopic examination would not only help in enumerating adhered bacterial cells, but also examine any lesion formation on the epithelial cells. By combining findings from the different suggested methods, this will definitely increase confidence in the data.

4.4 Assessing virulence between different EHEC O157:H7 strains in *Galleria mellonella* larvae infection model

The next phenotype assessed was virulence between strains with different Stx2-phage complements. *Galleria mellonella* larvae, as described in further details in the introduction section, were used as an alternative to a large animal model and serve as a relatively convenient and quantifiable infection model to establish some aspects of preliminary virulence interactions. *A priori* hypothesis was that Stx-phage carrying strains would be able to induce more damage and higher death rates in the larvae, while the isogenic mutants will not be as harmful or less damaging to the

larvae based on the fact that the parental strain genome have intact prophages that confer 'maximum' virulence, including Shiga toxin expression.

The data obtained indicated otherwise, the isogenic Stx-phage mutant strains for EHEC O157:H7 Strain 9000 and Sakai were able to kill more larvae than their parental strains containing Stx2a-phage(s). It is not known if Stx2 is expressed by the strains inside the larvae, or which virulence factor(s) is(are) responsible for causing fatal lesions as this warrants further experiments to be performed. Interestingly, the outcome was different for Strain 10671, where the survival rates were similar between Strain 10671 and its Stx2c-phage deficient strain. There were clearly strain-dependent effects on the larvae. It has been suggested that prophages are able to impact on expression of virulence factors in its bacterial host and in the presence of more than one prophage in the genome, this could result in potentiation of virulence as a result of interaction between the prophages present [547]. From the survival curves obtained in this study however, it can be proposed that the Stx2a prophages may repress or down regulate certain virulence traits, which are then expressed at a higher level upon curing of the Stx-phage. As discussed above for toxin production, competitive growth and adherence to epithelial cells, the differences in the outcome displayed among strains of different Stx-phage carriage suggests that these prophages are somehow interacting with some of the key virulence and survival traits, manipulating the behaviour of the bacterial host in order to promote its own survivability. Further studies applying this model could incorporate total bacterial count from the haemolymph of the larvae, inspection of histological sections of infected larvae to confirm colonisation, detection for any presence of Stx and Gb3, among others would supply useful information in explaining how Stx-phage cured strains, supposedly thought to be less virulent, caused higher death rate in the larvae, as compared to the 'wild-type' strains. Considering the fact that this infection model utilises a dramatically different host species than cattle, careful interpretation of data obtained is needed. From the data, it is evident that Stx2a phage integration can actually pacify certain strains in terms of innate interactions, although it appears the larvae are not susceptible to Shiga toxin, although this in part mirrors the cattle

situation. Perhaps a less aggressive strain can colonise to higher levels and for longer and this is promoted by the phage-bacterium relationship.

4.5 Conclusion

This chapter discussed the characterisation of several key traits of EHEC O157:H7 strains with the aim to assess if Stx-encoding phages contribute to the phenotypes displayed by its bacterial host. The relationship between the Stx-phage and EHEC O157:H7 could be viewed as mutually symbiotic as both entities are believed to positively support the survival of one another. The ability for the temperate Stx-phage to manipulate the bacterial host to ensure continuous propagation of the phage genes could simultaneously contribute to the survival of the bacteria. Vice versa, the prophages are more likely to be conserved in the bacterial genome as the genes provide superior traits. Under certain conditions, the balanced mutual symbiosis may change direction to either become parasitic (e.g. Stx-phage undergoing lytic phase which directly kills the bacterial hosts) or commensalism (e.g. lysogenisation ensuring maintenance and propagation of phage genes and at the same time, conferring resistance to the infected bacterial host that may also be used as a 'weapon' to attack competing bacterial strains). The impact of Stx-encoding phages and the EHEC O157:H7 host is believed to be complex, and the absence or presence of the Stx-phage does not necessarily result in modification of bacterial traits in the expected manner. The similar competitive growth and binding capacities of the two bovine isolates (Strain 9000 and Strain 10671) and the lack of synergism in total Stx production, despite the former strain containing an extra Stx2a-phage, and pacification (for 2 strains) of virulence in the *G. mellonella* larvae strongly suggest that the Stx-prophages interact with and are capable of altering the colonisation and virulence associated phenotypes of the host EHEC O157:H7 strain. Most of the findings here are preliminary as explanations of the regulatory mechanisms are missing. Moreover, the association between the Stx-phages and super-shedding remains unanswered. Several aspects of this chapter particularly on attachment and competitive growth warrants further investigation ideally carried out under *in vivo* conditions. As a start, cattle challenge experiments with EHEC O157:H7 strains of different Stx-phage status is currently on-going which may

provide crucial *in vivo* data on the phenotypic characteristics presented in this chapter for validation. It is also important at the same time to understand more about the biology of Stx-encoding phages from the Scottish EHEC O157:H7 strains which could then be merged with data from genomic analyses. Future findings from details of the sequencing data of the Stx-phages and the bovine EHEC strains carried out by other research group members, in addition to preliminary evolutionary work on Stx-phages [548] would facilitate the current understanding on the involvement of Stx-phages in EHEC O157:H7 colonisation at the bovine terminal rectum. Additionally, this would facilitate the development and improvement of current preventative strategies aimed at reducing EHEC O157:H7 shedding from cattle and ultimately transmission to humans.

Chapter 5

General Discussion and Conclusion

General Discussion

Shiga toxin is the virulence factor directly associated with the development of haemorrhagic uraemic syndrome (HUS) in humans following an episode of bloody diarrhoea [341], while the Stx-encoding prophages themselves have been implicated as the source of lineage diversification, persistence and emergence of important pathogenic EHEC O157:H7 isolates from humans and cattle [85]. The current study aimed to address the contributions of Shiga toxin and Shiga toxin-encoding bacteriophages (phages) towards intestinal colonisation of EHEC O157:H7 in the asymptomatic cattle host.

Chapter 2 explored the possibility of toxin-Gb3 receptor interactions at the principal colonisation site, identified as the bovine terminal rectum [33], as this has yet to be addressed and that Gb3 presence may indicate a significant role for the toxin during the process. The findings obtained, particularly from histological examinations were indicated that Gb3 is not present at significant levels at the preferred colonisation site of EHEC O157:H7 in cattle. This was true *in vivo* for the samples studied although further work is needed to support and confirm the absence of Gb3 on the rectal epithelium by determining the levels of Gb3 synthase or Gb3 lipid expression as well as histological evidence from a larger number of animals before completely ruling out the presence of Gb3 receptor at this site. Additionally, it was determined that Stx2, despite previous reports that it can initiate apoptosis and disrupt the cell cycle of epithelial cells, did not induce any obvious negative effects on the proliferation of intestinal epithelial cell lines investigated in this study, regardless of their Gb3 status and Stx sensitivity. It was not possible to assess the effects of Stx on proliferation of bovine terminal rectal cells, therefore generalisation of the findings with regard to cell proliferation needs further work to be carried out. Since it may not be feasible to examine effects of the toxin in live cattle, future work could utilise alternative approaches such as the 3-dimensional (3D) cell culture systems [549] of the bovine terminal rectum which could provide a better *in vitro* system than the two-dimensional continuous or primary cells, based on issues discussed in the discussion section of Chapter 2. EHEC O157:H7 could be added onto the cells following optimisation to induce Stx release thereby allowing

assessment of the effects of the toxin, rather than stimulating the cells with commercially obtained purified toxins as these may not give accurate observations since the properties may be different from the ones released from bacterial lysis. Simultaneously, providing the 3D cell culture system with a microaerobic environment [165, 205] will most likely enhance and refine the *in vitro* system to achieve a more realistic model, resembling the conditions *in vivo* that will increase the relevance of these experimental observations.

Since there was no strong evidence to associate Stx and the intestinal epithelial cells in Chapter 2, the aim of the study was shifted to focus on the impact of Stx and Stx-expressing EHEC O157:H7 strains on the immune cells residing the mucosal layer of the bovine terminal rectum. The consequences of toxin activity on these immune cells largely depends on the type of cell that is encountered [272]. The present study attempted to assess the responses of selected immune cell types (included those based on the findings of a previous study [250]) from the rectal mucosa of calves infected with two commonly isolated EHEC O157:H7 strains from cattle farms in Scotland [64]. The EHEC O157:H7 strains used to challenge the calves differed mainly in the Stx-phage type possessed and it was hypothesised that the strain containing the extra Stx2a phage, in addition to the Stx2c phage (also present in the other EHEC O157:H7 strain introduced in another group of calves) would significantly alter the bovine mucosal immune response. This concept was based on Stx2a being more potent than Stx2c and other Stx variants [69]. Potentially higher levels of Stxs may also be generated from EHEC O157:H7 Strain 9000 carrying two Stx phages (additive or synergistic), resulting in a more pronounced effect. Initially it was thought that the statistical differences could be associated with a down- or up-regulation of the expression of CD3⁺/CD4⁺, CD3⁺/γδ⁺ and CD21⁺ cells between calves in the group receiving EHEC O157:H7 Strain 9000 and control calves. However a closer look at the data revealed the lack in the total number of cells analysed (refer to Chapter 3, Discussion section 3.1). Had the total number of cells sampled for flow cytometry analysis determined, the direction of the bovine host immune response could be convincingly ascertained.

The inability of Stx2 to interfere with IFN- γ activation of the JAK/STAT1 pathway in intestinal epithelial cells contrasted with suppression previously reported [482, 483, 502]. It is believed that such inhibitory effects result from multifactorial, complex interactions between the bacteria and signalling system of intestinal epithelial cells [502]. To clarify the findings from Chapter 3, the EHEC O157:H7 infection of calves needs to be repeated to obtain more terminal rectal mucosal tissue that can be examined under an improved protocol particularly with regards to immunophenotyping the selected immune cells investigated in this study.

From the findings of Chapter 2 and 3 of the current study, Stx, if expressed during bovine intestinal colonisation, do not play any role as hypothesised earlier at both levels; the intestinal epithelial cells and the bovine intestinal immune cells of the terminal rectal mucosa. Chapter 4 then explored the possibility for the Stx-encoding phages, rather than Stx production, in determining the successful colonisation of the bovine terminal rectum. Four phenotypic characteristics of EHEC O157:H7 associated with colonisation and virulence were examined; total Stx production and toxicity, competition growth assays, adherence to epithelial cells and pathogenicity in a larvae infection model. In order to achieve results that may describe how EHEC behaves in the bovine terminal rectum, 10% bovine terminal rectal mucus was used as an alternative growth medium in most of the assays (in addition to LB or LB and SOS inducing agent) to provide culture conditions resembling that during colonisation *in vivo*. Both human isolates of EHEC O157:H7 PT21/28 grown in both LB and LB with MMC induction produced exceptionally high levels of total Stx compared to the defined bovine isolates assessed, which agrees with the findings of others [77, 78, 242, 550] and may explain why humans are more affected by the adverse effects of Stx than the cattle, apart from differences in Gb3 distribution and cellular susceptibility or resistance against the toxin [147, 273, 275, 352, 551]. More importantly, mucus of the bovine terminal rectum may contain inhibitory components against the expression of Stx by EHEC O157:H7, compared to LB. In addition, it was recently reported that microaerobic conditions provided to a vertical diffusion chamber system of human carcinoma intestinal cells to resemble the physiological levels of oxygen in intestinal lumen of living mice

(estimated to be low, at 1.4% atmospheric pressure) caused a reduction in total Stx production by EHEC O157:H7 [165]. This, taken together with the non-significant presence of Gb3 on bovine terminal rectal mucosa strongly indicates that Stx are not expressed or if expressed, only at very low levels at the colonisation site, presumably where the mucosal barrier is breached. In the event of Stx expression, the toxin would either enter the intestinal epithelial cells via a Gb3-independent manner and may follow a lysosomal degradation route [142] or travel across the epithelial layer to the lamina propria/lymph nodes via an interrupted epithelial barrier (e.g. due to the A/E lesions or Stx-induced damage) [159] or transcytose across epithelial monolayer efficiently under microaerobic conditions, enhanced in the presence of EHEC O157:H7 colonisation [165]. Then it can be presumed that the translocated toxins may modulate the immune responses ensuring persistence of replicating bacterial colonies without reduced interference from the bovine immune system, leading to higher numbers of bacterial shedding. Based on studies and modelling of individual animal shedding curves, it was estimated that the bovine innate immune response will negate bacterial replication and reduce bacterial attachment or increase epithelial detachment from the terminal rectum between 5 to 9 days after bacterial challenge [552]. The shedding curves in the calves infected with EHEC O157:H7 Strain 9000 PT21/28 peaked between 3 to 10 days post challenge at high levels ($> 10^3$ C.F.U/gram of faeces) [384]. It is therefore important for EHEC to be able to immediately establish intimate attachment as soon as it reaches the terminal rectum to allow ample time to replicate at a higher rate. It should however be reminded that these infection models were carried out with a large bolus of bacteria (10^{10}) which do not reflect infection events occurring in the real world and therefore may induce a much stronger response that might overwhelm and mask the immunomodulation events occurring within the animals. Transmission studies employing an improved calves infection model with EHEC O157:H7 of different Stx phage types is currently on going to clarify the shedding curves and further the understanding of such complex interaction during colonisation *in vivo*.

As “super-shedder” cattle tend to be associated with excreting Strain PT21/28 than other EHEC O157:H7 phage types, it was thought that this strain may replicate

faster than other strains due to the double Stx phage content present on its genome. Having assessed the competition growth rate assay results, the growth rate and fitness of PT21/28, its double Stx phage mutant strain as well as PT32, these did not seem to differ. It is also not known if the Stx phage mutants of the bovine isolates have developed resistance towards the Stx phage(s) previously present on the genome. From another point of view, Stx phages could be used as a ‘weapon’ attacking the susceptible, Stx phage negative strains and directly inducing lysis resulting in killing the ‘weaker’ strain [526]. The alternating peaks seen in the competition growth curves between the K12 and K12-SP5+ strain may demonstrate the predator-prey relationship mentioned [539]. Despite not observing the PT21/28 or PT32 as winners when competed against the isogenic Stx phage mutants, or between the two bovine isolates, the retention of the integrated prophages on the bacterial genome provides a strong basis for the phage to be beneficial to the bacterial host. More experiments are required, encompassing Stx phage characterisation and infectivity of EHEC O157:H7 strains to animal co-infection model with two strains (Stx phage + and mutants) that are able to reach and colonise the terminal rectum and similarly observe for any ‘winning’ strain, but in a highly complex environment, with the presence of commensal bacterial strains and other eukaryotes as well as other intestinal lumen conditions (oxygen levels, pH, temperature, nutrient availability).

EHEC O157:H7 adherence to intestinal epithelial cells was shown to be significantly be affected with the T3SS being repressed upon lysogeny, indicating the involvement of phage elements in the complex regulatory circuitry of T3SS [257]. In that study, the authors showed a significantly higher expression of EspD in PT32 than PT21/28 and suggested for the presence of Stx2a-phage to repress the T3SS upon lysogeny. They also presented results associating the cII protein of the Stx2 phage with the repression of the T3SS activation. The current findings in this study did not show striking differences in the binding capacities between the wild type and the Stx phage mutants of Strain PT21/28 and PT32. In addition, the Western blot for EspD expression in Strain PT21/28, Strain PT32 and the isogenic mutants for Stx2a/Stx2c phages indicated the absence of EspD expression in both of the isogenic

mutant strains, which contrasted with the findings by Xu, et al. [257]. At this point, it could only be speculated for the differences in phenotypes observed between the current and the previous studies to be related to the prophage and LEE regulatory networks, although evidence is required to prove this hypothesis. The insertion sequence recently detected by a member of the group that was proposed to contribute to the lack of Stxs production in the Strain 9000 ϕ Stx2c, could also be related to the T3SS and adherence phenotype observed in Strain 9000. Moreover, as indicated in the Discussion section of Chapter 4, there were issues encountered with the method used in this study to partly quantify bacterial binding to eukaryotic cells and therefore alternative ways to quantitate bound cells is required, such as flow cytometry which could produce more reliable, consistent and accurate results, in addition to providing other information including the number of bacterial cells attached to one host cell. Future work may also adopt the microaerobic, vertical chamber diffusion system protocol developed by Schuller and Phillips [205] to infect intestinal epithelial cells for a more optimised conditions and obtain better accuracy in assessing binding capacities between the EHEC O157:H7 strains. The authors also reported for an enhanced T3SS expression under low oxygen conditions, which may further optimise the experimental conditions and improve accuracy of the findings. Efforts to estimate important physiological parameters (oxygen levels, pH) at the bovine terminal rectum would therefore facilitate the development of a binding assay protocol that would produce results reflecting the actual binding conditions during a *in vivo* colonisation, in addition to using bovine intestinal epithelial cells rather than cells of human-origin. Lastly, the development of such *in vitro* models may be more cost-effective than carrying out experiments in live cattle.

The *Galleria mellonella* infection model with EHEC O157:H7 isolates provided an insight into the relative virulence levels, especially between the bovine isolates and their Stx phage mutants. The most significant outcome obtained was that the double Stx phage mutants had higher virulence level than its parental strains (PT21/28 and Sakai strains). This seems to contrast with the expectation that any strain that is able to produce Stx, in particular, Stx2a, should be able to induce severe clinical outcomes and high mortality rate than those without the same *stx* genes. It is

highly likely that the *G. mellonella* larvae are not susceptible to the adverse effects of Stxs. Moreover, the T3SS does not appear to be a factor contributing to virulence observed in the moth model (personal communications with Andy Roe, University of Glasgow, U.K.). This may explain the findings from Chapter 4 where despite having similar negligible levels of T3SS, the double Stx-phage knockout of Strain 9000 produced higher mortality rates than the single Stx-phage mutants and the parental Strain 9000. The differences in virulence levels of the strains are believed to be of other, unidentified factors which remains to be investigated. Little is known with regard to the innate and adaptive immune system of the *G. mellonella*, in addition to the lack of information on the real fate of the bacterial cells once inoculated into the larvae. Indeed we are still far in understanding and explaining the differences between the pathogenicity levels of EHEC O157:H7 in the larvae, justifying the need to unravel the events post-inoculation both in the bacteria and in the larvae.

Moving forward, perhaps the answer for other factors involved in the persistence and super-shedding behaviour of Stx-phage bearing EHEC O157:H7 strains lies in the bacterial-grazing protozoa residing in the bovine gut as eukaryotic commensals [553]. Published reports suggested that the bacterial predatory protozoa is an important factor in shaping the structure of bacterial strains inhabiting a particular ecosystem including that of EHEC O157:H7 [554-556]. Since the predatory-prey interactions could seriously reduce the population size of the EHEC O157:H7 in the ruminant reservoir, it was hypothesised that EHEC have evolved and developed anti-predatory mechanisms including Stx to primarily escape death by protozoan ingestion, before the Stx phages were maintained in the bacteria due to the benefits conferred. Later, Stx would have then evolved and adapted as a virulence factor creating pathogenesis in humans [557]. Stx was shown to be toxic to the predatory protozoa, *Tetrahymena thermophila* [558]. Moreover, EHEC O157:H7 cells were able to survive in the food vacuoles of *T. thermophila* following ingestion up to 90 min, a time length that is ample for the delivery of Stx to the protozoa [554, 559]. Interestingly, EHEC O157:H7 strains containing Stx prophages were favoured for ingestion by the *T. thermophila* over strains lacking the Stx phages [554]. To fully comprehend these interactions, more studies presenting consistent evidence are

needed. The strategy used by EHEC O157:H7 to survive and outlast the protozoa is probably akin to the macrophage ingestion of the bacteria where EHEC O157:H7 were able to survive and produce Stx whilst inside the macrophages [449]. This could also be used as a strategy to increase the affinity of immune cells towards the EHEC O157:H7-ingested protozoa for destruction, which will release Stxs produced by the ingested bacteria. The more aggressive a strain is, the more toxins will be expressed and therefore increasing the mortality rate of the protozoa while at the same time releasing higher magnitudes of Stxs in the intestine. There is going to be a very interesting ‘trade-off’ between the value of the toxin to the strain, prophage and the obvious point that the strain has to lyse to release Stxs. It may therefore be important for the strain to modify the behaviour to become less aggressive as a way to address that balance.

Conclusion

This thesis was dedicated to unravel the association between bovine intestinal colonisation by EHEC O157:H7 with both Stx and bacteriophages carrying the Stx genes. It was hypothesised that the successful propagation of EHEC O157:H7 is impacted by the integrated Stx prophages on the bacterial chromosome. However, despite carrying the *stx* genes encoding for the major virulence factor implicated in human infections, there was no evidence to support toxin production from EHEC O157:H7 by phage-directed lysis within the mucus of the terminal rectum. Besides, many non-EHEC strains are able to produce Stxs, including non-pathogenic, commensals or environmental strains by acquisition of the *stx* genes via lateral gene transfer events [94, 560, 561] and this may indicate for the presence of other more important factors that dictates the persistence of EHEC O157:H7 at the bovine gut. At the same time, Gb3, the Stx receptor acting as cell surface marker on toxin-sensitive cells, was not found to be significantly present along the terminal rectal epithelial mucosa layer. The lack of convincing evidence so far to support the role of Stxs together with the lack of significant Stx expression by the bovine isolated EHEC O157:H7 strains in bovine terminal rectal mucus strongly suggest that Stx production is not an important bacterial factor in determining the success of the bovine terminal rectum colonisation by EHEC O157:H7. The actions of Stx in

facilitating the bacterial colonisation process via enhancement of bacterial adherence to the host cells (nucleolin upregulation acting as intimin receptor [241]) may be significant under circumstances where Stx production is evident, particularly in susceptible, Gb3 positive human tissues.

On the role of Stx phages in EHEC O157:H7 colonisation, despite the lack of mechanistic explanation for alterations observed in colonisation and virulence traits among bacteria possessing different Stx phage types, evidence presented in Chapter 4 shows that **different types of Stx-encoding phages are able to influence important phenotypic traits of EHEC O157:H7 during colonisation at the bovine intestine**. Interactions involving the Stx phage, bacterial host and the bovine terminal rectum presumably occurs via a complex regulatory network to facilitate bacterial adaptation to the niche. Perhaps the Stx prophages are expressed in a chronological manner, for example by only a small subset of bacteria in the early hours of the interaction, to produce Stx which promotes the upregulation of the intimin receptor, nucleolin to strengthen the A/E lesion or by the act of infective phage particles infecting and killing the commensal species residing on the outer mucosal layer of the rectum, allowing replacement of the commensal flora by EHEC O157:H7. After a while a Stx phage could pose as a liability to the survival of EHEC O157:H7 as some of the susceptible strains could then be lysogenized and become resistant to Stx phages creating a new competitor that will receive all benefits conferred by the Stx phage. To overcome this, the EHEC O157:H7 may lose the Stx phage to avoid losing out to the emerging lysogen-converted strains which have been described to occur during certain phases of the life cycle of the non-motile sorbitol-fermenting *E. coli* O157 isolated from human stools [562]. The Stx phages could be regained into EHEC O157:H7 when the situation requires it to happen, for example before excretion out of the cattle to ensure possessing the correct repertoire of genes for survival and virulence upon transmission to human hosts.

The final conclusion of my work is **i) different Stx-encoding phages are able to control different phenotypic traits of EHEC O157:H7 during colonisation of the bovine intestine and ii) there was no clear evidence for Stx to**

play a role in EHEC O157:H7 colonisation at the bovine terminal rectum. On going work aims to understand Stx phage epidemiology and the differences portrayed by the EHEC O157:H7 with different types and combination of Stx phages.

References

1. Shulman ST, Friedmann HC, Sims RH: **Theodor Escherich: The First Pediatric Infectious Diseases Physician?** *Clinical Infectious Diseases* 2007, **45**(8):1025-1029.
2. Gan L, Chen S, Jensen GJ: **Molecular organization of Gram-negative peptidoglycan.** *Proceedings of the National Academy of Sciences* 2008, **105**(48):18953-18957.
3. Trueba FJ, Woldringh CL: **Changes in cell diameter during the division cycle of Escherichia coli.** *Journal of Bacteriology* 1980, **142**(3):869-878.
4. Huang KC, Mukhopadhyay R, Wen B, Gitai Z, Wingreen NS: **Cell shape and cell-wall organization in Gram-negative bacteria.** *Proceedings of the National Academy of Sciences* 2008, **105**(49):19282-19287.
5. Chang D-E, Smalley DJ, Tucker DL, Leatham MP, Norris WE, Stevenson SJ, Anderson AB, Grissom JE, Laux DC, Cohen PS: **Carbon nutrition of Escherichia coli in the mouse intestine.** *Proceedings of the National Academy of Sciences of the United States of America* 2004, **101**(19):7427-7432.
6. Fryklund B, Berglund B, Burman L, Tullus K: **Importance of the environment and the faecal flora of infants, nursing staff and parents as sources of gram-negative bacteria colonizing newborns in three neonatal wards.** *Infection* 1992, **20**(5):253-257.
7. Nowrouzian F, Hesselmar B, Saalman R, Strannegard I-L, Aberg N, Wold AE, Adlerberth I: **Escherichia coli in Infants' Intestinal Microflora: Colonization Rate, Strain Turnover, and Virulence Gene Carriage.** *Pediatr Res* 2003, **54**(1):8-14.
8. Mitsuoka T, Hayakawa K: **The fecal flora in man. I. Composition of the fecal flora of various age groups.** *Zentralblatt fur Bakteriologie, Parasitenkunde, Infektionskrankheiten und Hygiene Erste Abteilung Originale Reihe A: Medizinische Mikrobiologie und Parasitologie* 1973, **223**(2):333-342.
9. Tenaillon O, Skurnik D, Picard B, Denamur E: **The population genetics of commensal Escherichia coli.** *Nat Rev Micro* 2010, **8**(3):207-217.
10. Zhang Y, Laing C, Steele M, Ziebell K, Johnson R, Benson AK, Taboada E, Gannon VPJ: **Genome evolution in major Escherichia coli O157:H7 lineages.** *BMC Genomics* 2007, **8**:121-121.
11. Vanaja SK, Springman AC, Besser TE, Whittam TS, Manning SD: **Differential expression of virulence and stress fitness genes between Escherichia coli O157: H7 strains with clinical or bovine-biased genotypes.** *Applied and Environmental Microbiology* 2010, **76**(1):60-68.
12. Karmali MA, Gannon V, Sargeant JM: **Verocytotoxin-producing Escherichia coli (VTEC).** *Veterinary Microbiology* 2010, **140**(3-4):360-370.
13. Spears KJ, Roe AJ, Gally DL: **A comparison of enteropathogenic and enterohaemorrhagic Escherichia coli pathogenesis.** *FEMS Microbiology Letters* 2006, **255**(2):187-202.
14. Qadri F, Svennerholm A-M, Faruque A, Sack RB: **Enterotoxigenic Escherichia coli in developing countries: epidemiology, microbiology,**

- clinical features, treatment, and prevention.** *Clinical Microbiology Reviews* 2005, **18**(3):465-483.
15. Adachi JA, Jiang Z-D, Mathewson JJ, Verenkar MP, Thompson S, Martinez-Sandoval F, Steffen R, Ericsson CD, DuPont HL: **Enteroaggregative Escherichia coli as a major etiologic agent in traveler's diarrhea in 3 regions of the world.** *Clinical Infectious Diseases* 2001, **32**(12):1706-1709.
 16. Tarr PI: **Escherichia coli O157:H7: Clinical, Diagnostic, and Epidemiological Aspects of Human Infection.** *Clinical Infectious Diseases* 1995, **20**(1):1-8.
 17. Scaletsky IC, Fabbriotti SH, Carvalho RL, Nunes CR, Maranhão HS, Morais MB, Fagundes-Neto U: **Diffusely adherent Escherichia coli as a cause of acute diarrhea in young children in Northeast Brazil: a case-control study.** *Journal of clinical microbiology* 2002, **40**(2):645-648.
 18. Kaper JB, Nataro JP, Mobley HL: **Pathogenic Escherichia coli.** *Nature Reviews Microbiology* 2004, **2**(2):123-140.
 19. Nataro JP, Kaper JB: **Diarrheagenic escherichia coli.** *Clinical Microbiology Reviews* 1998, **11**(1):142-201.
 20. Besser M, R.E., Griffin M, P.M., Slutsker M, MPH, L.: **Escherichia coli O157: H7 gastroenteritis and the hemolytic uremic syndrome: An emerging infectious disease** *Annual Review of Medicine* 1999, **50**(1):355-367.
 21. Willshaw GA, Cheasty T, Smith HR, O'Brien SJ, Adak GK: **Verocytotoxin-producing Escherichia coli (VTEC) O157 and other VTEC from human infections in England and Wales: 1995–1998.** *Journal of Medical Microbiology* 2001, **50**(2):135-142.
 22. Cohen MB, Giannella RA: **Hemorrhagic colitis associated with Escherichia coli O157:H7.** *Advances in Internal Medicine* 1991, **37**:173-195.
 23. Boyce TG, Swerdlow DL, Griffin PM: **Escherichia coli O157: H7 and the hemolytic–uremic syndrome.** *New England Journal of Medicine* 1995, **333**(6):364-368.
 24. Michael M, Elliott EJ, Ridley GF, Hodson EM, Craig JC: **Interventions for haemolytic uraemic syndrome and thrombotic thrombocytopenic purpura.** *Cochrane Database Systematic Reviews* 2009.
 25. Pollock KGJ, Young D, Beattie TJ, Todd WTA: **Clinical surveillance of thrombotic microangiopathies in Scotland, 2003-2005.** *Epidemiology and Infection* 2008, **136**(1):115-121.
 26. Banatvala N, Griffin PM, Greene KD, Barrett TJ, Bibb WF, Green JH, Wells JG: **The United States National Prospective Hemolytic Uremic Syndrome Study: microbiologic, serologic, clinical, and epidemiologic findings.** *Journal of Infectious Diseases* 2001, **183**(7):1063-1070.
 27. Gyles CL: **Shiga toxin-producing Escherichia coli: an overview.** *Journal of Animal Science* 2007, **85**(13 Suppl):E45-E62.
 28. La Ragione RM, Best A, Woodward MJ, Wales AD: **Escherichia coli O157: H7 colonization in small domestic ruminants.** *FEMS Microbiology Reviews* 2009, **33**(2):394-410.

29. Paiba GA, Gibbens JC, Pascoe SJS: **Faecal carriage of verotoxin-producing Escherichia coli O157 in cattle and sheep at slaughter in Great Britain.** *Veterinary Record* 2002, **150**(19):593-598.
30. Elder RO, Keen JE, Siragusa GR, Barkocy-Gallagher GA, Koohmaraie M, Laegreid WW: **Correlation of enterohemorrhagic Escherichia coli O157 prevalence in feces, hides, and carcasses of beef cattle during processing.** *Proceedings of the National Academy of Sciences* 2000, **97**(7):2999-3003.
31. Naylor SW, Gally DL, Christopher Low J: **Enterohaemorrhagic E. coli in veterinary medicine.** *International Journal of Medical Microbiology* 2005, **295**(6-7):419-441.
32. Dean-Nystrom EA, Bosworth BT, Cray WC, Moon HW: **Pathogenicity of Escherichia coli O157:H7 in the intestines of neonatal calves.** *Infection and Immunity* 1997, **65**(5):1842-1848.
33. Naylor SW, Low JC, Besser TE, Mahajan A, Gunn GJ, Pearce MC, McKendrick IJ, Smith DGE, Gally DL: **Lymphoid follicle-dense mucosa at the terminal rectum is the principal site of colonization of enterohemorrhagic Escherichia coli O157 : H7 in the bovine host.** *Infection and Immunity* 2003, **71**(3):1505-1512.
34. Jones SA, Jorgensen M, Chowdhury FZ, Rodgers R, Hartline J, Leatham MP, Struve C, Krogfelt KA, Cohen PS, Conway T: **Glycogen and maltose utilization by Escherichia coli O157: H7 in the mouse intestine.** *Infection and Immunity* 2008, **76**(6):2531-2540.
35. Freter R: **Mechanisms of bacterial colonization of the mucosal surfaces of the gut.** In: *Virulence Mechanisms of Bacterial Pathogens.* edn. Washington, D.C.: American Society of Microbiology; 1988: 45-60.
36. Snider TA, Fabich AJ, Conway T, Clinkenbeard KD: **E. coli O157:H7 catabolism of intestinal mucin-derived carbohydrates and colonization.** *Veterinary Microbiology* 2009, **136**(1):150-154.
37. Bertin Y, Chaucheyras - Durand F, Robbe - Masselot C, Durand A, Foye A, Harel J, Cohen PS, Conway T, Forano E, Martin C: **Carbohydrate utilization by enterohaemorrhagic Escherichia coli O157: H7 in bovine intestinal content.** *Environmental Microbiology* 2013, **15**(2):610-622.
38. Fabich AJ, Jones SA, Chowdhury FZ, Cernosek A, Anderson A, Smalley D, McHargue JW, Hightower GA, Smith JT, Autieri SM *et al*: **Comparison of Carbon Nutrition for Pathogenic and Commensal Escherichia coli Strains in the Mouse Intestine.** *Infection and Immunity* 2008, **76**(3):1143-1152.
39. Beckham KSH, Connolly JPR, Ritchie JM, Wang D, Gawthorne JA, Tahoun A, Gally DL, Burgess K, Burchmore RJ, Smith BO: **The metabolic enzyme AdhE controls the virulence of Escherichia coli O157: H7.** *Molecular Microbiology* 2014, **93**(1):199-211.
40. Connolly JP, Finlay B, Roe AJ: **From ingestion to colonization: the influence of the host environment on regulation of the LEE encoded type III secretion system in enterohaemorrhagic Escherichia coli.** *Frontiers in Microbiology* 2015, **6**:568.
41. Locking ME, O'Brien SJ, Reilly WJ, Wright EM, Campbell DM, Coia JE, Browning LM, Ramsay CN: **Risk factors for sporadic cases of Escherichia**

- coli O157 infection: the importance of contact with animal excreta.** *Epidemiology and Infection* 2001, **127**(2):215-220.
42. Gyles CL, Prescott JF, Songer G, O'Thoen C: **Pathogenesis of Bacterial Pathogens in Animals.** In., Fourth edn. Ames: Blackwell Publishing; 2010.
 43. Caprioli A, Morabito S, Brugère H, Oswald E: **Enterohaemorrhagic Escherichia coli: emerging issues on virulence and modes of transmission.** *Veterinary research* 2005, **36**(3):289-311.
 44. Hepburn N, MacRae M, Ogden I: **Survival of Escherichia coli O157 in abattoir waste products.** *Letters in Applied Microbiology* 2002, **35**(3):233-236.
 45. Cody SH, Glynn MK, Farrar JA, Cairns KL, Griffin PM, Kobayashi J, Fyfe M, Hoffman R, King AS, Lewis JH: **An outbreak of Escherichia coli O157: H7 infection from unpasteurized commercial apple juice.** *Annals of Internal Medicine* 1999, **130**(3):202-209.
 46. Ackers M-L, Mahon BE, Leahy E, Goode B, Damrow T, Hayes PS, Bibb WF, Rice DH, Barrett TJ, Hutwagner L: **An outbreak of Escherichia coli O157: H7 infections associated with leaf lettuce consumption.** *Journal of Infectious Diseases* 1998, **177**(6):1588-1593.
 47. Michino H, Araki K, Minami S, Takaya S, Sakai N, Miyazaki M, Ono A, Yanagawa H: **Massive outbreak of Escherichia coli O157: H7 infection in schoolchildren in Sakai City, Japan, associated with consumption of white radish sprouts.** *American Journal of Epidemiology* 1999, **150**(8):787-796.
 48. Strachan NJC, Dunn GM, Ogden ID: **Quantitative risk assessment of human infection from Escherichia coli O157 associated with recreational use of animal pasture.** *International Journal of Food Microbiology* 2002, **75**(1):39-51.
 49. Snedeker KG, Shaw DJ, Locking ME, Prescott RJ: **Primary and secondary cases in Escherichia coli O157 outbreaks: a statistical analysis.** *BMC Infectious Diseases* 2009, **9**(1):144.
 50. Rangel JM, Sparling PH, Crowe C, Griffin PM, Swerdlow DL: **Epidemiology of Escherichia coli O157: H7 outbreaks, United States, 1982–2002.** *Emerging Infectious Diseases* 2005, **11**(4).
 51. Riley LW, Remis RS, Helgerson SD, McGee HB, Wells JG, Davis BR, Hebert RJ, Olcott ES, Johnson LM, Hargrett NT *et al*: **Hemorrhagic Colitis Associated with a Rare Escherichia coli Serotype.** *New England Journal of Medicine* 1983, **308**(12):681-685.
 52. O'Brien A, Melton A, Schmitt C, McKee M, Batts M, Griffin D: **Profile of Escherichia coli O157: H7 pathogen responsible for hamburger-borne outbreak of hemorrhagic colitis and hemolytic uremic syndrome in Washington.** *Journal of Clinical Microbiology* 1993, **31**(10):2799-2801.
 53. Bell BP, Goldoft M, Griffin PM, Davis MA, Gordon DC, Tarr PI, Bartleson CA, Lewis JH, Barrett TJ, Wells JG: **A multistate outbreak of Escherichia coli O157:H7-associated bloody diarrhea and hemolytic uremic syndrome from hamburgers. The Washington experience.** *Jama* 1994, **272**(17):1349-1353.

54. Taylor CM, White RH, Winterborn MH, Rowe B: **Haemolytic-uraemic syndrome: clinical experience of an outbreak in the West Midlands.** *BMJ* 1986, **292**(6534):1513-1516.
55. Pennington TH: **E. coli O157 outbreaks in the United Kingdom: past, present, and future.** *Infection and Drug Resistance* 2014, **7**:211-222.
56. Scheutz F, Nielsen EM, Frimodt-Moller J, Boisen N, Morabito S, Tozzoli R, Nataro J, Caprioli A: **Characteristics of the enteroaggregative Shiga toxin/verotoxin-producing Escherichia coli O104: H4 strain causing the outbreak of haemolytic uraemic syndrome in Germany, May to June 2011.** *Euro surveill* 2011, **16**(24):19889.
57. Hayashi T, Makino K, Ohnishi M, Kurokawa K, Ishii K, Yokoyama K, Han C-G, Ohtsubo E, Nakayama K, Murata T *et al*: **Complete Genome Sequence of Enterohemorrhagic Escherichia coli O157:H7 and Genomic Comparison with a Laboratory Strain K-12.** *DNA Research* 2001, **8**(1):11-22.
58. Perna NT, Plunkett G, 3rd, Burland V, Mau B, Glasner JD, Rose DJ, Mayhew GF, Evans PS, Gregor J, Kirkpatrick HA *et al*: **Genome sequence of enterohaemorrhagic Escherichia coli O157:H7.** *Nature* 2001, **409**(6819):529-533.
59. Strachan NJ, Dunn GM, Locking ME, Reid TM, Ogden ID: **Escherichia coli O157: Burger bug or environmental pathogen?** *International journal of food microbiology* 2006, **112**(2):129-137.
60. Chase-Topping M, Gally D, Low C, Matthews L, Woolhouse M: **Super-shedding and the link between human infection and livestock carriage of Escherichia coli O157.** *Nat Rev Micro* 2008, **6**(12):904-912.
61. Halliday JE, Chase-Topping ME, Pearce MC, McKendrick IJ, Allison L, Fenlon D, Low C, Mellor DJ, Gunn GJ, Woolhouse ME: **Herd-level risk factors associated with the presence of Phage type 21/28 E. coli O157 on Scottish cattle farms.** *BMC microbiology* 2006, **6**(1):99.
62. Sanz M, Viñas M, Parma A: **Prevalence of bovine verotoxin-producing Escherichia coli in Argentina.** *European journal of epidemiology* 1998, **14**(4):399-403.
63. Garvey P, McKeown P, Carroll A, McNamara E: **Epidemiology of Verotoxigenic E. coli in Ireland, 2005.** *Epi-Insight* 2006, **7**(9):2-3.
64. Pearce MC, Chase-Topping ME, McKendrick IJ, Mellor DJ, Locking ME, Allison L, Ternent HE, Matthews L, Knight HI, Smith AW: **Temporal and spatial patterns of bovine Escherichia coli O157 prevalence and comparison of temporal changes in the patterns of phage types associated with bovine shedding and human E. coli O157 cases in Scotland between 1998-2000 and 2002-2004.** *BMC microbiology* 2009, **9**(1):276.
65. Gunn G, McKendrick I, Ternent H, Thomson-Carter F, Foster G, Synge B: **An investigation of factors associated with the prevalence of verocytotoxin producing Escherichia coli O157 shedding in Scottish beef cattle.** *The Veterinary Journal* 2007, **174**(3):554-564.
66. Chase-Topping ME, McKendrick IJ, Pearce MC, MacDonald P, Matthews L, Halliday J, Allison L, Fenlon D, Low JC, Gunn G: **Risk factors for the**

- presence of high-level shedders of *Escherichia coli* O157 on Scottish farms. *Journal of clinical microbiology* 2007, **45**(5):1594-1603.
67. Money P, Kelly A, Gould S, Denholm - Price J, Threlfall E, Fielder M: **Cattle, weather and water: mapping *Escherichia coli* O157: H7 infections in humans in England and Scotland.** *Environmental microbiology* 2010, **12**(10):2633-2644.
 68. Lynn RM, O'Brien SJ, Taylor CM, Adak GK, Adak GK, Chart H, Cheasty T, Coia JE, Gillespie IA, Locking ME *et al*: **Childhood hemolytic uremic syndrome, United Kingdom and Ireland.** *Emerging Infectious Diseases* 2005, **11**(4):590-596.
 69. Fuller CA, Pellino CA, Flagler MJ, Strasser JE, Weiss AA: **Shiga Toxin Subtypes Display Dramatic Differences in Potency.** *Infection and Immunity* 2011, **79**(3):1329-1337.
 70. Zhang Y, Laing C, Zhang Z, Hallewell J, You C, Ziebell K, Johnson RP, Kropinski AM, Thomas JE, Karmali M *et al*: **Lineage and Host Source Are Both Correlated with Levels of Shiga Toxin 2 Production by *Escherichia coli* O157:H7 Strains.** *Applied and Environmental Microbiology* 2010, **76**(2):474-482.
 71. Matthews L, Reeve R, Gally DL, Low JC, Woolhouse MEJ, McAteer SP, Locking ME, Chase-Topping ME, Haydon DT, Allison LJ *et al*: **Predicting the public health benefit of vaccinating cattle against *Escherichia coli* O157.** *Proceedings of the National Academy of Sciences* 2013, **110**(40):16265-16270.
 72. Feng P, Lampel KA, Karch H, Whittam TS: **Genotypic and phenotypic changes in the emergence of *Escherichia coli* O157: H7.** *Journal of Infectious Diseases* 1998, **177**(6):1750-1753.
 73. Cowley L, Beckett S, Chase-Topping M, Perry N, Dallman T, Gally D, Jenkins C: **Analysis of whole genome sequencing for the *Escherichia coli* O157:H7 typing phages.** *BMC Genomics* 2015, **16**(1):1-13.
 74. Kim J, Nietfeldt J, Benson AK: **Octamer-based genome scanning distinguishes a unique subpopulation of *Escherichia coli* O157:H7 strains in cattle.** *Proceedings of the National Academy of Sciences* 1999, **96**(23):13288-13293.
 75. Dowd SE, Ishizaki H: **Microarray based comparison of two *Escherichia coli* O157: H7 lineages.** *BMC microbiology* 2006, **6**(1):30.
 76. Laing CR, Buchanan C, Taboada EN, Zhang Y, Karmali MA, Thomas JE, Gannon VP: **In silico genomic analyses reveal three distinct lineages of *Escherichia coli* O157: H7, one of which is associated with hypervirulence.** *BMC Genomics* 2009, **10**(1):287.
 77. Shringi S, Schmidt C, Katherine K, Brayton KA, Hancock DD, Besser TE: **Carriage of *stx2a* Differentiates Clinical and Bovine-Biased Strains of *Escherichia coli* O157.** *PLoS One* 2012, **7**(12):e51572.
 78. Lowe RMS, Baines D, Selinger LB, Thomas JE, McAllister TA, Sharma R: ***Escherichia coli* O157:H7 Strain Origin, Lineage, and Shiga Toxin 2 Expression Affect Colonization of Cattle.** *Applied and Environmental Microbiology* 2009, **75**(15):5074-5081.

79. Eppinger M, Mammel MK, Leclerc JE, Ravel JF, Cebula TA: **Genome signatures of Escherichia coli O157:H7 isolates from the bovine host reservoir.** *Applied and Environmental Microbiology* 2011, **77**(9):2916-2925.
80. Kyle JL, Cummings CA, Parker CT, Quinones B, Vatta P, Newton E, Huynh S, Swimley M, Degoricija L, Fontanoz S *et al*: **Escherichia coli serotype O55:H7 diversity supports parallel acquisition of bacteriophage at Shiga toxin phage insertion sites during evolution of the O157:H7 lineage.** *Journal of Bacteriology* 2012, **194**(8):1885-1896.
81. Bielaszewska M, Prager R, Köck R, Mellmann A, Zhang W, Tschäpe H, Tarr PI, Karch H: **Shiga Toxin Gene Loss and Transfer In Vitro and In Vivo during Enterohemorrhagic Escherichia coli O26 Infection in Humans.** *Applied and Environmental Microbiology* 2007, **73**(10):3144-3150.
82. Beutin L, Hammerl JA, Reetz J, Strauch E: **Shiga toxin-producing Escherichia coli strains from cattle as a source of the Stx2a bacteriophages present in enteroaggregative Escherichia coli O104: H4 strains.** *International Journal of Medical Microbiology* 2013, **303**(8):595-602.
83. Martínez-Castillo A, Muniesa M: **Implications of free Shiga toxin-converting bacteriophages occurring outside bacteria for the evolution and the detection of Shiga toxin-producing Escherichia coli.** *Frontiers in cellular and infection microbiology* 2014, **4**.
84. Allué-Guardia A, Martínez-Castillo A, Muniesa M: **Persistence of infectious Shiga toxin-encoding bacteriophages after disinfection treatments.** *Applied and environmental microbiology* 2014, **80**(7):2142-2149.
85. Timothy Dallman PMA, Lisa Byrne, Neil Perry, Liljana Petrovska, Richard Ellis, Lesley Allison, Mary Hanson, Anne Holmes, George J.Gunn, Margo E. ChaseJTopping, Mark E.J.Woolhouse, Kathie Grant , David L.Gally, John Wain , Claire Jenkins: **Phylogenomics of STEC O157:H7 demonstrates recent strain replacement in the cattle population in the United Kingdom.** In.; 2015.
86. Keusch GT, Jacewicz M: **The pathogenesis of Shigella diarrhea. V. Relationship of Shiga enterotoxin, neurotoxin, and cytotoxin.** *Journal of Infectious Diseases* 1975, **131**(Supplement):S33-S39.
87. Keusch GT, Grady GF, Mata LJ, McIver J: **The pathogenesis of Shigella Diarrhea: I. Enterotoxin production by Shigella dysenteriae 1.** *Journal of Clinical Investigation* 1972, **51**(5):1212.
88. Trofa AF, Ueno-Olsen H, Oiwa R, Yoshikawa M: **Dr. Kiyoshi Shiga: discoverer of the dysentery bacillus.** *Clinical infectious diseases* 1999, **29**(5):1303-1306.
89. Griffin PM, Tauxe RV: **The epidemiology of infections caused by Escherichia coli O157:H7, other enterohemorrhagic E. coli, and the associated hemolytic uremic syndrome.** *Epidemiologic Reviews* 1991, **12**(1):60-98.
90. Griffin PM, Ostroff SM, Tauxe RV, Greene KD, Wells JG, Lewis JH, Blake PA: **Illnesses associated with Escherichia coli O157:H7 infections. A broad clinical spectrum.** *Annals of Internal Medicine* 1988, **109**(9):705-712.
91. Mauro SA, Koudelka GB: **Shiga Toxin: Expression, Distribution, and Its Role in the Environment.** *Toxins* 2011, **3**(6):608-625.

92. Herold S, Karch H, Schmidt H: **Shiga toxin-encoding bacteriophages—genomes in motion.** *International journal of medical microbiology* 2004, **294**(2):115-121.
93. Muniesa M, Blanco JE, de Simón M, Serra-Moreno R, Blanch AR, Jofre J: **Diversity of stx2 converting bacteriophages induced from Shiga-toxin-producing Escherichia coli strains isolated from cattle.** *Microbiology* 2004, **150**(9):2959-2971.
94. García-Aljaro C, Muniesa M, Jofre J, Blanch AR: **Genotypic and phenotypic diversity among induced, stx2-carrying bacteriophages from environmental Escherichia coli strains.** *Applied and environmental microbiology* 2009, **75**(2):329-336.
95. Krüger A, Lucchesi PM: **Shiga toxins and stx phages: highly diverse entities.** *Microbiology* 2015, **161**(Pt 3):451-462.
96. Fortier L-C, Sekulovic O: **Importance of prophages to evolution and virulence of bacterial pathogens.** *Virulence* 2013, **4**(5):354-365.
97. James CE, Stanley KN, Allison HE, Flint HJ, Stewart CS, Sharp RJ, Saunders JR, McCarthy AJ: **Lytic and Lysogenic Infection of Diverse Escherichia coli and Shigella Strains with a Verocytotoxigenic Bacteriophage.** *Applied and environmental microbiology* 2001, **67**(9):4335-4337.
98. Allison HE: **Stx-phages: drivers and mediators of the evolution of STEC and STEC-like pathogens.** *Future Microbiology* 2007, **2**(2):165-174.
99. Barondess JJ, Beckwith J: **A bacterial virulence determinant encoded by lysogenic coliphage lambda.** *Nature* 1990, **346**(6287):871-874.
100. Brzuszkiewicz E, Thürmer A, Schuldes J, Leimbach A, Liesegang H, Meyer F-D, Boelter J, Petersen H, Gottschalk G, Daniel R: **Genome sequence analyses of two isolates from the recent Escherichia coli outbreak in Germany reveal the emergence of a new pathotype: Enterohemorrhagic Escherichia coli (EAHEC).** *Archives of microbiology* 2011, **193**(12):883-891.
101. Calderwood SB, and Mekalanos, J.J. : **Iron regulation of Shiga-like toxin expression in Escherichia coli is mediated by the fur locus.** *Journal of Bacteriology* 1987, **169**:4759-4764.
102. Sung LM, Jackson, M.P., O'Brien, A.D., and Holmes, R.K.: **Transcription of the Shiga-like toxin type II and Shiga-like toxin type II variant operons of Escherichia coli.** *Journal of Bacteriology* 1990, **172**:6386-6395.
103. Wagner PL, Neely MN, Zhang X, Acheson DWK, Waldor MK, Friedman DI: **Role for a Phage Promoter in Shiga Toxin 2 Expression from a Pathogenic Escherichia coli Strain.** *Journal of Bacteriology* 2001, **183**(6):2081-2085.
104. Wagner PL, Livny J, Neely MN, Acheson DWK, Friedman DI, Waldor MK: **Bacteriophage control of Shiga toxin 1 production and release by Escherichia coli.** *Molecular Microbiology* 2002, **44**(4):957-970.
105. Sperandio V, Pacheco AR: **Shiga Toxin in Enterohemorrhagic E.coli: regulation and novel antivirulence strategies.** *Frontiers in Cellular and Infection Microbiology* 2012, **2**(81):1-12.
106. Schmidt H: **Shiga-toxin-converting bacteriophages.** *Research in microbiology* 2001, **152**(8):687-695.

107. Wong CS, Jelacic S, Habeeb RL, Watkins SL, Tarr PI: **The risk of the hemolytic-uremic syndrome after antibiotic treatment of Escherichia coli O157:H7 infections.** *New England Journal of Medicine* 2000, **342**(26):1930-1936.
108. Shimizu T, Ohta, Y., & Noda, M. : **Shiga Toxin 2 Is Specifically Released from Bacterial Cells by Two Different Mechanisms.** *Infection and Immunity* 2009, **77**(7):2813-2823.
109. Strockbine NA, Marques L, Newland JW, Smith HW, Holmes RK, O'brien AD: **Two toxin-converting phages from Escherichia coli O157: H7 strain 933 encode antigenically distinct toxins with similar biologic activities.** *Infection and Immunity* 1986, **53**(1):135-140.
110. O'Loughlin EV, Robins-Browne RM: **Effect of Shiga toxin and Shiga-like toxins on eukaryotic cells.** *Microbes and Infection* 2001, **3**(6):493-507.
111. Lingwood CA, Binnington B, Manis A, Branch DR: **Globotriaosyl ceramide receptor function - Where membrane structure and pathology intersect.** *Febs Letters* 2010, **584**(9):1879-1886.
112. Melton-Celsa AR: **Shiga Toxin (Stx) Classification, Structure, and Function.** *Microbiol Spectr* 2014, **2**(2):1-21.
113. Odumosu O, Nicholas D, Yano H, Langridge W: **AB Toxins: A Paradigm Switch from Deadly to Desirable.** *Toxins* 2010, **2**(7):1612-1645.
114. Waddell T, Head S, Petric M, Cohen A, Lingwood C: **Globotriaosyl ceramide is specifically recognized by the Escherichia coli verocytotoxin 2.** *Biochemical and biophysical research communications* 1988, **152**(2):674-679.
115. DeGrandis S, Law H, Brunton J, Gyles C, Lingwood C: **Globotetraosylceramide is recognized by the pig edema disease toxin.** *Journal of Biological Chemistry* 1989, **264**(21):12520-12525.
116. Schnaar RL SA, Stanley P: **Glycosphingolipids.** In: *Essentials of Glycobiology.* Edited by Varki A CR, Esko JD, et al., 2nd edn. Cold Spring Harbor (NY): Cold Spring Harbor Laboratory Press; 2009.
117. Taube S, Jiang M, Wobus CE: **Glycosphingolipids as receptors for non-enveloped viruses.** *Viruses* 2010, **2**(4):1011-1049.
118. Fantini J, Maresca M, Hammache D, Yahi N, Delézay O: **Glycosphingolipid (GSL) microdomains as attachment platforms for host pathogens and their toxins on intestinal epithelial cells: Activation of signal transduction pathways and perturbations of intestinal absorption and secretion.** *Glycoconj J* 2000, **17**(3-4):173-179.
119. Clifford A L: **Role of verotoxin receptors in pathogenesis.** *Trends in Microbiology* 1996, **4**(4):147-153.
120. Maloney MD, Lingwood CA: **CD19 has a potential CD77 (globotriaosyl ceramide)-binding site with sequence similarity to verotoxin B-subunits: implications of molecular mimicry for B cell adhesion and enterohemorrhagic Escherichia coli pathogenesis.** *The Journal of Experimental Medicine* 1994, **180**(1):191-201.
121. Ghislain J, Lingwood CA, Fish EN: **Evidence for glycosphingolipid modification of the type 1 IFN receptor.** *The Journal of Immunology* 1994, **153**(8):3655-3663.

122. Mangeney M, Richard Y, Coulaud D, Tursz T, Wiels J: **CD77: an antigen of germinal center B cells entering apoptosis.** *European Journal of Immunology* 1991, **21**(5):1131-1140.
123. Johansson D, Kosovac E, Moharer J, Ljuslinder I, Brännström T, Johansson A, Behnam-Motlagh P: **Expression of verotoxin-1 receptor Gb3 in breast cancer tissue and verotoxin-1 signal transduction to apoptosis.** *BMC Cancer* 2009, **9**(1):67.
124. Furukawa K, Yokoyama K, Sato T, Wiels J, Hirayama Y, Ohta M, Furukawa K: **Expression of the Gb3/CD77 Synthase Gene in Megakaryoblastic Leukemia Cells-Implication in the Sensitivity to Verotoxins.** *Journal of Biological Chemistry* 2002, **277**(13):11247-11254.
125. Mangeney M, Lingwood CA, Taga S, Caillou B, Tursz T, Wiels J: **Apoptosis induced in Burkitt's lymphoma cells via Gb3/CD77, a glycolipid antigen.** *Cancer Research* 1993, **53**(21):5314-5319.
126. Falguières T, Maak M, von Weyhern C, Sarr M, Sastre X, Poupon M-F, Robine S, Johannes L, Janssen K-P: **Human colorectal tumors and metastases express Gb3 and can be targeted by an intestinal pathogen-based delivery tool.** *Molecular cancer therapeutics* 2008, **7**(8):2498-2508.
127. Arab S, Murakami M, Dirks P, Boyd B, Hubbard SL, Lingwood CA, Rutka JT: **Verotoxins inhibit the growth of and induce apoptosis in human astrocytoma cells.** *Journal of Neuro-oncology* 1998, **40**(2):137-150.
128. Kovbasnjuk O, Mourtazina R, Baibakov B, Wang T, Elowsky C, Choti MA, Kane A, Donowitz M: **The glycosphingolipid globotriaosylceramide in the metastatic transformation of colon cancer.** *Proceedings of the National Academy of Sciences of the United States of America* 2005, **102**(52):19087.
129. Okuda T, Tokuda N, Numata S-i, Ito M, Ohta M, Kawamura K, Wiels J, Urano T, Tajima O, Furukawa K *et al*: **Targeted Disruption of Gb3/CD77 Synthase Gene Resulted in the Complete Deletion of Globo-series Glycosphingolipids and Loss of Sensitivity to Verotoxins.** *Journal of Biological Chemistry* 2006, **281**(15):10230-10235.
130. Obrig TG, Seaner RM, Bentz M, Lingwood CA, Boyd B, Smith A, Narrow W: **Induction by Sphingomyelinase of Shiga Toxin Receptor and Shiga Toxin 2 Sensitivity in Human Microvascular Endothelial Cells.** *Infection and Immunity* 2003, **71**(2):845-849.
131. Pellizzari A, Pang H, Lingwood CA: **Binding of verocytotoxin 1 to its receptor is influenced by differences in receptor fatty acid content.** *Biochemistry* 1992, **31**(5):1363-1370.
132. Kiarash A, Boyd B, Lingwood CA: **Glycosphingolipid receptor function is modified by fatty acid content. Verotoxin 1 and verotoxin 2c preferentially recognize different globotriaosyl ceramide fatty acid homologues.** *Journal of Biological Chemistry* 1994, **269**(15):11138-11146.
133. Shin IS, Ishii S, Shin J, Sung K, Park B, Jang H, Kim B: **Globotriaosylceramide (Gb3) content in HeLa cells is correlated to Shiga toxin-induced cytotoxicity and Gb3 synthase expression.** *BMB reports* 2009, **42**(5):310.
134. Lingwood CA: **Role of verotoxin receptors in pathogenesis.** *Trends in Microbiology* 1996, **4**(4):147-153.

135. Khan F, Proulx F, Lingwood CA: **Detergent-resistant globotriaosyl ceramide may define verotoxin/glomeruli-restricted hemolytic uremic syndrome pathology.** *Kidney International* 2009, **75**(11):1209-1216.
136. Kovbasnjuk O, Edidin M, Donowitz M: **Role of lipid rafts in Shiga toxin 1 interaction with the apical surface of Caco-2 cells.** *Journal of Cell Science* 2001, **114**(22):4025.
137. Stricklett PK, Hughes AK, Ergonul Z, Kohan DE: **Molecular Basis for Up-Regulation by Inflammatory Cytokines of Shiga Toxin 1 Cytotoxicity and Globotriaosylceramide Expression.** *Journal of Infectious Diseases* 2002, **186**(7):976-982.
138. Kojima Y, Fukumoto S, Furukawa K, Okajima T, Wiels J, Yokoyama K, Suzuki Y, Urano T, Ohta M, Furukawa K: **Molecular Cloning of Globotriaosylceramide/CD77 Synthase, a Glycosyltransferase That Initiates the Synthesis of Globo Series Glycosphingolipids.** *Journal of Biological Chemistry* 2000, **275**(20):15152-15156.
139. Raa H, Grimmer S, Schwudke D, Bergan J, Wälchli S, Skotland T, Shevchenko A, Sandvig K: **Glycosphingolipid Requirements for Endosome-to-Golgi Transport of Shiga Toxin.** *Traffic* 2009, **10**(7):868-882.
140. Sandvig K, van Deurs B: **Entry of ricin and Shiga toxin into cells: molecular mechanisms and medical perspectives.** *Embo Journal* 2000, **19**(22):5943-5950.
141. Sandvig K, van Deurs B: **Endocytosis and intracellular sorting of ricin and Shiga toxin.** *FEBS letters* 1994, **346**(1):99-102.
142. Hoey DEE, Sharp L, Currie C, Lingwood CA, Gally DL, Smith DGE: **Verotoxin 1 binding to intestinal crypt epithelial cells results in localization to lysosomes and abrogation of toxicity.** *Cellular Microbiology* 2003, **5**(2):85-97.
143. Sandvig K: **Shiga toxins.** *Toxicon* 2001, **39**(11):1629-1635.
144. Sandvig K, Garred Ø, Prydz K, Kozlov JV, Hansen SH, van Deurs B: **Retrograde transport of endocytosed Shiga toxin to the endoplasmic reticulum.** 1992.
145. Sandvig K, Grimmer S, Lauvrak S, Torgersen M, Skretting G, van Deurs B, Iversen T: **Pathways followed by ricin and Shiga toxin into cells.** *Histochemistry and cell biology* 2002, **117**(2):131-141.
146. Johannes L, Römer W: **Shiga toxins—from cell biology to biomedical applications.** *Nature Reviews Microbiology* 2009, **8**(2):105-116.
147. Siegler RL, Obrig TG, Pysher TJ, Tesh VL, Denkers ND, Taylor FB: **Response to Shiga toxin 1 and 2 in a baboon model of hemolytic uremic syndrome.** *Pediatric Nephrology* 2003, **18**(2):92-96.
148. Rivas M, Miliwebsky E, Chinen I, Roldan C, Balbi L, Garcia B, Fiorilli G, Sosa-Estani S, Kincaid J, Rangel J: **Characterization and epidemiologic subtyping of Shiga toxin-producing Escherichia coli strains isolated from hemolytic uremic syndrome and diarrhea cases in Argentina.** *Foodborne Pathogens & Disease* 2006, **3**(1):88-96.
149. Gault G, Weill F, Mariani-Kurkdjian P, Jourdan-da Silva N, King L, Aldabe B, Charron M, Ong N, Castor C, Mace M: **Outbreak of haemolytic uraemic**

- syndrome and bloody diarrhoea due to *Escherichia coli* O104: H4, south-west France, June 2011. *Euro Surveill* 2011, **16**(26):Article2.
150. Keepers TR, Pstotka MA, Gross LK, Obrig TG: **A Murine Model of HUS: Shiga Toxin with Lipopolysaccharide Mimics the Renal Damage and Physiologic Response of Human Disease.** *Journal of the American Society of Nephrology* 2006, **17**(12):3404-3414.
 151. Stearns-Kurosawa DJ, Oh S-Y, Cherla RP, Lee M-S, Tesh VL, Papin J, Henderson J, Kurosawa S: **Distinct Renal Pathology and a Chemotactic Phenotype after Enterohemorrhagic *Escherichia coli* Shiga Toxins in Non-Human Primate Models of Hemolytic Uremic Syndrome.** *The American Journal of Pathology* 2013, **182**(4):1227-1238.
 152. Tesh VL, Burris J, Owens J, Gordon V, Wadolkowski E, O'brien A, Samuel J: **Comparison of the relative toxicities of Shiga-like toxins type I and type II for mice.** *Infection and Immunity* 1993, **61**(8):3392-3402.
 153. Holgersson J, Jovall PÅ, Breimer ME: **Glycosphingolipids of human large intestine: detailed structural characterization with special reference to blood group compounds and bacterial receptor structures.** *Journal of biochemistry* 1991, **110**(1):120.
 154. Philpott DJ, Ackerley CA, Kiliaan AJ, Karmali MA, Perdue MH, Sherman PM: **Translocation of verotoxin-1 across T84 monolayers: mechanism of bacterial toxin penetration of epithelium.** *Infection and Immunity* 1998, **66**(4):1680-1687.
 155. Yamasaki C, Natori Y, Zeng XT, Ohmura M, Yamasaki S, Takeda Y: **Induction of cytokines in a human colon epithelial cell line by Shiga toxin 1 (Stx1) and Stx2 but not by non-toxic mutant Stx1 which lacks N-glycosidase activity.** *FEBS letters* 1999, **442**(2-3):231-234.
 156. Smith WE, Kane AV, Campbell ST, Acheson DWK, Cochran BH, Thorpe CM: **Shiga Toxin 1 Triggers a Ribotoxic Stress Response Leading to p38 and JNK Activation and Induction of Apoptosis in Intestinal Epithelial Cells.** *Infection and immunity* 2003, **71**(3):1497-1504.
 157. Acheson DW, Moore R, De Breucker S, Lincicome L, Jacewicz M, Skutelsky E, Keusch GT: **Translocation of Shiga toxin across polarized intestinal cells in tissue culture.** *Infection and Immunity* 1996, **64**(8):3294-3300.
 158. Hurley BP, Jacewicz M, Thorpe CM, Lincicome LL, King AJ, Keusch GT, Acheson DWK: **Shiga Toxins 1 and 2 Translocate Differently across Polarized Intestinal Epithelial Cells.** *Infection and Immunity* 1999, **67**(12):6670-6677.
 159. Schuller S, Frankel G, Phillips AD: **Interaction of Shiga toxin from *Escherichia coli* with human intestinal epithelial cell lines and explants: Stx2 induces epithelial damage in organ culture.** *Cellular Microbiology* 2004, **6**(3):289-301.
 160. Hurley BP, Thorpe CM, Acheson DWK: **Shiga Toxin Translocation across Intestinal Epithelial Cells Is Enhanced by Neutrophil Transmigration.** *Infection and Immunity* 2001, **69**(10):6148-6155.
 161. Schuller S, Heuschkel R, Torrente F, Kaper JB, Phillips AD: **Shiga toxin binding in normal and inflamed human intestinal mucosa.** *Microbes and Infection* 2007, **9**(1):35-39.

162. Malyukova I, Murray KF, Zhu C, Boedeker E, Kane A, Patterson K, Peterson JR, Donowitz M, Kovbasnjuk O: **Macropinocytosis in Shiga toxin 1 uptake by human intestinal epithelial cells and transcellular transcytosis.** *American Journal of Physiology-Gastrointestinal and Liver Physiology* 2009, **296**(1):G78-G92.
163. Lukyanenko V, Malyukova I, Hubbard A, Delannoy M, Boedeker E, Zhu C, Cebotaru L, Kovbasnjuk O: **Enterohemorrhagic Escherichia coli infection stimulates Shiga toxin 1 macropinocytosis and transcytosis across intestinal epithelial cells.** *American Journal of Physiology-Cell Physiology* 2011, **301**(5):C1140-1149.
164. Garcia-del Portillo F, Finlay BB: **Salmonella invasion of nonphagocytic cells induces formation of macropinosomes in the host cell.** *Infection and Immunity* 1994, **62**(10):4641-4645.
165. Tran S-L, Billoud L, Lewis SB, Phillips AD, Schüller S: **Shiga toxin production and translocation during microaerobic human colonic infection with Shiga toxin-producing E.coli O157:H7 and O104:H4.** *Cellular Microbiology* 2014, **16**(8):1255-1266.
166. Pai C, Gordon R, Sims HV, Bryan LE: **Sporadic cases of hemorrhagic colitis associated with Escherichia coli O157:H7. Clinical, epidemiologic, and bacteriologic features.** *Annals of Internal Medicine* 1984, **101**(6):738-742.
167. Slutsker L, Ries AA, Greene KD, Wells JG, Hutwagner L, Griffin PM: **Escherichia coli O157:H7 diarrhea in the United States: clinical and epidemiologic features.** *Annals of Internal Medicine* 1997, **126**(7):505-513.
168. Desai M, Crawley-Boevey E, Verlander NQ, Brock A, Fraser G, Wade J, Heathcock R: **Factors associated with prolonged Escherichia coli O157 infection in a school outbreak.** *Public Health* 2013, **127**(6):582-585.
169. Arab S, Lingwood CA: **Intracellular targeting of the endoplasmic reticulum/nuclear envelope by retrograde transport may determine cell hypersensitivity to verotoxin via globotriaosyl ceramide fatty acid isoform traffic.** *Journal of Cellular Physiology* 1998, **177**(4):646-660.
170. Albanese A, Gerhardt E, Garcia H, Amigo N, Cataldi A, Zotta E, Ibarra C: **Inhibition of water absorption and selective damage to human colonic mucosa induced by Shiga toxin-2 are enhanced by Escherichia coli O157:H7 infection.** *International Journal of Medical Microbiology* 2015, **305**(3):348-354.
171. Fiorito P, Burgos J, Miyakawa M, Rivas M, Chillemi G, Berkowski D, Zotta E, Silberstein C, Ibarra C: **Effect of Shiga Toxin 2 on Water and Ion Transport in Human Colon In Vitro.** *Dig Dis Sci* 2000, **45**(3):480-486.
172. Creydt VP, Miyakawa MF, Martín F, Zotta E, Silberstein C, Ibarra C: **The Shiga toxin 2 B subunit inhibits net fluid absorption in human colon and elicits fluid accumulation in rat colon loops.** *Brazilian Journal of Medical and Biological Research* 2004, **37**:799-808.
173. Mead PS, Griffin PM: **Escherichia coli O157: H7.** *The Lancet* 1998, **352**(9135):1207-1212.
174. Griener TP, Mulvey, G. L., Marcato, P., Armstrong, G. D.: **Differential binding of Shiga toxin 2 to human and murine neutrophils.** *Journal of Medical Microbiology* 2007, **56**:1423-1430.

175. Brigotti M, Tazzari, P.L., Ravanelli, E., Carnicelli, D., Barbieri, S., Rocchi, L., Arfilli, V., Scavia, G., Ricci, F., Bontadini, A. and Alfieri, R.R.: **Endothelial damage induced by Shiga toxins delivered by neutrophils during transmigration.** *Journal of Leukocyte Biology* 2010, **88**(1):201-210.
176. Tania N Petruzzello-Pellegrini MM-N, Philip A Marsden **New insights into Shiga toxin-mediated endothelial dysfunction in hemolytic uremic syndrome.** *Virulence* 2013, **4**(6):556-563.
177. Louise CB, Obrig TG: **Shiga toxin-associated hemolytic-uremic syndrome: combined cytotoxic effects of Shiga toxin, interleukin-1 beta, and tumor necrosis factor alpha on human vascular endothelial cells in vitro.** *Infection and Immunity* 1991, **59**(11):4173-4179.
178. Petruzzello-Pellegrini TN YD, Page AV, Patel S, Soltyk AM, Matouk CC, Wong DK, Turgeon PJ, Fish JE, Ho JJ, et al. : **The CXCR4/CXCR7/SDF-1 pathway contributes to the pathogenesis of Shiga toxin-associated hemolytic uremic syndrome in humans and mice.** *Journal of Clinical Investigation* 2012, **122**:759-776.
179. Panicot-Dubois L TG, Furie BC, Furie B, Lombardo D, Dubois C.: **Bile salt-dependent lipase interacts with platelet CXCR4 and modulates thrombus formation in mice and humans.** *Journal of Clinical Investigation* 2007, **117**:3708-3719.
180. Nolasco LH TN, Bernardo A, Tao Z, Cleary TG, Dong JF, Moake JL. : **Hemolytic uremic syndrome-associated Shiga toxins promote endothelial cell secretion and impair ADAMTS13 cleavage of unusually large von Willebrand factor multimers.** *Blood* 2005, **106**:4199-4209.
181. Morigi M ZC, Figliuzzi M, Foppolo M, Micheletti G, Bontempelli M, Saronni M, Remuzzi G, Remuzzi A. : **Fluid shear stress modulates surface expression of adhesion molecules by endothelial cells.** *Blood* 1995, **85**:1696-1703.
182. Morigi M GM, Gastoldi S, Locatelli M, Buelli S, Pezzotta A, Pagani C, Noris M, Gobbi M, Stravalaci M, et al.: **Alternative pathway activation of complement by Shiga toxin promotes exuberant C3a formation that triggers microvascular thrombosis.** *Journal of Immunology* 2011, **187**:172-180.
183. Hughes AK, Ergonul Z, Stricklett PK, Kohan DE: **Molecular basis for high renal cell sensitivity to the cytotoxic effects of Shiga toxin-1: upregulation of globotriaosylceramide expression.** *Journal of Infectious Diseases* 2002, **187**(7):976-982.
184. Ergonul Z, Clayton F, Fogo AB, Kohan DE: **Shiga toxin-1 binding and receptor expression in human kidneys do not change with age.** *Pediatric Nephrology* 2003, **18**(3):246-253.
185. Eisenhauer PB, Chaturvedi P, Fine RE, Ritchie AJ, Pober JS, Cleary TG, Newburg DS: **Tumor Necrosis Factor Alpha Increases Human Cerebral Endothelial Cell Gb3 and Sensitivity to Shiga Toxin.** *Infection and Immunity* 2001, **69**(3):1889-1894.
186. Ramegowda B, Samuel JE, Tesh VL: **Interaction of Shiga toxins with human brain microvascular endothelial cells: cytokines as sensitizing agents.** *Journal of Infectious Diseases* 1999, **180**(4):1205-1213.

187. Siegler RL: **Spectrum of extrarenal involvement in postdiarrheal hemolytic-uremic syndrome.** *The Journal of Pediatrics* 1994, **125**(4):511-518.
188. Jacewicz MS, Acheson DWK, Binion DG, West GA, Lincicome LL, Fiocchi C, Keusch GT: **Responses of Human Intestinal Microvascular Endothelial Cells to Shiga Toxins 1 and 2 and Pathogenesis of Hemorrhagic Colitis.** *Infection and Immunity* 1999, **67**(3):1439-1444.
189. Siddiqui B, Whitehead JS, Kim Y: **Glycosphingolipids in human colonic adenocarcinoma.** *Journal of Biological Chemistry* 1978, **253**(7):2168-2175.
190. Zumbun SD, Hanson L, Sinclair JF, Freedy J, Melton-Celsa AR, Rodriguez-Canales J, Hanson JC, O'Brien AD: **Human intestinal tissue and cultured colonic cells contain globotriaosylceramide synthase mRNA and the alternate Shiga toxin receptor globotetraosylceramide.** *Infection and Immunity* 2010, **78**(11):4488-4499.
191. Gallegos KM, Conrady DG, Karve SS, Gunasekera TS, Herr AB, Weiss AA: **Shiga toxin binding to glycolipids and glycans.** *PLoS one* 2012, **7**(2):e30368.
192. Stevens MP, Frankel GM: **The Locus of Enterocyte Effacement and Associated Virulence Factors of Enterohemorrhagic Escherichia coli.** *Microbiol Spectr* 2014, **2**(4):1-25.
193. Garmendia J, Frankel G: **Operon structure and gene expression of the espJ--tccP locus of enterohaemorrhagic Escherichia coli O157:H7.** *FEMS Microbiology Letters* 2005, **247**(2):137-145.
194. Coburn B, Sekirov IF, Finlay BB: **Type III secretion systems and disease.** *Clinical Microbiology Reviews* 2007, **20**(4):535-549.
195. Zhou M, Guo Z, Duan Q, Hardwidge PR, Zhu G: **Escherichia coli type III secretion system 2: a new kind of T3SS?** *Veterinary Research* 2014, **45**(1):32-32.
196. Iyoda S, Watanabe H: **Positive effects of multiple pch genes on expression of the locus of enterocyte effacement genes and adherence of enterohaemorrhagic Escherichia coli O157 : H7 to HEp-2 cells.** *Microbiology* 2004, **150**(7):2357-2571.
197. Kendall MM, Gruber CC, Rasko DA, Hughes DT, Sperandio V: **Hfq virulence regulation in enterohemorrhagic Escherichia coli O157:H7 strain 86-24.** *Journal of Bacteriology* 2011, **193**(24):6843-6851.
198. Sperandio V, Torres AG, Girón JA, Kaper JB: **Quorum Sensing Is a Global Regulatory Mechanism in Enterohemorrhagic Escherichia coli O157:H7.** *Journal of Bacteriology* 2001, **183**(17):5187-5197.
199. Pacheco AR, Curtis MM, Ritchie JM, Munera D, Waldor MK, Moreira CG, Sperandio V: **Fucose sensing regulates bacterial intestinal colonization.** *Nature* 2012, **491**(7427):113-117.
200. Lam H, Oh D-C, Cava F, Takacs CN, Clardy J, de Pedro MA, Waldor MK: **D-amino acids govern stationary phase cell wall remodeling in bacteria.** *Science* 2009, **325**(5947):1552-1555.
201. Reading NC, Rasko DA, Torres AG, Sperandio V: **The two-component system QseEF and the membrane protein QseG link adrenergic and stress sensing to bacterial pathogenesis.** *Proceedings of the National Academy of Sciences* 2009, **106**(14):5889-5894.

202. Sperandio V, Torres AG, Kaper JB: **Quorum sensing Escherichia coli regulators B and C (QseBC): a novel two-component regulatory system involved in the regulation of flagella and motility by quorum sensing in E. coli.** *Molecular Microbiology* 2002, **43**(3):809-821.
203. Pacheco AR: **The Characterization of the Fucose Sensing Kinase (FUSK) and the Fucose Sensing Response Regulator (FUSR) and Their Role in Virulence Regulation in Enterohemorrhagic Escherichia Coli O157: H7.** University of Texas Southwestern; 2013.
204. Abe H, Tatsuno I, Tobe T, Okutani A, Sasakawa C: **Bicarbonate ion stimulates the expression of locus of enterocyte effacement-encoded genes in enterohemorrhagic Escherichia coli O157: H7.** *Infection and Immunity* 2002, **70**(7):3500-3509.
205. Schüller S, Phillips AD: **Microaerobic conditions enhance type III secretion and adherence of enterohaemorrhagic Escherichia coli to polarized human intestinal epithelial cells.** *Environmental Microbiology* 2010, **12**(9):2426-2435.
206. Balkovetz DF, & Katz, J. : **Bacterial invasion by a paracellular route: divide and conquer.** *Microbes and Infection* 2003, **5**(7):613-619.
207. Guttman JA, Li, Y., Wickham, M. E., Deng, W., Vogl, A. W., & Finlay, B. B. : **Attaching and effacing pathogen - induced tight junction disruption in vivo.** *Cellular Microbiology* 2006, **8**(4):634-645.
208. McNamara BP, Koutsouris, A., O'Connell, C. B., Nougayrède, J. P., Sonnenberg, M. S., & Hecht, G. : **Translocated EspF protein from enteropathogenic Escherichia coli disrupts host intestinal barrier function.** *Journal of Clinical Investigation* 2001, **107**(5):621.
209. Viswanathan VK, Koutsouris, A., Lukic, S., Pilkinton, M., Simonovic, I., Simonovic, M., & Hecht, G. : **Comparative analysis of EspF from enteropathogenic and enterohemorrhagic Escherichia coli in alteration of epithelial barrier function.** *Infection and Immunity* 2004, **72**(6):3218-3227.
210. Nougayrède JP, & Sonnenberg, M. S.: **Enteropathogenic Escherichia coli EspF is targeted to mitochondria and is required to initiate the mitochondrial death pathway.** *Cellular Microbiology* 2004, **6**(11):1097-1111.
211. Dean P, & Kenny, B. : **Intestinal barrier dysfunction by enteropathogenic Escherichia coli is mediated by two effector molecules and a bacterial surface protein.** *Molecular microbiology*, **54**(3), 665-675. *Molecular Microbiology* 2004, **54**(3):665-675.
212. Garmendia J, Frankel, G., & Crepin, V. F. : **Enteropathogenic and enterohemorrhagic Escherichia coli infections: translocation, translocation, translocation.** *Infection and Immunity* 2005, **73**(5):2573-2585.
213. Erdem AL, Avelino F, Xicohtencatl-Cortes J, Girón JA: **Host protein binding and adhesive properties of H6 and H7 flagella of attaching and effacing Escherichia coli.** *Journal of Bacteriology* 2007, **189**(20):7426-7435.
214. Moens S, Vanderleyden J: **Functions of bacterial flagella.** *Critical Reviews in Microbiology* 1996, **22**(2):67-100.

215. Nash E: **Effect of verotoxin on the bovine intestinal epithelial cell proteome.** University of Edinburgh; 2007.
216. McNeilly TN, Naylor SW, Mahajan A, Mitchell MC, McAteer S, Deane D, Smith DG, Low JC, Gally DL, Huntley JF: **Escherichia coli O157: H7 colonization in cattle following systemic and mucosal immunization with purified H7 flagellin.** *Infection and Immunity* 2008, **76**(6):2594-2602.
217. Xicohtencatl-Cortes J, Monteiro-Neto V, Saldaña Z, Ledesma MA, Puente JL, Girón JA: **The type 4 pili of enterohemorrhagic Escherichia coli O157: H7 are multipurpose structures with pathogenic attributes.** *Journal of Bacteriology* 2009, **191**(1):411-421.
218. Ledesma MA, Ochoa SA, Cruz A, Rocha-Ramirez LM, Mas-Oliva, Eslava CA, Giron JA, Xicohtencatl-Cortes J: **The hemorrhagic coli pilus (HCP) of Escherichia coli O157:H7 is an inducer of proinflammatory cytokine secretion in intestinal epithelial cells.** *PLoS One* 2010, **5**(8):e12127-e12127.
219. Fitzhenry R, Dahan S, Torres AG, Chong Y, Heuschkel R, Murch SF, Thomson M, Thomson M, Kaper JB, Frankel G *et al*: **Long polar fimbriae and tissue tropism in Escherichia coli O157:H7.** *Microbes and Infection* 2006, **8**(7):1741-1749.
220. McWilliams BD, Torres AG: **EHEC Adhesins.** *Microbiol Spectr* 2014, **2**(2):EHEC-0003.
221. Farfan MJ, Cantero LF, Vidal R, Botkin DJ, Torres AG: **Long polar fimbriae of enterohemorrhagic Escherichia coli O157:H7 bind to extracellular matrix proteins.** *Infection and Immunity* 2011, **79**(9):3744-3750.
222. Low AS, Dziva F, Torres AG, Martinez JL, Rosser T, Naylor S, Spears K, Holden N, Mahajan A, Findlay J *et al*: **Cloning, expression, and characterization of fimbrial operon F9 from enterohemorrhagic Escherichia coli O157:H7.** *Infection and Immunity* 2006, **74**(4):2233-2244.
223. Rendon MA, Saldana Z, Erdem AL, Monteiro-Neto V, Vazquez A, Kaper JB, Puente JL, Giron JA: **Commensal and pathogenic Escherichia coli use a common pilus adherence factor for epithelial cell colonization.** *Proceedings of the National Academy of Sciences* 2007, **104**(25):10637-10642.
224. Roe AJ, Currie C, Smith DG, Gally DL: **Analysis of type 1 fimbriae expression in verotoxigenic Escherichia coli: a comparison between serotypes O157 and O26.** *Microbiology* 2001, **147**(1):145-152.
225. Burland V, Shao Y, Perna NT, Plunkett G, Blattner FR, Sofia HJ: **The complete DNA sequence and analysis of the large virulence plasmid of Escherichia coli O157: H7.** *Nucleic Acids Research* 1998, **26**(18):4196-4204.
226. Welinder-Olsson C, Eriksson E, Kaijser B: **Virulence genes in verocytotoxigenic Escherichia coli strains isolated from humans and cattle.** *APMIS* 2005, **113**(9):577-585.
227. Ho TD, Davis BM, Ritchie JM, Waldor MK: **Type 2 Secretion Promotes Enterohemorrhagic Escherichia coli Adherence and Intestinal Colonization.** *Infection and Immunity* 2008, **76**(5):1858-1865.

228. Grys TE SM, Lathem WW, Welch RA. : **The StcE pro- tease contributes to intimate adherence of enterohemorrhagic Escherichia coli O157:H7 to host cells.** *Infection and Immunity* 2005, **73**:1295-1303.
229. Brunder W, Schmidt H, Karch H: **KatP, a novel catalase-peroxidase encoded by the large plasmid of enterohaemorrhagic Escherichia coli O157:H7.** *Microbiology* 1997, **142**(11):3305-3315.
230. Brockmeyer J, Bielaszewska M, Fruth A, Bonn ML, Mellmann A, Humpf H-U, Karch H: **Subtypes of the plasmid-encoded serine protease EspP in Shiga toxin-producing Escherichia coli: distribution, secretion, and proteolytic activity.** *Applied and Environmental Microbiology* 2007, **73**(20):6351-6359.
231. In J, Lukyanenko V, Foulke-Abel J, Hubbard AL, Delannoy M, Hansen A-M, Kaper JB, Boisen N, Nataro JP, Zhu C: **Serine protease EspP from enterohemorrhagic escherichia coli is sufficient to induce shiga toxin macropinocytosis in intestinal epithelium.** *PloS One* 2013, **8**(7):e69196.
232. In J, Foulke-Abel J, Zachos NC, Hansen A-M, Kaper JB, Bernstein HD, Halushka M, Blutt S, Estes MK, Donowitz M *et al*: **Enterohemorrhagic Escherichia coli Reduces Mucus and Intermicrovillar Bridges in Human Stem Cell-Derived Colonoids.** *CMGH Cellular and Molecular Gastroenterology and Hepatology* 2016, **2**(1):48-62.e43.
233. Brunder W, Schmidt H, Karch H: **EspP, a novel extracellular serine protease of enterohaemorrhagic Escherichia coli O157:H7 cleaves human coagulation factor V.** *Molecular Microbiology* 1997, **24**(4):767-778.
234. Dziva F, Mahajan A, Cameron P, Currie C, McKendrick IJ, Wallis TS, Smith DGE, Stevens MP: **EspP, a Type V-secreted serine protease of enterohaemorrhagic Escherichia coli O157:H7, influences intestinal colonization of calves and adherence to bovine primary intestinal epithelial cells.** *FEMS Microbiology Letters* 2007, **271**(2):258-264.
235. Chapman P, Ellin M, Ashton R, Shafique W: **Comparison of culture, PCR and immunoassays for detecting Escherichia coli O157 following enrichment culture and immunomagnetic separation performed on naturally contaminated raw meat products.** *International Journal of Food Microbiology* 2001, **68**(1):11-20.
236. Ogden I, Hepburn N, MacRae M: **The optimization of isolation media used in immunomagnetic separation methods for the detection of Escherichia coli O157 in foods.** *Journal of Applied Microbiology* 2001, **91**(2):373-379.
237. Karmali MA, Steele BT, Petric M, Lim C: **Sporadic cases of haemolytic-uraemic syndrome associated with faecal cytotoxin and cytotoxin-producing Escherichia coli in stools.** *The Lancet* 1983, **321**(8325):619-620.
238. Avery S, Small A, Reid C-A, Buncic S: **Pulsed-field gel electrophoresis characterization of Shiga toxin-producing Escherichia coli O157 from hides of cattle at slaughter.** *Journal of Food Protection* 2002, **65**(7):1172-1176.
239. Underwood AP, Dallman T, Thomson NR, Williams M, Harker K, Perry N, Adak B, Willshaw G, Cheasty T, Green J: **Public health value of next-generation DNA sequencing of enterohemorrhagic Escherichia coli isolates from an outbreak.** *Journal of Clinical Microbiology* 2013, **51**(1):232-237.

240. Boerlin P, McEwen SA, Boerlin-Petzold F, Wilson JB, Johnson RP, Gyles CL: **Associations between Virulence Factors of Shiga Toxin-Producing Escherichia coli and Disease in Humans.** *Journal of Clinical Microbiology* 1999, **37**(3):497-503.
241. Robinson CM, Sinclair JF, Smith MJ, O'Brien AD: **Shiga toxin of enterohemorrhagic Escherichia coli type O157:H7 promotes intestinal colonization.** *Proceedings of the National Academy of Sciences of the United States of America* 2006, **103**(25):9667-9672.
242. Ritchie JM, Wagner PI, Acheson DWK, Waldor MK: **Comparison of Shiga toxin production by hemolytic-uremic syndrome-associated and bovine-associated Shiga toxin-producing Escherichia coli isolates.** *Applied and Environmental Microbiology* 2003, **69**(2):1059-1066.
243. Baines D, Masson L, McAllister T: **Escherichia coli O157: H7-secreted cytotoxins are toxic to enterocytes and increase Escherichia coli O157: H7 colonization of jejunum and descending colon in cattle.** *Canadian Journal of Animal Science* 2008, **88**(1):41-50.
244. Dziva F, van Diemen PM, Stevens MP, Smith AJ, Wallis TS: **Identification of Escherichia coli O157 : H7 genes influencing colonization of the bovine gastrointestinal tract using signature-tagged mutagenesis.** *Microbiology* 2004, **150**(11):3631-3645.
245. Cornick NA, Booher SL, Casey TA, Moon HW: **Persistent Colonization of Sheep by Escherichia coli O157:H7 and Other E. coli Pathotypes.** *Applied and Environmental Microbiology* 2000, **66**(11):4926-4934.
246. Majoul I, Schmidt T, Pomasanova M, Boutkevich E, Kozlov Y, Soling H: **Differential expression of receptors for Shiga and Cholera toxin is regulated by the cell cycle.** *Journal of Cell Science* 2002, **115**:817-826.
247. Erwert RD, Eiting KT, Tupper JC, Winn RK, Harlan JM, Bannerman DD: **Shiga toxin induces decreased expression of the anti-apoptotic protein Mcl-1 concomitant with the onset of endothelial apoptosis.** *Microbiology Pathology* 2003, **35**:87-93.
248. Cherla RP, Lee S-Y, Tesh VL: **Shiga toxins and apoptosis.** *FEMS Microbiology Letters* 2003, **228**(2):159-166.
249. Ching JCY, Jones NL, Ceponis PJM, Karmali MA, Sherman PM: **Escherichia coli Shiga-Like Toxins Induce Apoptosis and Cleavage of Poly(ADP-Ribose) Polymerase via In Vitro Activation of Caspases.** *Infection and Immunity* 2002, **70**(8):4669-4677.
250. Mahajan A, Naylor S, Mills AD, Low JC, Mackellar A, Hoey DEE, Currie CG, Gally DL, Huntley J, Smith DGE: **Phenotypic and functional characterisation of follicle-associated epithelium of rectal lymphoid tissue.** *Cell and Tissue Research* 2005, **321**(3):365-374.
251. Arthur TM, Ahmed R, Chase-Topping M, Kalchayanand N, Schmidt JW, Bono JL: **Characterization of Escherichia coli O157: H7 Strains Isolated from Supershedding Cattle.** *Applied and Environmental Microbiology* 2013, **79**(14):4294-4303.
252. Menge C, Wieler LH, Schlapp T, Baljer G: **Shiga Toxin 1 from Escherichia coli Blocks Activation and Proliferation of Bovine Lymphocyte Subpopulations In Vitro.** *Infection and Immunity* 1999, **67**(5):2209-2217.

253. Menge C, Stamm I, Blessenohl M, Wieler LH, Baljer G: **Verotoxin 1 from Escherichia coli Affects Gb3/CD77+ Bovine Lymphocytes Independent of Interleukin-2, Tumor Necrosis Factor- α , and Interferon- α .** *Experimental Biology and Medicine* 2003, **228**(4):377-386.
254. Ruemmele F, Gurbindo C, Mansour A, Marchand R, Levy E, Seidman E: **Effects of Interferon γ on growth, apoptosis, and MHC class II expression of immature rat intestinal crypt (IEC - 6) cells.** *Journal of Cellular Physiology* 1998, **176**(1):120-126.
255. Steenbergen SM, Jirik JL, Vimr ER: **YjhS (NanS) Is Required for Escherichia coli To Grow on 9-O-Acetylated N-Acetylneuraminic Acid.** *Journal of Bacteriology* 2009, **191**(22):7134-7139.
256. Hughes KJ: **Understanding patterns of Escherichia coli O157: H7 shedding and colonisation in cattle and their role in transmission.** University of York; 2013.
257. Xu X, McAteer SP, Tree JJ, Shaw DJ, Wolfson EBK, Beatson SA, Roe AJ, Allison LJ, Chase-Topping ME, Mahajan A *et al*: **Lysogeny with Shiga Toxin 2-Encoding Bacteriophages Represses Type III Secretion in Enterohemorrhagic Escherichia coli.** *PLoS Pathog* 2012, **8**(5):e1002672.
258. Kiyokawa N, Taguchi T, Mori T, Uchida H, Sato N, Takeda T, Fujimoto J: **Induction of apoptosis in normal human renal tubular epithelial cells by Escherichia coli Shiga toxins 1 and 2.** *Journal of Infectious Diseases* 1998, **178**(1):178-184.
259. Hughes AK, Stricklett PK, Kohan DE: **Cytotoxic effect of Shiga toxin-1 on human proximal tubule cells1.** *Kidney International* 1998, **54**(2):426-437.
260. Meyers KEC, Kaplan BS: **Many cell types are Shiga toxin targets.** *Kidney International* 2000, **57**(6):2650-2651.
261. Obata F, Tohyama, K., Bonev, A.D., Kolling, G.L., Keepers, T.R., Gross, L.K., *et al*: **Shiga toxin 2 affects the central nervous system through receptor globotriaosylceramide localized to neurons.** *Journal of Infectious Diseases* 2008, **198**:1398-1406.
262. Johansson D, Johansson, A., Grankvist, K., Andersson, U., Henriksson, R., Bergstrom, P., *et al* : **Verotoxin-1 induction of apoptosis in Gb3-expressing human glioma cell lines.** *Cancer Biology and Therapy* 2006, **5**:1211-1217.
263. Miyamoto Y, Iimura M, Kaper JB, Torres AG, Kagnoff MF: **Role of Shiga toxin versus H7 flagellin in enterohaemorrhagic Escherichia coli signalling of human colon epithelium in vivo.** *Cellular microbiology* 2006, **8**(5):869-879.
264. Wadolkowski EA, Sung LM, Burris JA, Samuel JE, O'Brien AD: **Acute renal tubular necrosis and death of mice orally infected with Escherichia coli strains that produce Shiga-like toxin type II.** *Infection and Immunity* 1990, **58**(12):3959-3965.
265. Imai Y, Fukui T, Kurohane K, Miyamoto D, Suzuki Y, Ishikawa T, Ono Y, Miyake M: **Restricted expression of shiga toxin binding sites on mucosal epithelium of mouse distal colon.** *Infection and Immunity* 2003, **71**(2):985-990.
266. Kita E, Yunou Y, Kurioka T, Harada H, Yoshikawa S, Mikasa K, Higashi N: **Pathogenic mechanism of mouse brain damage caused by oral infection**

- with **Shiga toxin-producing Escherichia coli O157:H7**. *Infection and Immunity* 2000, **68**(3):1207-1214.
267. Keusch GT, Jacewicz M, Mobassaleh M, Donohue-Rolfe A: **Shiga toxin: intestinal cell receptors and pathophysiology of enterotoxic effects**. *Review of Infectious Diseases* 1991, **13**:304-310.
268. Ramegowda B, Tesh VL: **Differentiation-associated toxin receptor modulation, cytokine production, and sensitivity to Shiga-like toxins in human monocytes and monocytic cell lines**. *Infection and Immunity* 1996, **64**(4):1173-1180.
269. Ghosh SA, Polanowska-Grabowska RK, Fujii J, Obrig T, Gear AR: **Shiga toxin binds to activated platelets**. *Journal of Thrombosis and Homeostasis* 2004, **2**(3):499-506.
270. Pruijboom-Brees IM, Morgan TW, Ackermann MR, Nystrom ED, Samuel JE, Cornick NA, Moon HW: **Cattle lack vascular receptors for Escherichia coli O157:H7 Shiga toxins**. *Proceedings of the National Academy of Sciences of the United States of America* 2000, **97**(19):10325-10329.
271. Stamm I, Wuhler M, Geyer R, Baljer G, Menge C: **Bovine lymphocytes express functional receptors for Escherichia coli Shiga toxin 1**. *Microbial Pathogenesis* 2002, **33**(6):251-264.
272. Stamm I, Mohr M, Bridger PS, Schropfer E, Konig M, Stoffregen WC, Dean-Nystrom EA, Baljer G, Menge C: **Epithelial and mesenchymal cells in the bovine colonic mucosa differ in their responsiveness to Escherichia coli Shiga toxin 1**. *Infection and Immunity* 2008, **76**(11):5381-5391.
273. De Elaine H, Currie C, Else RW, Nutikka A, Lingwood CA, Gally DL, Smith DGE: **Expression of receptors for verotoxin 1 from Escherichia coli O157 on bovine intestinal epithelium**. *Journal of Medical Microbiology* 2002, **51**(2):143-149.
274. Menge C, Stamm I, Wuhler M, Geyer R, Wieler LH, Baljer G: **Globotriaosylceramide (Gb3/CD77) is synthesized and surface expressed by bovine lymphocytes upon activation in vitro**. *Veterinary Immunology and Immunopathology* 2001, **83**(1-2):19-36.
275. Menge C, Blessenohl M, Eisenberg T, Stamm I, Baljer G: **Bovine Ileal Intraepithelial Lymphocytes Represent Target Cells for Shiga Toxin 1 from Escherichia coli**. *Infection and Immunity* 2004, **72**(4):1896-1905.
276. Kim M, Binnington B, Sakac D, Fernandes KR, Shi SP, Lingwood CA, Branch DR: **Comparison of detection methods for cell surface globotriaosylceramide**. *Journal of Immunological Methods* 2011, **371**(1-2):48-60.
277. Orth D, Grif K, Khan AB, Naim A, Dierich MP, Würzner R: **The Shiga toxin genotype rather than the amount of Shiga toxin or the cytotoxicity of Shiga toxin in vitro correlates with the appearance of the hemolytic uremic syndrome**. *Diagnostic Microbiology and Infectious Disease* 2007, **59**(3):235-242.
278. Shimizu T, Sato T, Kawakami S, Ohta T, Noda M, Hamabata T: **Receptor affinity, stability and binding mode of Shiga toxins are determinants of toxicity**. *Microbial Pathogenesis* 2007, **43**(2-3):88-95.

279. Basu D, Tumer NE: **Do the A Subunits Contribute to the Differences in the Toxicity of Shiga Toxin 1 and Shiga Toxin 2?** *Toxins* 2015, **7**(5):1467-1485.
280. Lea N, Lord JM, Roberts LM: **Proteolytic cleavage of the A subunit is essential for maximal cytotoxicity of Escherichia coli O157:H7 Shiga-like toxin-1.** *Microbiology* 1999, **145**(5):999-1004.
281. Kroemer G, El-Deiry WS, Golstein P, Peter ME, Vaux D, Vandenabeele P, Zhivotovsky B, Blagosklonny MV, Malorni W, Knight RA *et al*: **Classification of cell death: recommendations of the Nomenclature Committee on Cell Death.** *Cell Death Differ* 2005, **12**(S2):1463-1467.
282. Melino G, Knight RA, Nicotera P: **How many ways to die? How many different models of cell death?** *Cell Death and Differentiation* 2005, **12**(2):1457-1462.
283. Golstein P: **Controlling cell death.** *Science* 1997, **275**(5303):1081.
284. Jones NL, Islur A, Haq R, Mascarenhas M, Karmali MA, Perdue MH, Zanke BW, Sherman PM: **Escherichia coli Shiga toxins induce apoptosis in epithelial cells that is regulated by the Bcl-2 family.** *American Journal of Physiology - Gastrointestinal and Liver Physiology* 2000, **278**(5):G811-G819.
285. Yoshida T, Fukada M, Koide N, Ikeda H, Sugiyama T, Kato Y, Ishikawa N, Yokochi T: **Primary Cultures of Human Endothelial Cells Are Susceptible to Low Doses of Shiga Toxins and Undergo Apoptosis.** *Journal of Infectious Diseases* 1999, **180**(6):2048-2052.
286. Van Setten PA, van Hinsbergh VW, Van den Heuvel LP, van der Velden TJ, van de Kar NC, Krebbers RJ, Karmali MA, Monnens LA: **Verocytotoxin inhibits mitogenesis and protein synthesis in purified human glomerular mesangial cells without affecting cell viability: evidence for two distinct mechanisms.** *Journal of the American Society of Nephrology* 1997, **8**(12):1877-1888.
287. Adler S, Bollu R: **Glomerular Endothelial Cell Injury Mediated by Shiga-Like Toxin-1.** *Kidney and Blood Pressure Research* 1998, **21**(1):13-21.
288. Keenan KP, Sharpnack DD, Collins H, Formal SB, O'Brien AD: **Morphologic evaluation of the effects of Shiga toxin and E coli Shiga-like toxin on the rabbit intestine.** *The American Journal of Pathology* 1986, **125**(1):69-80.
289. Bhattacharjee RN, Park K-S, Uematsu S, Okada K, Hoshino K, Takeda K, Takeuchi O, Akira S, Iida T, Honda T: **Escherichia coli verotoxin 1 mediates apoptosis in human HCT116 colon cancer cells by inducing overexpression of the GADD family of genes and S phase arrest.** *FEBS letters* 2005, **579**(29):6604-6610.
290. Liu J, Akahoshi T, Sasahana T, Kitasato H, Namai R, Sasaki T, Inoue M, Kondo H: **Inhibition of Neutrophil Apoptosis by Verotoxin 2 Derived from Escherichia coli O157:H7.** *Infection and Immunity* 1999, **67**(11):6203-6205.
291. Evan GI, Brown L, Whyte M, Harrington E: **Apoptosis and the cell cycle.** *Current Opinion in Cell Biology* 1995, **7**(6):825-834.
292. Pucci B, Kasten M, Giordano A: **Cell Cycle and Apoptosis.** *Neoplasia* 2000, **2**(4):291-299.

293. Kim M, Ashida H, Ogawa M, Yoshikawa Y, Mimuro H, Sasakawa C: **Bacterial Interactions with the Host Epithelium**. *Cell Host & Microbe* 2010, **8**(1):20-35.
294. Morinaga N, Yahiro K, Matsuura G, Moss J, Noda M: **Subtilase cytotoxin, produced by Shiga-toxigenic Escherichia coli, transiently inhibits protein synthesis of Vero cells via degradation of BiP and induces cell cycle arrest at G1 by downregulation of cyclin D1**. *Cellular Microbiology* 2008, **10**(4):921-929.
295. Bielaszewska M, Sinha B, Kuczius T, Karch H: **Cytolethal distending toxin from Shiga toxin-producing Escherichia coli O157 causes irreversible G(2)/M arrest, inhibition of proliferation, and death of human endothelial cells**. *Infection and Immunity* 2005, **73**(1):552-562.
296. Niehrs C, Acebron SP: **Mitotic and mitogenic Wnt signalling**. *The EMBO Journal* 2012, **31**(12):2705-2713.
297. Malumbres M, Barbacid M: **Cell cycle, CDKs and cancer: a changing paradigm**. *Nature Review Cancer* 2009, **9**(3):153-166.
298. Besson A, Dowdy SF, Roberts JM: **CDK inhibitors: cell cycle regulators and beyond**. *Developmental Cell* 2008, **14**(2):159-169.
299. Neal MD, Richardson WM, Sodhi CP, Russo A, Hackam DJ: **Intestinal Stem Cells and Their Roles During Mucosal Injury and Repair**. *Journal of Surgical Research* 2011, **167**(1):1-8.
300. Sheng H, Lim JY, Knecht HJ, Li J, Hovde CJ: **Role of Escherichia coli O157: H7 virulence factors in colonization at the bovine terminal rectal mucosa**. *Infection and Immunity* 2006, **74**(8):4685.
301. Falk PG, Hooper LV, Midtvedt T, Gordon JI: **Creating and maintaining the gastrointestinal ecosystem: what we know and need to know from gnotobiology**. *Microbiology and Molecular Biology Reviews* 1998, **62**(4):1157-1170.
302. Pudymaitis A, Lingwood CA: **Susceptibility to verotoxin as a function of the cell cycle**. *Journal of cellular physiology* 1992, **150**(3):632-639.
303. Siavoshian S, Segain J, Kornprobst M, Bonnet C, Cherbut C, Galmiche J, Blottiere H: **Butyrate and trichostatin A effects on the proliferation/differentiation of human intestinal epithelial cells: induction of cyclin D3 and p21 expression**. *Gut* 2000, **46**(4):507-514.
304. Mobassaleh M, Koul O, Mishra K, McCluer RH, Keusch GT: **Developmentally regulated Gb3 galactosyltransferase and alpha-galactosidase determine Shiga toxin receptors in intestine**. *American Journal of Physiology - Gastrointestinal and Liver Physiology* 1994, **267**(4):G618-G624.
305. Jacewicz M, Acheson D, Mobassaleh M, Donohue-Rolfe A, Balasubramanian K, Keusch G: **Maturational regulation of globotriaosylceramide, the Shiga-like toxin 1 receptor, in cultured human gut epithelial cells**. *Journal of Clinical Investigation* 1995, **96**(3):1328.
306. Duncan S, Booth I, Flint H, Stewart C: **The potential for the control of Escherichia coli O157 in farm animals**. *Journal of Applied Microbiology* 2000, **88**:157S.

307. Russell JB, Diez-Gonzalez F, Jarvis GN: **Potential effect of cattle diets on the transmission of pathogenic Escherichia coli to humans.** *Microbes and Infection* 2000, **2**(1):45-53.
308. Magnuson BA, Davis M, Hubele S, Austin PR, Kudva IT, Williams CJ, Hunt CW, Hovde CJ: **Ruminant gastrointestinal cell proliferation and clearance of Escherichia coli O157: H7.** *Infection and Immunity* 2000, **68**(7):3808.
309. Liu X, Lu R, Wu S, Sun J: **Salmonella regulation of intestinal stem cells through the Wnt/beta-catenin pathway.** *FEBS letters* 2010, **584**(5):911-916.
310. Tajrishi MM, Tuteja R, Tuteja N: **Nucleolin: The most abundant multifunctional phosphoprotein of nucleolus.** *Communicative & Integrative Biology* 2011, **4**(3):267-275.
311. van Dierendonck JH, Wijsman JH, Keijzer R, van de Velde CJ, Cornelisse CJ: **Cell-cycle-related staining patterns of anti-proliferating cell nuclear antigen monoclonal antibodies. Comparison with BrdUrd labeling and Ki-67 staining.** *The American Journal of Pathology* 1991, **138**(5):1165-1172.
312. Medema JP, Vermeulen L: **Microenvironmental regulation of stem cells in intestinal homeostasis and cancer.** *Nature* 2011, **474**(7351):318-326.
313. Kosinski C, Li VSW, Chan ASY, Zhang J, Ho C, Tsui WY, Chan TL, Mifflin RC, Powell DW, Yuen ST *et al*: **Gene expression patterns of human colon tops and basal crypts and BMP antagonists as intestinal stem cell niche factors.** *Proceedings of the National Academy of Sciences* 2007, **104**(39):15418-15423.
314. Short B: **A fifth amendment to the intestine's constitution.** *The Journal of Cell Biology* 2011, **192**(5):706.
315. de Lau W, Barker N, Clevers H: **WNT signaling in the normal intestine and colorectal cancer.** *Front Biosci* 2007, **12**:471-491.
316. van der Flier LG, Clevers H: **Stem Cells, Self-Renewal, and Differentiation in the Intestinal Epithelium.** In: *Annual Review of Physiology. Volume 71*, edn. Palo Alto: Annual Reviews; 2009: 241-260.
317. Clevers HC, Bevins CL: **Paneth cells: maestros of the small intestinal crypts.** *Annual Review of Physiology* 2013, **75**:289-311.
318. Rhim JS, Schell K, Creasy B, Case W: **Biological characteristics and viral susceptibility of an African green monkey kidney cell line (Vero).** *Experimental Biology and Medicine* 1969, **132**(2):670-678.
319. Masters JR: **HeLa cells 50 years on: the good, the bad and the ugly.** *Nature Reviews Cancer* 2002, **2**(4):315-319.
320. Bouzari S, Oloomi M, Azadmanesh K: **Study on induction of apoptosis on HeLa and Vero cells by recombinant shiga toxin and its subunits.** *Cytotechnology* 2009, **60**(1-3):105-113.
321. Mebus C, Kono M, Underdahl N, Twiehaus M: **Cell culture propagation of neonatal calf diarrhea (scours) virus.** *The Canadian Veterinary Journal* 1971, **12**(3):69.
322. Pansky B: **Medical embryology.** New York: Macmillan 1982.
323. Hanashima T, Miyake M, Yahiro K, Iwamaru Y, Ando A, Morinaga N, Noda M: **Effect of Gb3 in lipid rafts in resistance to Shiga-like toxin of mutant Vero cells.** *Microbial Pathogenesis* 2008, **45**(2):124-133.

324. Acheson D, Moore R, De Breucker S, Lincicome L, Jacewicz M, Skutelsky E, Keusch G: **Translocation of Shiga toxin across polarized intestinal cells in tissue culture.** *Infection and Immunity* 1996, **64**(8):3294.
325. Jacewicz MS, Mobassaleh M, Gross SK, Balasubramanian KA, Daniel PF, Raghavan S, McCluer RH, Keusch GT: **Pathogenesis of Shigella Diarrhea: XVII. A Mammalian Cell Membrane Glycolipid, Gb3, Is Required but Not Sufficient to Confer Sensitivity to Shiga Toxin.** *Journal of Infectious Diseases* 1994, **169**(3):538-546.
326. **CHO-K1 (ATCC® CCL-61™)**
327. Bosques CJ, Collins BE, Meador III JW, Sarvaiya H, Murphy JL, DelloRusso G, Bulik DA, Hsu I-H, Washburn N, Sipsey SF: **Chinese hamster ovary cells can produce galactose-[alpha]-1, 3-galactose antigens on proteins.** *Nature Biotechnology* 2010, **28**(11):1153-1156.
328. De Elaine H, Currie C, Else RW, Nutikka A, Lingwood CA, Gally DL, Smith DG: **Expression of receptors for verotoxin 1 from Escherichia coli O157 on bovine intestinal epithelium.** *Journal of Medical Microbiology* 2002, **51**(2):143-149.
329. Fujii Y, Numata S-i, Nakamura Y, Honda T, Furukawa K, Urano T, Wiels J, Uchikawa M, Ozaki N, Matsuo S-i *et al*: **Murine glycosyltransferases responsible for the expression of globo-series glycolipids: cDNA structures, mRNA expression, and distribution of their products.** *Glycobiology* 2005, **15**(12):1257-1267.
330. Lingwood CA: **Shiga toxin receptor glycolipid binding.** *Pathology and Utility Methods Molecular Medicine* 2003, **73**:165-186.
331. Fuchs E, Weber K: **Intermediate filaments: structure, dynamics, function and disease.** *Annual Review of Biochemistry* 1994, **63**(1):345-382.
332. Osborn M, Weber K: **Intermediate filament proteins: a multigene family distinguishing major cell lineages.** *Trends in Biochemical Sciences* 1986, **11**(11):469-472.
333. Lane E, Alexander C: **Use of keratin antibodies in tumor diagnosis.** In: *Seminars in Cancer Biology: 1990*; 1990: 165-179.
334. Moll R, Franke WW, Schiller DL, Geiger B, Krepler R: **The catalog of human cytokeratins: patterns of expression in normal epithelia, tumors and cultured cells.** *Cell* 1982, **31**(1):11-24.
335. Albaugh GP, Iyengar V, Lohani A, Malayeri M, Bala S, Nair PP: **Isolation of exfoliated colonic epithelial cells, a novel, non-invasive approach to the study of cellular markers.** *International Journal of Cancer* 1992, **52**(3):347-350.
336. Evans RM: **Vimentin: the conundrum of the intermediate filament gene family.** *Bioessays* 1998, **20**(1):79-86.
337. Mendez MG, Kojima S-I, Goldman RD: **Vimentin induces changes in cell shape, motility, and adhesion during the epithelial to mesenchymal transition.** *The FASEB Journal* 2010, **24**(6):1838-1851.
338. Jepson M, Mason C, Bennett M, Simmons N, Hirst B: **Co-expression of vimentin and cytokeratins in M cells of rabbit intestinal lymphoid follicle-associated epithelium.** *Histochem J* 1992, **24**(1):33-39.

339. Neefjes J, Jongsma MLM, Paul P, Bakke O: **Towards a systems understanding of MHC class I and MHC class II antigen presentation.** *Nat Rev Immunol* 2011, **11**(12):823-836.
340. Jinadasa RN, Bloom SE, Weiss RS, Duhamel GE: **Cytolethal distending toxin: a conserved bacterial genotoxin that blocks cell cycle progression, leading to apoptosis of a broad range of mammalian cell lineages.** *Microbiology* 2011, **157**(Pt 7):1851-1875.
341. Karmali MA, Petric M, Lim C, Fleming PC, Arbus GS, Lior H: **The association between idiopathic hemolytic uremic syndrome and infection by verotoxin-producing Escherichia coli.** *Journal of Infectious Diseases* 1985, **151**(5):775-782.
342. Okuda T, Nakayama K-i: **Identification and characterization of the human Gb3/CD77 synthase gene promoter.** *Glycobiology* 2008, **18**(12):1028-1035.
343. Lentz EK, Leyva-Illades, D., Lee, M. S., Cherla, R. P., & Tesh, V. L. : **Differential response of the human renal proximal tubular epithelial cell line HK-2 to Shiga toxin types 1 and 2.** *Infection and Immunity* 2011, **79**(9):3527-3540.
344. Chiou J-C, Li X-P, Remacha M, Ballesta JP, Tumer NE: **Shiga toxin 1 is more dependent on the P proteins of the ribosomal stalk for depurination activity than Shiga toxin 2.** *The International Journal of Biochemistry & Cell Biology* 2011, **43**(12):1792-1801.
345. Head S, Karmali M, Lingwood C: **Preparation of VT1 and VT2 hybrid toxins from their purified dissociated subunits. Evidence for B subunit modulation of a subunit function.** *Journal of Biological Chemistry* 1991, **266**(6):3617-3621.
346. Nakajima H, Kiyokawa N, Katagiri YU, Taguchi T, Suzuki T, Sekino T, Mimori K, Ebata T, Saito M, Nakao H: **Kinetic analysis of binding between Shiga toxin and receptor glycolipid Gb3Cer by surface plasmon resonance.** *Journal of Biological Chemistry* 2001, **276**(46):42915-42922.
347. Karve SS, Weiss AA: **Glycolipid binding preferences of Shiga toxin variants.** *PloS one* 2014, **9**(7):e101173.
348. Briske-Anderson MJ, Finley JW, Newman SM: **The Influence of Culture Time and Passage Number on the Morphological and Physiological Development of Caco-2 Cells.** *Experimental Biology and Medicine* 1997, **214**(3):248-257.
349. Sambuy Y, De Angelis I, Ranaldi G, Scarino M, Stammati A, Zucco F: **The Caco-2 cell line as a model of the intestinal barrier: influence of cell and culture-related factors on Caco-2 cell functional characteristics.** *Cell Biology and Toxicology* 2005, **21**(1):1-26.
350. Natoli M, Leoni BD, D'Agnano I, D'Onofrio M, Brandi R, Arisi I, Zucco F, Felsani A: **Cell growing density affects the structural and functional properties of Caco - 2 differentiated monolayer.** *Journal of Cellular Physiology* 2011, **226**(6):1531-1543.
351. Rousset M: **The human colon carcinoma cell lines HT-29 and Caco-2: two in vitro models for the study of intestinal differentiation.** *Biochimie* 1986, **68**(9):1035-1040.

352. Nart P, Naylor S, Huntley J, McKendrick I, Gally D, Low J: **Responses of Cattle to Gastrointestinal Colonization by Escherichia coli O157:H7.** *Infection and Immunity* 2008, **76**:5366-5372.
353. Liu B, Yin X, Feng Y, Chambers JR, Guo A, Gong J, Zhu J, Gyles CL: **Verotoxin 2 Enhances Adherence of Enterohemorrhagic Escherichia coli O157:H7 to Intestinal Epithelial Cells and Expression of β 1-Integrin by IPEC-J2 Cells.** *Applied and Environmental Microbiology* 2010, **76**(13):4461-4468.
354. Traore A, Baudrimont I, Ambaliou S, Dano S, Creppy E: **DNA breaks and cell cycle arrest induced by okadaic acid in Caco-2 cells, a human colonic epithelial cell line.** *Archives of Toxicology* 2001, **75**(2):110-117.
355. Nataro JP, Hicks S, Phillips AD, Vial PA, Sears CL: **T84 cells in culture as a model for enteroaggregative Escherichia coli pathogenesis.** *Infection and Immunity* 1996, **64**(11):4761-4768.
356. Miyazawa K, Hondo T, Kanaya T, Tanaka S, Takakura I, Itani W, Rose MT, Kitazawa H, Yamaguchi T, Aso H: **Characterization of newly established bovine intestinal epithelial cell line.** *Histochemistry and Cell Biology* 2010, **133**(1):125-134.
357. Chiba E, Villena J, Hosoya S, Takanashi N, Shimazu T, Aso H, Tohno M, Suda Y, Kawai Y, Saito T *et al*: **A newly established bovine intestinal epithelial cell line is effective for in vitro screening of potential antiviral immunobiotic microorganisms for cattle.** *Research in Veterinary Science* 2012, **93**(2):688-694.
358. Schäfer A-O: **Anorectal Anatomy.** In: *MRI of Rectal Cancer.* edn.: Springer; 2010: 5-13.
359. Liévin-Le Moal V, Servin AL: **The Front Line of Enteric Host Defense against Unwelcome Intrusion of Harmful Microorganisms: Mucins, Antimicrobial Peptides, and Microbiota.** *Clinical Microbiology Reviews* 2006, **19**(2):315-337.
360. Budras KD: **Bovine Anatomy: An Illustrated Text:** Schluetersche, Germany; 2003.
361. Neutra MR, Mantis NJ, Kraehenbuhl JP: **Collaboration of epithelial cells with organized mucosal lymphoid tissues.** *Nature Immunology* 2001, **2**(11):1004-1009.
362. Didierlaurent A, Sirard JC, Kraehenbuhl JP, Neutra MR: **How the gut senses its content.** *Cellular Microbiology* 2002, **4**(2):61-72.
363. Brandtzaeg P, Kiyono H, Pabst R, Russell M: **Terminology: nomenclature of mucosa-associated lymphoid tissue.** *Mucosal Immunology* 2008, **1**(1):31-37.
364. Parsons KR, Howard CJ, Jones BV, Sopp P: **Investigation of bovine gut associated lymphoid tissue (GALT) using monoclonal antibodies against bovine lymphocytes.** *Veterinary Pathology Online* 1989, **26**(5):396-408.
365. Landsverk T, Halleraker M, Aleksandersen M, McClure S, Hein W, Nicander L: **The intestinal habitat for organized lymphoid tissues in ruminants; comparative aspects of structure, function and development.** *Veterinary Immunology and Immunopathology* 1991, **28**(1):1-16.

366. Yasuda M, Jenne CN, Kennedy LJ, Reynolds JD: **The sheep and cattle Peyer's patch as a site of B-cell development.** *Veterinary Research* 2006, **37**(3):401-415.
367. Liebler EM, Pohlenz JF, Woode GN: **Gut-associated lymphoid tissue in the large intestine of calves. I. Distribution and histology.** *Veterinary Pathology Online* 1988, **25**(6):503-508.
368. Liebler EM, Pohlenz JF, Cheville NF: **Gut-associated lymphoid tissue in the large intestine of calves. II. Electron microscopy.** *Veterinary Pathology Online* 1988, **25**(6):509-515.
369. O'Leary AD, Sweeney EC: **Lymphoglandular complexes of the colon: structure and distribution.** *Histopathology* 1986, **10**(3):267-283.
370. Farris AB, Lauwers GY, Judith A, Ferry JA, Zukerberg LR: **The rectal tonsil: a reactive lymphoid proliferation that may mimic lymphoma.** *American Journal of Surgical Pathology* 2008, **32**(7):1075-1079.
371. Dagleish MP, Finlayson J, Steele PJ, Pang Y, Hamilton S, Eaton SL, Sales J, González L, Chianini F: **Immunophenotype of Cells within Cervine Rectoanal Mucosa-Associated Lymphoid Tissue and Mesenteric Lymph Nodes.** *Journal of Comparative Pathology* 2012, **146**(4):365-371.
372. González L, Dagleish MP, Bellworthy SJ, Sisó S, Stack MJ, Chaplin MJ, Davis LA, Hawkins SAC, Hughes J, Jeffrey M: **Postmortem diagnosis of preclinical and clinical scrapie in sheep by the detection of disease-associated PrP in their rectal mucosa.** *Veterinary Record* 2006, **158**(10):325-331.
373. Sheng H, Wang J, Lim JY, Davitt C, Minnich SA, Hovde CJ: **Internalization of Escherichia coli O157:H7 by bovine rectal epithelial cells.** *Frontiers in Microbiology* 2011, **2**.
374. Kudva IT, Dean-Nystrom EA: **Bovine recto-anal junction squamous epithelial (RSE) cell adhesion assay for studying Escherichia coli O157 adherence.** *Journal of Applied Microbiology* 2011, **111**(5):1283-1294.
375. Mahajan A, Currie CG, Mackie S, Tree J, McAteer S, McKendrick I, McNeilly TN, Roe A, La Ragione RM, Woodward MJ: **An investigation of the expression and adhesin function of H7 flagella in the interaction of Escherichia coli O157: H7 with bovine intestinal epithelium.** *Cellular Microbiology* 2009, **11**(1):121-137.
376. Sheng H, Davis MA, Knecht HJ, Hovde CJ: **Rectal Administration of Escherichia coli O157:H7: Novel Model for Colonization of Ruminants.** *Applied and Environmental Microbiology* 2004, **70**(8):4588-4595.
377. Aleksandersen M, Hein WR, Landsverk T, McClure S: **Distribution of lymphocyte subsets in the large intestinal lymphoid follicles of lambs.** *Immunology* 1990, **70**(3):391.
378. Nagi AM, Babiuk LA: **Bovine gut-associated lymphoid tissue--morphologic and functional studies. I. Isolation and characterization of leukocytes from the epithelium and lamina propria of bovine small intestine.** *Journal of Immunological Methods* 1987, **105**(1):23-37.
379. Nagi AM, Babiuk LA: **Characterization of surface markers of bovine gut mucosal leukocytes using monoclonal antibodies.** *Veterinary Immunology and Immunopathology* 1989, **22**(1):1-14.

380. Alberts B JA, Lewis J, et al. : **Helper T Cells and Lymphocyte Activation**. In: *Molecular Biology of the Cell*. 4th edition edn. New York: Garland Science; 2002.
381. Szabo SJ, Kim ST, Costa GL, Zhang X, Fathman CG, Glimcher LH: **A novel transcription factor, T-bet, directs Th1 lineage commitment**. *Cell* 2000, **100**(6):655-669.
382. Plevy SE, Landers CJ, Prehn J, Carramanzana NM, Deem RL, Shealy D, Targan SR: **A role for TNF-alpha and mucosal T helper-1 cytokines in the pathogenesis of Crohn's disease**. *The Journal of Immunology* 1997, **159**(12):6276-6282.
383. Romagnani S: **T-cell subsets (Th1 versus Th2)**. *Annals of Asthma and Immunology* 2000, **85**(1):9-21.
384. Corbishley A, Ahmad NI, Hughes K, Hutchings MR, McAteer SP, Connelley TK, Brown H, Gally DL, McNeilly TN: **Strain-Dependent Cellular Immune Responses in Cattle following Escherichia coli O157:H7 Colonization**. *Infection and Immunity* 2014, **82**(12):5117-5131.
385. Romagnani S: **Th1/Th2 cells**. *Inflammatory Bowel Diseases* 1999, **5**(4):285-294.
386. Reefer AJ, Carneiro RM, Custis NJ, Platts-Mills TA, Sung S-SJ, Hammer J, Woodfolk JA: **A role for IL-10-mediated HLA-DR7-restricted T cell-dependent events in development of the modified Th2 response to cat allergen**. *The Journal of Immunology* 2004, **172**(5):2763-2772.
387. Grewe M, Bruijnzeel-Koomen CA, Schöpf E, Thepen T, Langeveld-Wildschut AG, Ruzicka T, Krutmann J: **A role for Th1 and Th2 cells in the immunopathogenesis of atopic dermatitis**. *Immunology today* 1998, **19**(8):359-361.
388. Prete GD: **Human Th1 and Th2 lymphocytes: their role in the pathophysiology of atopy**. *Allergy* 1992, **47**(5):450-455.
389. Zaiss Dietmar MW, Gause William C, Osborne Lisa C, Artis D: **Emerging Functions of Amphiregulin in Orchestrating Immunity, Inflammation, and Tissue Repair**. *Immunity* 2015, **42**(2):216-226.
390. Hajikhan Mirzaei M, Esmaeilzadeh A: **Overexpression of MDA-7/IL-24 as an anticancer cytokine in gene therapy of thyroid carcinoma**. *Journal of Medical Hypotheses and Ideas* 2014, **8**(1):7-13.
391. Paul WE, Zhu J: **How are TH2-type immune responses initiated and amplified?** *Nat Rev Immunol* 2010, **10**(4):225-235.
392. Ghanekar SA, Nomura LE, Suni MA, Picker LJ, Maecker HT, Maino VC: **Gamma Interferon Expression in CD8+ T Cells Is a Marker for Circulating Cytotoxic T Lymphocytes That Recognize an HLA A2-Restricted Epitope of Human Cytomegalovirus Phosphoprotein pp65**. *Clinical and Diagnostic Laboratory Immunology* 2001, **8**(3):628-631.
393. Kelso A, Costelloe EO, Johnson BJ, Groves P, Buttigieg K, Fitzpatrick DR: **The genes for perforin, granzymes A-C and IFN-gamma are differentially expressed in single CD8(+) T cells during primary activation**. *International Immunology* 2002, **14**(6):605-613.
394. Hagiwara K, Domi M, Ando J: **Bovine colostrum CD8-positive cells are potent IFN-gamma-producing cells**. *Veterinary Immunology and Immunopathology* 2008, **124**(1):93-98.

395. McLane LM, Banerjee PP, Cosma GL, Makedonas G, Wherry EJ, Orange JS, Betts MR: **Differential localization of T-bet and Eomes in CD8 T-cell memory populations.** *The Journal of Immunology* 2013, **190**(7):3207-3215.
396. Berke G: **The CTL's kiss of death.** *Cell* 1995, **81**(1):9-12.
397. Martin-Fontecha A, Thomsen LI, Brett SF, Gerard C, Lipp M, Lanzavecchia A, Sallusto F: **Induced recruitment of NK cells to lymph nodes provides IFN-gamma for T(H)1 priming.** *Nature Immunology* 2004, **5**(12):1260-1265.
398. Trinchieri G: **Biology of natural killer cells.** *Advances in Immunology* 1989, **47**(187):376.
399. Degli-Esposti MA, Smyth MJ: **Close encounters of different kinds: dendritic cells and NK cells take centre stage.** *Nature Review Immunology* 2005, **5**(2):112-124.
400. Campbell KS, Hasegawa J: **Natural killer cell biology: An update and future directions.** *Journal of Allergy and Clinical Immunology* 2013, **132**(3):536-544.
401. Storset AK, Slettedal LO, Williams JL, Law A, Dissen E: **Natural killer cell receptors in cattle: a bovine killer cell immunoglobulin-like receptor multigene family contains members with divergent signaling motifs.** *European journal of Immunology* 2003, **33**(4):980-990.
402. Cohen GB, Gandhi RT, Davis DM, Mandelboim O, Chen BK, Strominger JL, Baltimore D: **The selective downregulation of class I major histocompatibility complex proteins by HIV-1 protects HIV-infected cells from NK cells.** *Immunity* 1999, **10**(6):661-671.
403. Boysen P, Storset AK: **Bovine natural killer cells.** *Veterinary Immunology and Immunopathology* 2009, **130**(3):163-177.
404. Walzer T, Jaeger S, Chaix J, Vivier E: **Natural killer cells: from CD3(-)NKp46(+) to post-genomics meta-analyses.** *Current Opinion in Immunology* 2007, **19**(3):365-372.
405. Storset AK, Kulberg S, Berg I, Boysen P, Hope JC, Dissen E: **NKp46 defines a subset of bovine leukocytes with natural killer cell characteristics.** *European Journal of Immunology* 2004, **34**(3):669-676.
406. Moretta A, Bottino C, Vitale M, Pende D, Cantoni C, Mingari MC, Biassoni R, Moretta L: **Activating receptors and coreceptors involved in human natural killer cell-mediated cytotoxicity.** *Annual Review of Immunology* 2001, **19**(1):197-223.
407. Bottino C, Castriconi R, Moretta L, Moretta A: **Cellular ligands of activating NK receptors.** *Trends in Immunology* 2005, **26**(4):221-226.
408. Gregoire C, Chasson L, Luci C, Tomasello E, Geissmann F, Vivier E, Walzer T: **The trafficking of natural killer cells.** *Immunological Reviews* 2007, **220**(1):169-182.
409. Boysen P, Olsen I, Berg I, Kulberg S, Johansen GM, Storset AK: **Bovine CD2-/NKp46+ cells are fully functional natural killer cells with a high activation status.** *BMC Immunology* 2006, **7**(1):10.
410. Boysen P, Gunnes G, Pende D, Valheim M, Storset AK: **Natural killer cells in lymph nodes of healthy calves express CD16 and show both cytotoxic and cytokine-producing properties.** *Developmental and Comparative Immunology* 2008, **32**(7):773-783.

411. Beagley K, Husband AJ: **Intraepithelial lymphocytes: origins, distribution, and function.** *Critical Reviews™ in Immunology* 1998, **18**(3).
412. Hayday A, Theodoridis E, Ramsburg E, Shires J: **Intraepithelial lymphocytes: exploring the Third Way in immunology.** *Nature Immunology* 2001, **2**(11):997-1003.
413. Walker CR, Hautefort I, Dalton JE, Overweg K, Egan CE, Bongaerts RJ, Newton DJ, Cruickshank SM, Andrew EM, Carding SR: **Intestinal intraepithelial lymphocyte-enterocyte crosstalk regulates production of bactericidal angiogenin 4 by Paneth cells upon microbial challenge.** *PLoS one* 2013, **8**(12):e84553.
414. Boismenu R, Havran WL: **$\gamma\delta$ T cells in host defense and epithelial cell biology.** *Clinical Immunology and Immunopathology* 1998, **86**(2):121-133.
415. Yang H, Antony PA, Wildhaber BE, Teitelbaum DH: **Intestinal intraepithelial lymphocyte $\gamma\delta$ -T cell-derived keratinocyte growth factor modulates epithelial growth in the mouse.** *The Journal of Immunology* 2004, **172**(7):4151-4158.
416. Mackay CR, Hein WR: **A large proportion of bovine T cells express the gamma delta T cell receptor and show a distinct tissue distribution and surface phenotype.** *International Immunology* 1989, **1**(5):540-545.
417. Guzman E, Hope J, Taylor G, Smith AL, Cubillos-Zapata C, Charleston B: **Bovine gammadelta T cells are a major regulatory T cell subset.** *The Journal of Immunology* 2014, **193**(1):208-222.
418. Vesosky B, O. T, J. T, Orme IM: **Gamma interferon production by bovine gamma delta T cells following stimulation with mycobacterial mycolylarabinogalactan peptidoglycan.** *Infection and Immunity* 2004, **72**(8):4612-4618.
419. Clevers H, MacHugh ND, Bensaid A, Dunlap S, Baldwin CL, Kaushal A, Iams K, Howard CJ, Morrison WI: **Identification of a bovine surface antigen uniquely expressed on CD4-CD8- T cell receptor gamma/delta+ T lymphocytes.** *European journal of Immunology* 1990, **20**(4):809-817.
420. Pierson W, Liston A: **A new role for interleukin-10 in immune regulation.** *Immunol Cell Biol* 2010, **88**(8):769-770.
421. LeBien TW, Tedder TF: **B lymphocytes: how they develop and function.** *Blood* 2008, **112**(5):1570-1580.
422. Chu PG, Arber DA: **CD79: a review.** *Applied Immunohistochemistry & Molecular Morphology* 2001, **9**(2):97-106.
423. Otero DC, Rickert RC: **CD19 Function in Early and Late B Cell Development. II. CD19 Facilitates the Pro-B/Pre-B Transition.** *The Journal of Immunology* 2003, **171**(11):5921-5930.
424. Parnes J, Pan C: **CD72, a negative regulator of B-cell responsiveness.** *Immunological Reviews* 2000, **176**:75-85.
425. Björck P, Elenström - Magnusson C, Rosén A, Severinson E, Paulie S: **CD23 and CD21 function as adhesion molecules in homotypic aggregation of human B lymphocytes.** *European Journal of Immunology* 1993, **23**(8):1771-1775.
426. Delcayre AX, Salas F, Mathur S, Kovats K, Lotz M, Lernhardt W: **Epstein Barr virus/complement C3d receptor is an interferon alpha receptor.** *The EMBO Journal* 1991, **10**(4):919.

427. Birkenbach M, Tong X, Bradbury L, Tedder T, Kieff E: **Characterization of an Epstein-Barr virus receptor on human epithelial cells.** *The Journal of Experimental Medicine* 1992, **176**(5):1405-1414.
428. Usui K, Honda S-i, Yoshizawa Y, Nakahashi-Oda C, Tahara-Hanaoka S, Shibuya K, Shibuya A: **Isolation and characterization of naïve follicular dendritic cells.** *Molecular Immunology* 2012, **50**(3):172-176.
429. Waters WR, Palmer MV, Nonnecke BJ, Thacker TC, Estes DM, Larsen MH, Jacobs WR, Andersen P, McNair J, Lyashchenko KP: **Signal regulatory protein α (SIRP α)+ cells in the adaptive response to ESAT-6/CFP-10 protein of tuberculous mycobacteria.** *PloS One* 2009, **4**(7):e6414.
430. Hussen J, Düvel A, Sandra O, Smith D, Sheldon IM, Zieger P, Schuberth H-J: **Phenotypic and functional heterogeneity of bovine blood monocytes.** *PloS One* 2013, **8**(8):e71502.
431. Shi C, Pamer EG: **Monocyte recruitment during infection and inflammation.** In: *Nature Reviews Immunology*. vol. 11; 2011: 762-774.
432. Chomarat P, Banchereau J, Davoust J, Karolina Palucka A: **IL-6 switches the differentiation of monocytes from dendritic cells to macrophages.** *Nat Immunol* 2000, **1**(6):510-514.
433. Chomarat P, Dantin C, Bennett L, Banchereau J, Palucka AK: **TNF Skews Monocyte Differentiation from Macrophages to Dendritic Cells.** *The Journal of Immunology* 2003, **171**(5):2262-2269.
434. Gordon S, Taylor PR: **Monocyte and macrophage heterogeneity.** *Nature Reviews Immunology* 2005, **5**(12):953-964.
435. Martinez FO, Helming L, Gordon S: **Alternative activation of macrophages: an immunologic functional perspective.** *Annual Review of Immunology* 2009, **27**:451-483.
436. Phillips A, Navabpour S, Hicks S, Dougan G, Wallis T, Frankel G: **Enterohaemorrhagic Escherichia coli O157: H7 target Peyer's patches in humans and cause attaching/effacing lesions in both human and bovine intestine.** *Gut* 2000, **47**(3):377.
437. Fitzhenry R, Pickard D, Hartland E, Reece S, Dougan G, Phillips A, Frankel G: **Intimin type influences the site of human intestinal mucosal colonisation by enterohaemorrhagic Escherichia coli O157: H7.** *Gut* 2002, **50**(2):180.
438. Fitzhenry RJ, Pickard DJ, Hartland EL, Reece S, Dougan G, Phillips AD, Frankel G: **Intimin type influences the site of human intestinal mucosa colonisation by enterohaemorrhagic Escherichia coli O157 : H7.** *Gut* 2002, **50**(2):180-185.
439. Neutra MR, Frey A, Kraehenbuhl JP: **Epithelial M cells: Gateways for mucosal infection and immunization.** *Cell* 1996, **86**(3):345-348.
440. Gebert A, Pabst R: **M cells at locations outside the gut.** *Seminars in Immunology* 1999, **11**(3):165-170.
441. Hamzaoui N, Kernéis S, Caliot E, Pringault E: **Expression and distribution of β 1 integrins in in vitro - induced M cells: implications for Yersinia adhesion to Peyer's patch epithelium.** *Cellular Microbiology* 2004, **6**(9):817-828.
442. McKee ML, Melton-Celsa AR, Moxley RA, Francis DH, O'Brien AD: **Enterohemorrhagic Escherichia coli O157: H7 requires intimin to**

- colonize the gnotobiotic pig intestine and to adhere to HEp-2 cells. *Infection and Immunity* 1995, **63**(9):3739-3744.
443. Clark MA, Hirst BH, Jepson MA: **M-cell surface beta1 integrin expression and invasin-mediated targeting of Yersinia pseudotuberculosis to mouse Peyer's patch M cells.** *Infection and Immunity* 1998, **66**(3):1237-1243.
444. Gebert A: **M-cells in the rabbit tonsil exhibit distinctive glycoconjugates in their apical membranes.** *International Review of Cytology* 1996, **167**:91-159.
445. Clark MA, Jepson MA, Simmons NL, Hirst BH: **Preferential interaction of Salmonella typhimurium with mouse Peyer's patch M cells.** *Research in Microbiology* 1994, **145**(7):543-552.
446. Autenrieth IB, Firsching R: **Penetration of M cells and destruction of Peyer's patches by Yersinia enterocolitica: an ultrastructural and histological study.** *Journal of Medical Microbiology* 1996, **44**(4):285-294.
447. Sansonetti PJ, Arondel J, Cantey JR, Prévost MC, Huerre M: **Infection of rabbit Peyer's patches by Shigella flexneri: effect of adhesive or invasive bacterial phenotypes on follicle-associated epithelium.** *Infection and Immunity* 1996, **64**(7):2752-2764.
448. Celli J, Finlay BB: **Bacterial avoidance of phagocytosis.** *Trends in Microbiology* 2002, **10**(5):232-237.
449. Etienne-Mesmin L, Chassaing B, Sauvanet P, Denizot J, Blanquet-Diot S, Darfeuille-Michaud A, Pradel N, Livrelli V: **Interactions with M cells and macrophages as key steps in the pathogenesis of enterohemorrhagic Escherichia coli infections.** *PLoS One* 2011, **6**(8):e23594.
450. Clark MA, Jepson MA: **Intestinal M cells and their role in bacterial infection.** *International Journal of Medical Microbiology* 2003, **293**(1):17-39.
451. Sharma VK, Casey TA: **Escherichia coli O157:H7 Lacking the qseBC-Encoded Quorum-Sensing System Outcompetes the Parental Strain in Colonization of Cattle Intestines.** *Applied and Environmental Microbiology* 2014, **80**(6):1882-1892.
452. Hoffman MA, Menge C, Casey TA, Laegreid W, Bosworth BT, Dean-Nystrom EA: **Bovine immune response to Shiga-toxigenic Escherichia coli O157: H7.** *Clinical and Vaccine Immunology* 2006, **13**(12):1322.
453. Menge C, Stamm I, van Diemen PM, Sopp P, Baljer G, Wallis TS, Stevens MP: **Phenotypic and functional characterization of intraepithelial lymphocytes in a bovine ligated intestinal loop model of enterohaemorrhagic Escherichia coli infection.** *Journal of Medical Microbiology* 2004, **53**(6):573-579.
454. Thorpe C, Hurley BP, Lincicome LL, Jacewicz MS, Keusch GT, Acheson DWK: **Shiga toxins stimulate secretion of interleukin-8 from intestinal epithelial cells.** *Infection and Immunity* 1999, **67**(11):5985.
455. Murata K, Higuchi T, Takada K, Oida K, Horie S, Ishii H: **Verotoxin-1 stimulation of macrophage-like THP-1 cells up-regulates tissue factor expression through activation of c-Yes tyrosine kinase: Possible signal transduction in tissue factor up-regulation.** *Biochimica et Biophysica Acta (BBA)-Molecular Basis of Disease* 2006, **1762**(9):835-843.

456. Cherla RP, Lee SY, Mees PL, Tesh VL: **Shiga toxin 1-induced cytokine production is mediated by MAP kinase pathways and translation initiation factor eIF4E in the macrophage-like THP-1 cell line.** *Journal of Leukocyte Biology* 2006, **79**(2):397-407.
457. van de Kar NC, Monnens LA, Karmali MA, van Hinsbergh VW: **Tumor necrosis factor and interleukin-1 induce expression of the verocytotoxin receptor globotriaosylceramide on human endothelial cells: implications for the pathogenesis of the hemolytic uremic syndrome.** *Blood* 1992, **80**(11):2755-2764.
458. Moussay E, Stamm I, Taubert A, Baljer G, Menge C: **Escherichia coli Shiga toxin 1 enhances il-4 transcripts in bovine ileal intraepithelial lymphocytes.** *Veterinary Immunology and Immunopathology* 2006, **113**(3-4):367-382.
459. Gobert AP, Vareille M, Glasser A-L, Hindre T, de Sablet T, Martin C: **Shiga toxin produced by enterohemorrhagic Escherichia coli inhibits PI3K/NF-kappaB signaling pathway in globotriaosylceramide-3-negative human intestinal epithelial cells.** *Journal of Immunology (Baltimore, Md : 1950)* 2007, **178**(12):8168-8174.
460. Ramana CV, Gil MP, Schreiber RD, Stark GR: **Stat1-dependent and-independent pathways in IFN-gamma-dependent signaling.** *Trends in Immunology* 2002, **23**(2):96-101.
461. Young HA, Hardy K: **Role of interferon-gamma in immune cell regulation.** *Journal of Leukocyte Biology* 1995, **58**(4):373-381.
462. Schoenborn JR, Wilson CB: **Regulation of interferon-gamma during innate and adaptive immune responses.** *Advances in Immunology* 2007, **96**:41-101.
463. Skeen MJ, Ziegler HK: **Activation of gamma delta T cells for production of IFN-gamma is mediated by bacteria via macrophage-derived cytokines IL-1 and IL-12.** *The Journal of Immunology* 1995, **154**(11):5832-5841.
464. Arase H, Arase N, Saito T: **Interferon gamma production by natural killer (NK) cells and NK1.1+ T cells upon NKR-P1 cross-linking.** *The Journal of Experimental Medicine* 1996, **183**(5):2391-2396.
465. Schroder K, Hertzog PJ, Ravasi T, Hume DA: **Interferon-gamma: an overview of signals, mechanisms and functions.** *Journal of Leukocyte Biology* 2004, **75**(2):163-189.
466. Desvignes L, Ernst JD: **Interferon-gamma-Responsive Nonhematopoietic Cells Regulate the Immune Response to Mycobacterium tuberculosis.** *Immunity* 2009, **31**(6):974-985.
467. Foster W, Li Y, Usas A, Somogyi G, Huard J: **Gamma interferon as an antifibrosis agent in skeletal muscle.** *Journal of Orthopaedic Research* 2003, **21**(5):798-804.
468. Agnello D, Lankford CR, Bream J, Morinobu A, Gadina M, O'Shea J, Frucht D: **Cytokines and Transcription Factors That Regulate T Helper Cell Differentiation: New Players and New Insights.** *J Clin Immunol* 2003, **23**(3):147-161.
469. Chang JH, Kim YJ, Han SH, Kang CY: **IFN-gamma-STAT1 signal regulates the differentiation of inducible Treg: potential role for ROS-**

- mediated apoptosis. *European Journal of Immunology* 2009, **39**(5):1241-1251.
470. Hu X, Ivashkiv LB: **Cross-regulation of signaling pathways by interferon- γ : implications for immune responses and autoimmune diseases.** *Immunity* 2009, **31**(4):539-550.
471. Rane SG, Reddy EP: **Janus kinases: components of multiple signaling pathways.** *Oncogene* 2000, **19**(49):5662-5679.
472. Calo V, Migliavacca M, Bazan V, Macaluso M, Buscemi M, Gebbia N, Russo A: **STAT proteins: from normal control of cellular events to tumorigenesis.** *Journal of Cellular Physiology* 2003, **197**(2):157-168.
473. Nguyen H, Ramana CV, Bayes J, Stark GR: **Roles of phosphatidylinositol 3-kinase in interferon-gamma-dependent phosphorylation of STAT1 on serine 727 and activation of gene expression.** *Journal of Biological Chemistry* 2001, **276**(36):33361-33368.
474. Wen Z, Zhong Z, Darnell JE, Jr.: **Maximal activation of transcription by Stat1 and Stat3 requires both tyrosine and serine phosphorylation.** *Cell* 1995, **82**(2):241-250.
475. Durbin JE, Hackenmiller R, Simon MC, Levy DE: **Targeted disruption of the mouse Stat1 gene results in compromised innate immunity to viral disease.** *Cell* 1996, **84**(3):443-450.
476. Meraz MA, White JM, Sheehan KC, Bach EA, Rodig SJ, Dighe AS, Kaplan DH, Riley JK, Greenlund AC, Campbell D *et al*: **Targeted disruption of the Stat1 gene in mice reveals unexpected physiologic specificity in the JAK-STAT signaling pathway.** *84* 1996, **3**(431-442).
477. Goldberg M, Belkowski LS, Bloom BR: **Regulation of macrophage function by interferon-gamma. Somatic cell genetic approaches in murine macrophage cell lines to mechanisms of growth inhibition, the oxidative burst, and expression of the chronic granulomatous disease gene.** *The Journal of Clinical Investigation* 1990, **85**(2):563-569.
478. Larkin J, Ahmed CM, Wilson TD, Johnson HM: **Regulation of interferon gamma signaling by suppressors of cytokine signaling and regulatory T cells.** *Frontiers in Immunology* 2013, **4**.
479. Carlow DA, Teh SJ, Teh HS: **Specific antiviral activity demonstrated by TGTP, a member of a new family of interferon-induced GTPases.** *The Journal of Immunology* 1998, **161**(5):2348-2355.
480. Jandu N, Shen S, Wickham ME, Prajapati R, Finlay BB, Karmali MA, Sherman PM: **Multiple seropathotypes of verotoxin-producing Escherichia coli (VTEC) disrupt interferon- γ -induced tyrosine phosphorylation of signal transducer and activator of transcription (Stat)-1.** *Microbial Pathogenesis* 2007, **42**(2-3):62-71.
481. Jandu N, Ceponis PJM, Kato S, Riff JD, McKay DM, Sherman PM: **Conditioned Medium from Enterohemorrhagic Escherichia coli-Infected T84 Cells Inhibits Signal Transducer and Activator of Transcription 1 Activation by Gamma Interferon.** *Infection and Immunity* 2006, **74**(3):1809-1818.
482. Ceponis PJM, McKay DM, Ching JCY, Pereira P, Sherman PM: **Enterohemorrhagic Escherichia coli O157:H7 Disrupts Stat1-Mediated**

- Gamma Interferon Signal Transduction in Epithelial Cells.** *Infection and Immunity* 2003, **71**(3):1396-1404.
483. Ho NK, Ossa JC, Silphaduang U, Johnson R, Johnson-Henry KC, Sherman PM: **Enterohemorrhagic Escherichia coli O157:H7 Shiga Toxins Inhibit Gamma Interferon-Mediated Cellular Activation.** *Infection and Immunity* 2012, **80**(7):2307-2315.
484. Ramana CV, Grammatikakis N, Chernov M, Nguyen H, Goh KC, Williams BR, Stark GR: **Regulation of c-myc expression by IFN-gamma through Stat1-dependent and -independent pathways.** *The EMBO Journal* 2000, **19**(2):263-272.
485. Wang S, Miura M, Jung YK, Zhu H, Gagliardini V, Shi L, Greenberg AH, Yuan J: **Identification and characterization of Ich-3, a member of the interleukin-1beta converting enzyme (ICE)/Ced-3 family and an upstream regulator of ICE.** *Journal of Biological Chemistry* 1996, **271**(34):20580-20587.
486. Asefa B, Klarmann KD, Copeland NG, Gilbert DJ, Jenkins NA, Keller JR: **The interferon-inducible p200 family of proteins: a perspective on their roles in cell cycle regulation and differentiation.** *Blood Cells, Molecules and Diseases* 2004, **32**(1):155-167.
487. Coqueret O: **New roles for p21 and p27 cell-cycle inhibitors: a function for each cell compartment?** *Trends in Cell Biology* 2003, **13**(2):65-70.
488. Chin YE, Kitagawa M, Su W-CS, You Z-H, Iwamoto Y, Fu X-Y: **Cell growth arrest and induction of cyclin-dependent kinase inhibitor p21WAF1/CIP1 mediated by STAT1.** *Science* 1996, **272**(5262):719-722.
489. Nava P, Koch S, Laukoetter MG, Lee WY, Kolegraff K, Capaldo CT, Beeman N, Addis C, Gerner-Smidt K, Neumaier I: **Interferon- γ regulates intestinal epithelial homeostasis through converging β -catenin signaling pathways.** *Immunity* 2010, **32**(3):392-402.
490. Chan JM, Bhinder G, Sham HP, Ryz N, Huang T, Bergstrom KS, Vallance BA: **CD4+ T cells drive goblet cell depletion during Citrobacter rodentium infection.** *Infection and Immunity* 2013, **81**(12):4649-4658.
491. Plattner BL, Hostetter JM: **Comparative Gamma Delta T Cell Immunology: A Focus on Mycobacterial Disease in Cattle.** *Veterinary Medicine International* 2011, **2011**:214384.
492. Tanaka S, Miyazawa K, Kuwano A, Watanabe K, Ohwada S, Aso H, Nishida S, Yamaguchi T: **Age - related changes in leukocytes and T cell subsets in peripheral blood of Japanese Black cattle.** *Animal Science Journal* 2008, **79**(3):368-374.
493. Bull TJ, Vrettou C, Linedale R, McGuinness C, Strain S, McNair J, Gilbert SC, Hope JC: **Immunity, safety and protection of an Adenovirus 5 prime-Modified Vaccinia virus Ankara boost subunit vaccine against Mycobacterium avium subspecies paratuberculosis infection in calves.** *Veterinary Research* 2014, **45**(1):112.
494. Chattha KS, Firth MA, Hodgins DC, Shewen PE: **Expression of complement receptor 2 (CD21), membrane IgM and the inhibitory receptor CD32 (Fc γ RIIb) in the lymphoid tissues of neonatal calves.** *Veterinary Immunology and Immunopathology* 2010, **137**(1):99-108.

495. Connelley T, Longhi C, Burrells A, Degnan K, Hope J, Allan AJ, Hammond JA, Storset AK, Morrison WI: **NKp46+CD3+ Cells: A Novel Nonconventional T Cell Subset in Cattle Exhibiting Both NK Cell and T Cell Features.** *The Journal of Immunology* 2014, **192**(8):3868-3880.
496. MacHugh N, Sopp P: **Bovine CD8 (BoCD8).** *Veterinary Immunology and Immunopathology* 1991, **27**(1):65-69.
497. Howard C, Clarke M, Sopp P, Brownlie J: **Immunity to bovine virus diarrhoea virus in calves: the role of different T-cell subpopulations analysed by specific depletion in vivo with monoclonal antibodies.** *Veterinary Immunology and Immunopathology* 1992, **32**(3):303-314.
498. **Protein Detection and Quantitation: Direct Detect® Spectrometer** [http://www.millipore.com/life_sciences/flx4/direct_detect-tab2=2]
499. Jandu N, Shen S, Wickham ME, Prajapati R, Finlay BB, Karmali MA, Sherman PM: **Multiple seropathotypes of verotoxin-producing Escherichia coli (VTEC) disrupt interferon-gamma-induced tyrosine phosphorylation of signal transducer and activator of transcription (Stat)-1.** *Microb Pathog* 2007, **42**(2-3):62-71.
500. Pollok RC, Farthing MJ, Bajaj-Elliott M, Sanderson IR, McDonald V: **Interferon gamma induces enterocyte resistance against infection by the intracellular pathogen Cryptosporidium parvum.** *Gastroenterology* 2001, **120**(1):99-107.
501. Plataniias LC, Fish EN: **Signaling pathways activated by interferons.** *Experimental Hematology* 1999, **27**(11):1583-1592.
502. Ho NK, Crandall I, Sherman PM: **Identifying Mechanisms by Which Escherichia coli O157:H7 Subverts Interferon-γ Mediated Signal Transducer and Activator of Transcription-1 Activation.** *PloS One* 2012, **7**(1):e30145.
503. Hoffman MA, Menge C, Casey TA, Laegreid W, Bosworth BT, Dean-Nystrom EA: **Bovine immune response to Shiga-toxigenic Escherichia coli O157: H7.** *Clinical and Vaccine Immunology* 2006, **13**(12):1322-1327.
504. Johnson RP, Cray W, Johnson ST: **Serum antibody responses of cattle following experimental infection with Escherichia coli O157: H7.** *Infection and Immunity* 1996, **64**(5):1879-1883.
505. Fröhlich J, Baljer G, Menge C: **Maternally and Naturally Acquired Antibodies to Shiga Toxins in a Cohort of Calves Shedding Shiga-Toxigenic Escherichia coli.** *Applied and Environmental Microbiology* 2009, **75**(11):3695-3704.
506. Rabinovitz BC, E G, Farinati T, A A, R G, Da V, C I, A C, Mercado EC: **Vaccination of pregnant cows with EspA, EspB, gamma-intimin, and Shiga toxin 2 proteins from Escherichia coli O157:H7 induces high levels of specific colostrum antibodies that are transferred to newborn calves.** *Journal of Dairy Science* 2012, **95**(6):3318-3326.
507. Nart P, Holden N, McAteer SP, Wang D, Flockhart AF, Naylor SW, Low JC, Gally DL, Huntley JF: **Mucosal antibody responses of colonized cattle to Escherichia coli O157 - secreted proteins, flagellin, outer membrane proteins and lipopolysaccharide.** *FEMS Immunology & Medical Microbiology* 2008, **52**(1):59-68.

508. Bretschneider G, Berberov E, Moxley RA: **Isotype-specific antibody responses against Escherichia coli O157: H7 locus of enterocyte effacement proteins in adult beef cattle following experimental infection.** *Veterinary Immunology and Immunopathology* 2007, **118**(3):229-238.
509. Potter AA, Klashinsky S, Li Y, Frey EF, Townsend H, Rogan D, Erickson G, Hinkley S, Klopfenstein T, Moxley RA *et al*: **Decreased shedding of Escherichia coli O157:H7 by cattle following vaccination with type III secreted proteins.** *Vaccine* 2004, **22**(3):362-369.
510. McNeilly TN, Mitchell MC, Rosser T, McAteer S, Low JC, Smith DG, Huntley JF, Mahajan A, Gally DL: **Immunization of cattle with a combination of purified intimin-531, EspA and Tir significantly reduces shedding of Escherichia coli O157: H7 following oral challenge.** *Vaccine* 2010, **28**(5):1422-1428.
511. Jandu N, Ho NKL, Donato KA, Karmali MA, Mascarenhas M, Duffy SP, Tailor C, Sherman PM: **Enterohemorrhagic *Escherichia coli* O157 : H7 Gene Expression Profiling in Response to Growth in the Presence of Host Epithelia.** *PloS one* 2009, **4**(3):e4889.
512. Blair JM, Richmond, G. E., Bailey, A. M., Ivens, A., & Piddock, L. J. : **Choice of bacterial growth medium alters the transcriptome and phenotype of Salmonella enterica Serovar Typhimurium.** *PloS One* 2013, **8**(5):e63912.
513. Bridger PS, Mohr M, Stamm I, Fröhlich J, Föllmann W, Birkner S, Metcalfe H, Werling D, Baljer G, Menge C: **Primary bovine colonic cells: a model to study strain-specific responses to Escherichia coli.** *Veterinary Immunology and Immunopathology* 2010, **137**(1):54-63.
514. Villena J, Aso H, Kitazawa H: **Regulation of Toll-like receptors-mediated inflammation by immunobiotics in bovine intestinal epitheliocytes: role of signalling pathways and negative regulators.** *Frontiers in Immunology* 2014, **5**.
515. Sun P, Zhou K, Wang S, Li P, Chen S, Lin G, Zhao Y, Wang T: **Involvement of mapk/NF-κB signaling in the activation of the cholinergic anti-inflammatory pathway in experimental colitis by chronic vagus nerve stimulation.** *PloS One* 2013, **8**(8):e69424.
516. Lim JY, Sheng H, Seo KS, Park YH, Hovde CJ: **Characterization of an Escherichia coli O157: H7 plasmid O157 deletion mutant and its survival and persistence in cattle.** *Applied and Environmental Microbiology* 2007, **73**(7):2037-2047.
517. Low JC, McKendrick IJ, McKechnie C, Fenlon D, Naylor SW, Currie C, Smith DGE, Smith DG, Allison LJ, Gally DL: **Rectal carriage of enterohemorrhagic Escherichia coli O157 in slaughtered cattle.** *Applied and Environmental Microbiology* 2005, **71**(1):93-97.
518. Matthews L, Low J, Gally D, Pearce M, Mellor D, Heesterbeek J, Chase-Topping M, Naylor S, Shaw D, Reid S: **Heterogeneous shedding of Escherichia coli O157 in cattle and its implications for control.** *Proceedings of the National Academy of Sciences of the United States of America* 2006, **103**(3):547-552.

519. Gamage SD, Patton AK, Hanson JF, Weiss AA: **Diversity and Host Range of Shiga Toxin-Encoding Phage**. *Infection and Immunity* 2004, **72**(12):7131-7139.
520. Ostroff SM, Tarr PI, Neill MA, Lewis JH, Hargrett-Bean N, Kobayashi JM: **Toxin genotypes and plasmid profiles as determinants of systemic sequelae in Escherichia coli O157: H7 infections**. *Journal of Infectious Diseases* 1989, **160**(6):994-998.
521. Gamage SD, Strasser JE, Chalk CL, Weiss AA: **Nonpathogenic Escherichia coli Can Contribute to the Production of Shiga Toxin**. *Infection and Immunity* 2003, **71**(6):3107-3115.
522. Gamage SD, McGannon CM, Weiss AA: **Escherichia coli serogroup O107/O117 lipopolysaccharide binds and neutralizes Shiga toxin 2**. *Journal of bacteriology* 2004, **186**(16):5506-5512.
523. Russo LM, Melton-Celsa AR, Smith MA, Smith MJ, O'Brien AD: **Oral intoxication of mice with Shiga toxin type 2a (Stx2a) and protection by anti-Stx2a monoclonal antibody 11E10**. *Infection and Immunity* 2014, **82**(3):1213-1221.
524. Vimr ER: **Unified Theory of Bacterial Sialometabolism: How and Why Bacteria Metabolize Host Sialic Acids**. *ISRN Microbiology* 2013, **2013**:26.
525. Brüssow H, Canchaya C, Hardt W-D: **Phages and the Evolution of Bacterial Pathogens: from Genomic Rearrangements to Lysogenic Conversion**. *Microbiology and Molecular Biology Reviews* 2004, **68**(3):560-602.
526. Gama JA, Reis AM, Domingues I, Mendes-Soares H, Matos AM, Dionisio F: **Temperate Bacterial Viruses as Double-Edged Swords in Bacterial Warfare**. *PloS One* 2013, **8**(3):e59043.
527. Johansson ME, Phillipson M, Petersson J, Velcich A, Holm L, Hansson GC: **The inner of the two Muc2 mucin-dependent mucus layers in colon is devoid of bacteria**. *Proceedings of the National Academy of Sciences* 2008, **105**(39):15064-15069.
528. Møller AK, Leatham MP, Conway T, Nuijten PJ, de Haan LA, Krogfelt KA, Cohen PS: **An Escherichia coli MG1655 lipopolysaccharide deep-rough core mutant grows and survives in mouse cecal mucus but fails to colonize the mouse large intestine**. *Infection and Immunity* 2003, **71**(4):2142-2152.
529. Grys TE, Walters LL, Welch RA: **Characterization of the StcE protease activity of Escherichia coli O157: H7**. *Journal of Bacteriology* 2006, **188**(13):4646-4653.
530. Low JC, McKendrick IJ, McKechnie C, Fenlon D, Naylor SW, Currie C, Smith DG, Allison L, Gally DL: **Rectal carriage of enterohemorrhagic Escherichia coli O157 in slaughtered cattle**. *Applied and Environmental Microbiology* 2005, **71**(1):93-97.
531. Hoffmann JA: **Innate immunity of insects**. *Current Opinion in Immunology* 1995, **7**(1):4-10.
532. Lionakis MS: **Drosophila and Galleria insect model hosts: new tools for the study of fungal virulence, pharmacology and immunology**. *Virulence* 2011, **2**(6):521-527.

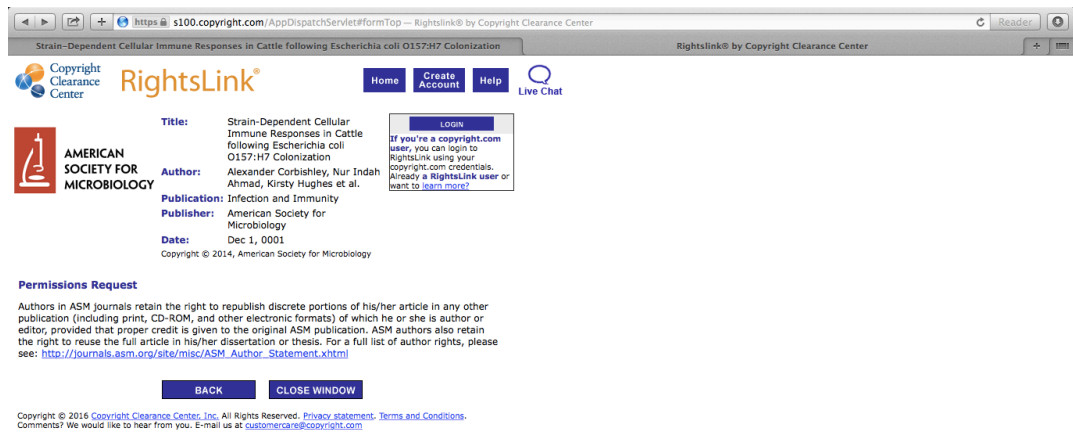
533. Ramarao N, Nielsen-Leroux C, Lereclus D: **The insect *Galleria mellonella* as a powerful infection model to investigate bacterial pathogenesis.** *Journal of Visualized Experiments: JoVE* 2011(70):e4392-e4392.
534. Roe AJ, Yull H, Naylor SW, Woodward MJ, Smith DGE, Gally DL: **Heterogeneous Surface Expression of EspA Translocon Filaments by *Escherichia coli* O157:H7 Is Controlled at the Posttranscriptional Level.** *Infection and Immunity* 2003, **71**(10):5900-5909.
535. Tahoun A, Siszler G, Spears K, McAteer S, Tree J, Paxton E, Gillespie TL, Martinez-Argudo I, Jepson MA, Shaw DJ: **Comparative Analysis of EspF Variants in Inhibition of *Escherichia coli* Phagocytosis by Macrophages and Inhibition of *E. coli* Translocation through Human-and Bovine-Derived M Cells.** *Infection and Immunity* 2011, **79**(11):4716-4729.
536. Griffiths AJF MJ, Suzuki DT, et al. New York: W. H. Freeman.: **Bacterial insertion sequences.** . In: *An Introduction to Genetic Analysis*. 2000.
537. Makino K, Ishii K, Yasunaga T, Hattori M, Yokoyama K, Yutsudo CH, Kubota Y, Yamaichi Y, Iida T, Yamamoto K: **Complete nucleotide sequences of 93-kb and 3.3-kb plasmids of an enterohemorrhagic *Escherichia coli* O157: H7 derived from Sakai outbreak.** *DNA Research* 1998, **5**(1):1-9.
538. Thingstad T, Lignell R: **Theoretical models for the control of bacterial growth rate, abundance, diversity and carbon demand.** *Aquatic Microbial Ecology* 1997, **13**(1):19-27.
539. Rodriguez-Valera F, Martin-Cuadrado A-B, Rodriguez-Brito B, Pašić L, Thingstad TF, Rohwer F, Mira A: **Explaining microbial population genomics through phage predation.** *Nature Reviews Microbiology* 2009, **7**(11):828-836.
540. Tree JJ, Granneman S, McAteer SP, Tollervey D, Gally DL: **Identification of bacteriophage-encoded anti-sRNAs in pathogenic *Escherichia coli*.** *Molecular cell* 2014, **55**(2):199-213.
541. Papenfort K, Vogel J: **Small RNA functions in carbon metabolism and virulence of enteric pathogens.** *Frontiers in Cellular and Infection Microbiology* 2014, **4**.
542. Torres AG, Kaper JB: **Multiple elements controlling adherence of enterohemorrhagic *Escherichia coli* O157: H7 to HeLa cells.** *Infection and Immunity* 2003, **71**(9):4985-4995.
543. Tarr PI, Bilge SS, Vary JC, Jelacic S, Habeeb RL, Ward TR, Baylor MR, Besser TE: **Iha: a novel *Escherichia coli* O157: H7 adherence-conferring molecule encoded on a recently acquired chromosomal island of conserved structure.** *Infection and Immunity* 2000, **68**(3):1400-1407.
544. Lloyd SJ, Ritchie JM, Torres AG: **Fimbriation and curliation in *Escherichia coli* O157:H7: a paradigm of intestinal and environmental colonization.** *Gut Microbes* 2012, **3**(3):272-276.
545. Low AS HN, Rosser T, Roe AJ, Constantinidou C, Hobman JL, Smith DG, Low JC, Gally DL. : **Analysis of fimbrial gene clusters and their expression in enterohaemorrhagic *Escherichia coli* O157:H7.** *Environmental Microbiology* 2006, **8**:1033-1047.
546. Samadder P X-CJ, Saldana Z, Jordan D, Tarr PI, Kaper JB, Giron JA.: **The *Escherichia coli* ycbQRST operon encodes fimbriae with laminin-**

- binding and epithelial cell adherence properties in Shiga-toxigenic E. coli O157:H7.** *Environmental Microbiology* 2009, **11**:1815-1826.
547. Asadulghani M, Ogura Y, Ooka T, Itoh T, Sawaguchi A, Iguchi A, Nakayama K, Hayashi T: **The defective prophage pool of Escherichia coli O157: prophage-prophage interactions potentiate horizontal transfer of virulence determinants.** *PLoS Pathog* 2009, **5**(5):e1000408.
548. Dallman T, Ashton P, Byrne L, Perry N, Petrovska L, Ellis R, Allison L, Hanson M, Holmes A, Gunn G *et al*: **Applying phylogenomics to understand the emergence of Shiga Toxin producing Escherichia coli O157:H7 strains causing severe human disease in the United Kingdom.** *Microbial Genomics* 2015, **16**(114.2015):10-1186.
549. Haycock JW: **3D cell culture: a review of current approaches and techniques:** Humana Press; 2011.
550. Murinda SE, Nguyen LT, Landers TL, Draughon FA, Mathew AG, Hogan JS, Smith KL, Hancock DD, Oliver SP: **Comparison of Escherichia coli Isolates from humans, food, and farm and companion animals for presence of Shiga toxin-producing E. coli virulence markers.** *Foodborne Pathogens and Disease* 2005, **1**(3):178-184.
551. Tesh VL, Samoel JE, Perera LP, Sharefkin JB, O'Brien AD: **Evaluation of the Role of Shiga and Shiga-like Toxins in Mediating Direct Damage to Human Vascular Endothelial Cells.** *Journal of Infectious Diseases* 1991, **164**(2):344-352.
552. Tildesley MJ, Gally DL, McNeilly TN, Low JC, Mahajan A, Savill NJ: **Insights into mucosal innate responses to Escherichia coli O157 : H7 colonization of cattle by mathematical modelling of excretion dynamics.** *Journal of The Royal Society Interface* 2012, **9**(68):518-527.
553. Mlay P, Phiri E, Pereka A, Balthazary S, Yakobo P: **The Type And Number Of Ciliate Protozoa In The Rumen, Omasum And Colon Of Tanzanian Short Horn Zebu Cattle.** *Tanzania Veterinary Journal* 2008, **25**(1):13-23.
554. Meltz Steinberg K, Levin BR: **Grazing protozoa and the evolution of the Escherichia coli O157:H7 Shiga toxin-encoding prophage.** *Proceedings of the Royal Society of London B: Biological Sciences* 2007, **274**(1621):1921-1929.
555. Barker J, Brown M: **Trojan horses of the microbial world: protozoa and the survival of bacterial pathogens in the environment.** *Microbiology* 1994, **140**(6):1253-1259.
556. C. E. Schmidt SS, T. E. Besser: **Naturally-Occurring Environmental Protozoa Graze Shigatoxigenic Escherichia coli O157:H7.** In: *American Society for Microbiology General Meeting: 2014; Boston, Massachusetts:* ASM; 2014.
557. Matz C, Kjelleberg S: **Off the hook—how bacteria survive protozoan grazing.** *Trends in Microbiology* 2005, **13**(7):302-307.
558. Lainhart W, Stolfa G, Koudelka GB: **Shiga toxin as a bacterial defense against a eukaryotic predator, Tetrahymena thermophila.** *Journal of Bacteriology* 2009, **191**(16):5116-5122.
559. Brandl MT: **Fitness of Human Enteric Pathogens on Plants and Implications for Food Safety1.** *Annual Review of Phytopathology* 2006, **44**(1):367-392.


560. Muniesa M, Jofre J: **Factors influencing the replication of somatic coliphages in the water environment.** *Antonie Van Leeuwenhoek* 2004, **86**(1):65-76.
561. Kelly BG, Vespermann A, Bolton DJ: **Horizontal gene transfer of virulence determinants in selected bacterial foodborne pathogens.** *Food and Chemical Toxicology* 2009, **47**(5):969-977.
562. Mellmann A, Lu S, Karch H, Xu J-g, Harmsen D, Schmidt MA, Bielaszewska M: **Recycling of Shiga Toxin 2 Genes in Sorbitol-Fermenting Enterohemorrhagic Escherichia coli O157:NM.** *Applied and Environmental Microbiology* 2008, **74**(1):67-72.

Appendix

Note on permission to reuse the article 'Strain-Dependent Cellular Immune Responses in Cattle following *Escherichia coli* O157:H7 colonisation' in this thesis:



The screenshot shows a web browser window with the URL <https://s100.copyright.com/AppDispatchServlet#formTop>. The page title is "Strain-Dependent Cellular Immune Responses in Cattle following Escherichia coli O157:H7 Colonization". The page features the Copyright Clearance Center logo and the RightsLink logo. Navigation links include Home, Create Account, Help, and Live Chat. The article metadata is as follows:

	Title: Strain-Dependent Cellular Immune Responses in Cattle following <i>Escherichia coli</i> O157:H7 Colonization
	Author: Alexander Corbishley, Nur Indah Ahmad, Kirsty Hughes et al.
	Publication: Infection and Immunity
	Publisher: American Society for Microbiology
	Date: Dec 1, 0001

Below the metadata is a "Permissions Request" section. It states: "Authors in ASM Journals retain the right to republish discrete portions of his/her article in any other publication (including print, CD-ROM, and other electronic formats) of which he or she is author or editor, provided that proper credit is given to the original ASM publication. ASM authors also retain the right to reuse the full article in his/her dissertation or thesis. For a full list of author rights, please see: http://journals.asm.org/site/misc/ASM_Author_Statement.xhtml". At the bottom of the page, there are "BACK" and "CLOSE WINDOW" buttons, and a copyright notice: "Copyright © 2016 Copyright Clearance Center, Inc. All Rights Reserved. Privacy statement Terms and Conditions. Comments? We would like to hear from you. E-mail us at customerservice@copyright.com".

Strain-Dependent Cellular Immune Responses in Cattle following *Escherichia coli* O157:H7 Colonization

Alexander Corbishley,^{a,b} Nur Indah Ahmad,^b Kirsty Hughes,^c Michael R. Hutchings,^c Sean P. McAteer,^b Timothy K. Connelley,^b Helen Brown,^b David L. Gally,^b Tom N. McNeilly^a

Moredun Research Institute, Pentlands Science Park, Bush Loan, Penicuik, United Kingdom^a; The Roslin Institute, University of Edinburgh, Easter Bush, Midlothian, United Kingdom^b; SRUC, Edinburgh, United Kingdom^c

Enterohemorrhagic *Escherichia coli* (EHEC) O157:H7 causes hemorrhagic diarrhea and potentially fatal renal failure in humans. Ruminants are considered to be the primary reservoir for human infection. Vaccines that reduce shedding in cattle are only partially protective, and their underlying protective mechanisms are unknown. Studies investigating the response of cattle to colonization generally focus on humoral immunity, leaving the role of cellular immunity unclear. To inform future vaccine development, we studied the cellular immune responses of cattle during EHEC O157:H7 colonization. Calves were challenged either with a phage type 21/28 (PT21/28) strain possessing the Shiga toxin 2a (Stx2a) and Stx2c genes or with a PT32 strain possessing the Stx2c gene only. T-helper cell-associated transcripts at the terminal rectum were analyzed by reverse transcription-quantitative PCR (RT-qPCR). Induction of gamma interferon (IFN- γ) and T-bet was observed with peak expression of both genes at 7 days in PT32-challenged calves, while upregulation was delayed, peaking at 21 days, in PT21/28-challenged calves. Cells isolated from gastrointestinal lymph nodes demonstrated antigen-specific proliferation and IFN- γ release in response to type III secreted proteins (T3SPs); however, responsiveness was suppressed in cells isolated from PT32-challenged calves. Lymph node cells showed increased expression of the proliferation marker Ki67 in CD4⁺ T cells from PT21/28-challenged calves, NK cells from PT32-challenged calves, and CD8⁺ and $\gamma\delta$ T cells from both PT21/28- and PT32-challenged calves following *ex vivo* restimulation with T3SPs. This study demonstrates that cattle mount cellular immune responses during colonization with EHEC O157:H7, the temporality of which is strain dependent, with further evidence of strain-specific immunomodulation.

Enterohemorrhagic *Escherichia coli* (EHEC) O157:H7 is a bacterial zoonotic disease of global importance (1). Ruminants, particularly cattle, are the predominant reservoir, and humans become infected following fecal contamination of food, the environment, and water (2–6). Many cases are sporadic (7); however, large outbreaks occur periodically. While colonization of cattle is largely asymptomatic (8), humans typically develop painful hemorrhagic diarrhea. A significant minority of patients progress to potentially fatal hemolytic-uremic syndrome (HUS), a form of renal failure resulting from Shiga toxin (Stx; also known as verotoxin)-induced endothelial dysfunction (9).

Significant efforts have been made in abattoirs and meat-processing plants to reduce the contamination of beef produce reaching the consumer. While these efforts have been partially successful, food-borne outbreaks have not been eliminated, and environmental transmission remains unmitigated. A range of on-farm interventions have been proposed to reduce bacterial shedding by cattle, including dietary manipulation, phage therapy, antimicrobial treatment, probiotic administration, and vaccination (10–15). Recent reviews and meta-analyses have identified probiotics and vaccines as the most tractable and efficacious control measures (12, 16, 17). Two commercial vaccines have been developed to date. One involves a method of extraction from bacteria cultured under iron-restricted conditions that enriches for membrane components (EpiTopix, Willmar, MN, USA). The other is a supernatant preparation that contains type III secreted proteins (T3SPs) (Econiche; Bioniche Life Sciences, Belleville, Ontario, Canada). Vaccination of cattle with recombinant T3SPs has been demonstrated to reduce colonization rates in cattle, an effect enhanced by the addition of H7 flagellin (18, 19).

To our knowledge, the mechanism of protection of these vac-

cines has not been demonstrated. EHEC O157:H7 uses its type III secretion system (T3SS) to deliver a range of effector proteins to host epithelial cells (20, 21). The T3SS includes an EspA translocon filament, capped by the pore-forming EspB/EspD (EspB/D) complex. The construction of the translocon and the delivery of effector proteins by the T3SS are carefully regulated (22). Injected effectors include the translocated intimin receptor (Tir), which binds to the bacterial surface protein intimin and is central to the formation of actin pedestals and intimate attaching and effacing (A/E) lesions (23). It is reasonable to hypothesize that antibodies directed against the structural components of the T3SS, such as EspA/B/D, or against adhesion factors, such as intimin and its cognate receptor Tir, may block bacterial binding. In support of this hypothesis, vaccination of sows with intimin has been shown to reduce the level of EHEC O157:H7 colonization of suckling piglets (24), presumably through antibody-mediated blocking of bacterial binding. In addition, bovine colostrum has been shown to reduce T3SS-mediated hemolysis *in vitro* (25), and passive transfer of EspB, intimin, and neutralizing antibodies against Stx2

Received 7 August 2014 Returned for modification 2 September 2014

Accepted 16 September 2014

Published ahead of print 29 September 2014

Editor: R. P. Morrison

Address correspondence to Tom N. McNeilly, tom.mcneilly@moredun.ac.uk.

Supplemental material for this article may be found at <http://dx.doi.org/10.1128/IAI.02462-14>.

Copyright © 2014, American Society for Microbiology. All Rights Reserved.

doi:10.1128/IAI.02462-14

TABLE 1 EHEC O157:H7 strains used in this study

Strain	Shiga toxin gene(s)	Phage type	Origin	Modification(s)	Source or reference
9000 (WX009000S01E)	<i>stx_{2a}</i> , <i>stx_{2c}</i>	PT21/28	Cattle feces	None	86
Zap1380	<i>stx_{2a}</i> , <i>stx_{2c}</i>	PT21/28	Strain 9000	Nal ^f	This study
10671 (WX010671S01E)	<i>stx_{2c}</i>	PT32	Cattle feces	None	86
Zap1381	<i>stx_{2c}</i>	PT32	Strain 10671	Nal ^f	This study
Zap193 (NCTC 12900) (WT)	None	NA ^b	NCTC ^a	None	NCTC
Zap1143 (Δ <i>sepL</i> mutant)	None	NA	Strain Zap193	Nal ^f , Δ <i>sepL</i>	52

^a National Collection of Type Cultures (NCTC), Public Health England (<https://www.phe-culturecollections.org.uk/collections/nctc.aspx>).

^b NA, not available.

to calves has been demonstrated following maternal vaccination (26). H7 flagellin has also been demonstrated to act as an adhesion factor, and anti-H7 antibodies reduce the level of binding of bacteria to primary cell cultures (27).

Despite high antibody titers following vaccination with these antigens, vaccination is only partially protective (13, 14, 28–31), while antibody titers are inconsistently correlated with bacterial shedding (32–34). The serological response of cattle to colonization has also been studied extensively, and antibodies against O157 lipopolysaccharide (LPS), H7, Tir, intimin, EspA, EspB, EspD, EspM2, NleA, TccP, Stx1, and Stx2 have been demonstrated (25, 33–36). Despite this, prior exposure to EHEC O157:H7 results in only partial and transient protection against reinfection (33, 34, 37).

While cattle can shed detectable levels of EHEC O157:H7 for a considerable period, most animals are able to clear the infection successfully (37–39). Given the limitations of antibody-mediated protection, it is likely that other innate and adaptive responses play important roles in bacterial clearance. It is also rational to hypothesize that once a microcolony has formed on an epithelial cell, and its cellular processes are thus being manipulated by secreted bacterial effectors, the best way of effectively clearing the infection is to dispose of the colonized cell. This raises the prospect of an important role for cellular immunity in bacterial clearance. However, to our knowledge, only two studies have considered the role of cellular immunity during EHEC O157:H7 colonization in ruminants; these identified lymphoproliferative cellular responses to heat-killed EHEC O157:H7 (40) and recombinant antigens (41) in bovine peripheral blood mononuclear cells and ovine rectal lymph node cells, respectively. The case for a protective cellular immune response is further strengthened by the observations that colonized bovine epithelial cells are exfoliated *in vivo* (42) and that some strains are efficiently internalized by bovine epithelial cells both *in vivo* and *in vitro* (43).

While colonization of mice by *Citrobacter rodentium* has been used as a model for study of the interaction of an A/E lesion-forming bacterium with its mammalian host (44), none of the mouse models reported to date have demonstrated convincing colonization and A/E lesion formation with EHEC O157:H7 (45–51). The relevance of studies on mice to the interaction of EHEC O157:H7 with its natural bovine host is therefore unclear. In addition to being the natural reservoir of infection, cattle can also be sampled repeatedly during colonization, allowing one to control for interanimal variation resulting from the use of outbred populations.

We hypothesized that by quantifying T-helper cell-associated gene transcripts at the terminal rectums of cattle during the course

of EHEC O157:H7 colonization, it would be possible to identify and determine the direction of the cellular immune response at the primary site of colonization. Our results show that there is a T_H type 1 skew to the response at the rectal mucosa, the temporal nature of which differs by strain, and that colonization with both the PT21/28 and the PT32 strain results in an increase in the proportion of CD4⁺ T cells within the rectal mucosal T-cell population. We also present data analyzing regional lymph node responses to bacterial proteins that suggest a role for both innate and adaptive cellular immunity in the bovine response to colonization.

MATERIALS AND METHODS

Bacterial strains, inocula, and T3SP preparation. The strains used in this study are listed in Table 1. Glycerol stocks were resuscitated on lysogeny broth (LB) agar and were incubated at 37°C overnight. To generate the inocula for the calf studies, a single colony of strain 9000 (phage type 21/28 [PT21/28]), PT32 strain 10671, Zap1380 (a naturally derived nalidixic acid [Nal]-resistant variant of 9000), or Zap1381 (a naturally derived Nal-resistant variant of 10671) was used to inoculate separate flasks of LB, which were incubated at 37°C overnight. Inocula for each calf were prepared by mixing 5 ml of an overnight LB culture of 9000 with 5 ml of an overnight LB culture of Zap1380 or by mixing 5 ml of an overnight LB culture of 10671 with 5 ml of an overnight LB culture of Zap1381, representing a final dose of $\sim 1 \times 10^9$ CFU per calf.

To generate the T3SP preparations for the study of antigen recall responses, a single colony of Zap193 (wild type [WT]) or Zap1143 (Δ *sepL*) was used to inoculate 10 ml LB, which was incubated at 37°C (200 rpm) overnight. The WT strain secretes predominantly structural components of the T3SS, while the Δ *sepL* strain instead secretes a wider variety of effector proteins (52). Two milliliters of the overnight culture was used to inoculate 500 ml minimal essential medium (MEM)-HEPES (Sigma-Aldrich, Gillingham, United Kingdom), which was cultured at 37°C (200 rpm) to an optical density at 600 nm (OD₆₀₀) of 0.8. Bacteria were pelleted, and supernatants were filter sterilized (0.2- μ m low protein binding filters; Millipore, Watford, United Kingdom). Proteins were precipitated overnight at 4°C using trichloroacetic acid (VWR International, Luttermouth, United Kingdom) at a final concentration of 10% (vol/vol). Precipitated proteins were pelleted at $5,000 \times g$ for 30 min at 4°C and the supernatant discarded. Pellets were suspended in 1.5 M Tris-HCl (pH 8.8) and were dialyzed in phosphate-buffered saline (PBS) across a regenerated cellulose membrane with a molecular size cutoff rating of 3.5 kDa (Spectrum Labs, Breda, The Netherlands). Protein preparations were checked by separation using sodium dodecyl sulfate-polyacrylamide gel electrophoresis (SDS-PAGE) and were stained with Coomassie blue (Invitrogen, Paisley, United Kingdom) (see Fig. S1 in the supplemental material). The total-protein concentration was estimated using a bicinchoninic protein assay kit (Pierce Biotechnology, Rockford, IL, USA) and was read using a microplate reader at 562 nm (Dydx Technologies, Worthing, United Kingdom). The lipopolysaccharide (LPS) concentra-

tion was estimated using the EndoLISA kit (Hyglos GmbH, Bernried, Germany) and was read using a Synergy HT microplate reader (BioTek, Winooski, VT, USA) fitted with 360/40-nm wavelength excitation and 460/40-nm wavelength emission filters.

Animal experiments. Oral bacterial challenge was performed at the Moredun Research Institute (MRI) under Home Office license 60/3179. Ethical approval was obtained from the MRI Animal Experiments Committee. Two groups of six conventionally reared male dairy calves were randomly assigned to separate rooms in the MRI High Security Unit (HSU). Two calves were housed in conventional pens. The average age of the calves at the time of challenge was 12 ± 2 weeks. At this age, all the animals were weaned, i.e., they were ruminants yet small enough to be handled safely in the HSU. Fecal samples obtained from each calf prior to challenge were confirmed to be negative for EHEC O157:H7 by immunomagnetic separation (IMS) performed according to the manufacturer's instructions (anti-EHEC O157 Dynabeads; Invitrogen). Five additional age-matched calves that had been used as controls in other studies were used as sources of additional lymph node and rectal mucosal samples. Fecal samples collected postmortem from these calves were screened for the presence of EHEC O157:H7 using IMS. EHEC O157:H7 was not isolated from any of the samples.

Four calves in one HSU room were orally challenged by orogastric intubation with 500 ml PBS containing 10 ml of an overnight LB culture of strain 9000 and its naturally derived Nal-resistant variant. Four calves in the other HSU room were orally challenged in the same way with strain 10671 and its naturally derived Nal-resistant variant. The other two calves (sentinels) in each HSU room were administered 500 ml PBS only.

Three days after oral challenge, 10 g surface feces taken directly from the rectum was suspended in 90 ml sterile PBS. Samples were collected daily for the first 2 weeks and then every other day. Tenfold serial dilutions were prepared in PBS, and 100 μ l from three dilutions across a 1,000-fold range of dilutions was plated out in triplicate onto cefixime-tellurite sorbitol MacConkey agar (CT-SMAC) plates. Resuspended feces were stored at 4°C overnight. Plates were incubated at 37°C overnight and colonies enumerated at the most suitable dilution. Five to 10 colonies from each plate were confirmed as O157 positive by using a latex agglutination kit (Oxoid, Basingstoke, United Kingdom). The CFU per gram of feces was calculated by multiplying the mean colony count of the triplicate plates by the appropriate dilution factor. Where no colonies were observed, broth enrichment was carried out with 1 ml of the resuspended feces added to 9 ml tryptone soya broth (TSB; Oxoid). TSBs were incubated at 37°C overnight and were plated onto CT-SMAC plates. Overnight bacterial growth was tested for O157 by latex agglutination. Feces that were negative by direct plating but positive after broth enrichment were assigned a value of 10 CFU/g.

Rectal biopsy specimens were taken at -5, 7, 14, 21, and 31 days postchallenge. A local anesthetic was applied to the anal sphincter (5% EMLA; Astra Zeneca, Luton, United Kingdom). A rectal speculum (Veterinary Instrumentation, Sheffield, United Kingdom) was used to access the rectal mucosa. Pinch biopsy specimens from the rectal mucosa were taken from two opposing sites approximately 5 cm proximal to the recto-anal junction. The position of each biopsy specimen was recorded, and the site was avoided at subsequent samplings. Biopsy specimens were immediately placed into RNAlater (Ambion, Paisley, United Kingdom) and were stored at 4°C overnight before storage at -80°C.

At the end of the trial (31 to 33 days), calves were killed using 60 ml intravenous pentobarbital (Animalcare, York, United Kingdom). Rectal lymph nodes (RLN), mesenteric lymph nodes (MLN) (100 cm proximal to the ileocecolic junction) and prescapular lymph nodes (PsLN) were collected and were transported in 35 ml preparation medium (Hanks buffered saline solution [HBSS] without calcium and magnesium, 2% heat-inactivated [56°C, 30 min] fetal calf serum [HI-FCS], 10 mg/ml gentamicin [Sigma-Aldrich], 200 IU/ml penicillin, and 200 μ g/ml streptomycin). A 0.5-cm-wide strip of rectal mucosa was dissected and was placed in

PBS containing 2 mg/ml polymyxin B (Sigma-Aldrich) for subsequent isolation of rectal mucosal lymphocytes.

Assessment of gene expression. RNA was extracted from the rectal biopsy specimens using the RNeasy Plus minikit (Qiagen, Hilden, Germany). Biopsy specimens were disrupted in Precellys CK28 tubes using 5 23-s cycles at 6,200 rpm in a tissue homogenizer (Peqlab, Salisbury Green, United Kingdom). Tubes were put on ice for 2 min between cycles. Residual DNA was digested on the column with DNase I (Qiagen). The RNA yield was measured using a NanoDrop ND1000 spectrophotometer (Thermo Scientific, Waltham, MA, USA) and RNA quality assessed using an RNA 6000 Nano kit for total RNA and a model 2100 Bioanalyzer (Agilent Technologies, Wokingham, United Kingdom). All RNA samples had an RNA integrity number (RIN) score of >7.0.

cDNA was synthesized as per the manufacturer's instructions, using SuperScript II (Invitrogen) reverse transcriptase (RT), RNaseOUT (Invitrogen), a deoxynucleoside triphosphate (dNTP) mixture (Invitrogen), and oligo(dT)₂₅ primers (Sigma-Aldrich), from 1 μ g RNA, where 0.5 μ g was pooled from each of the two biopsy specimens taken at each time point. The reaction volume was 20 μ l. Cycling conditions were as follows: 42°C for 2 min followed by the addition of reverse transcriptase, 42°C for 50 min, and 70°C for 15 min. cDNA was diluted 3-fold using PCR water and was stored at -20°C prior to use.

Quantitative PCR (qPCR) was conducted in triplicate in 96-well qPCR plates using Precision master mix with ROX (Primer Design, Southampton, United Kingdom) and an ABI Prism 7000 or ABI Prism 7500 (Applied Biosystems, Paisley, United Kingdom) qPCR instrument as per the manufacturer's instructions. The reaction volume was 20 μ l. Cycling conditions were 95°C for 15 min and 50 cycles of 95°C for 15 s and 60°C for 60 s, during which time fluorescence was read, followed by melting curve analysis.

Reference genes were selected using the bovine geNorm kit (Primer Design) containing primers for ATP5B, eukaryotic initiation factor 2, subunit beta (EIF2B2), actin, beta (ACTB), succinate dehydrogenase complex, subunit A (SDHA), RPL12, and glyceraldehyde-3-phosphate dehydrogenase (GAPDH). qPCRs were prepared using 5 μ l cDNA from each time point for three animals. qBasePLUS2 software, version 2.4 (Biogazelle, Zwijnaarde, Belgium), was used to select the GAPDH and ATP5B genes as the most stably expressed genes. Primers and standard curve plasmids for GAPDH and ATP5B were supplied by Primer Design and were used as per the manufacturer's instructions. All other primers in this study were supplied by Eurofins Genomics (Acton, United Kingdom).

Plasmids for standard curve generation for bovine interleukin 10 (IL-10), transforming growth factor β 1 (TGF- β 1), gamma interferon (IFN- γ), tumor necrosis factor alpha (TNF- α), IL-4, and IL-13 were available in-house. Fragments of bovine FoxP3, RAR-related orphan receptor C (RORC), IL-17, IL-22, T-bet, and GATA3 were cloned using the external primers shown in Table S1 in the supplemental material, which were designed using Primer BLAST (NCBI, Bethesda, MD, USA), and their specificity was checked against the *Bos taurus* RefSeq mRNA database. Gene fragments were generated using KOD Hot Start (Millipore) DNA polymerase, a dNTP mixture (Invitrogen), and bovine cDNA synthesized from one rectal biopsy sample as per the manufacturer's instructions. The reaction volume was 50 μ l. Cycling was carried out according to the following touchdown PCR (53) protocol: 95°C for 3 min; 15 cycles of 95°C for 30 s, 70°C decreasing by 1°C per cycle for 45 s, and 72°C for 60 s; 20 cycles of 95°C for 30 s, 55°C for 45 s, and 72°C for 60 s; and 70°C for 10 min. PCR products were run on a 2% agarose gel and bands of the expected size excised and purified using the QIAquick gel extraction kit (Qiagen). Two microliters of the purified amplicon mixture was A-tailed by incubation with 5 U of GoTaq DNA polymerase (Promega, Southampton, United Kingdom), 2 μ l 5 \times GoTaq DNA master mix (Promega), 1 μ l 2 mM dATP (Invitrogen), and 4 μ l PCR water for 30 min at 70°C. A-tailed amplicons were ligated into pGEM-T Easy vector plasmids (Promega) as per the manufacturer's instructions.

TABLE 2 Antibodies used in this study

Reactivity	Clone/host	Isotype	Conjugate	Supplier
Bovine CD3	MM1A	IgG1	None	Washington State University, Pullman, WA
Bovine CD4	ILA12	IgG2a	None	In-house
Bovine CD8	ILA105	IgG2a	None	In-house
Bovine TcR1-N24(δ)	GB21A	IgG2b	None	Washington State University, Pullman, WA
Bovine NKp46	AKS1	IgG1	Alexa Fluor 488	AbD Serotec, Oxford, UK
Bovine IFN- γ	CC302	IgG1	Alexa Fluor 647	AbD Serotec, Oxford, UK
Mouse IgG	Goat	NA ^a	Alexa Fluor 488	Molecular Probes, Paisley, UK
Ki67	Rabbit	NA	None	Abcam, Cambridge, UK
Rabbit Ig	Goat	NA	Alexa Fluor 405	Molecular Probes
Mouse IgG1	Goat	NA	Alexa Fluor 647	Molecular Probes
Mouse IgG2a	Goat	NA	Phycoerythrin	Molecular Probes
Mouse IgG2b	Goat	NA	Alexa Fluor 488	Molecular Probes

^a NA, not applicable.

Plasmids were used to transform JM109 competent cells (Promega) as per the manufacturer's instructions, and the transformed cells were plated onto LB agar containing 100 μ g/ml ampicillin, 80 μ g/ml 5-bromo-4-chloro-3-indolyl- β -D-galactopyranoside (X-gal), and 500 μ M isopropyl- β -D-thiogalactopyranoside (IPTG). Two white colonies for each transformation were checked by colony PCR using the internal primers shown in Table S2 in the supplemental material. Internal primers were taken from the literature or were designed using Primer BLAST (NCBI). Specificity was checked against the *Bos taurus* RefSeq mRNA database. One PCR-positive colony for each gene was used to inoculate 10 ml LB, and the mixture was incubated at 37°C (200 rpm) overnight. Plasmids were purified using the Wizard Plus SV Miniprep DNA purification system (Promega). Plasmids were sequenced by Eurofins Genomics using the T7 and M13 rev (–29) primers. Sequences were checked against the *Bos taurus* RefSeq RNA database using BLAST (NCBI), and internal primers (see Table S2) were checked using the Sequence Manipulation Suite, version 2 (Bioinformatics Organization, MA, USA). Plasmid molecular weight was estimated using the Sequence Manipulation Suite by updating the published plasmid sequence with the inserted sequences. One microgram of plasmid DNA was linearized using the restriction enzyme NdeI (Promega) at 37°C for 30 min. Linearization was confirmed by agarose gel electrophoresis. Digests were purified using the QIAquick PCR purification kit (Qiagen); DNA was quantified; and linearized plasmids were diluted using PCR water to 10⁹ copies per μ l.

Plasmids were diluted across the dynamic ranges indicated in Table S3 in the supplemental material and were used to generate a standard curve for each gene on each qPCR plate run. qPCR mixtures were prepared using 1 μ l cDNA/well. For ATP5B, GAPDH, IFN- γ , T-bet, IL-17, RORC, TNF- α , and IL-10, Precision master mix was used as per the geNorm experiment described above. For the lower-copy-number transcripts GATA3, FoxP3, IL-4, IL-22, IL-13, and TGF- β 1, the SYBR GreenER qPCR SuperMix (Invitrogen) was used as per the manufacturer's instructions. Reactions were performed in duplicate, and the reaction volume was 25 μ l. Cycling conditions were 50°C for 2 min, 95°C for 10 min, and 40 cycles of 95°C for 15 s and 60°C for 60 s, during which time fluorescence was read, followed by melting curve analysis.

Standard curves were calculated from the threshold cycle (C_T) values using ABI Prism 7000 SDS software, version 1.2.3 (Applied Biosystems), and the calculated gene copies/ μ l cDNA were exported in comma-separated variable files. An SQL script (MySQL Community Server, version 5.1) was used to calculate the arithmetic mean for the technical repeats and then to normalize the copy number/ μ l cDNA for each gene to the geometric mean copy number/ μ l cDNA for the reference genes ATP5B and GAPDH as described previously (54).

Analysis of mucosal T-cell populations. Rectal mucosal strips collected postmortem were cut into 1-cm by 2-cm pieces, placed in 25 ml digestion medium consisting of Dulbecco's modified Eagle medium (DMEM; Sigma-Aldrich) supplemented with 10% HI-FCS, 75 IU/ml col-

lagenase (Sigma-Aldrich), and 20 μ g/ml dispase I neutral protease, grade 1 (Roche, Basel, Switzerland), and incubated at 37°C (200 rpm) for 90 min. The digested samples were shaken vigorously and were centrifuged at 405 \times g for 5 min. The supernatant was passed through a 100- μ m filter (BD Biosciences, San Jose, CA), made up to 50 ml with lymphocyte medium (RPMI 1640 [Gibco], 10% HI-FCS, 200 mM L-glutamine [Invitrogen], 0.004% β -mercaptoethanol [Sigma-Aldrich], 100 IU/ml penicillin, and 100 μ g/ml streptomycin [Invitrogen]), and centrifuged at 405 \times g for 5 min. The supernatant was discarded and the pellet resuspended in 50 ml lymphocyte medium. This process was repeated until the supernatant was clear after centrifugation. The pellet was resuspended in 10 ml lymphocyte medium; cells were enumerated; and a V bottom 96-well plate was seeded with 1 \times 10⁶ cells/well. Unless otherwise stated, incubations were carried out for 30 min at 4°C, and 2% fluorescence-activated cell sorting (FACS) buffer (2% HI-FCS in PBS) was used for washes and antibody dilutions. The antibodies used are listed in Table 2. Unstained, no-primary-antibody, and single-stained controls were prepared. The cells were washed once, resuspended, and incubated with anti-bovine CD3 and anti-bovine CD4, CD8, or TcR1-N24(δ). The cells were washed three times, resuspended, and incubated with anti-mouse IgG1 and anti-mouse IgG2a or anti-mouse IgG2b for 20 min. The cells were subsequently washed and were resuspended in 2% FACS buffer. Data were acquired using a FACSCalibur flow cytometer (BD Biosciences) with a total of 10,000 events collected in the gated region. Compensation and analysis were conducted using FlowJo, version 7.5 (Tree Star, Ashland, OR, USA).

Ex vivo restimulation experiments. Lymph nodes extracted post-mortem were first washed twice with 25 ml preparation medium and then placed in a 100-mm by 25-mm petri dish containing 15 ml preparation medium. The nodes were repeatedly incised and were then transferred to a stomacher bag and placed in a stomacher for 30 s. The contents were then filtered through a 70- μ m nylon filter (Fisher Scientific, Loughborough, United Kingdom) and were made up to 20 ml with preparation medium. The suspension was underlaid with 10 ml Ficoll-Paque (GE Healthcare, Little Chalfont, United Kingdom) and was centrifuged at 800 \times g for 30 min at 4°C. The mononuclear cells were harvested from the top of the Ficoll layer and were washed twice in PBS before being resuspended in lymphocyte medium. Spare cells were resuspended in 10% (vol/vol) dimethyl sulfoxide (DMSO; Sigma-Aldrich) in HI-FCS and were stored in cryovials at 1 \times 10⁷ cells/ml in liquid nitrogen. Round-bottom 96-well plates were seeded with 1 \times 10⁵ cells/well and were stimulated with 5 μ g/ml WT or Δ sepl T3SPs. Controls included concanavalin A (ConA: 5 μ g/ml; Sigma-Aldrich), lymphocyte medium, and 38 or 78 endotoxin units (EU)/ml O111:B4 LPS (Sigma-Aldrich), corresponding to the LPS concentration of the WT or Δ sepl T3SPs, respectively. Cultures were incubated for 5 days under a humidified 5% CO₂ atmosphere at 37°C. Cultures were pulsed with 1 μ Ci/well of [³H]thymidine (PerkinElmer, Waltham, MA) for the final 18 h of incubation by removing 50 μ l of the supernatant and replacing it with [³H]thymidine-containing lympho-

cyte medium. The removed supernatants were stored at -20°C prior to use. Cells were harvested onto glass fiber filters (PerkinElmer, Waltham, MA, USA). [^3H]thymidine incorporation was quantified using an automated scintillation counter (PerkinElmer) and was expressed as counts per minute, with each test performed in triplicate. Stimulation indices (SI) were calculated by dividing the mean value for ConA by the mean value for the medium control or by dividing the mean value for the T3SPs by the mean value for the relevant LPS control.

IFN- γ release was measured using high-binding 96-well enzyme-linked immunosorbent assay (ELISA) plates (Corning, Amsterdam, The Netherlands) and a commercial bovine IFN- γ ELISA kit (Mabtech AB, Nacka Strand, Sweden) as per the manufacturers' instructions. Results below the limit of detection were assigned a value of 16 pg/ml. The supernatants of triplicate wells harvested as described above were pooled, and IFN- γ was assayed in duplicate. IFN- γ release indices were calculated by dividing the mean value for ConA by the mean value for the medium control or by dividing the mean value for the T3SPs by the mean value for the relevant LPS control.

Proliferation marker expression. For each animal, one vial of rectal lymph node cells stored in liquid nitrogen was resuscitated in lymphocyte medium and was used to seed round-bottom 96-well plates at 5×10^5 cells/well. Cells were stimulated in duplicate with 5 $\mu\text{g}/\text{ml}$ heat-treated (110°C for 30 min) WT T3SPs. Controls and culture conditions were as described above. Brefeldin A (10 $\mu\text{g}/\text{ml}$; Sigma-Aldrich) was added for the final 5 h of incubation by removing 50 μl of the supernatant and replacing it with spiked lymphocyte medium. Duplicate stimulated cultures were first pooled and then split evenly between 6 wells of a 96 well round-bottom plate.

The antibodies used are listed in Table 2. Unless stated otherwise, incubation was carried out for 30 min at 4°C , and 5% FACS buffer (5% HI-FCS, 0.02% sodium azide in PBS) was used for washes and antibody dilutions. Unstained, no-primary-antibody, single-stained, and fluorescence-minus-one (FMO) controls were prepared. Cells were pelleted, resuspended, and incubated with anti-bovine CD4, CD8, TcR1-N24(δ), or NKP46. Cells were washed twice, resuspended, and incubated with anti-mouse IgG. Cells were washed twice with PBS and were incubated with Live/Dead Fixable Near-IR reactive dye (Invitrogen) in 0.1% DMSO in PBS. Cells were washed in PBS and were fixed using 1% paraformaldehyde for 10 min at room temperature. Cells were washed in PBS and were permeabilized overnight in permeabilization/block buffer (5% FACS buffer, 0.2% saponin [Sigma-Aldrich], 20% heat-inactivated mouse serum [Invitrogen]). Cells were pelleted, resuspended, and incubated for 1 h with anti-bovine IFN- γ and anti-Ki67 in permeabilization buffer (5% FACS buffer, 0.2% saponin). Cells were washed twice in permeabilization buffer, resuspended, and incubated for 1 h with anti-rabbit Ig in permeabilization buffer. Cells were washed twice in permeabilization buffer and were resuspended in PBS. The entire sample was analyzed using a MACS-Quant flow cytometer (Miltenyi Biotec, Surrey, United Kingdom). Compensation and data analysis were conducted using FlowJo, version 10.0.7 (Tree Star). The gating strategy is shown in Fig. S2 in the supplemental material.

Statistical analysis. Statistical analysis of RT-qPCR data was performed using SAS, version 9.3 (SAS Institute Inc., Cary, NC, USA). All other statistical analyses and plotting of graphs were performed using R, version 3.1.0 (55), and the ggplot2 (56), lattice (57), nlme (58), lme4 (59), plyr (60), reshape (61), multcomp (62), grid (55), gridExtra (63), and lmeans (64) packages.

T-helper cell-associated gene copy numbers were analyzed for the four orally challenged calves in each group and the two control calves. The fold change in gene expression from the prechallenge level was calculated for each gene and was \log_{10} transformed. These log values were analyzed using linear mixed models, with \log_{10} prechallenge gene copies, experimental group, days postchallenge, and the interaction of the experimental group with the number of days postchallenge fitted as fixed effects. Ani-

mals were fitted as random effects. The use of log values ensured that normality requirements for the mixed model were satisfied.

Flow cytometry counts of surface marker-positive versus surface marker-negative CD3 $^{+}$ T cells isolated from the terminal rectum were analyzed using generalized linear models. These fitted the experimental group as the only explanatory variable and fitted a dispersion parameter to allow for overdispersion in the data. Comparisons between each pair of experimental groups were made using Tukey tests. Flow cytometry counts of Ki67-positive versus Ki67-negative, surface marker-positive rectal lymph node cells were also analyzed using generalized linear models with the experimental group, the *ex vivo* stimulant, and the interaction of the experimental group with the *ex vivo* stimulant fitted as explanatory variables, and a dispersion parameter was included to allow for overdispersion in the binomial data. Comparisons between each pair of experimental groups were made using Tukey tests.

\log_{10} -transformed thymidine incorporation, IFN- γ release, stimulation indices, and IFN- γ release indices were analyzed using linear mixed models with restricted maximum likelihood. The models fitted the experimental group, *ex vivo* stimulant, and lymph node as fixed effects. Additionally, two-way interactions between every two main effects were tested and were retained in the model if significant. The animal, the interaction of the animal with the lymph node, and the interaction of the animal with the stimulant were fitted as random effects. Comparisons between each pair of experimental groups were made using Tukey tests. When there was a significant interaction between the experimental group and the lymph node or stimulant, pairwise comparisons were made within the results for each lymph node or stimulant, again using Tukey tests.

RESULTS

Bacterial shedding. Individual shedding curves for each calf are shown in Fig. 1. EHEC O157:H7 was detectable at $>10^3$ CFU/g feces in all orally challenged calves from the first sampling at 3 days postchallenge until days 8 and 10 for the PT32 and PT21/28 strains, respectively, with peak shedding occurring between days 3 and 7. Bacteria were present at $>10^3$ CFU/g in both sentinel calves in the PT21/28 group from the first sampling until day 10, with peak shedding occurring at days 6 and 8. Shedding did not exceed 10^3 CFU/g until day 4 for one of the two PT32 sentinel calves and exceeded 10^3 CFU/g only on day 8 for the other, with peak shedding occurring at days 7 and 8. Shedding after day 10 was more heterogeneous in all calves, with some animals exceeding 10^3 CFU/g at multiple samplings while others remained below 10^3 CFU/g for the remainder of the study. These results confirm that the subsequent immunological analyses were conducted on successfully colonized animals.

Gene expression at the terminal rectum during colonization. The inflammatory transcript TNF- α , T $_H$ 1-associated transcripts IFN- γ and T-bet, T $_H$ 2-associated transcripts IL-4, IL-13, and GATA3, T $_H$ 17-associated transcripts IL-17, IL-22, and RORC, and regulatory T cell (T $_{\text{Reg}}$)-associated transcripts IL-10, TGF- β 1, and FoxP3 were quantified in rectal biopsy specimens taken from orally challenged calves at -5, 7, 14, 21, and 31 days postchallenge. Since the exact time of challenge was unknown for the sentinel animals, only transcript data from the orally challenged calves were analyzed. Transcripts for IL-4 and IL-13 were below the limit of quantification of 100 and 1,000 copies per μl of cDNA, respectively (data not shown). The \log_{10} -transformed relative change in expression from the prechallenge level was calculated for the remaining data and was analyzed using linear mixed models for each transcript of interest. The tests of the fixed effects for each model are shown in Table S4 in the supplemental material. The predicted

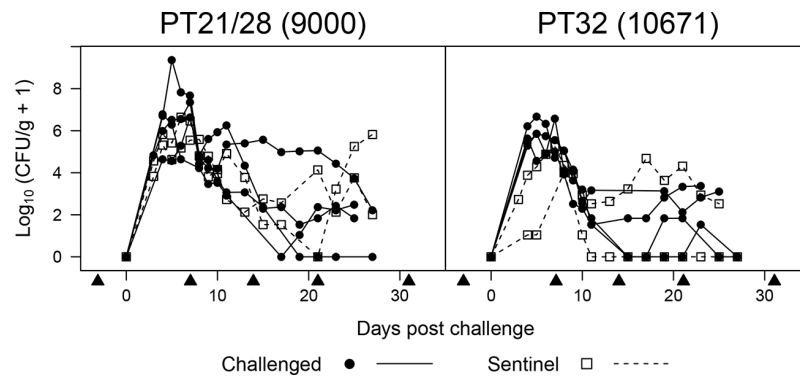


FIG 1 Fecal shedding of EHEC O157:H7 by experimentally infected weaned calves. Six calves were housed in each of two separate HSU rooms. Four calves in each HSU room were dosed with EHEC O157:H7 (strain 9000 in one room and strain 10671 in the other) by orogastric intubation (challenged), while two calves in each room received PBS only (sentinel). Each curve represents an individual animal. Arrowheads indicate rectal biopsy time points.

means and 95% confidence intervals (95% CI) of the model outputs are shown in Fig. 2 and Table S5 in the supplemental material.

Analysis of TNF- α as a general inflammatory indicator was included. There was no statistically significant change in expression at any time point in either control or challenge groups, indicating that the biopsy procedure and challenge did not induce a detectable inflammatory response. Levels of GATA3, the only T_H2 -associated transcript that could be quantified, increased gradually and peaked with 2.23-fold (95% CI, 1.20- to 4.14-fold; $P = 0.0134$) and 2.65-fold (95% CI, 1.56- to 4.50-fold; $P = 0.001$) increases at 21 days postchallenge in the PT21/28 and PT32 groups, respectively. There was no statistically significant change in the control group.

The patterns of expression of the T_H1 -associated transcripts were noticeably different for the two strains. IFN- γ expression in the PT32-challenged calves increased 2.79-fold (95% CI, 1.72- to 4.52-fold; $P = 0.0002$) by 7 days postchallenge and declined gradually, remaining significantly above prechallenge levels until 21 days postchallenge. This was in stark contrast to induction in the PT21/28-challenged calves, where IFN- γ expression remained unchanged until its peak at 21 days of 2.47 times prechallenge levels (95% CI, 1.51 to 4.04 times prechallenge levels; $P = 0.001$). There was no change in IFN- γ expression in the control animals. Changes in T-bet expression in PT32-challenged calves also peaked at 7 days (2.93-fold; 95% CI, 1.93- to 4.44-fold; $P < 0.0001$), but T-bet expression declined more rapidly than IFN- γ expression, to below prechallenge levels by 14 days (0.61-fold; 95% CI, 0.4- to 0.92-fold; $P = 0.0214$), where it remained until the end of the trial. T-bet expression in the PT21/28-challenged group was noticeably different, with biphasic induction at 7 days (1.69-fold; 95% CI, 1.11- to 2.59-fold; $P = 0.0169$) and 21 days (2.09-fold; 95% CI, 1.37- to 3.19-fold; $P = 0.0016$). In the control group, T-bet expression was significantly lower than prechallenge levels at 7 (0.38-fold; 95% CI, 0.21- to 0.69-fold; $P = 0.0026$), 21 (0.22-fold; 95% CI, 0.12- to 0.39-fold; $P < 0.0001$), and 31 (0.53-fold; 95% CI, 0.29- to 0.95-fold; $P = 0.0346$) days postchallenge. For all three groups, T-bet expression was significantly below prechallenge levels by day 31. Taken together, these results suggest a strong T_H1 type 1 skew in the response to colonization, the temporal dynamics of which differed by strain.

None of the three T_H17 -associated transcripts IL-17, IL-22, and RORC demonstrated a statistically significant increase in ex-

pression following challenge. IL-22 expression was somewhat variable within the control and PT32-challenged groups, as evidenced by the wide 95% CI. IL-17 expression remained unchanged until day 31, when it was significantly lower than prechallenge levels in the control group (0.57-fold; 95% CI, 0.32- to 0.99-fold; $P = 0.0467$) and in PT21/28-challenged calves (0.55-fold; 95% CI, 0.37- to 0.81-fold; $P = 0.0047$). RORC expression followed a similar pattern, with statistically significant downregulation in PT21/28-challenged calves (0.56-fold; 95% CI, 0.37- to 0.85-fold; $P = 0.0089$), PT32-challenged calves (0.57-fold; 95% CI, 0.38- to 0.87-fold; $P = 0.0111$), and control calves (0.50-fold; 95% CI, 0.28- to 0.89-fold; $P = 0.0218$) by 14 days. IL-22 expression in the PT21/28 group was down at day 7 (0.43-fold; 95% CI, 0.20- to 0.89-fold; $P = 0.0257$), with no other statistically significant changes in expression until day 31, when it was reduced in the PT21/28 (0.36-fold; 95% CI, 0.17- to 0.76-fold; $P = 0.0094$) and PT32 (0.44-fold; 95% CI, 0.21- to 0.92-fold; $P = 0.0314$) groups.

The T_{Reg} -associated transcripts TGF- $\beta1$ and FoxP3 demonstrated strong induction in control calves at 7 days, with changes of 12.64-fold (95% CI, 4.89- to 32.70-fold; $P < 0.0001$) and 4.67-fold (95% CI, 1.50- to 14.54-fold; $P = 0.0102$), respectively. Unlike FoxP3 expression, which returned to baseline, TGF- $\beta1$ expression remained elevated until the end of the study. This was in contrast to IL-10 expression, which was unchanged in the control calves until it was downregulated on day 31 (0.42-fold; 95% CI, 0.24- to 0.74-fold; $P = 0.0047$). All three genes were downregulated at various time points relative to prechallenge levels in PT21/28-challenged calves: IL-10 was downregulated on days 7 (0.58-fold; 95% CI, 0.40- to 0.84-fold; $P = 0.0062$) and 21 (0.66-fold; 95% CI, 0.46- to 0.96-fold; $P = 0.0295$), TGF- $\beta1$ was downregulated from day 7 (0.05-fold; 95% CI, 0.02- to 0.11-fold; $P < 0.0001$) until the end of the trial, and FoxP3 was downregulated on day 7 only (0.35-fold; 95% CI, 0.13- to 0.96-fold; $P = 0.0423$). In contrast, IL-10 expression remained unchanged in PT32-challenged calves; however, TGF- $\beta1$ expression was upregulated from day 14 (2.38-fold; 95% CI, 1.53- to 3.71-fold; $P = 0.0005$) until the end of the trial, and FoxP3 was upregulated on day 21 only (2.77-fold; 95% CI, 1.15- to 6.67-fold; $P = 0.0249$) in this group.

T cell subsets at the terminal rectum after colonization. Lymphocytes were isolated from the terminal rectum postmortem and were analyzed by flow cytometry. The numbers of CD4⁺, CD8⁺, and $\gamma\delta$ T-cell receptor-positive ($\gamma\delta$ TCR⁺) T cells as proportions

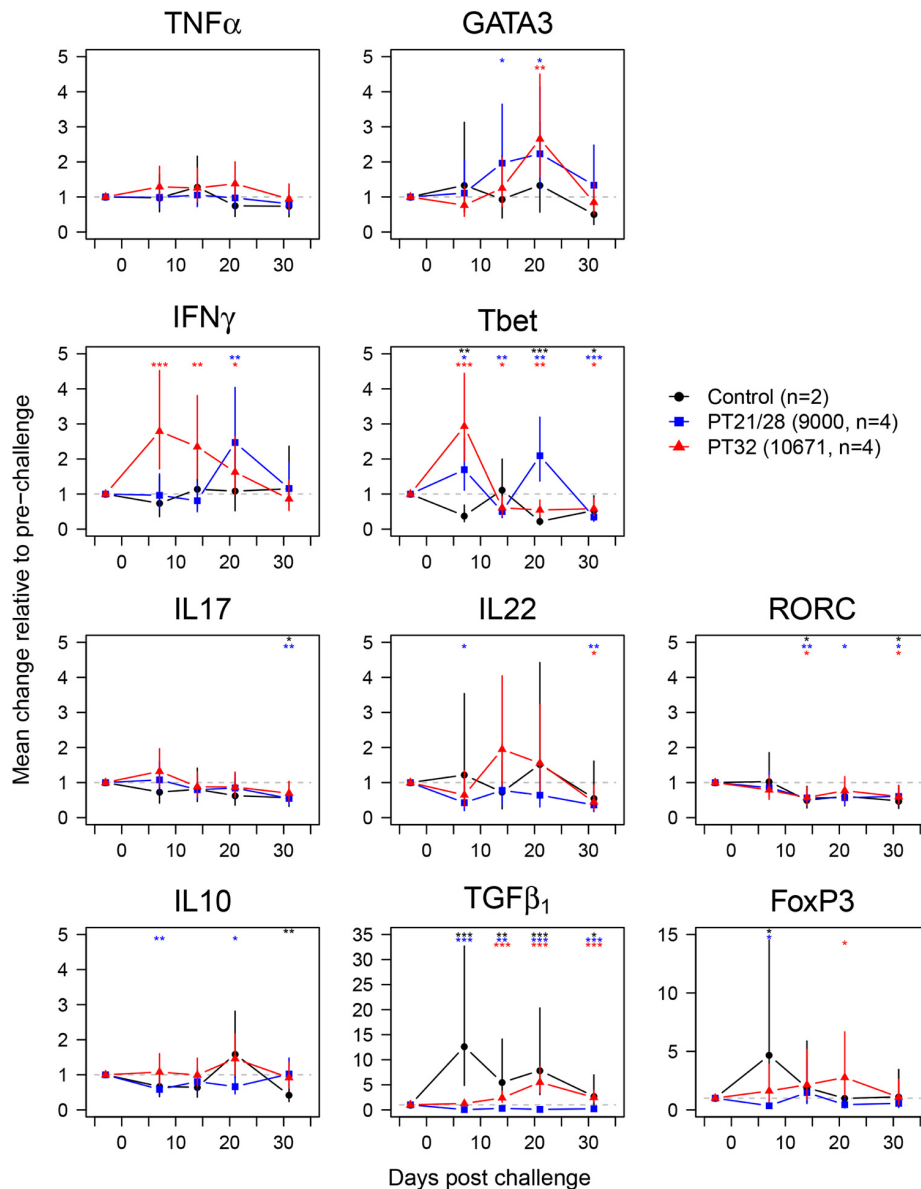


FIG 2 Gene expression at the terminal rectums of calves orally challenged with EHEC O157:H7. Data represent predicted means and 95% confidence intervals from linear-mixed-model analyses of changes in \log_{10} -transformed gene expression from prechallenge levels. Statistically significant differences from prechallenge levels are indicated for control (black symbols), strain 9000 (PT21/28)-challenged (blue symbols), and strain 10671 (PT32)-challenged (red symbols) calves. *, $P < 0.05$; **, $P < 0.01$; ***, $P < 0.001$.

of $CD3^+$ cells are presented in Fig. 3. The experimental group was a statistically significant variable for the proportions of $CD4^+$ (degrees of freedom [df] = 2; deviance = 7,852.1; $P = 0.0009$) and $CD8^+$ (df = 2; deviance = 1,209.1; $P = 0.0335$) T cells but not for the proportions of $\gamma\delta TCR^+$ T cells (df = 2; deviance = 1,290.1; $P = 0.1006$). Tukey comparisons confirmed that the proportions of $CD4^+$ cells were significantly higher at 58.8% (95% CI, 48.4 to 68.5%; Z-score [z] = 3.602; $P = 0.0009$) in the PT21/28-challenged calves and 63.5% (95% CI, 54.8 to 71.4%; $z = 4.496$; $P < 0.0001$) in the PT32-challenged calves than in the control group (31.4%; 95% CI, 22.5 to 41.9%), suggesting a $CD4^+$ T-cell infiltrate into the rectal mucosa in challenged calves. The proportion

of $CD8^+$ cells was significantly lower, at 15.8% (95% CI, 11.5 to 21.2%; $z = -2.892$; $P = 0.0106$), in the PT21/28-challenged calves than in the control group (27.5%; 95% CI, 21.8 to 34.1%).

Ex vivo restimulation of regional lymph node cells. Fresh lymph node cells were extracted postmortem and were restimulated for 5 days with concentrated bacterial secreted protein preparations that include primarily T3SPs. Responses to a wild-type (WT) T3SP preparation consisting predominantly of translocon proteins were compared to responses to a T3SP preparation from an isogenic $\Delta sepL$ mutant containing minimal translocon-associated proteins but increased amounts of secreted effector proteins (52). To distinguish between antigen-specific responses and non-

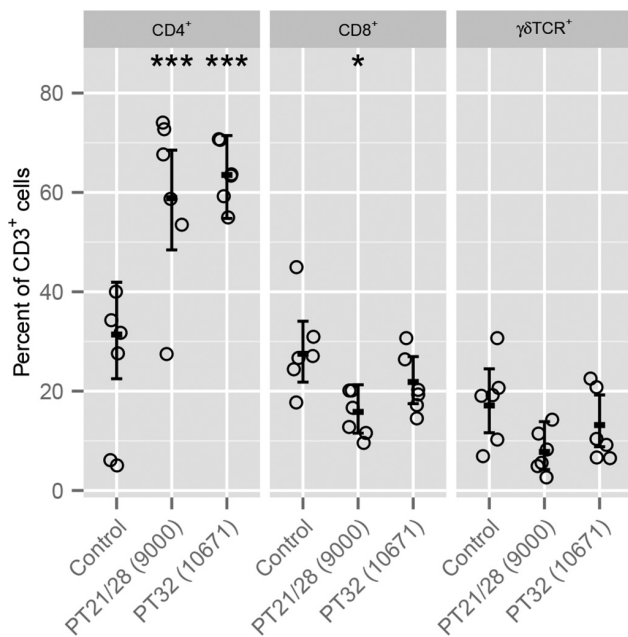


FIG 3 Flow cytometry analysis of CD3⁺ T-cell subsets at the terminal rectums of EHEC O157:H7-colonized calves postmortem. Circles represent results for individual animals. Error bars represent the predicted means and 95% confidence intervals from generalized linear model analysis for each T-cell subset. The significance of differences found by Tukey comparisons between challenged and age-matched control calves is indicated as follows: *, $P < 0.05$; **, $P < 0.01$; ***, $P < 0.001$.

specific proliferation in response to LPS, control wells were spiked with EHEC O111:B4 LPS, so that the final concentration of LPS in control wells was matched to that in the T3SP preparations (WT LPS and $\Delta sepL$ LPS). Levels of thymidine incorporation and IFN- γ release are presented in Fig. 4 as the fold change from the level for the respective LPS control (Fig. 4A and B) and as absolute thymidine incorporation (Fig. 4C) and IFN- γ concentration (Fig. 4D).

Antigen-specific responses. The stimulation index (fold change in thymidine incorporation from that for the relevant LPS control) provides an assessment of antigen-specific proliferation in response to the two T3SP preparations. Model selection showed that the interaction between the *ex vivo* stimulant and the lymph node was significant ($P = 0.0078$), demonstrating that the antigen-specific responses were different within each lymph node. Tukey comparisons (see Table S6 in the supplemental material) show that the stimulation index for the $\Delta sepL$ T3SPs was 1.77-fold higher (standard error [SE] = 1.16; t ratio [TR] = 3.8; $P = 0.0058$) than that for the WT T3SPs at the RLN and 2.83-fold higher (SE = 1.16; TR = 6.9; $P < 0.0001$) at the MLN, but there was no difference at the control PsLN (SE = 1.16; TR = 2.5; $P = 0.1391$). The stimulation index for the $\Delta sepL$ T3SP was 15.7-fold higher (SE = 1.28; TR = 11.0; $P < 0.0001$) at the RLN and 8.9-fold higher (SE = 1.28; TR = 8.7; $P < 0.0001$) at the MLN than at the PsLN, but there was no difference between the RLN and MLN (SE = 1.28; TR = 2.3; $P = 0.2342$). The stimulation index values for the WT T3SP, however, differed for the three different types of lymph nodes, with 2.8-fold (SE = 1.28; TR = 4.1; $P = 0.0024$) and 13.0-fold (SE = 1.28; TR = 10.2; $P < 0.0001$) higher values at the RLN

than at the MLN and PsLN, respectively, and a 4.6-fold higher value (SE = 1.28; TR = 6.1; $P < 0.0001$) at the MLN than at the PsLN.

Given the T_H type 1 skew identified by RT-qPCR in response to colonization, IFN- γ release was used as a second readout for lymphocyte activation and was again expressed as the fold increase over the level for the relevant LPS control (IFN- γ release index). None of the mixed-model interactions were significant, indicating that the difference between the T3SP preparations was the same across all the lymph nodes. Tukey comparisons (see Table S7 in the supplemental material) demonstrate that the IFN- γ release index was 2.4-fold higher (SE = 1.21; $z = 4.5$; $P < 0.0001$) for the $\Delta sepL$ T3SP than for the WT T3SP. The index was also 7.2-fold higher (SE = 1.58; $z = 4.3$; $P < 0.0001$) at the RLN and 4.3-fold higher (SE = 1.58; $z = 3.2$; $P = 0.00578$) at the MLN than at the PsLN. There was no difference between the RLN and MLN (SE = 1.58; $z = 1.1$; $P = 0.61659$).

Overall responsiveness of regional lymph node cells. The interaction plots (Fig. 4C and D) indicate that both total thymidine incorporation and IFN- γ release (i.e., values not normalized to the LPS control) in response to the T3SP preparations and LPS were lower at the RLN and PsLN in PT32-challenged calves than in PT21/28-challenged calves. This observation was confirmed by formal statistical testing. For thymidine incorporation, the interactions between the experimental group and the lymph node ($P = 0.0079$) and between the *ex vivo* stimulant and the lymph node ($P < 0.0001$) were significant. Tukey comparisons between experimental groups within each type of lymph node (see Table S8 in the supplemental material) show lower levels of thymidine incorporation—2.64-fold lower (SE = 1.44; TR = 2.6; $P = 0.0355$) at the RLN and 3.4-fold lower (SE = 1.44; TR = 3.3; $P = 0.0071$) at the PsLN—across all *ex vivo* stimulant groups (ConA, medium only, WT T3SP, WT LPS, $\Delta sepL$ T3SP, and $\Delta sepL$ LPS) for PT32-challenged calves than for PT21/28-challenged calves.

For IFN- γ release, the interactions between the experimental group and the *ex vivo* stimulant ($P = 0.0061$), between the experimental group and the lymph node ($P = 0.0043$), and between the *ex vivo* stimulant and the lymph node ($P < 0.0001$) were all significant. Tukey comparisons of IFN- γ release between experimental groups within each node-*ex vivo* stimulant combination (see Table S9 in the supplemental material) showed that at the RLN, only the antigen-specific responses varied by experimental group. The WT T3SPs resulted in a 12.2-fold (SE = 2.06; TR = 3.5; $P = 0.0035$) reduction in IFN- γ release in PT32-challenged calves from that in PT21/28-challenged calves. As with thymidine incorporation, there were no significant differences at the MLN, while at the PsLN, IFN- γ release was 7.1-fold (SE = 2.06; TR = 2.7; $P = 0.0251$), 28.7-fold (SE = 2.06; TR = 4.7; $P = 0.0001$), 10.6-fold (SE = 2.06; TR = 3.3; $P = 0.0061$), 13.4-fold (SE = 2.06; TR = 3.6; $P = 0.0025$), and 8.8-fold (SE = 2.06; TR = 3.0; $P = 0.0119$) higher in PT21/28-challenged calves than in PT32-challenged calves in response to medium only, WT T3SPs, WT LPS, $\Delta sepL$ T3SPs, and $\Delta sepL$ LPS, respectively.

Immunophenotyping of proliferating rectal lymph node cells in response to WT T3SP. Resuscitated RLN cells were incubated for 5 days with ConA, medium only, treated WT T3SPs, or EHEC O111:B4 LPS. The proportions within each subset of cells expressing the proliferation marker Ki67 are presented in Fig. 5. Data were analyzed using generalized linear models, and analysis-of-deviance tables are shown in Table S10 in the supplemental

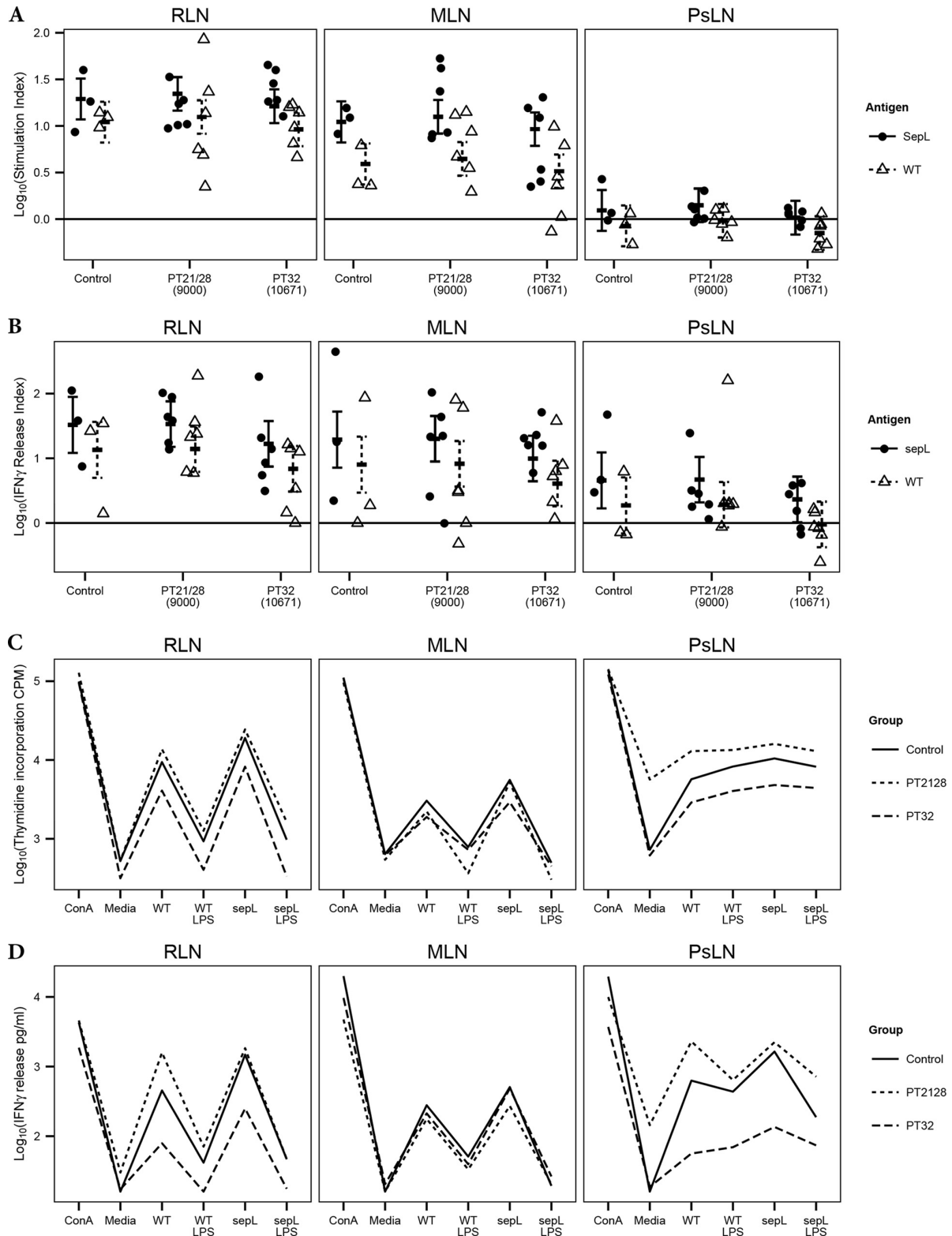


FIG 4 Proliferation of, and IFN- γ release by, bovine lymph node cells isolated postmortem and restimulated *ex vivo* for 5 days with either 5 μ g/ml ConA, medium only, 5 μ g/ml EHEC O157:H7 T3SPs from the *sepL* deletion strain Zap1143 (Δ *sepL*) or its isogenic wild-type (WT) strain Zap193, or medium containing a matched concentration of commercial EHEC O111:B4 LPS. Δ *sepL* T3SP preparations contain mainly secreted effector proteins, while WT T3SP preparations consist mainly of structural translocon components. The use of these two different T3SP preparations allows the relative contributions of structural and effector proteins to antigen recall responses to be compared. Cells were isolated from rectal lymph nodes (RLN), mesenteric lymph nodes (MLN), and prescapular lymph nodes (PsLN). (A and B) Proliferation (A) and IFN- γ release (B) are expressed as indices, representing fold changes in the response to T3SPs from levels with the relevant LPS controls. Circles represent individual animals. (C and D) Interaction plots illustrate mean thymidine incorporation (C) and IFN- γ release (D) by lymph node cells from each experimental group in response to different stimuli. Error bars represent predicted means and 95% confidence intervals from linear-mixed-model analysis.

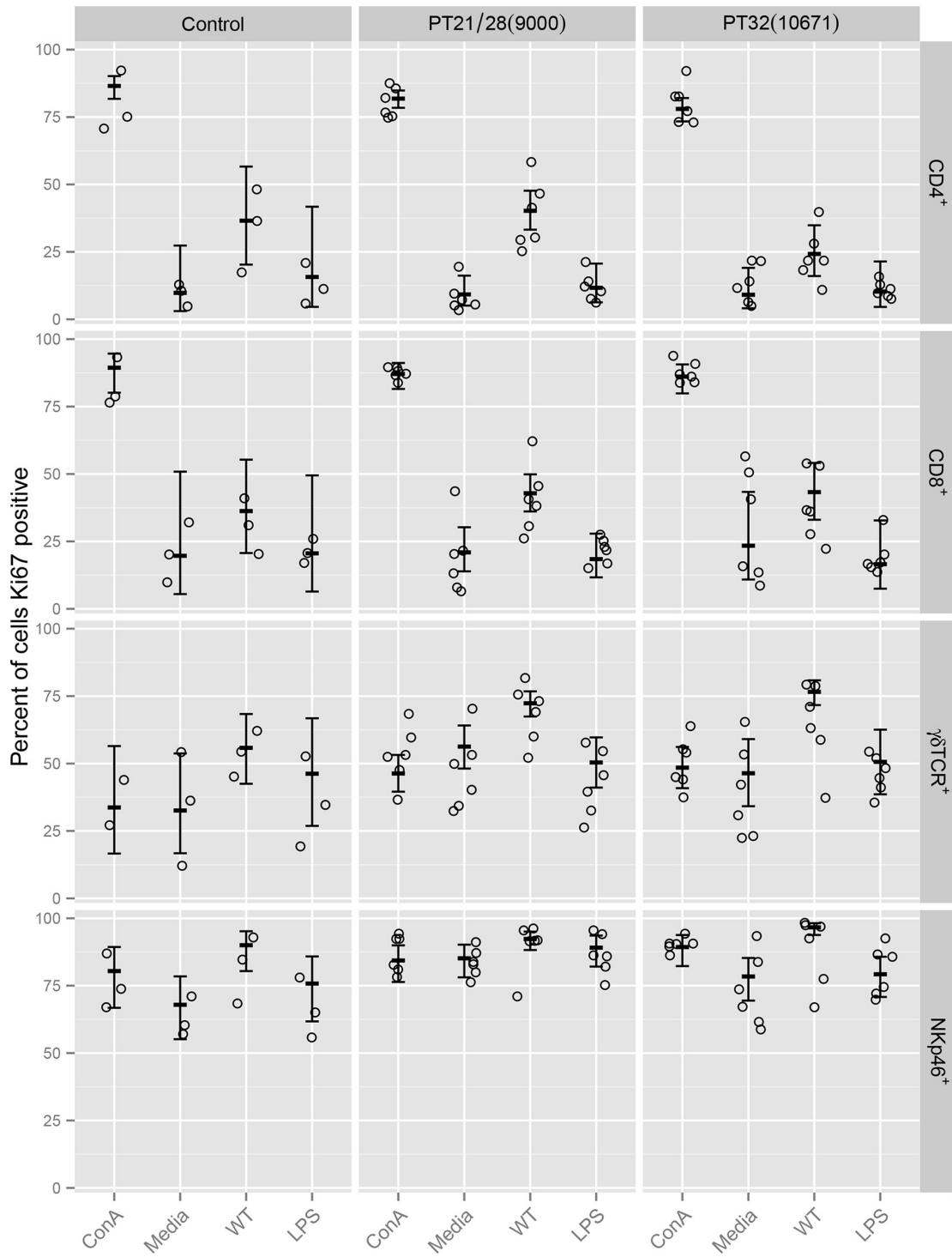


FIG 5 Flow cytometry analysis of proliferation marker (Ki67) expression by different lymphocyte subsets isolated postmortem from the rectal lymph nodes of control and EHEC O157:H7-challenged calves. Frozen cells were resuscitated and were restimulated *ex vivo* for 5 days with 5 μ g/ml ConA, medium only, 5 μ g/ml treated EHEC O157:H7 T3SPs (WT), or medium containing a matched concentration of commercial EHEC O111:B4 LPS (LPS). Circles represent individual animals. Error bars represent predicted means and 95% confidence intervals from generalized-linear-model analysis for each lymphocyte subset.

material. Retaining the interaction between the experimental group and the *ex vivo* stimulant in the models caused comparisons between experimental groups to be based on unweighted averages across the stimulants.

Tukey comparisons for each model are shown in Table S11 in the supplemental material. For all four cell types, there was no significant change in the proportion of cells staining positive for Ki67 in response to LPS compared to the medium control, while the proportions of CD4⁺ and CD8⁺ cells, but not $\gamma\delta$ TCR⁺ or NKp46⁺ cells, staining Ki67 positive increased in response to ConA. These results confirm that none of the cell types proliferated in response to LPS, while only the CD4⁺ and CD8⁺ T cells proliferated in response to ConA.

In PT21/28- but not PT32-challenged animals, a significantly higher proportion of CD4⁺ T cells stained Ki67 positive in response to WT T3SPs than in response to the LPS control. Conversely, in PT32- but not PT21/28-challenged animals, there was a significantly higher proportion of NKp46⁺ cells staining Ki67 positive in response to WT T3SPs than in response to the LPS control. In both groups of challenged calves, a higher proportion of CD8⁺ and $\gamma\delta$ TCR⁺ T cells stained Ki67 positive in response to WT T3SPs than in response to the LPS control.

DISCUSSION

The objective of this study was to characterize the temporal pattern of expression of a panel of transcripts associated with different T-helper cell polarizations at the terminal rectum, which is the principal site of EHEC O157:H7 colonization in calves (65). These results were then used to inform experiments in which regional lymph node cells were extracted and restimulated *ex vivo* with T3SP antigens.

Since the results of this study will be used to guide future vaccine development, the selection of clinically relevant strains was an important consideration. In the United Kingdom, PT21/28 strains are associated with higher levels of shedding in cattle than PT32 strains (66) and represent the predominant isolates from human HUS cases (67). In addition, PT21/28 strains are more likely to possess both Stx2a and Stx2c genes, whereas bovine PT32 strains are more likely to possess the Stx2c genes only (68). While cattle do not suffer from the same severe endothelial sequelae of Stx exposure as humans, there is a significant body of evidence that Stx can affect bovine leukocyte function (40, 69–74). Given the important epidemiological differences between these phage types and their propensity to possess different Stx types, we wanted to compare components of the cellular immune response in cattle following colonization with representative PT21/28 and PT32 strains. The strains used in this study were selected because they had common characteristics of these phage types in cattle. PT21/28 strain 9000 contains both Stx2a- and Stx2c-encoding genes and was isolated from a bovine fecal pat with relatively high EHEC O157:H7 levels, while PT32 strain 10671 contains Stx2c only and was isolated from a bovine fecal pat with relatively low EHEC O157:H7 levels.

Both these strains successfully colonized all the orally challenged cattle and were efficiently transmitted to the two sentinel calves. This study does not have the power to make comparisons between the shedding profiles of orally challenged and those of sentinel calves or between the transmissibilities of the two strains; however, these results will be used to inform power calculations leading to larger trials that will specifically address these questions.

While EHEC O157:H7 can be isolated from multiple sites within the bovine gastrointestinal tract, efficient colonization with A/E lesion formation has been demonstrated at the terminal rectum (65). This offers the opportunity to use minimally invasive rectal biopsy specimens to study the interaction between the bacteria and the mucosal surface at different stages during colonization. It was our hypothesis that by studying the expression of genes associated with different T-helper cell polarizations, it would be possible to determine whether a T-helper response is induced at the site of infection, as well as the type of this response within the T_H1, T_H2, T_H17, and T_{Reg} paradigm. Since mathematical modeling of bacterial shedding dynamics suggests that bacterial replication on the mucosal surface declines precipitously 5 to 7 days following oral challenge (75), biopsy specimens were taken at 7 days after challenge and weekly until the end of the study. Previous work using a bovine-specific cDNA microarray to analyze rectal biopsy specimens taken up to 7 days postchallenge demonstrated differential expression of 49 genes in response to colonization across a range of pathways (76). None of the genes analyzed in our study were identified as differentially regulated by the previous microarray approach. Because a subset of 1,676 genes was present on the microarray and the list of these genes is no longer available (Robert Collier, University of Arizona, personal communication), we are unable to determine whether the T-helper cell-associated transcripts we have analyzed were included in that previous study.

Rectal mucosal biopsy specimens were taken at different positions at each sampling time point to avoid resampling the same sites. The stability of TNF- α expression in the control animals indicates that the experimental protocol did not result in a general inflammatory response within the mucosa. In addition, the lack of induction of TNF- α in the challenge groups would also indicate that this cytokine is not an important component of the bovine response to colonization at the terminal rectum. This is significant, because TNF- α is upregulated during *C. rodentium* colonization in mice (77), while pretreatment of bovine colonic explants with TNF- α has been shown to upregulate mucin secretion and reduce EHEC O157:H7 colonization (78). The observation that TNF- α is not induced at the terminal rectum would imply that this pathway is not active *in vivo* and is likely to contribute to the difference between the pathogenicity of *C. rodentium* in mice, which results in weight loss, moderate mortality, and colonic hyperplasia (79, 80), and that of EHEC O157:H7 in cattle, where the infection is asymptomatic and demonstrates only a mild neutrophilic infiltrate, suggesting that while immunogenic, colonization is not a major inflammatory event (42).

The induction of both IFN- γ and T-bet during colonization is indicative of a T_H type 1 polarized response at the terminal rectum, which is further supported by the inability to detect either IL-4 or IL-13 transcripts. This is in keeping with studies of *C. rodentium* in mice, which has been shown to induce IFN- γ but not IL-4 (77), while experiments using knockout mice have confirmed the importance of IFN- γ in bacterial clearance (81).

The lack of a detectable T_H17 response in this study, in conjunction with the significant downregulation of RORC, suggests that there are additional important differences between the bovine response to EHEC O157:H7 and the response to *C. rodentium* in mice, where IL-22, IL17A, and IL-23 p19 are upregulated during colonization (82), while IL-23 (*p19*^{-/-}) (83), IL-22 (82), IL17A, and IL17F (84) knockout mice demonstrate increased pathology and deficiencies in controlling bacterial replication.

The strain differences in this study were striking. In PT32-challenged calves, as might be anticipated, both IFN- γ and T-bet demonstrated maximal induction around the time of peak shedding at 7 days postchallenge. In PT21/28-challenged calves, however, maximal induction for both genes occurred at 21 days postchallenge, with moderate induction of T-bet but not IFN- γ at 7 days. This strain-specific uncoupling of the IFN- γ and T-bet responses in early infection and the delayed induction of a convincing T_H type 1 response were surprising. IFN- γ can be produced by a wide variety of leukocytes, and T-bet can be expressed by both innate lymphoid cells and lymphocytes (85). It is therefore not possible to infer whether the differences in the dynamics of gene expression observed in the PT21/28-challenged animals are due to innate versus adaptive mechanisms or to a change in the kinetics of the response. While research to determine the complete genome sequences of the two challenge strains is ongoing, it is already known that the PT21/28 strain contains both Stx2a and Stx2c lysogens, whereas the PT32 strain contains Stx2c only. The toxin type and level of production may, in part, account for differences, but we also know that there are complex regulatory interactions between prophages and bacterial host gene expression, including colonization factors (86) and core genome regulatory elements (87). Additional *in vitro* and *in vivo* work with isogenic Stx and Stx-encoding bacteriophage knockout strains is planned to explore these concepts in more detail.

TGF- β 1 and FoxP3 were both upregulated in the control animals, suggesting a T_{Reg} skew. It is unclear whether this is incidental. Interestingly, the induction of both genes is dampened or absent in the challenged calves compared to unchallenged controls, with only moderate induction in PT32-challenged animals and downregulation in the PT21/28-challenged animals. This provides further evidence supporting a convincing T_H1 skew and the reciprocal downregulation of T_{Reg} responses.

The induction of GATA3 at 21 days postinfection suggests that there may be a role for T_H type 2 immunity later during the course of infection. B-cell-deficient mice have demonstrated impaired clearance of *C. rodentium* and reduced bacterial shedding following systemic administration of immune sera (88), despite a strong T_H type 1 response during early stages of infection, suggesting that while the initial response is biased toward cellular immunity, the role of humoral immunity and/or the presence of a healing response (89) may be important as colonization progresses.

In an attempt to understand the impact of colonization on the T-cell subsets at the terminal rectum, lymphocytes were extracted postmortem and were double stained for CD3 and either CD4, CD8, or $\gamma\delta$ TCR. The increase in the proportion of CD4⁺ T cells is indicative of a T-helper cell infiltrate and is strongly suggestive of an adaptive component in the response to colonization. To investigate this further, regional lymph node cells were restimulated *ex vivo* with two different T3SP preparations. Since we had identified a strong T_H type 1 response, IFN- γ release was used alongside thymidine incorporation as a readout of lymphocyte activation. Previous studies using heat-killed bacteria to restimulate ruminant lymphocytes have not controlled for the presence of LPS (40), and our results show that the responsiveness of cells to LPS differs by lymph node, with PsLN cells being more responsive than intestinal lymph node cells. Once the effects of LPS had been controlled for, antigen-specific proliferation and IFN- γ release in response to both T3SP preparations were significantly higher in cells isolated from the two intestinal lymph nodes than in those from

the control PsLN, confirming enhanced recognition of EHEC O157:H7 antigens at sites anatomically relevant to colonization. There was no difference between the experimental groups, suggesting that the experimental animals had previously been exposed to some of the T3SP antigens and/or epitopes used in this study, although the animals were screened for EHEC O157 colonization at multiple times prior to the challenges. An alternative but less likely explanation for the response is that these protein preparations could contain effectors that drive lymphocyte proliferation, as is the case with the staphylococcal superantigen TSST (toxic shock syndrome toxin) (90), although one would predict that proliferation would be equivalent throughout all lymph nodes if this were the case. Of interest was the significantly stronger response from all the lymph nodes to the Δ *sepL* T3SP. Since LPS was controlled for and these preparations were matched by protein concentration, it is reasonable to hypothesize that the secreted effectors are potentially more immunogenic than the structural components. While vaccines containing native secreted and recombinant T3SP structural proteins have been shown to reduce shedding in cattle (13, 28, 29), our current results lend further weight to the consideration of secreted effector proteins in EHEC O157:H7 cattle vaccines and work to define the most immunogenic of these in terms of a T_H1 response.

The observation that cells from the RLN and PsLN of PT32-challenged animals are less responsive than those from control and PT21/28-challenged animals is suggestive of systemic immunomodulation by this strain. Paradoxically, however, this effect was not observed at the MLN. This effect was missed when we were examining the stimulation and IFN- γ release indices due to the reduction in responsiveness also affecting the medium and LPS controls. Currently, it is unclear what may be responsible for this immunomodulation. While Stx activity is a prime candidate, it is interesting that it was the Stx2c-positive PT32 strain, and not the PT21/28 strain, which contains both Stx2a and Stx2c, that demonstrated this repression, suggesting that factors other than Stx may be involved.

In an effort to understand which cell types were involved in responding to T3SPs at the RLN and consequently which cell types might be attenuated by PT32 challenge, the proliferation of the different lymphocyte subsets was characterized by flow cytometry. Heat-inactivated protein preparations were used to exclude the possibility of effector bioactivity driving proliferative responses. CD8⁺ and $\gamma\delta$ TCR⁺ T cells from colonized animals demonstrated statistically significant proliferation in response to the T3SPs, independently of LPS and any potential biological activity of the preparations. It is interesting that these antigens are able to drive both $\gamma\delta$ TCR⁺ and CD8⁺ T-cell proliferation, suggesting a role for $\gamma\delta$ T cells in the response to colonization and the selection of CD8 T-cell clones that are responsive to major histocompatibility complex (MHC) class I-presented EHEC O157:H7 peptides. While CD8⁺ T-cell-depleted mice do not demonstrate a deficit in *C. rodentium* clearance (91), the injection of bacterial effector proteins into host cells via the T3SS means that bacterially derived peptides may be presented on MHC class I molecules. Mathematical modeling of proteasome degradation, TAP processing, and MHC class I loading in humans suggests that secreted EHEC O157:H7 effectors have an altered amino acid composition like that of viral proteins, enabling them to reduce the efficiency by which they are presented by MHC class I molecules (92). The lack of a protective CD8⁺ T-cell response in mice to an A/E lesion-

forming organism does not necessarily mean that these cells do not play an important role in host immunity to EHEC O157:H7 in cattle.

The CD4⁺ T-cell proliferative response to WT T3SPs seen in PT21/28-challenged calves was absent in PT32-challenged calves, while the NK cell proliferative response seen in PT32-challenged calves was absent in PT21/28-challenged calves. This may indicate that the PT32 strain is effectively cleared via innate mechanisms in contrast to the PT21/28 strain, which may be able to evade components of the innate response, resulting in a stronger adaptive response. Alternatively, the PT32 strain may specifically target adaptive immunity by suppressing CD4⁺ T-cell function. NK cells have recently been demonstrated to play an important role in *C. rodentium* clearance (93). If innate immunity is an important component of the immune response in cattle, it may explain why rechallenge experiments demonstrate only a partial and short-term protective effect following bacterial clearance (33). Further work is required to better understand the interaction of these strains with bovine leukocytes.

This study is the first to definitively demonstrate a T_H type 1 immune response to EHEC O157:H7 in cattle. The temporal differences in this response between the two strains studied raise important questions about strain-dependent strategies used by these pathogens to evade host immunity and prolong persistence in the gastrointestinal tract. The roles of innate versus adaptive cellular immunity have not been dissected in this study; however, both are likely to be important, and the organism appears to be directly targeting CD4⁺ T-cell and/or NK cell function through as yet unidentified mechanisms. The serological responses to EHEC O157:H7 vaccination have been extensively studied; however, future vaccine development will need to measure the impact of vaccination on cellular immunity and to test the hypothesis that while high antibody titers may be important in blocking bacterial adhesion, cellular immune responses are required for bacterial clearance. In addition, the targeting of immunomodulatory virulence factors to improve vaccine efficacy should be considered.

ACKNOWLEDGMENTS

This work was supported by DEFRA project 020714. The MRI and SRUC receive funding from the Scottish Government. D.L.G. and S.P.M. are supported by a BBSRC Institute strategic program at the Roslin Institute. A.C. is supported by a Bioniche Life Sciences, Inc., Ph.D. studentship and BBSRC funding. N.I.A. is supported by the Malaysian Ministry of Education.

We thank Dragan Rogan for his contribution to initial discussions on the role of cellular immunity in the control of *E. coli* O157 colonization in cattle. We thank the Moredun Research Institute Bioservices Division for excellent care of experimental animals.

REFERENCES

- Chase-Topping M, Gally D, Low C, Matthews I, Woolhouse M. 2008. Super-shedding and the link between human infection and livestock carriage of *Escherichia coli* O157. *Nat. Rev. Microbiol.* 6:904–912. <http://dx.doi.org/10.1038/nrmicro2029>.
- Olsen SJ, Miller G, Breuer T, Kennedy M, Higgins C, Walford J, McKee G, Fox K, Bibb W, Mead P. 2002. A waterborne outbreak of *Escherichia coli* O157:H7 infections and hemolytic uremic syndrome: implications for rural water systems. *Emerg. Infect. Dis.* 8:370–375. <http://dx.doi.org/10.3201/eid0804.000218>.
- Health Canada. 2000. Waterborne outbreak of gastroenteritis associated with a contaminated municipal water supply, Walkerton, Ontario, May–June 2000. *Can. Commun. Dis. Rep.* 26:170–173.
- Armstrong GL, Hollingsworth J, Morris JG, Jr. 1996. Emerging food-borne pathogens: *Escherichia coli* O157:H7 as a model of entry of a new pathogen into the food supply of the developed world. *Epidemiol. Rev.* 18:29–51. <http://dx.doi.org/10.1093/oxfordjournals.epirev.a017914>.
- Ostroff SM, Griffin PM, Tauxe RV, Shipman LD, Greene KD, Wells JG, Lewis JH, Blake PA, Kobayashi JM. 1990. A statewide outbreak of *Escherichia coli* O157:H7 infections in Washington State. *Am. J. Epidemiol.* 132:239–247.
- Ihekweazu C, Carroll K, Adak B, Smith G, Pritchard GC, Gillespie IA, Verlander NQ, Harvey-Vince L, Reacher M, Edeghere O, Sultan B, Cooper R, Morgan G, Kinross PTN, Boxall NS, Iversen A, Bickler G. 2012. Large outbreak of verocytotoxin-producing *Escherichia coli* O157 infection in visitors to a petting farm in South East England, 2009. *Epidemiol. Infect.* 140:1400–1413. <http://dx.doi.org/10.1017/S0950268811002111>.
- Locking ME, O'Brien SJ, Reilly WJ, Wright EM, Campbell DM, Coia JE, Browning LM, Ramsay CN. 2001. Risk factors for sporadic cases of *Escherichia coli* O157 infection: the importance of contact with animal excreta. *Epidemiol. Infect.* 127:215–220. <http://dx.doi.org/10.1017/S0950268801006045>.
- Dean-Nystrom EA, Bosworth BT, Cray WC, Jr, Moon HW. 1997. Pathogenicity of *Escherichia coli* O157:H7 in the intestines of neonatal calves. *Infect. Immun.* 65:1842–1848.
- Karmali MA. 2004. Infection by Shiga toxin-producing *Escherichia coli*: an overview. *Mol. Biotechnol.* 26:117–122. <http://dx.doi.org/10.1385/MB:26:2:117>.
- Rozema EA, Stephens TP, Bach SJ, Okine EK, Johnson RP, Stanford K, McAllister TA. 2009. Oral and rectal administration of bacteriophages for control of *Escherichia coli* O157:H7 in feedlot cattle. *J. Food Prot.* 72:241–250. <http://dx.doi.org/10.1016/j.jprot.2009.01.001>.
- Callaway TR, Carr MA, Edrington TS, Anderson RC, Nisbet DJ. 2009. Diet, *Escherichia coli* O157:H7, and cattle: a review after 10 years. *Curr. Issues Mol. Biol.* 11:67–79.
- Sargeant JM, Amezcua MR, Rajic A, Waddell L. 2007. Pre-harvest interventions to reduce the shedding of *E. coli* O157 in the faeces of weaned domestic ruminants: a systematic review. *Zoonoses Public Health* 54:260–277. <http://dx.doi.org/10.1111/j.1863-2378.2007.01059.x>.
- Potter AA, Klashinsky S, Li Y, Frey E, Townsend H, Rogan D, Erickson G, Hinkley S, Klopfenstein T, Moxley RA, Smith DR, Finlay BB. 2004. Decreased shedding of *Escherichia coli* O157:H7 by cattle following vaccination with type III secreted proteins. *Vaccine* 22:362–369. <http://dx.doi.org/10.1016/j.vaccine.2003.08.007>.
- Fox JT, Thomson DU, Drouillard JS, Thornton AB, Burkhardt DT, Emery DA, Nagaraja TG. 2009. Efficacy of *Escherichia coli* O157:H7 siderophore receptor/porin proteins-based vaccine in feedlot cattle naturally shedding *E. coli* O157. *Foodborne Pathog. Dis.* 6:893–899. <http://dx.doi.org/10.1089/fpd.2009.0336>.
- Stevens MP, van Diemen PM, Dziva F, Jones PW, Wallis TS. 2002. Options for the control of enterohaemorrhagic *Escherichia coli* in ruminants. *Microbiology* 148:3767–3778.
- Varela NP, Dick P, Wilson J. 2013. Assessing the existing information on the efficacy of bovine vaccination against *Escherichia coli* O157:H7: a systematic review and meta-analysis. *Zoonoses Public Health* 60:253–268. <http://dx.doi.org/10.1111/j.1863-2378.2012.01523.x>.
- Snedeker KG, Campbell M, Sargeant JM. 2012. A systematic review of vaccinations to reduce the shedding of *Escherichia coli* O157 in the faeces of domestic ruminants. *Zoonoses Public Health* 59:126–138. <http://dx.doi.org/10.1111/j.1863-2378.2011.01426.x>.
- McNeilly TN, Naylor SW, Mahajan A, Mitchell MC, McAteer S, Deane D, Smith DG, Low JC, Gally DL, Huntley JF. 2008. *Escherichia coli* O157:H7 colonization in cattle following systemic and mucosal immunization with purified H7 flagellin. *Infect. Immun.* 76:2594–2602. <http://dx.doi.org/10.1128/IAI.01452-07>.
- McNeilly TN, Mitchell MC, Rosser T, McAteer S, Low JC, Smith DG, Huntley JF, Mahajan A, Gally DL. 2010. Immunization of cattle with a combination of purified intimin-531, EspA and Tir significantly reduces shedding of *Escherichia coli* O157:H7 following oral challenge. *Vaccine* 28:1422–1428. <http://dx.doi.org/10.1016/j.vaccine.2009.10.076>.
- Wong AR, Pearson JS, Bright MD, Munera D, Robinson KS, Lee SF, Frankel G, Hartland EL. 2011. Enteropathogenic and enterohaemorrhagic *Escherichia coli*: even more subversive elements. *Mol. Microbiol.* 80:1420–1438. <http://dx.doi.org/10.1111/j.1365-2958.2011.07661.x>.
- Jarvis KG, Kaper JB. 1996. Secretion of extracellular proteins by entero-

- hemorrhagic *Escherichia coli* via a putative type III secretion system. *Infect. Immun.* 64:4826–4829.
22. Tree JJ, Wolfson EB, Wang D, Roe AJ, Gally DL. 2009. Controlling injection: regulation of type III secretion in enterohaemorrhagic *Escherichia coli*. *Trends Microbiol.* 17:361–370. <http://dx.doi.org/10.1016/j.tim.2009.06.001>.
 23. DeVinney R, Stein M, Reinscheid D, Abe A, Ruschkowski S, Finlay BB. 1999. Enterohemorrhagic *Escherichia coli* O157: H7 produces Tir, which is translocated to the host cell membrane but is not tyrosine phosphorylated. *Infect. Immun.* 67:2389–2398.
 24. Dean-Nystrom EA, Gansheroff LJ, Mills M, Moon HW, O'Brien AD. 2002. Vaccination of pregnant dams with intimin_{O157} protects suckling piglets from *Escherichia coli* O157:H7 infection. *Infect. Immun.* 70:2414–2418. <http://dx.doi.org/10.1128/IAI.70.5.2414-2418.2002>.
 25. Vilte DA, Larzabal M, Cataldi AA, Mercado EC. 2008. Bovine colostrum contains immunoglobulin G antibodies against intimin, EspA, and EspB and inhibits hemolytic activity mediated by the type three secretion system of attaching and effacing *Escherichia coli*. *Clin. Vaccine Immunol.* 15: 1208–1213. <http://dx.doi.org/10.1128/CVI.00027-08>.
 26. Rabinovitz BC, Gerhardt E, Tironi Farinati C, Abdala A, Galarza R, Vilte DA, Ibarra C, Cataldi A, Mercado EC. 2012. Vaccination of pregnant cows with EspA, EspB, γ -intimin, and Shiga toxin 2 proteins from *Escherichia coli* O157:H7 induces high levels of specific colostrum antibodies that are transferred to newborn calves. *J. Dairy Sci.* 95:3318–3326. <http://dx.doi.org/10.3168/jds.2011-5093>.
 27. Mahajan A, Currie CG, Mackie S, Tree J, McAteer S, McKendrick I, McNeilly TN, Roe A, La Ragione RM, Woodward MJ, Gally DL, Smith DG. 2009. An investigation of the expression and adhesin function of H7 flagella in the interaction of *Escherichia coli* O157: H7 with bovine intestinal epithelium. *Cell. Microbiol.* 11:121–137. <http://dx.doi.org/10.1111/j.1462-5822.2008.01244.x>.
 28. Allen KJ, Rogan D, Finlay BB, Potter AA, Asper DJ. 2011. Vaccination with type III secreted proteins leads to decreased shedding in calves after experimental infection with *Escherichia coli* O157. *Can. J. Vet. Res.* 75:98–105.
 29. Van Donkersgoed J, Hancock D, Rogan D, Potter AA. 2005. *Escherichia coli* O157:H7 vaccine field trial in 9 feedlots in Alberta and Saskatchewan. *Can. Vet. J.* 46:724–728.
 30. Thomson DU, Loneragan GH, Thornton AB, Lechtenberg KF, Emery DA, Burkhardt DT, Nagaraja TG. 2009. Use of a siderophore receptor and porin proteins-based vaccine to control the burden of *Escherichia coli* O157:H7 in feedlot cattle. *Foodborne Pathog. Dis.* 6:871–877. <http://dx.doi.org/10.1089/fpd.2009.0290>.
 31. Thornton AB, Thomson DU, Loneragan GH, Fox JT, Burkhardt DT, Emery DA, Nagaraja TG. 2009. Effects of a siderophore receptor and porin proteins-based vaccination on fecal shedding of *Escherichia coli* O157:H7 in experimentally inoculated cattle. *J. Food Prot.* 72:866–869.
 32. Bretschneider G, Berberov EM, Moxley RA. 2007. Isotype-specific antibody responses against *Escherichia coli* O157:H7 locus of enterocyte effacement proteins in adult beef cattle following experimental infection. *Vet. Immunol. Immunopathol.* 118:229–238. <http://dx.doi.org/10.1016/j.vetimm.2007.06.005>.
 33. Naylor SW, Flockhart A, Nart P, Smith DG, Huntley J, Gally DL, Low JC. 2007. Shedding of *Escherichia coli* O157:H7 in calves is reduced by prior colonization with the homologous strain. *Appl. Environ. Microbiol.* 73:3765–3767. <http://dx.doi.org/10.1128/AEM.02670-06>.
 34. Johnson RP, Cray WC, Jr, Johnson ST. 1996. Serum antibody responses of cattle following experimental infection with *Escherichia coli* O157:H7. *Infect. Immun.* 64:1879–1883.
 35. Pirro F, Wieler LH, Failing K, Bauerfeind R, Baljer G. 1995. Neutralizing antibodies against Shiga-like toxins from *Escherichia coli* in colostrum and sera of cattle. *Vet. Microbiol.* 43:131–141. [http://dx.doi.org/10.1016/0378-1135\(94\)00089-F](http://dx.doi.org/10.1016/0378-1135(94)00089-F).
 36. Asper DJ, Karmali MA, Townsend H, Rogan D, Potter AA. 2011. Serological response of Shiga toxin-producing *Escherichia coli* type III secreted proteins in sera from vaccinated rabbits, naturally infected cattle, and humans. *Clin. Vaccine Immunol.* 18:1052–1057. <http://dx.doi.org/10.1128/CVI.00068-11>.
 37. Sanderson MW, Besser TE, Gay JM, Gay CC, Hancock DD. 1999. Fecal *Escherichia coli* O157:H7 shedding patterns of orally inoculated calves. *Vet. Microbiol.* 69:199–205. [http://dx.doi.org/10.1016/S0378-1135\(99\)00106-6](http://dx.doi.org/10.1016/S0378-1135(99)00106-6).
 38. Carlson BA, Nightingale KK, Mason GL, Ruby JR, Choat WT, Loneragan GH, Smith GC, Sofos JN, Belk KE. 2009. *Escherichia coli* O157:H7 strains that persist in feedlot cattle are genetically related and demonstrate an enhanced ability to adhere to intestinal epithelial cells. *Appl. Environ. Microbiol.* 75:5927–5937. <http://dx.doi.org/10.1128/AEM.00972-09>.
 39. Cray WC, Jr, Moon HW. 1995. Experimental infection of calves and adult cattle with *Escherichia coli* O157:H7. *Appl. Environ. Microbiol.* 61: 1586–1590.
 40. Hoffman MA, Menge C, Casey TA, Laegreid W, Bosworth BT, Dean-Nystrom EA. 2006. Bovine immune response to Shiga-toxicogenic *Escherichia coli* O157:H7. *Clin. Vaccine Immunol.* 13:1322–1327. <http://dx.doi.org/10.1128/CVI.00205-06>.
 41. Vande Walle K, De Zutter L, Cox E. 2011. Oral infection with a Shiga toxin-negative *Escherichia coli* O157:H7 strain elicits humoral and cellular responses but does not protect sheep from colonisation with the homologous strain. *Vet. Microbiol.* 148:317–322. <http://dx.doi.org/10.1016/j.vetmic.2010.09.012>.
 42. Nart P, Naylor SW, Huntley JF, McKendrick IJ, Gally DL, Low JC. 2008. Responses of cattle to gastrointestinal colonization by *Escherichia coli* O157:H7. *Infect. Immun.* 76:5366–5372. <http://dx.doi.org/10.1128/IAI.01223-07>.
 43. Sheng H, Wang J, Lim JY, Davitt C, Minnich SA, Hovde CJ. 2011. Internalization of *Escherichia coli* O157:H7 by bovine rectal epithelial cells. *Front. Microbiol.* 2:32. <http://dx.doi.org/10.3389/fmicb.2011.00032>.
 44. Frankel G, Phillips AD, Novakova M, Field H, Candy DC, Schauer DB, Douce G, Dougan G. 1996. Intimin from enteropathogenic *Escherichia coli* restores murine virulence to a *Citrobacter rodentium eaeA* mutant: induction of an immunoglobulin A response to intimin and EspB. *Infect. Immun.* 64:5315–5325.
 45. Wadolkowski EA, Burris JA, O'Brien AD. 1990. Mouse model for colonization and disease caused by enterohemorrhagic *Escherichia coli* O157: H7. *Infect. Immun.* 58:2438–2445.
 46. Conlan JW, Perry MB. 1998. Susceptibility of three strains of conventional adult mice to intestinal colonization by an isolate of *Escherichia coli* O157: H7. *Can. J. Microbiol.* 44:800–805. <http://dx.doi.org/10.1139/w98-056>.
 47. Isogai E, Isogai H, Kimura K, Hayashi S, Kubota T, Fujii N, Takeshi K. 1998. Role of tumor necrosis factor alpha in gnotobiotic mice infected with an *Escherichia coli* O157:H7 strain. *Infect. Immun.* 66:197–202.
 48. Nagano K, Taguchi K, Hara T, Yokoyama S, Kawada K, Mori H. 2003. Adhesion and colonization of enterohemorrhagic *Escherichia coli* O157:H7 in cecum of mice. *Microbiol. Immunol.* 47:125–132. <http://dx.doi.org/10.1111/j.1348-0421.2003.tb02795.x>.
 49. Mundy R, Girard F, FitzGerald AJ, Frankel G. 2006. Comparison of colonization dynamics and pathology of mice infected with enteropathogenic *Escherichia coli*, enterohaemorrhagic *E. coli* and *Citrobacter rodentium*. *FEMS Microbiol. Lett.* 265:126–132. <http://dx.doi.org/10.1111/j.1574-6968.2006.00481.x>.
 50. Fernandez-Brando RJ, Miliwebsky E, Mejias MP, Baschkier A, Panek CA, Abrey-Recalde MJ, Cabrera G, Ramos MV, Rivas M, Palermo MS. 2012. Shiga toxin-producing *Escherichia coli* O157: H7 shows an increased pathogenicity in mice after the passage through the gastrointestinal tract of the same host. *J. Med. Microbiol.* 61:852–859. <http://dx.doi.org/10.1099/jmm.0.041251-0>.
 51. Mohawk KL, Melton-Celsa AR, Zangari T, Carroll EE, O'Brien AD. 2010. Pathogenesis of *Escherichia coli* O157:H7 strain 86-24 following oral infection of BALB/c mice with an intact commensal flora. *Microb. Pathog.* 48:131–142. <http://dx.doi.org/10.1016/j.micpath.2010.01.003>.
 52. Wang D, Roe AJ, McAteer S, Shipston MJ, Gally DL. 2008. Hierarchical type III secretion of translocators and effectors from *Escherichia coli* O157:H7 requires the carboxy terminus of SepL that binds to Tir. *Mol. Microbiol.* 69:1499–1512. <http://dx.doi.org/10.1111/j.1365-2958.2008.06377.x>.
 53. Korbie DJ, Mattick JS. 2008. Touchdown PCR for increased specificity and sensitivity in PCR amplification. *Nat. Protoc.* 3:1452–1456. <http://dx.doi.org/10.1038/nprot.2008.133>.
 54. Vandesompele J, De Preter K, Pattyn F, Poppe B, Van Roy N, De Paep A, Speleman F. 2002. Accurate normalization of real-time quantitative RT-PCR data by geometric averaging of multiple internal control genes. *Genome Biol.* 3:RESEARCH0034. <http://dx.doi.org/10.1186/gb-2002-3-7-research0034>.
 55. R Core Team. 2014. R: a language and environment for statistical computing. R Foundation for Statistical Computing, Vienna, Austria. <http://www.R-project.org/>.
 56. Wickham H. 2009. ggplot2: elegant graphics for data analysis. Springer, New York, NY.

57. Sarkar D. 2008. Lattice: multivariate data visualization with R. Springer, New York, NY.
58. Pinheiro J, Bates D, DebRoy S, Sarkar D, R Core Team. 2014. nlme: linear and nonlinear mixed effects models. R package, version 3.1-117. <http://CRAN.R-project.org/package=nlme>.
59. Bates D, Maechler M, Bolker B, Walker S. 2014. lme4: linear mixed-effects models using Eigen and S4. R package, version 1.1-6. <http://CRAN.R-project.org/package=lme4>.
60. Wickham H. 2011. The split-apply-combine strategy for data analysis. J. Stat. Software 40(1). <http://www.jstatsoft.org/v40/i01/>.
61. Wickham H. 2007. Reshaping data with the reshape package. J. Stat. Software 21(12). <http://www.jstatsoft.org/v21/i12/paper>.
62. Hothorn T, Bretz F, Westfall P. 2008. Simultaneous inference in general parametric models. Biom. J. 50:346–363. <http://dx.doi.org/10.1002/bimj.200810425>.
63. Auguie B. 2012. gridExtra: functions in Grid graphics. R package, version 0.9.1. <http://CRAN.R-project.org/package=gridExtra>.
64. Lenth RV. 2014. lsmeans: least-squares means. R package, version 2.00-5. <http://CRAN.R-project.org/package=lsmeans>.
65. Naylor SW, Low JC, Besser TE, Mahajan A, Gunn GJ, Pearce MC, McKendrick IJ, Smith DG, Gally DL. 2003. Lymphoid follicle-dense mucosa at the terminal rectum is the principal site of colonization of enterohemorrhagic *Escherichia coli* O157:H7 in the bovine host. Infect. Immun. 71:1505–1512. <http://dx.doi.org/10.1128/IAI.71.3.1505-1512.2003>.
66. Chase-Topping ME, McKendrick IJ, Pearce MC, MacDonald P, Matthews L, Halliday J, Allison L, Fenlon D, Low JC, Gunn G, Woolhouse ME. 2007. Risk factors for the presence of high-level shedders of *Escherichia coli* O157 on Scottish farms. J. Clin. Microbiol. 45:1594–1603. <http://dx.doi.org/10.1128/JCM.01690-06>.
67. Lynn RM, O'Brien SJ, Taylor CM, Adak GK, Chart H, Cheasty T, Coia JE, Gillespie IA, Locking ME, Reilly WJ, Smith HR, Waters A, Willshaw GA. 2005. Childhood hemolytic uremic syndrome, United Kingdom and Ireland. Emerg. Infect. Dis. 11:590–596. <http://dx.doi.org/10.3201/eid1104.040833>.
68. Matthews L, Reeve R, Gally DL, Low JC, Woolhouse MEJ, McAteer SP, Locking ME, Chase-Topping ME, Haydon DT, Allison LJ, Hanson MF, Gunn GJ, Reid SWJ. 2013. Predicting the public health benefit of vaccinating cattle against *Escherichia coli* O157. Proc. Natl. Acad. Sci. U. S. A. 110:16265–16270. <http://dx.doi.org/10.1073/pnas.1304978110>.
69. Moussay E, Stamm I, Taubert A, Baljer G, Menge C. 2006. *Escherichia coli* Shiga toxin 1 enhances IL-4 transcripts in bovine ileal intraepithelial lymphocytes. Vet. Immunol. Immunopathol. 113:367–382. <http://dx.doi.org/10.1016/j.vetimm.2006.06.007>.
70. Menge C, Eisenberg T, Stamm I, Baljer G. 2006. Comparison of binding and effects of *Escherichia coli* Shiga toxin 1 on bovine and ovine granulocytes. Vet. Immunol. Immunopathol. 113:392–403. <http://dx.doi.org/10.1016/j.vetimm.2006.06.009>.
71. Menge C, Stamm I, Van Diemen PM, Sopp P, Baljer G, Wallis TS, Stevens MP. 2004. Phenotypic and functional characterization of intraepithelial lymphocytes in a bovine ligated intestinal loop model of enterohaemorrhagic *Escherichia coli* infection. J. Med. Microbiol. 53:573–579. <http://dx.doi.org/10.1099/jmm.0.45530-0>.
72. Menge C, Blessenohl M, Eisenberg T, Stamm I, Baljer G. 2004. Bovine ileal intraepithelial lymphocytes represent target cells for Shiga toxin 1 from *Escherichia coli*. Infect. Immun. 72:1896–1905. <http://dx.doi.org/10.1128/IAI.72.4.1896-1905.2004>.
73. Menge C, Stamm I, Blessenohl M, Wieler LH, Baljer G. 2003. Verotoxin 1 from *Escherichia coli* affects Gb3/CD77⁺ bovine lymphocytes independent of interleukin-2, tumor necrosis factor-alpha, and interferon-alpha. Exp. Biol. Med. (Maywood) 228:377–386.
74. Menge C, Wieler LH, Schlapp T, Baljer G. 1999. Shiga toxin 1 from *Escherichia coli* blocks activation and proliferation of bovine lymphocyte subpopulations in vitro. Infect. Immun. 67:2209–2217.
75. Tildesley MJ, Gally DL, McNeilly TN, Low JC, Mahajan A, Savill NJ. 2012. Insights into mucosal innate responses to *Escherichia coli* O157:H7 colonization of cattle by mathematical modelling of excretion dynamics. J. R. Soc. Interface 9:518–527. <http://dx.doi.org/10.1098/rsif.2011.0293>.
76. Li J, Hovde CJ. 2007. Expression profiles of bovine genes in the rectoanal junction mucosa during colonization with *Escherichia coli* O157:H7. Appl. Environ. Microbiol. 73:2380–2385. <http://dx.doi.org/10.1128/AEM.02262-06>.
77. Higgins LM, Frankel G, Douce G, Dougan G, MacDonald TT. 1999. *Citrobacter rodentium* infection in mice elicits a mucosal Th1 cytokine response and lesions similar to those in murine inflammatory bowel disease. Infect. Immun. 67:3031–3039.
78. Xue Y, Zhang H, Wang H, Hu J, Du M, Zhu M-J. 2014. Host inflammatory response inhibits *Escherichia coli* O157:H7 adhesion to gut epithelium through augmentation of mucin expression. Infect. Immun. 82:1921–1930. <http://dx.doi.org/10.1128/IAI.01589-13>.
79. Schauer DB, Zabel BA, Pedraza IF, O'Hara CM, Steigerwalt AG, Brenner DJ. 1995. Genetic and biochemical characterization of *Citrobacter rodentium* sp. nov.. J. Clin. Microbiol. 33:2064–2068.
80. Barthold SW, Coleman GL, Jacoby RO, Livestone EM, Jonas AM. 1978. Transmissible murine colonic hyperplasia. Vet. Pathol. 15:223–236. <http://dx.doi.org/10.1177/030098587801500209>.
81. Simmons CP, Goncalves NS, Ghaem-Maghani M, Bajaj-Elliott M, Clare S, Neves B, Frankel G, Dougan G, MacDonald TT. 2002. Impaired resistance and enhanced pathology during infection with a noninvasive, attaching-effacing enteric bacterial pathogen, *Citrobacter rodentium*, in mice lacking IL-12 or IFN- γ . J. Immunol. 168:1804–1812. <http://dx.doi.org/10.4049/jimmunol.168.4.1804>.
82. Zheng Y, Valdez PA, Danilenko DM, Hu Y, Sa SM, Gong Q, Abbas AR, Modrusan Z, Ghilardi N, de Sauvage FJ, Ouyang W. 2008. Interleukin-22 mediates early host defense against attaching and effacing bacterial pathogens. Nat. Med. 14:282–289. <http://dx.doi.org/10.1038/nm1720>.
83. Mangan PR, Harrington LE, O'Quinn DB, Helms WS, Bullard DC, Elson CO, Hatton RD, Wahl SM, Schoeb TR, Weaver CT. 2006. Transforming growth factor-beta induces development of the T_H17 lineage. Nature 441:231–234. <http://dx.doi.org/10.1038/nature04754>.
84. Ishigame H, Kakuta S, Nagai T, Kadoki M, Nambu A, Komiyama Y, Fujikado N, Tanahashi Y, Akitsu A, Kotaki H, Sudo K, Nakae S, Sasakawa C, Iwakura Y. 2009. Differential roles of interleukin-17A and -17F in host defense against mucocutaneous bacterial infection and allergic responses. Immunity 30:108–119. <http://dx.doi.org/10.1016/j.immuni.2008.11.009>.
85. Sciume G, Hirahara K, Takahashi H, Laurence A, Villarino AV, Singleton KL, Spencer SP, Wilhelm C, Poholek AC, Vahedi G, Kanno Y, Belkaid Y, O'Shea JJ. 2012. Distinct requirements for T-bet in gut innate lymphoid cells. J. Exp. Med. 209:2331–2338. <http://dx.doi.org/10.1084/jem.20122097>.
86. Xu X, McAteer SP, Tree JJ, Shaw DJ, Wolfson EB, Beatson SA, Roe AJ, Allison LJ, Chase-Topping ME, Mahajan A, Tozzoli R, Woolhouse ME, Morabito S, Gally DL. 2012. Lysogeny with Shiga toxin 2-encoding bacteriophages represses type III secretion in enterohemorrhagic *Escherichia coli*. PLoS Pathog. 8:e1002672. <http://dx.doi.org/10.1371/journal.ppat.1002672>.
87. Tree JJ, Granneman S, McAteer SP, Tollervey D, Gally DL. 2014. Identification of bacteriophage-encoded anti-sRNAs in pathogenic *Escherichia coli*. Mol. Cell 55:199–213. <http://dx.doi.org/10.1016/j.molcel.2014.05.006>.
88. Maaser C, Housley MP, Iimura M, Smith JR, Vallance BA, Finlay BB, Schreiber JR, Varki NM, Kagnoff MF, Eckmann L. 2004. Clearance of *Citrobacter rodentium* requires B cells but not secretory immunoglobulin A (IgA) or IgM antibodies. Infect. Immun. 72:3315–3324. <http://dx.doi.org/10.1128/IAI.72.6.3315-3324.2004>.
89. Allen JE, Wynn TA. 2011. Evolution of Th2 immunity: a rapid repair response to tissue destructive pathogens. PLoS Pathog. 7:e1002003. <http://dx.doi.org/10.1371/journal.ppat.1002003>.
90. Poindexter NJ, Schlievert PM. 1985. Toxic-shock-syndrome toxin 1-induced proliferation of lymphocytes: comparison of the mitogenic response of human, murine, and rabbit lymphocytes. J. Infect. Dis. 151:65–72. <http://dx.doi.org/10.1093/infdis/151.1.65>.
91. Simmons CP, Clare S, Ghaem-Maghani M, Uren TK, Rankin J, Huett A, Goldin R, Lewis DJ, MacDonald TT, Strugnell RA, Frankel G, Dougan G. 2003. Central role for B lymphocytes and CD4⁺ T cells in immunity to infection by the attaching and effacing pathogen *Citrobacter rodentium*. Infect. Immun. 71:5077–5086. <http://dx.doi.org/10.1128/IAI.71.9.5077-5086.2003>.
92. Maman Y, Nir-Paz R, Louzoun Y. 2011. Bacteria modulate the CD8⁺ T cell epitope repertoire of host cytosol-exposed proteins to manipulate the host immune response. PLoS Comput. Biol. 7:e1002220. <http://dx.doi.org/10.1371/journal.pcbi.1002220>.
93. Reid-Yu SA, Small CL, Coombes BK. 2013. CD3⁻ NK1.1⁺ cells aid in the early induction of a Th1 response to an attaching and effacing enteric pathogen. Eur. J. Immunol. 43:2638–2649. <http://dx.doi.org/10.1002/eji.201343435>.